Helder Rui Cardoso da Cruz

DINÂMICA OSCILATÓRIA CORTICAL E SUBCORTICAL NO PROCESSAMENTO DA INFORMAÇÃO NOCICEPTIVA: ASPECTOS SENSORIAIS E COGNITIVOS

Orientação do Professor Doutor Vasco Miguel Clara Lopes Galhardo

Dissertação apresentada à Faculdade de Medicina da Universidade do Porto para a obtenção do grau de Doutor em Neurociências

Departamento de Biologia Experimental

Faculdade de Medicina da Universidade do Porto

PORTO, 2012

DISSERTAÇÃO DE CANDIDATURA AO GRAU DE DOUTOR EM NEUROCIÊNCIAS

APRESENTADA À FACULDADE DE MEDICINA DA UNIVERSIDADE DO PORTO

Orientação do Professor Doutor Vasco Miguel Clara Lopes Galhardo

HELDER RUI CARDOSO DA CRUZ

DINÂMICA OSCILATÓRIA CORTICAL E SUBCORTICAL NO PROCESSAMENTO DA INFORMAÇÃO NOCICEPTIVA: ASPECTOS SENSORIAIS E COGNITIVOS

JÚRI NOMEADO PARA A PROVA DE DOUTORAMENTO

PRESIDENTE
Reitor da Universidade do Porto

VOGAIS
Deolinda Maria Valente Alves Lima Teixeira
Professora Catedrática da Faculdade de Medicina da Universidade do Porto

João José Oliveira Malva
Investigador Principal da Faculdade de Medicina da Universidade de Coimbra

Rui Costa
Investigador Principal do Champalimaud Centre for the Unknown

Rui Manuel Cardoso Vaz
Professor Catedrático convidado da Faculdade de Medicina da Universidade do Porto

Vasco Miguel Clara Lopes Galhardo
Professor Auxiliar da Faculdade de Medicina da Universidade do Porto e orientador da tese

CORPO CATEDRÁTICO

DA FACULDADE DE MEDICINA DO PORTO

Professores Efectivos

Alberto Manuel Barros da Silva
Altamiro Manuel Rodrigues Costa Pereira
Álvaro Jerónimo Leal Machado de Aguiar
António Carlos Freitas Ribeiro Saraiva
Daniel Filipe Lima Moura
Deolinda Maria Valente Alves Lima Teixeira
Francisco Fernando Rocha Gonçalves
Isabel Maria Amorim Pereira Ramos
João Francisco Montenegro Andrade Lima Bernardes
Jorge Manuel Mergulhão Castro Tavares
José Agostinho Marques Lopes
José Carlos Neves da Cunha Areias
José Eduardo Torres Eckenroth Guimarães
José Henrique Dias Pinto de Barros
José Manuel Lopes Teixeira Amarante
José Manuel Pereira Dias de Castro Lopes
Manuel Alberto Coimbra Sobrinho Simões
Manuel António Caldeira Pais Clemente
Manuel Jesus Falcão Pestana Vasconcelos
Maria Amélia Duarte Ferreira
Maria Dulce Cordeiro Madeira
Maria Fátima Machado Henriques Carneiro
Maria Leonor Martins Soares David
Patrício Manuel Vieira Araújo Soares Silva
Rui Manuel Almeida Mota Cardoso
Rui Manuel Lopes Nunes

Professores Jubilados ou Aposentados

Abel José Sampaio da Costa Tavares
Abel Vitorino Trigo Cabral
Alexandre Alberto Guerra Sousa Pinto
Amândio Gomes Sampaio Tavares
António Augusto Lopes Vaz
António Carvalho Almeida Coimbra
António Fernandes da Fonseca
António Fernandes Oliveira Barbosa Ribeiro Braga
António Germano Pina Silva Leal
António José Pacheco Palha
António Luís Tomé da Rocha Ribeiro
António Manuel Sampaio de Araújo Teixeira
Belmiro dos Santos Patrício
Cândido Alves Hipólito Reis
Carlos Rodrigo Magalhães Ramalhão
Cassiano Pena de Abreu e Lima
Daniel Santos Pinto Serrão
Eduardo Jorge Cunha Rodrigues Pereira
Fernando de Carvalho Cerqueira Magro Ferreira
Fernando Tavarela Veloso
Francisco de Sousa Lé
Henrique José Ferreira Gonçalves Lecour de Menezes
Joaquim Germano Pinto Machado Correia da Silva
José Augusto Fleming Torrinha
José Carvalho de Oliveira
José Fernando Barros Castro Correia
José Luís Medina Vieira
José Manuel Costa Mesquita Guimarães
Levi Eugénio Ribeiro Guerra
Luís Alberto Martins Gomes de Almeida
Manuel Augusto Cardoso de Oliveira
Manuel Machado Rodrigues Gomes
Manuel Maria Paula Barbosa
Maria da Conceição Fernandes Marques Magalhães
Maria Isabel Amorim de Azevedo
Mário José Cerqueira Gomes Braga
Serafim Correia Pinto Guimarães
Valdemar Miguel Botelho dos Santos Cardoso
Walter Friedrich Alfred Osswald

Ao Professor Doutor Vasco Miguel Clara Lopes Galhardo

Aos meus Pais e Irmão

PREFÁCIO

O trabalho de dissertação de doutoramento que se apresenta é fruto de uma colaboração intensa de diversas pessoas às quais desejo manifestar os meus sinceros agradecimentos.

De um modo muito especial ao meu orientador, Professor Doutor Vasco Galhardo, o principal responsável pelo meu sucesso como investigador. Pela disponibilidade demonstrada para a minha formação desde o primeiro dia em que integrei este grupo, numa área de investigação totalmente nova para mim, e que culmina agora com o sucesso dos trabalhos aqui apresentados.

Aos colegas de laboratório com os quais ao longo dos últimos anos tive o privilégio de interagir, que ultrapassam a mera relação laboral amizade. Dra. Clara Monteiro, Doutor Miguel Pais Vieira, Doutor Paulo Aguiar, Eng. Luís Mendonça, Dra. Mafalda Sousa, Doutor Albino Oliveira Maia, Dra. Manuela Pinto, Dra. Margarida Dourado, Dra. Mariana Raimundo.

Uma palavra de agradecimento às pessoas que materializaram as colaborações estabelecidas durante a execução da presente dissertação, que impulsionaram o sucesso de dois dos trabalhos aqui apresentados com o conjugar de sinergias. Ao Professor Doutor Luís Antunes e Doutora Aura Silva do Laboratório de Ciência Animal do IBMC/UTAD. Ao Professor Doutor Koichi Sameshima da Universidade de São Paulo e aos seus alunos, Daniel Takahashi e Luíz Lana. Ao Doutor Damien Gervasoni e ao Doutor Lin Shih-Chieh da Universidade de Duke.

Aos meus pais pelo apoio incondicional em todas as fases de elaboração deste trabalho.

À Fundação para a Ciência e Tecnologia pela concessão da bolsa de doutoramento para a execução da presente dissertação (*).

A todos o meu profundo agradecimento.

(*) Bolsa de Doutoramento FCT Ref.ª SFRH/BD/2007/42500

Em obediência ao disposto no Decreto-Lei n.º388/70, Artigo 8.º, parágrafo 2, declaro que efectuei o planeamento e execução das experiências, observação do material e análise de resultados e participei activamente na redacção de todas as publicações que fazem parte integrante desta dissertação:

I. Cardoso-Cruz H, Sameshima K, Lima D, Galhardo V (2011) *Dynamics of circadian thalamocortical flow of information during a peripheral neuropathic pain condition.* Frontiers in Integrative Neuroscience 5:43.
DOI: 10.3389/fnint.2011.00043

II. Silva A, Cardoso-Cruz H, Silva F, Galhardo V, Antunes L (2010) *Comparison of anesthetic depth indexes based on thalamocortical local field potentials in rats.* Anesthesiology 112(2):355-363.
DOI: 10.1097/ALN.0b013e3181ca3196

III. Cardoso-Cruz H, Lima D, Galhardo V (2011) *Instability of spatial encoding by CA1 hippocampal place cells after peripheral nerve injury.* European Journal of Neuroscience 33(12):2255-2264.
DOI: 10.1111/j.1460-9568.2011.07721.x

IV. Cardoso-Cruz H, Lima D, Galhardo V (2012) *Reduced hippocampal-prefrontal cortex connectivity in neuropathic pain rats performing a spatial working memory task*. Submetido.

V. Cardoso-Cruz H, Sousa M, Vieira J, Lima D, Galhardo V (2012) *Uncovering information interactions between medial prefrontal cortex and mediodorsal thalamus circuit in rats performing a spatial working memory task under a chronic pain condition.* Submetido.

ABREVIATURAS UTILIZADAS NA INTRODUÇÃO E CONSIDERAÇÕES FINAIS

ACC, Córtex cingulado anterior
BDNF, *Brain-derived neurotrophic factor*
CA, *Cornu Ammonis*
CL, Núcleo talâmico centro-lateral
dCA1, região dorsal do *Cornu Ammonis* primário hipocampal
DG, Giro dentado
EC, Córtex entorrinal
EEG, Electroencefalografia
EMG, Electromiografia
HF, Formação hipocampal
LC, *Locus Coeruleus*
LFP, Potencial de campo local
LGN, Núcleo geniculado lateral
LTS, *Low-threshold calcium spikes*
LTP, *Low-term potentiation*
MD, Tálamo médio-dorsal
MEG, Magnetoencefalografia
mPFC, Córtex pré-frontal medial
NMDA, N -metil D-Aspartato
PAG, Substância cinzenta periaqueductal
PFC, Córtex préfrontal
REM, *Rapid-eye-movement*
SI, Córtex somatosensitivo primário
SII, Córtex somatosensitivo secundário
SNC, Sistema nervoso central
SWS, *Slow-wave-sleep*
TC, Tálamo-cortical
TCD, Disritmia tálamo-cortical
TNF-α, Factor de necrose tumoral *alpha*
TS, Estado de transição
VPL, Núcleo talâmico ventro-porterior-lateral
VPM, Núcleo talâmico ventro-posterior-medial
WK, estado de vigília
WM, Memória de trabalho
WT, *Whisker-twitching*

ÍNDICE

INTRODUÇÃO I

1. OSCILAÇÕES NO CÉREBRO

A actividade basal no cérebro é caracterizada por oscilações espontâneas a nível das áreas sensoriais (Gray et al., 1989; Neville and Haberly, 2003), motoras (Raij et al., 2004) e associativas (Hasselmo et al., 2002a; Montgomery and Buzsáki, 2007). As interacções entre os diferentes ritmos de oscilação neuronais são utilizadas pelo cérebro para a realização dinâmica de computações de integração, processamento e armazenamento de informação. Estas oscilações têm origem no somatório de potenciais pós-sinápticos excitatórios e inibitórios oriundos da actividade simultânea de centenas de neurónios. Esta actividade pode ser quantificada com eléctrodos inseridos no espaço extracelular intracranial (potenciais de campo local ou *local field potentials* - LFPs) ou de forma não invasiva com eléctrodos posicionados na superfície do crânio (electroencefalografia - EEG).

A existência de variações nas oscilações espontâneas nos potenciais eléctricos do cérebro em bandas de frequência que vão dos 0.5 a 250 Hz, é o argumento definitivo de que o cérebro possui uma actividade contínua e autónoma, não se limitando a receber estímulos e a organizar respostas motoras a esses mesmos estímulos. A coexistência e interacção de diversos ritmos em padrões oscilatórios complexos, mesmo durante estados de inconsciência, como o sono, coma, anestesia geral e em estados epilépticos, mostram que a actividade cerebral é incessante e que apenas depende parcialmente da entrada de informação sensorial (Laureys et al., 2004; Owen et al., 2006). Efectivamente, algumas das oscilações mais importantes são as decorrentes da transição entre o estado de vigília e o estado de sono (Steriade and Timofeev, 2003; Gervasoni et al., 2004; Llinás and Steriade, 2006) ou da transição dos estados de consciência para inconsciência associados a protocolos de anestesia (Schneider and Kochs, 2007; Velly et al., 2007; Silva et al., 2010).

1.1. BANDAS DE FREQUÊNCIA DAS OSCILAÇÕES

Hans Berger (1873-1941) é considerado um dos cientistas pioneiros no campo da electrofisiologia. Foi responsável pelos primeiros registos de EEG em humanos, pela introdução da nomenclatura actual de classificação dos diferentes ritmos do cérebro baseada em letras do alfabeto grego, e pelas primeiras descrições de alterações nos sinais oscilatórios em epilepsia. Berger introduziu o conceito de bandas de frequência ao

descrever uma oscilação primordial no cérebro a que chamou “ondas alfa” (entre os 9 e os 12 Hz) que eram suprimidas pelas “ondas beta” (entre os 12 e os 30 hz) quando o sujeito abria os olhos durante o registo encefalográfico.

Actualmente, consideram-se ainda a existência de uma banda *delta* (abaixo dos 4Hz), e aquelas que são as bandas de frequência mais estudadas actualmente: as oscilações *theta* (4-9 Hz) e as oscilações *gamma* (acima dos 30 Hz). No caso particular das oscilações em *theta* foram muito estudadas ao nível do hipocampo de roedores, nomeadamente durante a execução de comportamentos (Buzsaki, 2002), navegação espacial (Skaggs et al., 1996), processos de memória (Hasselmo et al., 2002a; Hasselmo et al., 2002b) e sono (Louie and Wilson, 2001). Todavia, os ritmos *theta* também estão presentes em outras áreas corticais (Lakatos et al., 2005; Canolty et al., 2006) e subcorticais (DeCoteau et al., 2007). Este padrão de actividade está na génese de uma teoria que atribuiu a estas oscilações a função da sincronização da actividade entre diversas estruturas neocorticais e o hipocampo, que por sua vez processaria a informação e a devolveria ao neocórtex (Miller, 1989).

Após a ênfase inicial atribuída ao ritmo *theta* originada pelos estudos das décadas de 60 e 70 (Vanderwolf, 1969; Kramis et al., 1975), a atenção foi voltada para o estudo das oscilações mais rápidas na banda *gamma*. As oscilações *gamma* podem ser observadas durante a associação sensorial visual (Gray et al., 1989; Singer and Gray, 1995; Rols et al., 2001), olfactiva (Neville and Haberly, 2003) e auditiva (Brosch et al., 2002), em processos de atenção selectiva (Jensen and Colgin, 2007), actividade epiléptica (Lévesque et al., 2009) e durante a transmissão de informação e seu armazenamento (Lisman et al., 2005; Driver et al., 2007; Montgomery and Buzsáki, 2007). No hipocampo os mecanismos de oscilação acima dos 40 Hz envolvem redes de células inibitórias contendo conexões axónicas por “*gap-junctions*” (Mann and Paulsen, 2005). Os interneurónios possuem padrões de disparo rápidos, sendo capazes de disparar continuamente a cada oscilação *gamma* (Harris et al., 2003; Senior et al., 2008), exercendo uma inibição cíclica sobre as células piramidais, criando desta forma janelas temporais nas quais pode ocorrer sincronização do disparo (Klausberger and Somogyi, 2008).

No cérebro existem também interacções entre diferentes bandas de frequência (Chrobak et al., 2000; Lakatos et al., 2005; Canolty et al., 2006). Por exemplo, a fase

theta é conhecida por influenciar as oscilações em *gamma* entre o hipocampo e os circuitos corticais. Este tipo de interacções está envolvido na organização sequencial dos processos de memória e sua leitura e manutenção (Chrobak et al., 2000; Sederberg et al., 2003; Lisman and Grace, 2005; Siapas et al., 2005; Izaki and Akema, 2008; Sirota et al., 2008).

1.2. OSCILAÇÕES E ESTIMULAÇÃO NOCICEPTIVA

As oscilações observadas em diferentes circuitos do cérebro reflectem um estado funcional global do sistema, sendo utilizadas pelo cérebro como mecanismos de alerta para perturbações do seu normal funcionamento (Ploner et al., 2006). A dor é um dos factores conotados com a perturbação destas oscilações espontâneas ao nível dos diferentes circuitos cortico-subcorticais (Corbetta and Shulman, 2002; Mouraux et al., 2003; Ohara et al., 2004), através da inibição ou potenciação de ritmos oscilatórios (Backonja et al., 1991; Veerasarn and Stohler, 1992; Chang et al., 2002; Ploner et al., 2006). Esta função de alerta para a dor pode estar enquadrada num fenómeno de facilitação do processamento sensorial (Ploner et al., 2004) e motor (Raij et al., 2004), como preparação da reacção a estímulos agressivos.

No que respeita ao processamento da informação nociceptiva, encontram-se na literatura a identificação de padrões de oscilação específicos em algumas áreas do cérebro. Um dos padrões mais estudado é o de pacientes com dor neurogénica que exibem um aumento da coerência de oscilação no eixo tálamo-cortical ao nível da banda de frequência *theta* (Sarnthein and Jeanmonod, 2008), o qual é um dos argumentos que suporta o conceito de disritmia tálamo-cortical (DTC) sugerido como responsável desta patologia (a DTC é abordada em maior detalhe no ponto 2.1.3 desta Introdução). Para além da banda *theta* também foram descritas alterações noutros domínios de frequência induzidas pelo processamento de informação nociceptiva. Registos EEG provaram existir um aumento da actividade na banda de frequência *alpha* (9-15 Hz) ao nível do neocórtex, áreas somatosensitivas (Babiloni et al., 2002; Babiloni et al., 2003) e córtex insular (Franciotti et al., 2009) durante estimulação nociceptiva. Estes padrões oscilatórios foram também observados em associação com oscilações do tipo *theta* ao nível do córtex somatosensitivo secundário (Hsiao et al., 2008). Em humanos foi observado um aumento da actividade cortical na banda em *beta* (15-30 Hz) associada a

alterações do processamento sensorial (Lalo et al., 2007) e ao nível do córtex cingulado durante a estimulação dolorosa por laser (Stancák et al., 2010). A banda *beta* foi também observada no córtex somatosensitivo primário e secundário, córtex insular e córtex parietal posterior em pacientes com dor neurogénica (Stern et al., 2006). No que diz respeito às oscilações do tipo *gamma* foram identificadas no córtex somatosensitivo (Gross et al., 2007), córtex cingulado (Legrain et al., 2009) e outras áreas corticais, estando positivamente correlacionadas com a percepção de estímulos nociceptivos e com os padrões de atenção decorrentes da dor (Hauck et al., 2007; Tiemann et al., 2010).

2. A COMPLEXIDADE DA DOR

A percepção da dor é uma experiência essencial para a sobrevivência dos organismos mais complexos. Com excepção dos indivíduos com insensibilidade congénita para a dor (Nagasako et al., 2003), todas as pessoas irão experimentar vários tipos de dor ao longo da sua vida. Na maioria dos pacientes com dor crónica, o síndrome avança para condições muito para além do mero indicador de estímulos nocivos, tornando-se uma condição patológica. Nos últimos anos, a dor crónica tem sido inserida num grupo de patologias que requer especial atenção e tratamento, tendo aumentado o interesse para a descrição e compreensão dos mecanismos associados à integração da informação nociceptiva por diversos circuitos do cérebro.

Melzack e Casey (1968) propuseram a repartição dos circuitos de processamento da dor em dois sistemas paralelos: o lateral e o medial. O sistema lateral - constituído pelo córtex somatosensitivo (primário e secundário), núcleos laterais e mediais do tálamo e medula espinhal - está envolvido na componente sensorial e discriminativa da dor, isto é, na detecção e percepção da origem, intensidade, duração e modalidade do estímulo nociceptivo (Casey and Morrow, 1983b; Casey et al., 1996; Urban and Gebhart, 1999). O sistema medial - constituído por várias estruturas do sistema límbico como o hipocampo, córtex frontal, córtex cingulado, ínsula, amígdala e vários núcleos do tronco cerebral - está relacionado com os aspectos cognitivos e afectivos da dor, ou seja, a relação entre a dor e a memória, a capacidade de tolerância à dor, bem como a racionalização e interpretação afectiva da dor (Willis, 1985; Rainville, 2002; Baliki et al., 2006; Apkarian et al., 2009).

A visão actual é que estes dois sistemas não são activados isoladamente, mas que estão interligados a diversos níveis de modo a interactuarem recíproca e interactivamente (Besson, 1999; Melzack, 1999; Neugebauer et al., 2009). A apoiar essa hipótese, diversos estudos de neuroimagiologia funcional demonstraram o envolvimento em simultâneo de diversas regiões do cérebro na resposta à estimulação dolorosa (Ploghaus et al., 2001; Bantick et al., 2002; Tracey, 2005; Dick and Rashiq, 2007; Ploner et al., 2011). Esses estudos estão na base do conceito de "neuromatriz da dor", que propõe a existência de um processamento multidimensional dependente da geração de padrões de actividade distribuídos por vários circuitos no cérebro (Legrain et al., 2011). Esta teoria põe de parte a ideia de um sistema reduzido ao conceito cartesiano, de dor como uma sensação produzida por uma lesão, inflamação ou outro tipo de patologia no tecido, e introduz o conceito de dor como um reflexo de experiências resultantes da influência de múltiplos factores decorrentes da integração da informação sensorial-discriminativa, afecto-motivacional e cognitiva-evaluativa (Price, 2000; Rainville, 2002; Apkarian, 2008). É habitualmente assumido que a dor crónica não causa apenas perturbações sensoriais (dor espontânea, hiperalgesia e alodínea), mas está também envolvida em diversas alterações funcionais do cérebro (estados de ansiedade, amnésia, insónia ou depressão) (Lautenbacher et al., 2006; Moriarty et al., 2011). Partindo deste pressuposto é necessário não limitar o estudo dos mecanismos associados à dor crónica, a apenas os baixos níveis da neuromatriz e amplia-los até outras estruturas a nível cortical e subcortical. A seguir serão abordados em detalhe dois dos circuitos que servem como suporte à valência multidimensional da dor: o circuito tálamo-cortical e o circuito fronto-hipocampal.

2.1. O CIRCUITO TÁLAMO-CORTICAL

O sistema tálamo-cortical é por excelência um circuito envolvido na integração de informação e na interconexão com outros circuitos (Contreras et al., 1996; Llinás et al., 1998). As áreas corticais e talâmicas são densamente e reciprocamente interconectadas (Steriade, 1999; Jones, 2001; Castro-Alamancos, 2004), embora as projecções descendentes do córtex para o tálamo sejam sete a dez vezes superiores às projecções ascendentes do tálamo para o córtex (Bourassa and Deschênes, 1995; Bourassa et al., 1995; Liu and Sandk hler, 1995).

Diversos estudos aplicando técnicas *in vivo* em animais anestesiados e acordados têm abordado o papel funcional do sistema tálamo-cortical (Llinás and Jahnsen, 1982; Llinás, 1988; Contreras et al., 1996; Fanselow and Nicolelis, 1999; Steriade, 1999, 2001). Os padrões temporais e espaciais da actividade cortico-talâmica demonstraram uma grande variabilidade, sugerindo que o circuito suporta uma vasta gama de interacções que são necessárias para a análise da informação sensorial, programação motora e funções cognitivas (Mogilner et al., 1993; Steriade et al., 1993; Alitto and Usrey, 2003; Ribary, 2005). Um dos aspectos funcionais mais relevantes é a transição constante que existe no tálamo entre um estado fisiológico de actividade em disparo tónico (em que os potenciais de acção originam uma alternação entre despolarização e hiperpolarização neuronal) e um estado fisiológico de disparo em *burst* (em que os neurónios permanecem num regime hiperpolarizado que leva à geração autoperpetuada de potenciais de acção cálcio-dependentes). Alguns investigadores defendem que a informação sensorial é transmitida do tálamo para o córtex unicamente durante padrões de actividade tónica, e que nenhuma informação é transmitida durante o padrão de actividade em *burst* (Steriade et al., 1993). Esta ideia foi recentemente posta em causa com dados experimentais, que demonstraram que neurónios talâmicos podem transmitir informação sensorial durante os dois estados fisiológicos de actividade (Guido and Weyand, 1995; Weyand et al., 2001). No entanto a natureza do sinal transmitido difere entre os dois modos de actividade. Fanselow e colaboradores (2001) demonstraram que os *burst* talâmicos podem ocorrer durante os estados de vigília, todavia a sua prevalência é menor quando comparada com o estado de sono denominado por *slow-wave-sleep* (SWS). Este padrão foi encontrado no sistema tálamo-cortical na sequência das oscilações na banda 7-12 Hz durante o movimento rítmico dos bigodes do rato ("*whisker-twitching"*) (Fanselow and Nicolelis, 1999). Durante o modo de disparo em *burst* os neurónios talâmicos estão afinados para detecção de alterações rápidas dos sinais sensoriais e transmissão da informação da sua presença para o córtex (Fanselow and Nicolelis, 1999; Fanselow et al., 2001; Nicolelis and Fanselow, 2002a, b; Wiest and Nicolelis, 2003).

Apesar de nas últimas duas décadas se terem dado passos significativos no conhecimento do papel do eixo tálamo-cortical no processamento da informação sensorial, ainda estão pendentes várias questões ao nível da compreensão da relação

entre a dinâmica das oscilações exibidas e as condições de plasticidade deste circuito durante os quadros de dor crónica.

2.1.1. CICLO DE VIGÍLIA-SONO

A actividade eléctrica talâmica e cortical reflecte os diferentes estados comportamentais inseridos no ciclo de vigília-sono dos vertebrados (ritmo circadiano) (Steriade et al., 1993; Destexhe et al., 1999). Em particular, a transição do estado de vigília para o sono, que é caracterizada por oscilações a nível dos padrões de actividade dos neurónios talâmicos que alternam entre um modo de actividade tónico e um modo de actividade em *burst* (Ribeiro et al., 2010).

Durante o estado de vigília (*awake state* - WK), o eixo tálamo-cortical apresenta oscilações na banda de frequência *theta* e oscilações rápidas de menor amplitude (bandas de frequência *beta* e *gamma*, superiores a 15 Hz) (Steriade et al., 1993; Destexhe et al., 1999). O estado de vigília pode ser subdividido em dois padrões comportamentais distintos (Gervasoni et al., 2004). O primeiro é o estado de exploração activa, durante a qual o animal está envolvido em comportamentos exploratórios (locomoção, identificação de texturas com as vibrissas e olfacção), e é caracterizado por oscilações de baixa-amplitude nos LFPs corticais e elevada potência espectral em *theta* e *gamma*. O segundo é um estado de baixa actividade no qual o animal se apresenta parado mas desperto, ou absolutamente imóvel ou a executar comportamentos estereotipados, como por exemplo movimentos de *grooming*. Neste caso, os comportamentos são caracterizados por oscilações de baixa-amplitude nos LFPs corticais e uma relativa elevada potência espectral em *theta* e também em *gamma,* embora inferior ao padrão de exploração activa. Nos roedores foi também descrito um terceiro padrão durante o estado de vigília que é caracterizado pelo movimento rítmico das vibrissas associado à exploração activa do espaço ("*whisker-twitching"*, WT), e que apresenta oscilações cortico-talâmicas de grande amplitude na gama de frequência entre os 7 e 12 Hz (Nicolelis et al., 1995; Fanselow and Nicolelis, 1999).

Ao contrário do estado de vigília, a entrada no período de sono é marcada por oscilações corticais lentas de baixa amplitude (ondas *delta* 1-4 Hz e "*spindles*" – eventos curtos de oscilação a 7-14 Hz) (Steriade et al., 1993; Achermann and Borbely, 1997; Destexhe et al., 1999), caracterizando um estado denominado por *slow-wave-sleep* (SWS). A nível comportamental durante o estado de SWS os animais permanecem imóveis, com os olhos fechados e exibem movimentos respiratórios lentos e regulares. Os primeiros estudos de sono com registo de EEG associaram o estado SWS a uma redução drástica da actividade cerebral e consequente

desconexão das aferências sensoriais (Davis et al., 1937), isto devido à predominância de oscilações corticais de baixa amplitude que deram precisamente o nome a este estado. Todavia, essa ideia foi rapidamente posta de parte, quando se verificou que as oscilações do estado SWS coexistem com oscilações em frequências mais elevadas, como por exemplo na banda *gamma* (Steriade, 2006a), e que a actividade de neurónios durante o SWS em diversas regiões do cérebro, aumenta após experiências relevantes decorridas durante o período de vigília antecedente (Wilson and McNaughton, 1994; Ribeiro and Nicolelis, 2004). Sabe-se ainda que as oscilações lentas do estado SWS actuam como mecanismos de sincronização da actividade dispersa em diversas áreas cerebrais, em especial no circuito tálamo-cortical (Steriade, 2006a, b). As oscilações do estado SWS variam consoante o nível de profundidade do sono: numa fase inicial é caracterizado pela exibição de "*spindles*" sobrepostas a ondas *delta*, mas numa fase mais avançada as oscilações em *delta* tornam-se mais proeminentes.

Um terceiro estado do ciclo vigília-sono é o estado REM (de *rapid-eye-movement*), que é um estado de sono superficial, caracterizado por movimentos rápidos dos globos oculares e grande actividade de sonhos. No estado REM o córtex e estruturas subcorticais apresentam oscilações *gamma* rápidas similares às observadas no estado de vigília (Vanderwolf, 1969; Steriade et al., 1993), e o hipocampo apresenta oscilações características em *theta* denominadas por ritmo *theta* hipocampal (Vanderwolf, 1969; Buzsaki, 2002).

O estado de SWS é seguido por um estado intermédio de transição (TS) caracterizado por oscilações instáveis entre as bandas *delta*, *theta* e *alpha*. Este estado foi observado no rato (Gottesmann, 1992; Benington et al., 1994) durante as transições entre o estado SWS e o estado REM. Mais recentemente, Mandile e colaboradores utilizando métodos computacionais de alta resolução temporal para a análise de padrões de EEG, identificaram também este tipo de oscilação durante as transições entre o estado SWS e o estado de vigília (Mandile et al., 1996; Mandile et al., 2000; Piscopo et al., 2001), embora apresente neste caso uma duração superior aos episódios observados na transição entre SWS e REM.

A importância das oscilações do eixo cortico-talâmico durante o ciclo circadiano não se restringe à identificação do estado de vigília correspondente. Diversos autores têm proposto que as oscilações cerebrais observadas durante o sono, podem desempenhar um importante papel no fortalecimento de processos de memória. A ideia central é de que, após os períodos de vigília, os estímulos sensoriais são fortalecidos, armazenados e consolidados através das oscilações que ocorrem nos ciclos sucessivos de SWS e REM, durante os quais não há a interferência de novos estímulos sensoriais, permitindo a livre reverberação dos eventos

ocorridos durante o período de vigília (Ribeiro and Nicolelis, 2004; Born, 2010; Born and Wilhelm, 2011).

Um último ponto de interesse para esta dissertação está relacionado com a relação que pode estabelecer entre o ciclo de vigília-sono e a processamento de informação dolorosa. Diversos estudos realizados em humanos (Moldofsky and Scarisbrick, 1976; Lentz et al., 1999; Lautenbacher et al., 2006) e em modelos animais (Carli et al., 1987; Landis et al., 1988; Onen et al., 2001; Kontinen et al., 2003; Mendelson et al., 2003; Monassi et al., 2003; Schutz et al., 2003; Keay et al., 2004; Millecamps et al., 2005) têm abordado essa interacção entre dor e perturbações no ciclo de vigília-sono. Em humanos, dados clínicos referenciam um aumento do nível de sensibilidade à dor em patologias associadas à privação do sono (Moldofsky and Scarisbrick, 1976; Drewes et al., 1998; Lentz et al., 1999; Kundermann et al., 2004a; Kundermann et al., 2004b; Lautenbacher et al., 2006). Por outro lado, modelos animais ilustram o envolvimento da privação do estado REM na diminuição do limiar necessário para a percepção de dor (Hicks and Sawrey, 1978; Onen et al., 2001).

É importante assinalar que em animais a maior parte do conhecimento da relação entre a dor e as perturbações do sono advém de modelos de estimulação aguda. No que diz respeito a modelos de dor de cariz neuropático ainda são escassos os estudos e os que existem com base na análise da actividade cerebral são centrados numa abordagem comportamental e limitados a períodos curtos ou a uma única sessão de registo da actividade cerebral (Andersen and Tufik, 2003; Kontinen et al., 2003; Monassi et al., 2003; Keay et al., 2004). Por outro lado, não existem estudos a descrever quais as alterações na dinâmica tálamo-cortical após a instalação de uma condição de dor neuropática em função do ciclo de vigília-sono, apesar de alguns estudos abordarem as alterações nesse circuito durante a estimulação dolorosa aguda ou imediatamente a seguir à injecção de formol (Wang et al., 2003; Huang et al., 2006). Partindo destes prossupostos, um dos pontos de interesse da presente dissertação está relacionado com a compreensão da relação entre os diferentes regimes de oscilação do circuito tálamo-cortical e o processamento da informação nociceptiva num quadro de dor neuropática.

2.1.2. TRANSIÇÃO DA CONSCIÊNCIA PARA INCONSCIÊNCIA

Um segundo processo em que as oscilações do eixo tálamo-cortical desempenham um papel relevante, é o da transição entre estados de consciência e inconsciência aquando da aplicação de anestésicos centrais. O que ocorre na interacção funcional entre o tálamo e córtex durante a anestesia profunda, e qual destas áreas é primordialmente afectada pelos anestésicos de uso comum, gera ainda bastante

controvérsia (Schneider and Kochs, 2007; Zhou et al., 2011). A maior parte das teorias enuncia que a redução do nível de consciência ocorre por uma redução gradual da quantidade de informação ou por uma diminuição da capacidade de integração sensorial do eixo cortico-talâmico (Tononi, 2004; Alkire et al., 2008; Kim et al., 2012), ou mesmo pela interrupção da transferência de informação no circuito TC (Alkire et al., 2007; Zhou et al., 2011). Este paradigma tem gerado alguma controvérsia nos últimos anos por existirem dois modelos conceptuais para as transições de consciência. Alguns investigadores apontam o córtex como o principal alvo envolvido no processo de transição para o estado de inconsciência (Velly et al., 2007), enquanto outros sugerem que o tálamo é o principal alvo da anestesia geral (Alkire et al., 2007). O tálamo desempenha um papel importante no suporte do nível de consciência a dois níveis (Llinás et al., 1998; Ribary, 2005). Primeiro, na integração da informação sensorial e motora, componente importante do estado de consciência; e em segundo, no controlo da actividade cortical originada na formação reticular. Todavia, qual a importância das oscilações dinâmicas que ocorrem entre os circuitos corticais e talâmicos durante as transições de consciência, e de que forma essas oscilações podem representar padrões sinalizadores dessas transições ainda permanece pouco estudado. Na literatura, alguns estudos demonstraram existir uma redução da conectividade funcional tálamo-cortical durante a perda de consciência (Mhuircheartaigh et al., 2010; Borsook and Becerra, 2011) e em estados vegetativos (Zhou et al., 2011). A maior parte dos modelos indica que essa redução acontece por uma supressão da actividade tálamo-cortical em frequências mais rápidas (Ching et al., 2010; Kreuzer et al., 2010; Hudetz et al., 2011; Silva et al., 2011).

Um dos problemas que existe actualmente é a falta de bons métodos quantitativos para analisar as oscilações em pacientes, e por outro lado a escassez de trabalhos em animais ao nível da optimização de índices para a monitorização da profundidade da anestesia. Os monitores comerciais disponíveis para a análise do nível de anestesia são baseados na análise superficial do sinal EEG espontâneo. Todos eles utilizam eléctrodos na cabeça do paciente, registando maioritariamente a actividade cortical (lobo frontal). O mais popular dos monitores de anestesia é o "*Bispectral Index*" (BIS), e tem vindo a ser utilizado de forma generalizada na prática anestésica como um potencial utensílio para reduzir a incidência de sensibilização durante a anestesia (Myles

et al., 2004). Vários estudos de performance de monitores de anestesia demonstram que o BIS é o mais eficiente na análise das transições entre os estados de consciência e inconsciência (Glass et al., 1997; Struys et al., 2003), enquanto outros demonstraram que não é o mais indicado para a monitorização da administração de anestesia gasosa volátil (Avidan et al., 2008), aumentando desta forma a controvérsia da sua utilização. Novos métodos têm vindo a ser implementados para aumentar a eficiência dos algoritmos utilizados pelos monitores de anestesia. Algumas das melhorias passam pela recolha de sinais mais robustos do que a actividade EEG, que permitam a análise das oscilações que ocorrem em frequências mais elevadas e consequente correcção dos algoritmos dos índices utilizados para monitorizar a profundidade da anestesia (Ching et al., 2010; Silva et al., 2010; Hudetz et al., 2011).

2.1.3. A DISRITMIA TÁLAMO-CORTICAL

São diversas as propostas de modelos conceptuais para explicar a neurofisiologia da dor e dos mecanismos aliados à sua cronicidade (Treede et al., 1999; Peyron et al., 2000; Apkarian et al., 2005). Um destes modelos é o da disritmia tálamo-cortical (DTC) que sugere que a perturbação do equilíbrio nas interacções tálamo-corticais está na origem da cronicidade dolorosa associada à maioria das lesões neuropáticas (Llinás et al., 1998; Llinás et al., 1999). A DTC pode ser sumarizada por uma sequência de eventos (Llinás et al., 1999). A lesão desencadeia uma desaferenciação dos estímulos excitatórios ao nível dos neurónios talâmicos que resulta numa hiperpolarização da sua membrana celular. No estado hiperpolarizado, a desactivação dos canais "T" de cálcio leva os neurónios talâmicos a um padrão de actividade em *burst* que funciona como um amplificador não especifico da actividade nas bandas de frequência *theta* e *gamma* a nível dos módulos tálamo-corticais (Llinás and Jahnsen, 1982; Llinás and Steriade, 2006). Em particular este modelo propõe que a alteração nessas duas bandas de actividade oscilatória funciona como sintoma positivo do síndrome doloroso, e são o suporte fisiológico para a sua manutenção (Walton et al., 2010).

Este modelo é baseado em múltiplos aspectos: por um lado, dados clínicos demonstraram que intervenções cirúrgicas de lesão terapêutica do núcleo central-lateral do tálamo aliviam a dor neurogénica (Jeanmonod et al., 2001); por outro lado, muitos pacientes com dor central neuropática apresentam padrões de actividade em *burst* que

estão conotados com potenciais de cálcio de baixo limiar no tálamo (Lenz et al., 1989; Jeanmonod et al., 1993; Jeanmonod et al., 1996); finalmente, em registos de EEG/EMG de pacientes com dor central neuropática, foi observado um aumento da actividade na banda de frequência *theta* e *gamma*, bem como um desvio do pico da banda *theta* para frequências mais baixas que o habitual (Llinás et al., 1999; Sarnthein et al., 2006; Stern et al., 2006).

Um dos aspectos mais interessantes do modelo da DTC é a proposta de que a dor central se origina por um "edge effect" que resulta da interacção entre neurónios tálamo-corticais com diferentes níveis tónicos de actividade nas bandas *theta* e *gamma* (Llinás et al., 2005). Habitualmente, um foco cortical de actividade *gamma* impede a propagação dessa mesma actividade para outras populações corticais adjacentes, por um processo de inibição lateral mediado por interneurónios GABAérgicos. O modelo propõe que o aumento de actividade *theta* talâmica de baixa frequência vai induzir uma diminuição da inibição lateral cortical, levando a uma propagação de picos de actividade em *gamma* que estão associadas ao processamento doloroso (Chen and Rappelsberger, 1994). Este aumento da actividade *gamma* cortical em pacientes com dor crónica foi já descrito em registos de MEG (Llinás et al., 1999) e em pacientes com dor neurogénica (Sarnthein et al., 2006).

2.2. O CIRCUITO FRONTO-HIPOCAMPAL

A formação hipocampal recebe a maior parte do fluxo de informação neocortical directamente por uma via cortico-hipocampal e indirectamente por uma via septo-hipocampal (Vertes, 2006). A via directa cortico-hipocampal faz chegar ao hipocampo uma grande quantidade de informação sensorial vinda de áreas associativas do neocórtex e em menor quantidade vinda de áreas sensoriais primárias (Liu and Chen, 2009). Este circuito extende-se desde o córtex SI e SII, até às estruturas insulares e corticais, e depois até à amigdala, córtex entorrinal e hipocampo, e converge finalmente nas mesmas estruturas que são directamente activadas pelas vias do tracto espinho-talâmico (Friedman et al., 1986; Liu and Chen, 2009). Ao nível funcional este circuito é um dos pontos de convergência entre a via lateral e medial de processamento da dor e

permite a integração de informação relativa às características sensoriais da dor com informação de processos de aprendizagem e memória (Price, 2000; Klossika et al., 2006).

A via indirecta septo-hipocampal representa uma via alternativa de chegada da informação nociceptiva à formação hipocampal, e é responsável pela maior parte da informação de natureza colinérgica (Khanna and Zheng, 1999; Zheng and Khanna, 1999). Esta via apresenta diversas conecções funcionais com outras áreas do cérebro, entre as quais o hipotálamo, o *locus coeruleus*, substância cinzenta periaqueductal (PAG), os núcleos da rafe e também o córtex cerebral (Vertes, 2006).

A primeira grande evidência do papel do hipocampo na integração da informação nociceptiva surgiu com os estudos de Khanna e colaboradores, que provaram existir uma activação de neurónios do hipocampo após a indução do modelo animal de dor inflamatória por injecção periférica de formol (Khanna, 1997; Zheng and Khanna, 1999). Por outro lado, a hipocampoctomia parcial ou total em primatas e humanos provou resultar em alterações da percepção da dor (Gol et al., 1963; Gol and Faibish, 1967), enquanto no rato lesões eléctricas do hipocampo medial e dorsal, reduziram a sua capacidade de evitar a aplicação de estímulos nociceptivos (Teitelbaum and Milner, 1963; Blanchard and Fial, 1968). Algumas abordagens farmacológicas demonstraram ainda uma redução dos comportamentos nociceptivos após a aplicação no hipocampo de lidocaína ou de um antagonista dos receptores de NMDA (McKenna and Melzack, 1992, 2001), serotonina (Soleimannejad et al., 2006), $GABA_A$ (Favaroni Mendes and Menescal-de-Oliveira, 2008), óxido nitrico (Echeverry et al., 2004), e após a modulação noradrenérgica da via septo-hipocampal (Aloisi, 1997; Aloisi et al., 1997).

O córtex pré-frontal (PFC) está associado a diversas funções cognitivas e emocionais incluindo a atenção, a decisão, a recompensa e a "working memory" (Gusnard et al., 2001; Phelps et al., 2004). Em humanos, diversos estudos demonstraram que as diversas subregiões do PFC desempenham um papel importante na dor aguda; o córtex prefrontal medial (mPFC) está envolvido na sinalização do aspecto desagradável da dor (Lorenz et al., 2002); o córtex anterior cingulado (ACC) medeia a componente afectiva das respostas à dor (Rainville et al., 1997) e o efeito placebo (Wager et al., 2004); e que as respostas de anticipação à dor estão positivamente correlacionadas com a actividade do ACC e do mPFC (Porro et al., 2002). Pacientes com o sindrome doloroso complexo regional do tipo I (CRPS, *complex regional pain syndrome*) e dor crónica

manifestam a existência de défices na performance de tarefas emocionais de decisão com risco associado como o teste *Iowa Gambling* (Apkarian et al., 2004b), o qual implica o envolvimento do mPFC. Neste caso, os pacientes com CRPS-1 apresentam uma performance muito próxima da obtida por pacientes com lesões no PFC. Por outro lado, em pacientes com dor crónica a extensão da activação do mPFC durante a dor espontânea, componente emocional e disfunções cognitivas estão também correlacionadas com a intensidade e a duração da dor (Baliki et al., 2006). Estudos de ressonância magnética demonstraram ainda que a dor crónica está associada a uma redução da densidade de matéria cinzenta em várias regiões do PFC (Apkarian et al., 2004a; Kuchinad et al., 2007), e que pacientes com CRPS-1 apresentam uma reorganização do quadro de actividade dessa região (Baliki et al., 2006; Schweinhardt et al., 2008).

Em animais, alguns estudos têm fornecido também evidências do envolvimento das áreas corticais pré-frontais na nocicepção aguda e inflamatória. Registos electrofisiológicos no rato (Fuchs et al., 1996; Yamamura et al., 1996; Zhang et al., 2004) e no coelho (Sikes and Vogt, 1992) demonstraram que existem neurónios nociceptivos na região ventral do mPFC, e que esta região é activada por estimulação nociceptiva (Traub et al., 1996; Albutaihi et al., 2004). Por outro lado, a modulação da neurotransmissão desta região provou contribuir para uma redução da sensibilidade táctil em animais com lesão periférica do nervo ciático (Millecamps et al., 2007; Centeno et al., 2009). Mais recentemente foi também identificada a existência de uma reorganização morfológica e funcional de base celular no mPFC durante condições de dor neuropática (Metz et al., 2009), e que estas alterações poderão estar associadas à manifestação de défices na performance cognitiva.

Apesar de já serem conhecidos alguns aspectos referentes à acção da dor na formação hipocampal e nas regiões corticais pré-frontais, ainda é desconhecida sua acção em termos dos circuitos de interligação entre essas regiões, aos quais se sabe, desempenham um papel crucial ao nível dos processos mnemónicos. Um último ponto de interesse para esta dissertação está relacionado com a relação que a dor pode ter na alteração da eficiência da conectividade do circuito fronto-hipocampal, a qual poderá explicar em parte a ocorrência de défices na componente cognitiva exibida por pacientes com dor crónica.

2.2.1. A DOR E A COMPONENTE COGNITIVA

A dor e a atenção interagem reciprocamente (Eccleston, 1995; Dick et al., 2002). É usualmente assumido que a distracção reduz a sensação de dor e é igualmente assumido que a dor altera os níveis de atenção reduzindo a performance na execução de tarefas cognitivas complexas (Ford et al., 2008; Buhle and Wager, 2010; Moriarty et al., 2011). Juntos, estes pressupostos sugerem um equilíbrio entre o processamento de informação dolorosa e o desempenho cognitivo na execução de outras tarefas, podendo-se inferir que se existir um limite aos recursos cognitivos exigidos para os dois processos, o desempenho cognitivo esteja condicionado nos pacientes com dor crónica ou mesmo em episódios transitórios de dor (Norman, 1967; Oosterman et al., 2009).

Vários estudos na literatura analisam os mecanismos de domínio cognitivo que podem ser influenciados pela dor, entre os quais se destacam estudos em modelos animais (Dubner et al., 1981; Hayes et al., 1981; Hoffman et al., 1981; Casey and Morrow, 1983a, b; Boyette-Davis et al., 2008; Boyette-Davis and Fuchs, 2009), pacientes com dor crónica (Park et al., 2001; Dick et al., 2002; Glass et al., 2005; Dick and Rashiq, 2007; Seminowicz and Davis, 2007; Dick et al., 2008; Sarnthein and Jeanmonod, 2008) ou em voluntários saudáveis expostos a estímulos dolorosos (Bingel et al., 2002; Brooks et al., 2002; Bingel et al., 2004; Hoffman et al., 2004; Zambreanu et al., 2005; Ploner et al., 2011). Em humanos, é no entanto importante referir a existência de algumas discrepâncias entre os dados clínicos, as quais residem provavelmente no facto da utilização de diferentes metodologias, variações nos grupos de pacientes a nível dos sintomas e diferentes níveis de dor (Buhle and Wager, 2010; Moriarty et al., 2011). No caso dos estudos em voluntários saudáveis expostos a estimulação dolorosa durante a execução de tarefas também foram encontradas algumas discrepâncias: enquanto em alguns estudos os participantes evidenciam menor nível de dor à medida que as tarefas propostas são mais complexas (Dowman, 2004; Hoffman et al., 2004; Coen et al., 2008), noutros não apresentam qualquer alteração (Pud and Sapir, 2006; Seminowicz and Davis, 2007). Todavia, apenas um número restrito de estudos reporta um declínio das capacidades cognitivas em função da dor (Crombez et al., 2002; Houlihan et al., 2004;

Bingel et al., 2007), enquanto a maior parte não revela qualquer alteração (Wiech et al., 2005; Pud and Sapir, 2006; Seminowicz and Davis, 2007).

Por outro lado, estudos em modelos animais demonstram também existir um efeito negativo causado pela dor na performance cognitiva de roedores, quer em condições de dor inflamatória, quer em condições de dor neuropática (revisão em, Moriarty et al., 2011). A nível de modelos inflamatórios de dor foram encontrados défices na atenção (Cain et al., 1997; Millecamps et al., 2004; Boyette-Davis et al., 2008; Pais-Vieira et al., 2009a), nos mecanismos de decisão emocional (Pais-Vieira et al., 2009b; Ji et al., 2010), na aprendizagem espacial (Cain, 1997; Lindner et al., 1999) e na memória de referência espacial (Cain, 1997; Lindner et al., 1999; Millecamps et al., 2004). Alguns dos défices observados nos modelos inflamatórios de dor foram também observados em condições de dor neuropática ao nível da aprendizagem e memória espacial (Leite-Almeida et al., 2009; Hu et al., 2010). Todavia, a dor neuropática está também associada a alterações nos aspectos de flexibilidade cognitiva (Leite-Almeida et al., 2009) e aprendizagem de condições adversas (Suzuki et al., 2007).

Os dados obtidos nos estudos em humanos e modelos animais, em conjunto explicam o modelo conceptual bidireccional da relação entre a dor e a performance, nomeadamente a nível da compreensão dos processos partilhados pela dor e performance cognitiva. Todavia, a forma como os circuitos envolvidos em funções cognitivas estão afectados pela dor e como a dor é processada por esses circuitos permanece ainda pouco conhecida.

2.2.2. INTEGRAÇÃO DA INFORMAÇÃO ESPACIAL

Os neurónios piramidais das áreas CA1 e CA3 do hipocampo apresentam a capacidade de codificar a localização espacial do animal, e são por essa particularidade denominados por "*place cells*", pois aumentam a sua frequência de disparo quando o animal se encontra numa posição particular do seu meio ambiente (o seu campo espacial ou "*spatial field*") (O' Keefe and Dostrovsky, 1971; O' Keefe and Nadel, 1978) (Fox and Ranck, 1981). O "*spatial field*" é habitualmente estável ao longo de várias visitas ao mesmo ambiente, mesmo no caso do animal ser retirado do ambiente de teste por longos períodos (Muller and Kubie, 1987; Thompson and Best, 1990). Alguns estudos demonstraram que alterações nas características espaciais ou conteúdo motivacional do

meio ambiente de teste podem afectar a estabilidade dos "*spatial fields*" (Muller and Kubie, 1987; Markus et al., 1995; Kobayashi et al., 1997; Wood et al., 2000; Moita et al., 2004). Essa estabilidade pode ser ainda alterada por manipulações farmacológicas do hipocampo (Kentros et al., 1998; Rotenberg et al., 2000; Dragoi et al., 2003) ou por lesão directa do hipocampo ou de outras áreas interconectadas (McNaughton et al., 1989; Mizumori et al., 1994; Leutgeb and Mizumori, 1999; Muir and Bilkey, 2001; Liu et al., 2003).

Para além da informação espacial, o hipocampo está também envolvido na regulação de diversos aspectos comportamentais associados à adaptação a situações adversas, incluindo a dor (Khanna and Sinclair, 1992; Khanna et al., 2004; Soleimannejad et al., 2006). Os neurónios do hipocampo respondem à estimulação dolorosa (Delgado, 1955; Halgren et al., 1978; Khanna, 1997; Wei et al., 2000; Soleimannejad et al., 2006; Tai et al., 2006; Zheng and Khanna, 2008) e estudos de imagiologia em humanos comprovaram a activação da formação hipocampal durante estimulação dolorosa aguda (Ploghaus et al., 2000; Ploghaus et al., 2001; Bingel et al., 2002). Por outro lado, a inactivação da transmissão sináptica do hipocampo revelou ter atenuado o comportamento nociceptivo em ratos sujeitos ao modelo do formol (McKenna and Melzack, 1992; Khanna, 1997; McKenna and Melzack, 2001). Em termos do funcionamento do hipocampo, alguns estudos demonstraram que a dor crónica altera a expressão de c-Fos (Ceccarelli et al., 2003; Carter et al., 2011), perturba os mecanismos de LTP "*long-term-potentiation*" (Kodama et al., 2007; Zhao et al., 2009), reduz o nível de BDNF (Duric and McCarson, 2005; Hu et al., 2010) e causa diminuições na volumetria do hipocampo (Lutz et al., 2008; Younger et al., 2010). Contudo, ainda são desconhecidos os efeitos da dor em funções cruciais do hipocampo como na integração de informação espacial e na geração dos mapas espaciais.

2.2.3. WORKING MEMORY DE REFERÊNCIA ESPACIAL

A memória de trabalho ou "working memory" é geralmente definida como um mecanismo central relacionado com a retenção temporária de informação em curtos intervalos de tempo (Goldman-Rakic, 1995; Baddeley, 1996; Fuster, 1997; Dudchenko, 2004). Esta capacidade é crucial para a formação de associações entre estímulos, que é antecedente e necessária a todas as funções cognitivas. A memória de trabalho pode

estar associada a estímulos sensoriais simples, a objectos ou associada à localização espacial do sujeito (Olton and Samuelson, 1976; Deadwyler et al., 1996; Delatour and Gisquet-Verrier, 1996; Floresco et al., 1997).

Em roedores, as tarefas de alternação são utilizadas para investigar a relação entre a actividade do córtex pré-frontal e a memória de referência espacial, utilizando labirintos em forma de "T", labirintos radiais e labirintos em figura de "8", (Floresco et al., 1997; Murphy and Segal, 1997; Zahrt et al., 1997; Baeg et al., 2003; Schoenbaum et al., 2003; Phillips et al., 2004). Para além do córtex pré-frontal, o hipocampo também está envolvido nas tarefas de memória de trabalho, em particular em tarefas que envolvem intervalos longos de tempo de retenção da memória adquirida (Lee and Kesner, 2003). Lesões nestas duas regiões cerebrais permitiram comprovar, em primeiro lugar, que a formação hipocampal desempenha um papel importante na fase inicial da aprendizagem de tarefas comportamentais por roedores, não afectando as fases finais do processo de aprendizagem (Anagnostaras et al., 1999; Eichenbaum, 2000; Maviel et al., 2004; Gaskin et al., 2009). O inverso acontece quando se lesiona o córtex pré-frontal medial (mPFC), havendo lugar a um défice na fase final da curva de aprendizagem e não na fase inicial (Shaw and Aggleton, 1993; Delatour and Gisquet-Verrier, 1996; Floresco et al., 1997; Kyd and Bilkey, 2003; Takehara et al., 2003).

Anatomicamente, as duas regiões partilham interconexões funcionais, directamente através da conexão da via excitatória mono-sináptica na parte ventral da região CA1 do hipocampo e parte ventral do *subiculum* (Ferino et al., 1987; Laroche et al., 2000; Thierry et al., 2000), e indirectamente através do tálamo mediodorsal (MD) até à parte dorsal da região CA1 do hipocampo (Vertes, 2006). Esta última está especificamente envolvida no processamento da informação espacial (Moser et al., 1993) e a inibição desse circuito provou estar associado ao desenvolvimento de défices de memória espacial (Floresco et al., 1997; Wang and Cai, 2006). Um ponto-chave neste circuito é o tálamo MD, uma vez que a sua lesão demonstrou estar associada ao desenvolvimento de deficies de memoria espacial (Isseroff et al., 1982) e amnésia (Mitchell and Dalrymple-Alford, 2005; Mitchell et al., 2008). O tálamo MD partilha projecções até ao córtex cingulado anterior (ACC) (Wang and Shyu, 2004; Chai et al., 2010), o qual está envolvido na integração dos aspectos afecto-motivacionais da dor (Rainville et al., 1997; Treede et al., 1999; Wang et al., 2003; Shyu et al., 2010).

As interacções mPFC-hipocampo decorrentes dos processos de memória de trabalho ocorrem por um aumento da coerência na banda de frequência *theta* (Jones and Wilson, 2005b, a; Siapas et al., 2005), na qual os neurónios do mPFC alternam entre padrões de disparo em fase e não fase dependendo do contexto comportamental (Hyman et al., 2005). Essas interacções são mais evidentes no período que precede a tomada de uma decisão e diminuem quando são tomadas decisões erradas (Jones and Wilson, 2005b, a). Este tipo de padrões de actividade representa uma forte evidência para a integração funcional entre o mPFC e o hipocampo.

Em humanos também são observados défices de memória de trabalho em diversos quadros clínicos, como em lesões traumáticas do cérebro (McDowell et al., 1997), síndrome de Down (Vallar and Papagno, 1993), esquizofrenia (Green, 2006), autismo (Frank et al., 1996) e dor crónica (Ling et al., 2007; Luerding et al., 2008).

Estas observações foram comprovadas por estudos de imagiologia que demonstraram a sua activação em processos de memória e aprendizagem durante a aplicação aguda de estímulação dolorosa (Peyron et al., 1998; Ploghaus et al., 2000; Ducreux et al., 2006; Schweinhardt et al., 2006). Recentemente, estudos com modelos animais de dor neuropatica demonstraram que a memória espacial é afectada em modelos de dor crónica (Leite-Almeida et al., 2009; Hu et al., 2010). Todavia, a forma como a condição de dor afecta o funcionamento do circuito mPFC-hipocampal ainda não está totalmente esclarecida. É conhecido o envolvimento da região mPFC em processos de modulação da dor (Seifert et al., 2009; Devoize et al., 2011), e que reorganizações morfologicas e funcionais da população de neurónios da região mPFC estão na base do aparecimento de defices cognitivos durante uma condição de dor neuropática (Metz et al., 2009). A nível da hipocampo foi recentemente reportado um incremento da produção TNF-α até nível patológico após a lesão periférica do nervo ciático. Estes dados foram conotados com o desenvolvimento de défices de memória de trabalho devido a uma inibição do LTP hippocampal (Ren et al., 2011).

Apesar de todo o conhecimento obtido nos últimos anos, ainda permanece pouco claro qual o efeito da dor no circuito fronto-hipocampal ao nível da partilha, manutenção, e processamento de informação que são aspectos cruciais para os processos mnemónicos.

3. OBJECTIVOS GERAIS

As interacções oscilativas entre os diferentes circuitos do cérebro reflectem um estado funcional global do sistema e são utilizadas pelo cérebro como um mecanismo de alerta para perturbações do seu normal funcionamento, sendo a dor crónica um dos factores que contribui para essa perturbação. É usualmente assumido que a dor quando evoluiu para estados de persistência ou crónicos, não causa apenas perturbações e disfunções sensoriais, mas está também envolvida em diversas alterações funcionais do cérebro, entre os quais se destacam os processos cognitivos.

Os objectivos a que esta dissertação se propõe, referem-se à compreensão da relação entre as oscilações sincrónicas dos vários níveis de processamento da informação nociceptiva e de que forma elas são dependentes das condições de plasticidade dos circuitos do cérebro responsáveis pelas dimensões sensori-discriminativa, afecto-motivacional e cognitiva da percepção da dor.

Na primeira parte procedi à caracterização da neurofisiologia das oscilações de informação tálamo-corticais. Esta análise foi efectuada a dois níveis. Primeiro, através da análise dos vários padrões oscilatórios do ciclo de vigília-sono após a instalação de uma condição de dor crónica de cariz neuropática. Em segundo, nas transições dos estados de consciência para inconsciência, nos quais existe uma redução gradual da quantidade de informação sensorial integrada pelo circuito.

Na segunda parte procedi à caracterização dos mecanismos de plasticidade no processamento da informação nociceptiva durante a competição com funções associativas e cognitivas. Esta análise foi efectuada a dois níveis do circuito fronto-hipocampal. Primeiro, na integração e processamento da informação associada à geração dos mapas espaciais pelos neurónios piramidais da região CA1 dorsal do hipocampo. Em segundo, ao nível do circuito fronto-hipocampal durante a codificação e retenção da memória de referência espacial, aspecto crucial para a performance de tarefas cognitivas.

4. REFERÊNCIAS BIBLIOGRÁFICAS

Achermann P, Borbely AA (1997) Low-frequency (<1 Hz) oscillations in the human sleep electroencephalogram. Neuroscience 81:213-222.

Albutaihi IA, DeJongste MJ, Ter Horst GJ (2004) An integrated study of heart pain and behavior in freely moving rats (using fos as a marker for neuronal activation). Neurosignals 13:207-226.

Alitto HJ, Usrey WM (2003) Corticothalamic feedback and sensory processing. Curr Opin Neurobiol 13:440-445.

Alkire MT, Hudetz AG, Tononi G (2008) Consciousness and anesthesia. Science 322:876-880.

Alkire MT, McReynolds JR, Hahn EL, Trivedi AN (2007) Thalamic microinjection of nicotine reverses sevoflurane-induced loss of righting reflex in the rat. Anesthesiology 107:264-272.

Aloisi AM (1997) Sex differences in pain-induced effects on the septo-hippocampal system. Brain Res Brain Res Rev 25:397-406.

Aloisi AM, Casamenti F, Scali C, Pepeu G, Carli G (1997) Effects of novelty, pain and stress on hippocampal extracellular acetylcholine levels in male rats. Brain Res 748:219-226.

Anagnostaras SG, Maren S, Fanselow MS (1999) Temporally graded retrograde amnesia of contextual fear after hippocampal damage in rats: within-subjects examination. J Neurosci 19:1106-1114.

Andersen ML, Tufik S (2003) Sleep patterns over 21-day period in rats with chronic constriction of sciatic nerve. Brain Research 984:84-92.

Apkarian AV (2008) Pain perception in relation to emotional learning. Curr Opin Neurobiol 18:464-468.

Apkarian AV, Baliki MN, Geha PY (2009) Towards a theory of chronic pain. Prog Neurobiol 87:81-97.

Apkarian AV, Bushnell MC, Treede RD, Zubieta JK (2005) Human brain mechanisms of pain perception and regulation in health and disease. Eur J Pain 9:463-484.

Apkarian AV, Sosa Y, Sonty S, Levy RM, Harden RN, Parrish TB, Gitelman DR (2004a) Chronic back pain is associated with decreased prefrontal and thalamic gray matter density. J Neurosci 24:10410-10415.

Apkarian AV, Sosa Y, Krauss BR, Thomas PS, Fredrickson BE, Levy RE, Harden RN, Chialvo DR (2004b) Chronic pain patients are impaired on an emotional decision-making task. Pain 108:129-136.

Avidan MS, Zhang L, Burnside BA, Finkel KJ, Searleman AC, Selvidge JA, Saager L, Turner MS, Rao S, Bottros M, Hantler C, Jacobsohn E, Evers AS (2008) Anesthesia awareness and the bispectral index. N Engl J Med 358:1097-1108.

Babiloni C, Babiloni F, Carducci F, Cincotti F, Rosciarelli F, Arendt-Nielsen L, Chen AC, Rossini PM (2002) Human brain oscillatory activity phase-locked to painful electrical stimulations: a multi-channel EEG study. Hum Brain Mapp 15:112-123.

Babiloni C, Brancucci A, Babiloni F, Capotosto P, Carducci F, Cincotti F, Arendt-Nielsen L, Chen AC, Rossini PM (2003) Anticipatory cortical responses during the expectancy of a predictable painful stimulation. A high-resolution electroencephalography study. Eur J Neurosci 18:1692-1700.

Backonja M, Howland EW, Wang J, Smith J, Salinsky M, Cleeland CS (1991) Tonic changes in alpha power during immersion of the hand in cold water. Electroencephalogr Clin Neurophysiol 79:192-203.

Baddeley A (1996) The fractionation of working memory. Proc Natl Acad Sci USA 93:13468-13472.

Baeg EH, Kim YB, Huh K, Mook-Jung I, Kim HT, Jung MW (2003) Dynamics of population code for working memory in the prefrontal cortex. Neuron 40:177-188.

Baliki MN, Chialvo DR, Geha PY, Levy RM, Harden RN, Parrish TB, Apkarian AV (2006) Chronic pain and the emotional brain: specific brain activity associated with spontaneous fluctuations of intensity of chronic back pain. J Neurosci 26:12165-12173.

Bantick SJ, Wise RG, Ploghaus A, Clare S, Smith SM, Tracey I (2002) Imaging how attention modulates pain in humans using functional MRI. Brain 125:310-319.

Benington JH, Kodali SK, Heller HC (1994) Scoring Transitions to Rem-Sleep in Rats Based on the Eeg Phenomena of Pre-Rem Sleep - An Improved Analysis of Sleep Structure. Sleep 17:28-36.

Besson JM (1999) The Neurobiology of pain. The Lancet 353:1610-1615.

Bingel U, Glascher J, Weiller C, Buchel C (2004) Somatotopic representation of nociceptive information in the putamen: an event-related fMRI study. Cereb Cortex 14:1340-1345.

Bingel U, Rose M, Gläscher J, Büchel C (2007) fMRI reveals how pain modulates visual object processing in the ventral visual stream. Neuron 55:157-167.

Bingel U, Quante M, Knab R, Bromm B, Weiller C, Buchel C (2002) Subcortical structures involved in pain processing: evidence from single-trial fMR1. Pain 99:313-321.

Blanchard RJ, Fial RA (1968) Effects of limbic lesions on passive avoidance and reactivity to shock. J Comp Physiol Psychol 66:606-612.
Born J (2010) Slow-wave sleep and the consolidation of long-term memory. World J Biol Psychiatry 11 Suppl 1:16-21.
Born J, Wilhelm I (2011) System consolidation of memory during sleep. Psychol Res. 76(2):192-203.
Borsook D, Becerra L (2011) CNS animal fMRI in pain and analgesia. Neurosci Biobehav Rev 35:1125-1143.
Bourassa J, Deschênes M (1995) Corticothalamic projections from the primary visual cortex in rats: a single fiber study using biocytin as an anterograde tracer. Neuroscience 66:253-263.
Bourassa J, Pinault D, Deschênes M (1995) Corticothalamic projections from the cortical barrel field to the somatosensory thalamus in rats: a single-fibre study using biocytin as an anterograde tracer. Eur J Neurosci 7:19-30.
Boyette-Davis JA, Fuchs PN (2009) Differential effects of paclitaxel treatment on cognitive functioning and mechanical sensitivity. Neurosci Lett 453:170-174.
Boyette-Davis JA, Thompson CD, Fuchs PN (2008) Alterations in attentional mechanisms in response to acute inflammatory pain and morphine administration. Neuroscience 151:558-563.
Brooks JC, Nurmikko TJ, Bimson WE, Singh KD, Roberts N (2002) fMRI of thermal pain: effects of stimulus laterality and attention. Neuroimage 15:293-301.
Brosch M, Budinger E, Scheich H (2002) Stimulus-related gamma oscillations in primate auditory cortex. J Neurophysiol 87:2715-2725.
Buhle J, Wager TD (2010) Performance-dependent inhibition of pain by an executive working memory task. Pain 149:19-26.
Buzsaki G (2002) Theta oscillations in the hippocampus. Neuron 33:325-340.
Cain CK, Francis JM, Plone MA, Emerich DF, Lindner MD (1997) Pain-related disability and effects of chronic morphine in the adjuvant-induced arthritis model of chronic pain. Physiol Behav 62:199-205.
Cain DP (1997) Prior non-spatial pretraining eliminates sensorimotor disturbances and impairments in water maze learning caused by diazepam. Psychopharmacology (Berl) 130:313-319.
Canolty RT, Edwards E, Dalal SS, Soltani M, Nagarajan SS, Kirsch HE, Berger MS, Barbaro NM, Knight RT (2006) High gamma power is phase-locked to theta oscillations in human neocortex. Science 313:1626-1628.
Carli G, Montesano A, Rapezzi S, Paluffi G (1987) Differential-Effects of Persistent Nociceptive Stimulation on Sleep Stages. Behav Brain Res 26:89-98.
Carter JL, Lubahn C, Lorton D, Osredkar T, Der TC, Schaller J, Evelsizer S, Flowers S, Ruff N, Reese B, Bellinger DL (2011) Adjuvant-induced arthritis induces c-Fos chronically in neurons in the hippocampus. J Neuroimmunol 230:85-94.
Casey KL, Morrow TJ (1983a) Nocifensive responses to cutaneous thermal stimuli in the cat: stimulus-response profiles, latencies, and afferent activity. J Neurophysiol 50:1497-1515.
Casey KL, Morrow TJ (1983b) Ventral posterior thalamic neurons differentially responsive to noxious stimulation of the awake monkey. Science 221:675-677.
Casey KL, Minoshima S, Morrow TJ, Koeppe RA (1996) Comparison of human cerebral activation patterns during cutaneous warmth, heat pain, and deep cold pain. J Neurophysiol 76:571-581.
Castro-Alamancos M (2004) Dynamics of sensory thalamocortical synaptic networks during information processing states. Prog Neurobiol 74:213-247.
Ceccarelli I, Scaramuzzino A, Massafra C, Aloisi AM (2003) The behavioral and neuronal effects induced by repetitive nociceptive stimulation are affected by gonadal hormones in male rats. Pain 104:35-47.
Centeno MV, Mutso A, Millecamps M, Apkarian AV (2009) Prefrontal cortex and spinal cord mediated anti-neuropathy and analgesia induced by sarcosine, a glycine-T1 transporter inhibitor. Pain 145:176-183.
Chai SC, Kung JC, Shyu BC (2010) Roles of the anterior cingulate cortex and medial thalamus in short-term and long-term aversive information processing. Mol Pain 6:42.
Chang PF, Arendt-Nielsen L, Chen AC (2002) Differential cerebral responses to aversive auditory arousal versus muscle pain: specific EEG patterns are associated with human pain processing. Exp Brain Res 147:387-393.
Chen AC, Rappelsberger P (1994) Brain and human pain: topographic EEG amplitude and coherence mapping. Brain Topogr 7:129-140.
Ching S, Cimenser A, Purdon PL, Brown EN, Kopell NJ (2010) Thalamocortical model for a propofol-induced alpha-rhythm associated with loss of consciousness. Proc Natl Acad Sci U S A 107:22665-22670.

Chrobak JJ, Lörincz A, Buzsáki G (2000) Physiological patterns in the hippocampo-entorhinal cortex system. Hippocampus 10:457-465.

Coen SJ, Aziz Q, Yágüez L, Brammer M, Williams SC, Gregory LJ (2008) Effects of attention on visceral stimulus intensity encoding in the male human brain. Gastroenterology 135:2065-2074, 2074.e2061.

Contreras D, Destexhe A, Sejnowski TJ, Steriade M (1996) Control of spatiotemporal coherence of a thalamic oscillation by corticothalamic feedback. Science 274:771-774.

Corbetta M, Shulman GL (2002) Control of goal-directed and stimulus-driven attention in the brain. Nat Rev Neurosci 3:201-215.

Crombez G, Eccleston C, Van den Broeck A, Van Houdenhove B, Goubert L (2002) The effects of catastrophic thinking about pain on attentional interference by pain: no mediation of negative affectivity in healthy volunteers and in patients with low back pain. Pain Res Manag 7:31-39.

Davis H, Davis PA, Loomis AL, Harvey EN, Hobart G (1937) Changes in human brain potentials during the onset of sleep. Science 86:448-450.

Deadwyler SA, Bunn T, Hampson RE (1996) Hippocampal ensemble activity during spatial delayed-nonmatch-to- sample performance in rats. J Neurosci 16:354-372.

DeCoteau WE, Thorn C, Gibson DJ, Courtemanche R, Mitra P, Kubota Y, Graybiel AM (2007) Learning-related coordination of striatal and hippocampal theta rhythms during acquisition of a procedural maze task. Proc Natl Acad Sci U S A 104(13):5644-5649.

Delatour B, Gisquet-Verrier P (1996) Prelimbic cortex specific lesions disrupt delayed-variable response tasks in the rat. Behav Neurosci 110:1282-1298.

Delgado JMR (1955) Cerebral Structures Involved in Transmission and Elaboration of Noxious Stimulation. J Neurophysiol 18:261-275.

Destexhe A, Contreras D, Steriade M (1999) Spatiotemporal analysis of local field potentials and unit discharges in cat cerebral cortex during natural wake and sleep states. Journal of Neuroscience 19:4595-4608.

Devoize L, Alvarez P, Monconduit L, Dallel R (2011) Representation of dynamic mechanical allodynia in the ventral medial prefrontal cortex of trigeminal neuropathic rats. Eur J Pain 15(7):676-682.

Dick B, Eccleston C, Crombez G (2002) Attentional functioning in fibromyalgia, rheumatoid arthritis, and musculoskeletal pain patients. Arthritis Rheum 47:639-644.

Dick BD, Rashiq S (2007) Disruption of attention and working memory traces in individuals with chronic pain. Anesth Analg 104:1223-1229.

Dick BD, Verrier MJ, Harker KT, Rashiq S (2008) Disruption of cognitive function in Fibromyalgia Syndrome. Pain 139:610-616.

Dowman R (2004) Distraction produces an increase in pain-evoked anterior cingulate activity. Psychophysiology 41:613-624.

Dragoi G, Harris KD, Buzsaki G (2003) Place representation within hippocampal networks is modified by long-term potentiation. Neuron 39:843-853.

Drewes AM, Svendsen L, Taagholt SJ, Bjerregard K, Nielsen KD, Hansen B (1998) Sleep in rheumatoid arthritis: a comparison with healthy subjects and studies of sleep/wake interactions. BrJ Rheumatol 37:71-81.

Driver JE, Racca C, Cunningham MO, Towers SK, Davies CH, Whittington MA, LeBeau FE (2007) Impairment of hippocampal gamma-frequency oscillations in vitro in mice overexpressing human amyloid precursor protein (APP). Eur J Neurosci 26:1280-1288.

Dubner R, Hoffman DS, Hayes RL (1981) Neuronal activity in medullary dorsal horn of awake monkeys trained in a thermal discrimination task. III. Task-related responses and their functional role. J Neurophysiol 46:444-464.

Ducreux D, Attal N, Parker F, Bouhassira D (2006) Mechanisms of central neuropathic pain: a combined psychophysical and fMRI study in syringomyelia. Brain 129:963-976.

Dudchenko PA (2004) An overview of the tasks used to test working memory in rodents. NeurosciBiobehavRev 28:699-709.

Duric V, McCarson KE (2005) Hippocampal neurokinin-1 receptor and brain-derived neurotrophic factor gene expression is decreased in rat models of pain and stress. Neuroscience 133:999-1006.

Eccleston C (1995) Chronic pain and distraction: an experimental investigation into the role of sustained and shifting attention in the processing of chronic persistent pain. BehavResTher 33:391-405.

Echeverry MB, Guimarães FS, Del Bel EA (2004) Acute and delayed restraint stress-induced changes in nitric oxide producing neurons in limbic regions. Neuroscience 125:981-993.

Eichenbaum H (2000) A cortical-hippocampal system for declarative memory. Nat Rev Neurosci 1:41-50.
Fanselow EE, Nicolelis MAL (1999) Behavioral modulation of tactile responses in the rat somatosensory system. J Neurosci 19:7603-7616.
Fanselow EE, Sameshima K, Baccala LA, Nicolelis MA (2001) Thalamic bursting in rats during different awake behavioral states. Proc Natl Acad Sci U S A 98:15330-15335.
Favaroni Mendes LA, Menescal-de-Oliveira L (2008) Role of cholinergic, opioidergic and GABAergic neurotransmission of the dorsal hippocampus in the modulation of nociception in guinea pigs. Life Sci 83:644-650.
Ferino F, Thierry AM, Glowinski J (1987) Anatomical and electrophysiological evidence for a direct projection from Ammon's horn to the medial prefrontal cortex in the rat. Exp Brain Res 65:421-426.
Floresco SB, Seamans JK, Phillips AG (1997) Selective roles for hippocampal, prefrontal cortical, and ventral striatal circuits in radial-arm maze tasks with or without a delay. J Neurosci 17:1880-1890.
Ford GK, Moriarty O, McGuire BE, Finn DP (2008) Investigating the effects of distracting stimuli on nociceptive behaviour and associated alterations in brain monoamines in rats. Eur J Pain 12:970-979.
Fox SE, Ranck JB, Jr. (1981) Electrophysiological characteristics of hippocampal complex-spike cells and theta cells. Exp Brain Res 41:399-410.
Franciotti R, Ciancetta L, Della Penna S, Belardinelli P, Pizzella V, Romani GL (2009) Modulation of alpha oscillations in insular cortex reflects the threat of painful stimuli. Neuroimage 46:1082-1090.
Frank Y, Seiden J, Napolitano B (1996) Visual event related potentials and reaction time in normal adults, normal children, and children with attention deficit hyperactivity disorder: differences in short-term memory processing. Int J Neurosci 88:109-124.
Friedman DP, Murray EA, O'Neill JB, Mishkin M (1986) Cortical connections of the somatosensory fields of the lateral sulcus of macaques: evidence for a corticolimbic pathway for touch. J Comp Neurol 252:323-347.
Fuchs PN, Balinsky M, Melzack R (1996) Electrical stimulation of the cingulum bundle and surrounding cortical tissue reduces formalin-test pain in the rat. Brain Res 743:116-123.
Fuster JM (1997) Network memory. Trends Neurosci 20:451-459.
Gaskin S, Tardif M, Mumby DG (2009) Patterns of retrograde amnesia for recent and remote incidental spatial learning in rats. Hippocampus 19:1212-1221.
Gervasoni D, Lin SC, Ribeiro S, Soares ES, Pantoja J, Nicolelis MA (2004) Global forebrain dynamics predict rat behavioral states and their transitions. J Neurosci 24:11137-11147.
Glass JM, Park DC, Minear M, Crofford LJ (2005) Memory beliefs and function in fibromyalgia patients. JPsychosomRes 58:263-269.
Glass PS, Bloom M, Kearse L, Rosow C, Sebel P, Manberg P (1997) Bispectral analysis measures sedation and memory effects of propofol, midazolam, isoflurane, and alfentanil in healthy volunteers. Anesthesiology 86:836-847.
Gol A, Faibish GM (1967) Effects of human hippocampal ablation. J Neurosurg 26:390-398.
Gol A, Kellaway P, Shapiro M, Hurst CM (1963) Studies of hippocampectomy in the monkey, baboon, and cat. Behavioral changes and a preliminary evaluation of cognitive function. Neurology 13:1031-1041.
Goldman-Rakic PS (1995) Architecture of the prefrontal cortex and the central executive. Ann N Y Acad Sci 769:71-83.
Gottesmann C (1992) Detection of 7 Sleep-Waking Stages in the Rat. Neurosci Biobehav Rev 16:31-38.
Gray CM, König P, Engel AK, Singer W (1989) Oscillatory responses in cat visual cortex exhibit inter-columnar synchronization which reflects global stimulus properties. Nature 338:334-337.
Green MF (2006) Cognitive impairment and functional outcome in schizophrenia and bipolar disorder. J Clin Psychiatry 67:e12.
Gross J, Schnitzler A, Timmermann L, Ploner M (2007) Gamma oscillations in human primary somatosensory cortex reflect pain perception. PLoS Biol 5:e133.
Guido W, Weyand T (1995) Burst responses in thalamic relay cells of the awake behaving cat. J Neurophysiol 74:1782-1786.
Gusnard DA, Akbudak E, Shulman GL, Raichle ME (2001) Medial prefrontal cortex and self-referential mental activity: relation to a default mode of brain function. Proc Natl Acad Sci U S A 98:4259-4264.

Halgren E, Walter RD, Cherlow DG, Crandall PH (1978) Mental Phenomena Evoked by Electrical-Stimulation of Human Hippocampal Formation and Amygdala. Brain 101:83-117.
Harris KD, Csicsvari J, Hirase H, Dragoi G, Buzsáki G (2003) Organization of cell assemblies in the hippocampus. Nature 424:552-556.
Hasselmo ME, Bodelón C, Wyble BP (2002a) A proposed function for hippocampal theta rhythm: separate phases of encoding and retrieval enhance reversal of prior learning. Neural Comput 14:793-817.
Hasselmo ME, Hay J, Ilyn M, Gorchetchnikov A (2002b) Neuromodulation, theta rhythm and rat spatial navigation. Neural Netw 15:689-707.
Hauck M, Lorenz J, Engel AK (2007) Attention to painful stimulation enhances gamma-band activity and synchronization in human sensorimotor cortex. J Neurosci 27:9270-9277.
Hayes RL, Dubner R, Hoffman DS (1981) Neuronal activity in medullary dorsal horn of awake monkeys trained in a thermal discrimination task. II. Behavioral modulation of responses to thermal and mechanical stimuli. J Neurophysiol 46:428-443.
Hicks RA, Sawrey JM (1978) Rem-Sleep Deprivation and Stress Susceptibility in Rats. Psychological Record 28:187-191.
Hoffman DS, Dubner R, Hayes RL, Medlin TP (1981) Neuronal activity in medullary dorsal horn of awake monkeys trained in a thermal discrimination task. I. Responses to innocuous and noxious thermal stimuli. J Neurophysiol 46:409-427.
Hoffman HG, Richards TL, Coda B, Bills AR, Blough D, Richards AL, Sharar SR (2004) Modulation of thermal pain-related brain activity with virtual reality: evidence from fMRI. Neuroreport 15:1245-1248.
Houlihan ME, McGrath PJ, Connolly JF, Stroink G, Allen Finley G, Dick B, Phi TT (2004) Assessing the effect of pain on demands for attentional resources using ERPs. Int J Psychophysiol 51:181-187.
Hsiao FJ, Chen WT, Liao KK, Wu ZA, Ho LT, Lin YY (2008) Oscillatory characteristics of nociceptive responses in the SII cortex. Can J Neurol Sci 35:630-637.
Hu Y, Yang J, Wang Y, Li W (2010) Amitriptyline rather than lornoxicam ameliorates neuropathic pain-induced deficits in abilities of spatial learning and memory. Eur J Anaesthesiol 27:162-168.
Huang J, Chang J, Woodward D, Baccalá L, Han J, Wang J, Luo F (2006) Dynamic neuronal responses in cortical and thalamic areas during different phases of formalin test in rats. Exp Neurol 200:124-134.
Hudetz AG, Vizuete JA, Pillay S (2011) Differential effects of isoflurane on high-frequency and low-frequency γ oscillations in the cerebral cortex and hippocampus in freely moving rats. Anesthesiology 114:588-595.
Hyman JM, Zilli EA, Paley AM, Hasselmo ME (2005) Medial prefrontal cortex cells show dynamic modulation with the hippocampal theta rhythm dependent on behavior. Hippocampus 15:739-749.
Isseroff A, Rosvold HE, Galkin TW, Goldman-Rakic PS (1982) Spatial memory impairments following damage to the mediodorsal nucleus of the thalamus in rhesus monkeys. Brain Res 232:97-113.
Izaki Y, Akema T (2008) Gamma-band power elevation of prefrontal local field potential after posterior dorsal hippocampus-prefrontal long-term potentiation induction in anesthetized rats. Exp Brain Res 184.
Jeanmonod D, Magnin M, Morel A (1993) Thalamus and neurogenic pain: physiological, anatomical and clinical data. Neuroreport 4:475-478.
Jeanmonod D, Magnin M, Morel A (1996) Low-threshold calcium spike bursts in the human thalamus. Common physiopathology for sensory, motor and limbic positive symptoms. Brain 119 (Pt 2):363-375.
Jeanmonod D, Magnin M, Morel A, Siegemund M (2001) Surgical control of the human thalamocortical dysrhythmia: I. Central lateral thalamotomy in neurogenic pain,. Thalamus Related Syst 1:71-79.
Jensen O, Colgin LL (2007) Cross-frequency coupling between neuronal oscillations. Trends Cogn Sci 11:267-269.
Ji G, Sun H, Fu Y, Li Z, Pais-Vieira M, Galhardo V, Neugebauer V (2010) Cognitive impairment in pain through amygdala-driven prefrontal cortical deactivation. J Neurosci 30:5451-5464.
Jones E (2001) The thalamic matrix and thalamocortical synchrony. Trends Neurosci 24:595-601.
Jones MW, Wilson MA (2005a) Phase precession of medial prefrontal cortical activity relative to the hippocampal theta rhythm. Hippocampus 15:867-873.
Jones MW, Wilson MA (2005b) Theta rhythms coordinate hippocampal-prefrontal interactions in a spatial memory task. PLoS Biol 3:e402.

Keay KA, Monassi CR, Levison DB, Bandler R (2004) Peripheral nerve injury evokes disabilities and sensory dysfunction in a subpopulation of rats: a closer model to human chronic neuropathic pain? Neurosci Lett 361:188-191.
Kentros C, Hargreaves E, Hawkins RD, Kandel ER, Shapiro M, Muller RV (1998) Abolition of long-term stability of new hippocampal place cell maps by NMDA receptor blockade. Science 280:2121-2126.
Khanna S (1997) Dorsal hippocampus field CA1 pyramidal cell responses to a persistent versus an acute nociceptive stimulus and their septal modulation. Neuroscience 77:713-721.
Khanna S, Sinclair J (1992) Responses in the CA1 region of the rat hippocampus to a noxious stimulus. Exp Neurol 117:28-35.
Khanna S, Zheng F (1999) Morphine reversed formalin-induced CA1 pyramidal cell suppression via an effect on septohippocampal neural processing. Neuroscience 89:61-71.
Khanna S, Chang LS, Jiang F, Koh HC (2004) Nociception-driven decreased induction of Fos protein in ventral hippocampus field CA1 of the rat. Brain Res 1004:167-176.
Kim SP, Hwang E, Kang JH, Kim S, Choi JH (2012) Changes in the thalamocortical connectivity during anesthesia-induced transitions in consciousness. Neuroreport 23:294-298.
Klausberger T, Somogyi P (2008) Neuronal diversity and temporal dynamics: the unity of hippocampal circuit operations. Science 321:53-57.
Klossika I, Flor H, Kamping S, Bleichhardt G, Trautmann N, Treede RD, Bohus M, Schmahl C (2006) Emotional modulation of pain: a clinical perspective. Pain 124:264-268.
Kobayashi T, Nishijo H, Fukuda M, Bures J, Ono T (1997) Task-dependent representations in rat hippocampal place neurons. J Neurophysiol 78:597-613.
Kodama D, Ono H, Tanabe M (2007) Altered hippocampal long-term potentiation after peripheral nerve injury in mice. Eur J Pharmacol 574:127-132.
Kontinen VK, Ahnaou A, Drinkenburg WH, Meert TF (2003) Sleep and EEG patterns in the chronic constriction injury model of neuropathic pain. Physiol Behav 78:241-246.
Kramis R, Vanderwolf CH, Bland BH (1975) Two types of hippocampal rhythmical slow activity in both the rabbit and the rat: relations to behavior and effects of atropine, diethyl ether, urethane, and pentobarbital. Exp Neurol 49:58-85.
Kreuzer M, Hentschke H, Antkowiak B, Schwarz C, Kochs EF, Schneider G (2010) Cross-approximate entropy of cortical local field potentials quantifies effects of anesthesia--a pilot study in rats. BMC Neurosci 11:122.
Kuchinad A, Schweinhardt P, Seminowicz DA, Wood PB, Chizh BA, Bushnell MC (2007) Accelerated brain gray matter loss in fibromyalgia patients: premature aging of the brain? J Neurosci 27:4004-4007.
Kundermann B, Krieg JC, Schreiber W, Lautenbacher S (2004a) The effect of sleep deprivation on pain. Pain ResManag 9:25-32.
Kundermann B, Spernal J, Huber MT, Krieg JC, Lautenbacher S (2004b) Sleep deprivation affects thermal pain thresholds but not somatosensory thresholds in healthy volunteers. PsychosomMed 66:932-937.
Kyd RJ, Bilkey DK (2003) Prefrontal cortex lesions modify the spatial properties of hippocampal place cells. Cereb Cortex 13:444-451.
Lakatos P, Shah AS, Knuth KH, Ulbert I, Karmos G, Schroeder CE (2005) An oscillatory hierarchy controlling neuronal excitability and stimulus processing in the auditory cortex. J Neurophysiol 94:1904-1911.
Lalo E, Gilbertson T, Doyle L, Di Lazzaro V, Cioni B, Brown P (2007) Phasic increases in cortical beta activity are associated with alterations in sensory processing in the human. Exp Brain Res 177:137-145.
Landis CA, Robinson CR, Levine JD (1988) Sleep Fragmentation in the Arthritic Rat. Pain 34:93-99.
Laroche S, Davis S, Jay TM (2000) Plasticity at hippocampal to prefrontal cortex synapses: dual roles in working memory and consolidation. Hippocampus 10:438-446.
Laureys S, Owen AM, Schiff ND (2004) Brain function in coma, vegetative state, and related disorders. Lancet Neurol 3:537-546.
Lautenbacher S, Kundermann B, Krieg JC (2006) Sleep deprivation and pain perception. Sleep MedRev 10:357-369.
Lee I, Kesner RP (2003) Time-dependent relationship between the dorsal hippocampus and the prefrontal cortex in spatial memory. J Neurosci 23:1517-1523.
Legrain V, Crombez G, Mouraux A (2011) Controlling attention to nociceptive stimuli with working memory. PLoS One 6:e20926.

Legrain V, Damme SV, Eccleston C, Davis KD, Seminowicz DA, Crombez G (2009) A neurocognitive model of attention to pain: behavioral and neuroimaging evidence. Pain 144:230-232.
Leite-Almeida H, Almeida-Torres L, Mesquita AR, Pertovaara A, Sousa N, Cerqueira JJ, Almeida A (2009) The impact of age on emotional and cognitive behaviours triggered by experimental neuropathy in rats. Pain 144:57-65.
Lentz MJ, Landis CA, Rothermel J, Shaver JL (1999) Effects of selective slow wave sleep disruption on musculoskeletal pain and fatigue in middle aged women. J Rheumatol 26:1586-1592.
Lenz FA, Kwan HC, Dostrovsky JO, Tasker RR (1989) Characteristics of the bursting pattern of action potentials that occurs in the thalamus of patients with central pain. Brain Res 496:357-360.
Leutgeb S, Mizumori SJY (1999) Excitotoxic septal lesions result in spatial memory deficits and altered flexibility of hippocampal single-unit representations. J Neurosci 19:6661-6672.
Lindner MD, Plone MA, Francis JM, Cain CK (1999) Chronic morphine reduces pain-related disability in a rodent model of chronic, inflammatory pain. Exp Clin Psychopharmacol 7:187-197.
Ling J, Campbell C, Heffernan TM, Greenough CG (2007) Short-term prospective memory deficits in chronic back pain patients. Psychosom Med 69:144-148.
Lisman JE, Grace AA (2005) The hippocampal-VTA loop: controlling the entry of information into long-term memory. Neuron 46:703-713.
Lisman JE, Talamini LM, Raffone A (2005) Recall of memory sequences by interaction of the dentate and CA3: a revised model of the phase precession. Neural Netw 18:1191-1201.
Liu MG, Chen J (2009) Roles of the hippocampal formation in pain information processing. Neurosci Bull 25:237-266.
Liu X, Muller RU, Huang LT, Kubie JL, Rotenberg A, Rivard B, Cilio MR, Holmes GL (2003) Seizure-induced changes in place cell physiology: relationship to spatial memory. J Neurosci 23:11505-11515.
Liu XG, Sandk hler J (1995) Long-term potentiation of C-fiber-evoked potentials in the rat spinal dorsal horn is prevented by spinal N-methyl-D-aspartic acid receptor blockage. Neurosci Lett 191:43-46.
Llinás R, Jahnsen H (1982) Electrophysiology of mammalian thalamic neurones in vitro. Nature 297:406-408.
Llinás R, Ribary U, Contreras D, Pedroarena C (1998) The neuronal basis for consciousness. Philos Trans R Soc Lond B Biol Sci 353:1841-1849.
Llinás R, Ribary U, Jeanmonod D, Kronberg E, Mitra P (1999) Thalamocortical dysrhythmia: A neurological and neuropsychiatric syndrome characterized by magnetoencephalography. Proc Natl Acad Sci U S A 96:15222-15227.
Llinás R, Urbano FJ, Leznik E, Ramírez RR, van Marle HJ (2005) Rhythmic and dysrhythmic thalamocortical dynamics: GABA systems and the edge effect. Trends Neurosci 28:325-333.
Llinás RR (1988) The intrinsic electrophysiological properties of mammalian neurons: insights into central nervous system function. Science 242:1654-1659.
Llinás RR, Steriade M (2006) Bursting of thalamic neurons and states of vigilance. J Neurophysiol 95:3297-3308.
Lorenz J, Cross DJ, Minoshima S, Morrow TJ, Paulson PE, Casey KL (2002) A unique representation of heat allodynia in the human brain. Neuron 35:383-393.
Louie K, Wilson M (2001) Temporally structured replay of awake hippocampal ensemble activity during rapid eye movement sleep. Neuron 29:145-156.
Luerding R, Weigand T, Bogdahn U, Schmidt-Wilcke T (2008) Working memory performance is correlated with local brain morphology in the medial frontal and anterior cingulate cortex in fibromyalgia patients: structural correlates of pain-cognition interaction. Brain 131:3222-3231.
Lutz J, Jager L, de Quervain D, Krauseneck T, Padberg F, Wichnalek M, Beyer A, Stahl R, Zirngibl B, Morhard D, Reiser M, Schelling G (2008) White and gray matter abnormalities in the brain of patients with fibromyalgia: a diffusion-tensor and volumetric imaging study. Arthritis Rheum 58:3960-3969.
Lévesque M, Langlois JM, Lema P, Courtemanche R, Bilodeau GA, Carmant L (2009) Synchronized gamma oscillations (30-50 Hz) in the amygdalo-hippocampal network in relation with seizure propagation and severity. Neurobiol Dis 35:209-218.
Mandile P, Vescia S, Montagnese P, Romano F, Giuditta A (1996) Characterization of transition sleep episodes in baseline EEG recordings of adult rats. Physiol Behav 60:1435-1439.
Mandile P, Vescia S, Montagnese P, Piscopo S, Cotugno M, Giuditta A (2000) Post-trial sleep sequences including transition sleep are involved in avoidance learning of adult rats. Behav Brain Res 112:23-31.

Mann EO, Paulsen O (2005) Mechanisms underlying gamma ('40 Hz') network oscillations in the hippocampus--a mini-review. Prog Biophys Mol Biol 87:67-76.
Markus EJ, Qin YL, Leonard B, Skaggs WE, McNaughton BL, Barnes CA (1995) Interactions between location and task affect the spatial and directional firing of hippocampal neurons. J Neurosci 15:7079-7094.
Maviel T, Durkin TP, Menzaghi F, Bontempi B (2004) Sites of neocortical reorganization critical for remote spatial memory. Science 305:96-99.
McDowell S, Whyte J, D'Esposito M (1997) Working memory impairments in traumatic brain injury: evidence from a dual-task paradigm. Neuropsychologia 35:1341-1353.
McKenna JE, Melzack R (1992) Analgesia produced by lidocaine microinjection into the dentate gyrus. Pain 49:105-112.
McKenna JE, Melzack R (2001) Blocking NMDA receptors in the hippocampal dentate gyrus with AP5 produces analgesia in the formalin pain test. Exp Neurol 172:92-99.
McNaughton BL, Barnes CA, Meltzer J, Sutherland RJ (1989) Hippocampal granule cells are necessary for normal spatial learning but not for spatially-selective pyramidal cell discharge. Exp Brain Res 76:485-496.
Melzack R (1999) From the gate to the neuromatrix. Pain Suppl 6:S121-126.
Melzack R, Casey KL (1968) Sensory, motivational and central control determinants of pain. In: The Skin Senses (Kenshalo DR, ed), pp 423-443. Springfield: C.C.Thomas.
Mendelson WB, Bergmann BM, Tung A (2003) Baseline and post-deprivation recovery sleep in SCN-lesioned rats. Brain Res 980:185-190.
Metz AE, Yau HJ, Centeno MV, Apkarian AV, Martina M (2009a) Morphological and functional reorganization of rat medial prefrontal cortex in neuropathic pain. Proc Natl Acad Sci U S A 106:2423-2428.
Mhuircheartaigh RN, Rosenorn-Lanng D, Wise R, Jbabdi S, Rogers R, Tracey I (2010) Cortical and subcortical connectivity changes during decreasing levels of consciousness in humans: a functional magnetic resonance imaging study using propofol. J Neurosci 30:9095-9102.
Millecamps M, Etienne M, Jourdan D, Eschalier A, Ardid D (2004) Decrease in non-selective, non-sustained attention induced by a chronic visceral inflammatory state as a new pain evaluation in rats. Pain 109:214-224.
Millecamps M, Jourdan D, Leger S, Etienne M, Eschalier A, Ardid D (2005) Circadian pattern of spontaneous behavior in monarthritic rats - A novel global approach to evaluation of chronic pain and treatment effectiveness. Arthritis Rheum 52:3470-3478.
Millecamps M, Centeno MV, Berra HH, Rudick CN, Lavarello S, Tkatch T, Apkarian AV (2007) D-cycloserine reduces neuropathic pain behavior through limbic NMDA-mediated circuitry. Pain 132:108-123.
Miller R (1989) Cortico-hippocampal interplay: self-organizing phase-locked loops for indexing
memory. Psychobiology 17:115-128.
Mitchell AS, Dalrymple-Alford JC (2005) Dissociable memory effects after medial thalamus lesions in the rat. Eur J Neurosci 22:973-985.
Mitchell AS, Browning PG, Wilson CR, Baxter MG, Gaffan D (2008) Dissociable roles for cortical and subcortical structures in memory retrieval and acquisition. J Neurosci 28:8387-8396.
Mizumori S, Miya D, Ward K (1994) Reversible inactivation of the lateral dorsal thalamus disrupts hippocampal place representation and impairs spatial learning. Brain Res 644:168-174.
Mogilner A, Grossman JA, Ribary U, Joliot M, Volkmann J, Rapaport D, Beasley RW, Llinás RR (1993) Somatosensory cortical plasticity in adult humans revealed by magnetoencephalography. Proc Natl Acad Sci U S A 90:3593-3597.
Moita MA, Rosis S, Zhou Y, LeDoux JE, Blair HT (2004) Putting fear in its place: remapping of hippocampal place cells during fear conditioning. J Neurosci 24:7015-7023.
Moldofsky H, Scarisbrick P (1976) Induction of neurasthenic musculoskeletal pain syndrome by selective sleep stage deprivation. PsychosomMed 38:35-44.
Monassi CR, Bandler R, Keay KA (2003) A subpopulation of rats show social and sleep-waking changes typical of chronic neuropathic pain following peripheral nerve injury. Eur J Neurosci 17:1907-1920.
Montgomery SM, Buzsáki G (2007) Gamma oscillations dynamically couple hippocampal CA3 and CA1 regions during memory task performance. Proc Natl Acad Sci U S A 104:14495-14500.
Moriarty O, McGuire BE, Finn DP (2011) The effect of pain on cognitive function: A review of clinical and preclinical research. Prog Neurobiol.

Moser E, Moser MB, Andersen P (1993) Spatial learning impairment parallels the magnitude of dorsal hippocampal lesions, but is hardly present following ventral lesions. J Neurosci 13:3916-3925.
Mouraux A, Guérit JM, Plaghki L (2003) Non-phase locked electroencephalogram (EEG) responses to CO2 laser skin stimulations may reflect central interactions between A partial partial differential- and C-fibre afferent volleys. Clin Neurophysiol 114:710-722.
Muir G, Bilkey D (2001) Instability in the place field location of hippocampal place cells after lesions centered on the perirhinal cortex. J Neurosci 21:4016-4025.
Muller RU, Kubie JL (1987) The effects of changes in the environment on the spatial firing of hippocampal complex-spike cells. J Neurosci 7:1951-1968.
Murphy DD, Segal M (1997) Morphological plasticity of dendritic spines in central neurons is mediated by activation of cAMP response binding protein. Proc Natl Acad Sci USA 94:1482-1487.
Myles PS, Leslie K, McNeil J, Forbes A, Chan MT (2004) Bispectral index monitoring to prevent awareness during anaesthesia: the B-Aware randomised controlled trial. Lancet 363:1757-1763.
Nagasako EM, Oaklander AL, Dworkin RH (2003) Congenital insensitivity to pain: an update. Pain 101:213-219.
Neugebauer V, Galhardo V, Maione S, Mackey SC (2009) Forebrain pain mechanisms. Brain Res Rev 60:226-242.
Neville KR, Haberly LB (2003) Beta and gamma oscillations in the olfactory system of the urethane-anesthetized rat. J Neurophysiol 90:3921-3930.
Nicolelis MAL, Fanselow EE (2002a) Dynamic shifting in thalamocortical processing during different behavioural states. PhilTransRSocLondB 357:1753-1758.
Nicolelis MAL, Fanselow EE (2002b) Thalamocortical optimization of tactile processing according to behavioral state. Nat Neurosci 5:517-523.
Nicolelis MAL, Baccala LA, Lin RC, Chapin JK (1995) Sensorimotor encoding by synchronous neural ensemble activity at multiple levels of the somatosensory system. Science 268:1353-1358.
Norman DA (1967) Temporal confusions and limited capacity processors. Acta Psychol (Amst) 27:293-297.
O' Keefe J, Dostrovsky J (1971) Hippocampus as A Spatial Map - Preliminary Evidence from Unit Activity in Freely-Moving Rat. Brain Res 34:5.
O' Keefe J, Nadel L (1978) The hippocampus as a cognitive map.: Oxford: Clarendon.
Ohara S, Crone NE, Weiss N, Lenz FA (2004) Attention to a painful cutaneous laser stimulus modulates electrocorticographic event-related desynchronization in humans. Clin Neurophysiol 115:1641-1652.
Olton DS, Samuelson RJ (1976) Remembrance of places passed: Spatial memory in rats. JExpPsycholAnim BehavProcess 2:97-116.
Onen SH, Alloui A, Gross A, Eschallier A, Dubray C (2001) The effects of total sleep deprivation, selective sleep interruption and sleep recovery on pain tolerance thresholds in healthy subjects. J Sleep Res 10:35-42.
Oosterman JM, de Vries K, Dijkerman HC, de Haan EH, Scherder EJ (2009) Exploring the relationship between cognition and self-reported pain in residents of homes for the elderly. Int Psychogeriatr 21:157-163.
Owen AM, Coleman MR, Boly M, Davis MH, Laureys S, Pickard JD (2006) Detecting awareness in the vegetative state. Science 313:1402.
Pais-Vieira M, Lima D, Galhardo V (2009a) Sustained attention deficits in rats with chronic inflammatory pain. Neurosc Lett 463:98-102.
Pais-Vieira M, Mendes-Pinto MM, Lima D, Galhardo V (2009b) Cognitive impairment of prefrontal-dependent decision-making in rats after the onset of chronic pain. Neuroscience 161:671-679.
Park DC, Glass JM, Minear M, Crofford LJ (2001) Cognitive function in fibromyalgia patients. Arthritis Rheum 44:2125-2133.
Peyron R, Laurent B, Garcia-Larrea L (2000) Functional imaging of brain responses to pain. A review and meta-analysis (2000). NeurophysiolClin 30:263-288.
Peyron R, García-Larrea L, Grégoire MC, Convers P, Lavenne F, Veyre L, Froment JC, Mauguière F, Michel D, Laurent B (1998) Allodynia after lateral-medullary (Wallenberg) infarct. A PET study. Brain 121:345-356.
Phelps EA, Delgado MR, Nearing KI, LeDoux JE (2004) Extinction learning in humans: role of the amygdala and vmPFC. Neuron 43:897-905.
Phillips AG, Ahn S, Floresco SB (2004) Magnitude of dopamine release in medial prefrontal cortex predicts accuracy of memory on a delayed response task. J Neurosci 24:547-553.

Piscopo S, Mandile P, Montagnese P, Cotugno M, Giuditta A, Vescia S (2001) Trains of sleep sequences are indices of learning capacity in rats. Behav Brain Res 120:13-21.
Ploghaus A, Tracey I, Clare S, Gati JS, Rawlins JNP, Matthews PM (2000) Learning about pain: The neural substrate of the prediction error for aversive events. Proc Natl Acad Sci U S A 97:9281-9286.
Ploghaus A, Narain C, Beckmann CF, Clare S, Bantick S, Wise R, Matthews PM, Rawlins JNP, Tracey I (2001) Exacerbation of pain by anxiety is associated with activity in a hippocampal network. J Neurosci 21:9896-9903.
Ploner M, Pollok B, Schnitzler A (2004) Pain facilitates tactile processing in human somatosensory cortices. J Neurophysiol 92:1825-1829.
Ploner M, Gross J, Timmermann L, Pollok B, Schnitzler A (2006) Pain suppresses spontaneous brain rhythms. Cereb Cortex 16:537-540.
Ploner M, Lee MC, Wiech K, Bingel U, Tracey I (2011) Flexible cerebral connectivity patterns subserve contextual modulations of pain. Cereb Cortex 21:719-726.
Porro CA, Baraldi P, Pagnoni G, Serafini M, Facchin P, Maieron M, Nichelli P (2002) Does anticipation of pain affect cortical nociceptive systems? J Neurosci 22:3206-3214.
Price DD (2000) Psychological and neural mechanisms of the affective dimension of pain. Science 288:1769-1772.
Pud D, Sapir S (2006) The effects of noxious heat, auditory stimulation, a cognitive task, and time on task on pain perception and performance accuracy in healthy volunteers: a new experimental model. Pain 120:155-160.
Raij TT, Forss N, Stancák A, Hari R (2004) Modulation of motor-cortex oscillatory activity by painful Adelta- and C-fiber stimuli. Neuroimage 23:569-573.
Rainville P (2002) Brain mechanisms of pain affect and pain modulation. Curr Opin Neurobiol 12:195-204.
Rainville P, Duncan GH, Price DD, Carrier B, Bushnell MC (1997) Pain affect encoded in human anterior cingulate but not somatosensory cortex. Science 277:968-971.
Ren WJ, Liu Y, Zhou LJ, Li W, Zhong Y, Pang RP, Xin WJ, Wei XH, Wang J, Zhu HQ, Wu CY, Qin ZH, Liu G, Liu XG (2011) Peripheral Nerve Injury Leads to Working Memory Deficits and Dysfunction of the Hippocampus by Upregulation of TNF-α in Rodents. Neuropsychopharmacology 36(5):979-992.
Ribary U (2005) Dynamics of thalamo-cortical network oscillations and human perception. Prog Brain Res 150:127-142.
Ribeiro S, Nicolelis MA (2004) Reverberation, storage, and postsynaptic propagation of memories during sleep. Learn Mem 11:686-696.
Ribeiro TL, Copelli M, Caixeta F, Belchior H, Chialvo DR, Nicolelis MA, Ribeiro S (2010) Spike avalanches exhibit universal dynamics across the sleep-wake cycle. PLoS ONE 5:e14129.
Rols G, Tallon-Baudry C, Girard P, Bertrand O, Bullier J (2001) Cortical mapping of gamma oscillations in areas V1 and V4 of the macaque monkey. Vis Neurosci 18:527-540.
Rotenberg A, Abel T, Hawkins RD, Kandel ER, Muller RU (2000) Parallel instabilities of long-term potentiation, place cells, and learning caused by decreased protein kinase A activity. J Neurosci 20:8096-8102.
Sarnthein J, Jeanmonod D (2008) High thalamocortical theta coherence in patients with neurogenic pain. Neuroimage 39:1910-1917.
Sarnthein J, Stern J, Aufenberg C, Rousson V, Jeanmonod D (2006) Increased EEG power and slowed dominant frequency in patients with neurogenic pain. Brain 129:55-64.
Schneider G, Kochs EF (2007) The search for structures and mechanisms controlling anesthesia-induced unconsciousness. Anesthesiology 107:195-198.
Schoenbaum G, Setlow B, Ramus SJ (2003) A systems approach to orbitofrontal cortex function: recordings in rat orbitofrontal cortex reveal interactions with different learning systems. Behav Brain Res 146:19-29.
Schutz TCB, Andersen ML, Tufik S (2003) Sleep alterations in an experimental orofacial pain model in rats. Brain Res 993:164-171.
Schweinhardt P, Kalk N, Wartolowska K, Chessell I, Wordsworth P, Tracey I (2008) Investigation into the neural correlates of emotional augmentation of clinical pain. Neuroimage 40:759-766.
Schweinhardt P, Glynn C, Brooks J, McQuay H, Jack T, Chessell I, Bountra C, Tracey I (2006) An fMRI study of cerebral processing of brush-evoked allodynia in neuropathic pain patients. Neuroimage 32:256-265.
Sederberg PB, Kahana MJ, Howard MW, Donner EJ, Madsen JR (2003) Theta and gamma oscillations during encoding predict subsequent recall. J Neurosci 23(34):10809-10814.

Seifert F, Bschorer K, De Col R, Filitz J, Peltz E, Koppert W, Maihöfner C (2009) Medial prefrontal cortex activity is predictive for hyperalgesia and pharmacological antihyperalgesia. J Neurosci 29:6167-6175.

Seminowicz DA, Davis KD (2007) Interactions of pain intensity and cognitive load: the brain stays on task. Cereb Cortex 17:1412-1422.

Senior TJ, Huxter JR, Allen K, O'Neill J, Csicsvari J (2008) Gamma oscillatory firing reveals distinct populations of pyramidal cells in the CA1 region of the hippocampus. J Neurosci 28(9):2274-2286.

Shaw C, Aggleton JP (1993) The effects of fornix and medial prefrontal lesions on delayed non-matching-to-sample by rats. Behav Brain Res 54:91-102.

Shyu BC, Sikes RW, Vogt LJ, Vogt BA (2010) Nociceptive processing by anterior cingulate pyramidal neurons. J Neurophysiol 103:3287-3301.

Siapas AG, Lubenov EV, Wilson MA (2005) Prefrontal phase locking to hippocampal theta oscillations. Neuron 46:141-151.

Sikes RW, Vogt BA (1992) Nociceptive neurons in area 24 of rabbit cingulate cortex. Journal of Neurophysiology 68:1720-1732.

Silva A, Cardoso-Cruz H, Silva F, Galhardo V, Antunes L (2010) Comparison of anesthetic depth indexes based on thalamocortical local field potentials in rats. Anesthesiology 112:355-363.

Silva A, Ferreira DA, Venâncio C, Souza AP, Antunes LM (2011) Performance of electroencephalogram-derived parameters in prediction of depth of anaesthesia in a rabbit model. Br J Anaesth 106:540-547.

Singer W, Gray CM (1995) Visual feature integration and the temporal correlation hypothesis. Annual Review of Neurosciences 18:555-586.

Sirota A, Montgomery S, Fujisawa S, Isomura Y, Zugaro M, Buzsáki G (2008) Entrainment of neocortical neurons and gamma oscillations by the hippocampal theta rhythm. Neuron 60:683-697.

Skaggs WE, McNaughton BL, Wilson MA, Barnes CA (1996) Theta phase precession in hippocampal neuronal populations and the compression of temporal sequences. Hippocampus 6:149-172.

Soleimannejad E, Semnanian S, Fathollahi Y, Naghdi N (2006) Microinjection of ritanserin into the dorsal hippocampal CA1 and dentate gyrus decrease nociceptive behavior in adult male rat. Behav Brain Res 168:221-225.

Stancák A, Polácek H, Bukovský S (2010) Bursts of 15-30 Hz oscillations following noxious laser stimulus originate in posterior cingulate cortex. Brain Res 1317:69-79.

Steriade M (1999) Coherent oscillations and short-term plasticity in corticothalamic networks. Trends Neurosci 22:337-345.

Steriade M (2001) Impact of network activities on neuronal properties in corticothalamic systems. J Neurophysiol 86:1-39.

Steriade M (2006a) Grouping of brain rhythms in corticothalamic systems. Neuroscience 137:1087-1106.

Steriade M (2006b) Neuronal substrates of spike-wave seizures and hypsarrhythmia in corticothalamic systems. Adv Neurol 97:149-154.

Steriade M, Timofeev I (2003) Neuronal plasticity in thalamocortical networks during sleep and waking oscillations. Neuron 37:563-576.

Steriade M, McCormick DA, Sejnowski TJ (1993) Thalamocortical Oscillations in the Sleeping and Aroused Brain. Science 262:679-685.

Stern J, Jeanmonod D, Sarnthein J (2006) Persistent EEG overactivation in the cortical pain matrix of neurogenic pain patients. Neuroimage 31:721-731.

Struys MM, Vereecke H, Moerman A, Jensen EW, Verhaeghen D, De Neve N, Dumortier FJ, Mortier EP (2003) Ability of the bispectral index, autoregressive modelling with exogenous input-derived auditory evoked potentials, and predicted propofol concentrations to measure patient responsiveness during anesthesia with propofol and remifentanil. Anesthesiology 99:802-812.

Suzuki T, Amata M, Sakaue G, Nishimura S, Inoue T, Shibata M, Mashimo T (2007) Experimental neuropathy in mice is associated with delayed behavioral changes related to anxiety and depression. Anesth Analg 104:1570-1577.

Tai SK, Huang FD, Moochhala S, Khanna S (2006) Hippocampal theta state in relation to formalin nociception. Pain 121:29-42.

Takehara K, Kawahara S, Kirino Y (2003) Time-dependent reorganization of the brain components underlying memory retention in trace eyeblink conditioning. J Neurosci 23:9897-9905.

Teitelbaum H, Milner P (1963) Activity changes following partial hippocampal lesions in rats. J Comp Physiol Psychol 56:284-289.

Thierry AM, Gioanni Y, Dégénétais E, Glowinski J (2000) Hippocampo-prefrontal cortex pathway: anatomical and electrophysiological characteristics. Hippocampus 10:411-419.
Thompson LT, Best PJ (1990) Long-term stability of the place-field activity of single units recorded from the dorsal hippocampus of freely behaving rats. Brain Res 509:299-308.
Tiemann L, Schulz E, Gross J, Ploner M (2010) Gamma oscillations as a neuronal correlate of the attentional effects of pain. Pain 150:302-308.
Tononi G (2004) An information integration theory of consciousness. BMC Neurosci 5:42.
Tracey I (2005) Nociceptive processing in the human brain. Curr Opin Neurobiol 15:478-487.
Traub RJ, Silva E, Gebhart GF, Solodkin A (1996) Noxious colorectal distention induced-c-Fos protein in limbic brain structures in the rat. Neurosci Lett 215:165-168.
Treede RD, Kenshalo DR, Jr., Gracely RH, Jones AKP (1999) The cortical representation of pain. Pain 79:105-111.
Urban MO, Gebhart GF (1999) Supraspinal contributions to hyperalgesia. Proc Natl Acad Sci U S A 96:7687-7692.
Vallar G, Papagno C (1993) Preserved vocabulary acquisition in Down's syndrome: the role of phonological short-term memory. Cortex 29:467-483.
Vanderwolf CH (1969) Hippocampal Electrical Acitvity and Voluntary Movement in Rat. Electroencephalography and Clinical Neurophysiology 26:407-408.
Veerasarn P, Stohler CS (1992) The effect of experimental muscle pain on the background electrical brain activity. Pain 49:349-360.
Velly LJ, Rey MF, Bruder NJ, Gouvitsos FA, Witjas T, Regis JM, Peragut JC, Gouin FM (2007) Differential dynamic of action on cortical and subcortical structures of anesthetic agents during induction of anesthesia. Anesthesiology 107:202-212.
Vertes RP (2006) Interactions among the medial prefrontal cortex, hippocampus and midline thalamus in emotional and cognitive processing in the rat. Neuroscience 142:1-20.
Wager TD, Rilling JK, Smith EE, Sokolik A, Casey KL, Davidson RJ, Kosslyn SM, Rose RM, Cohen JD (2004) Placebo-induced changes in FMRI in the anticipation and experience of pain. Science 303:1162-1167.
Walton K, Dubois M, Llinás R (2010) Abnormal thalamocortical activity in patients with Complex Regional Pain Syndrome (CRPS) Type I. Pain 150:41-51.
Wang CC, Shyu BC (2004) Differential projections from the mediodorsal and centrolateral thalamic nuclei to the frontal cortex in rats. Brain Res 995:226-235.
Wang GW, Cai JX (2006) Disconnection of the hippocampal-prefrontal cortical circuits impairs spatial working memory performance in rats. Behav Brain Res 175:329-336.
Wang J, Luo F, Chang J, Woodward D, Han J (2003) Parallel pain processing in freely moving rats revealed by distributed neuron recording. Brain Res 992:263-271.
Wei F, Xu ZC, Qu Z, Milbrandt J, Zhuo M (2000) Role of EGR1 in hippocampal synaptic enhancement induced by tetanic stimulation and amputation. J Cell Biol 149:1325-1333.
Weyand TG, Boudreaux M, Guido W (2001) Burst and tonic response modes in thalamic neurons during sleep and wakefulness. J Neurophysiol 85:1107-1118.
Wiech K, Seymour B, Kalisch R, Stephan KE, Koltzenburg M, Driver J, Dolan RJ (2005) Modulation of pain processing in hyperalgesia by cognitive demand. Neuroimage 27:59-69.
Wiest MC, Nicolelis MAL (2003) Behavioral detection of tactile stimuli during 7-12 Hz cortical oscillations in awake rats. Nat Neurosci 6:913-914.
Willis WD (1985) Nociceptive pathways: anatomy and physiology of nociceptive ascending pathways. PhilTransRSocLondB 308:253-268.
Wilson MA, McNaughton BL (1994) Reactivation of hippocampal ensemble memories during sleep. Science 265:676-679.
Wood ER, Dudchenko PA, Robitsek RJ, Eichenbaum H (2000) Hippocampal neurons encode information about different types of memory episodes occurring in the same location. Neuron 27:623-633.
Yamamura H, Iwata K, Tsuboi Y, Toda K, Kitajima K, Shimizu N, Nomura H, Hibiya J, Fujita S, Sumino R (1996) Morphological and electrophysiological properties of ACCx nociceptive neurons in rats. Brain Research 735:83-92.
Younger JW, Shen YF, Goddard G, Mackey SC (2010) Chronic myofascial temporomandibular pain is associated with neural abnormalities in the trigeminal and limbic systems. Pain 149:222-228.

Zahrt J, Taylor JR, Mathew RG, Arnsten AF (1997) Supranormal stimulation of D1 dopamine receptors in the rodent prefrontal cortex impairs spatial working memory performance. J Neurosci 17:8528-8535.

Zambreanu L, Wise RG, Brooks JC, Iannetti GD, Tracey I (2005) A role for the brainstem in central sensitisation in humans. Evidence from functional magnetic resonance imaging. Pain 114:397-407.

Zhang R, Tomida M, Katayama Y, Kawakami Y (2004) Response durations encode nociceptive stimulus intensity in the rat medial prefrontal cortex. Neuroscience 125:777-785.

Zhao XY, Liu MG, Yuan DL, Wang Y, He Y, Wang DD, Chen XF, Zhang FK, Li H, He XS, Chen J (2009) Nociception-induced spatial and temporal plasticity of synaptic connection and function in the hippocampal formation of rats: a multi-electrode array recording. Mol Pain 5:55.

Zheng F, Khanna S (1999) Hippocampal field CA1 interneuronal nociceptive responses: modulation by medial septal region and morphine. Neuroscience 93:45-55.

Zheng F, Khanna S (2008) Intra-hippocampal tonic inhibition influences formalin pain-induced pyramidal cell suppression, but not excitation in dorsal field CA1 of rat. Brain Res Bull 77:374-381.

Zhou J, Liu X, Song W, Yang Y, Zhao Z, Ling F, Hudetz AG, Li SJ (2011) Specific and nonspecific thalamocortical functional connectivity in normal and vegetative states. Conscious Cogn 20:257-268.

PUBLICAÇÕES II

PUBLICAÇÃO 1

frontiers in
INTEGRATIVE NEUROSCIENCE

ORIGINAL RESEARCH ARTICLE
published: 23 August 2011
doi: 10.3389/fnint.2011.00043

Dynamics of circadian thalamocortical flow of information during a peripheral neuropathic pain condition

Helder Cardoso-Cruz[1,2], Koichi Sameshima[3], Deolinda Lima[1,2] and Vasco Galhardo[1,2]*

[1] *Departamento de Biologia Experimental, Faculdade de Medicina, Universidade do Porto, Porto, Portugal*
[2] *Instituto de Biologia Molecular e Celular, Grupo de Morfofisiologia do Sistema Somatosensitivo, Universidade do Porto, Porto, Portugal*
[3] *Departamento de Radiologia, Faculdade de Medicina, Universidade de São Paulo, São Paulo, SP, Brasil*

Edited by:
Elizabeth B. Torres, Rutgers University, USA

Reviewed by:
Albino J. Oliveira-Maia, Champalimaud Foundation, Portugal
John F. Araujo, Federal University of Rio Grande do Norte, Brazil

***Correspondence:**
Vasco Galhardo, Instituto de Biologia Molecular e Celular, Rua do Campo Alegre, 823, 4150-180 Porto, Portugal.
e-mail: galhardo@med.up.pt

It is known that the thalamocortical loop plays a crucial role in the encoding of sensory–discriminative features of painful stimuli. However, only a few studies have addressed the changes in thalamocortical dynamics that may occur after the onset of chronic pain. Our goal was to evaluate how the induction of chronic neuropathic pain affected the flow of information within the thalamocortical loop throughout the brain states of the sleep–wake cycle. To address this issue we recorded local field potentials (LFPs) – both before and after the establishment of neuropathic pain in awake freely moving adult rats chronically implanted with arrays of multielectrodes in the lateral thalamus and primary somatosensory cortex. Our results show that the neuropathic injury induced changes in the number of wake and slow-wave-sleep (SWS) state episodes, and especially in the total number of transitions between brain states. Moreover, partial directed coherence – analysis revealed that the amount of information flow between cortex and thalamus in neuropathic animals decreased significantly, indicating that the overall thalamic activity had less weight over the cortical activity. However, thalamocortical LFPs displayed higher phase-locking during awake and SWS episodes after the nerve lesion, suggesting faster transmission of relevant information along the thalamocortical loop. The observed changes are in agreement with the hypothesis of thalamic dysfunction after the onset of chronic pain, and may result from diminished inhibitory effect of the primary somatosensory cortex over the lateral thalamus.

Keywords: spared nerve injury model, intracranial recordings, thalamocortical, partial directed coherence, rat

INTRODUCTION

Although classically viewed as indicators of sleep–arousal transitions (McCormick and Bal, 1997), thalamocortical oscillations are now known to play an important role in the perception of visual, auditory, and somatosensory stimuli (Jones, 2001; Sherman and Guillery, 2002; Ribary, 2005; Massimini et al., 2009). Recent studies have shown that the disruption of this oscillatory activity in the thalamocortical loop impairs attentional control, affects the normal processing of sensory information, and disrupts the recall of previous sensory experiences (Lumer et al., 1997; Wiest and Nicolelis, 2003; de Labra et al., 2007; Meehan et al., 2008; Ray et al., 2009). In what concerns pain perception, the functional loop between neurons of the primary somatosensory cortex and lateral thalamic nuclei is known for a long time to be fundamental in the processing of the sensory–discriminative features of painful stimuli that are transmitted through the spinothalamic tract (Willis, 2007; Lima, 2008). However, recent studies have proposed a larger sensory role for thalamocortical oscillations by suggesting that disruption of their fine balance could be at the onset of neurogenic pain by a process known as thalamocortical dysrhythmia, in which slower brain rhythms are produced by a disruption of inhibitory feedback in thalamic neurons (Llinás et al., 1999). This hypothesis is supported by the clinical observation that chronic pain patients have a shift in their EEG spectrum toward lower dominant frequencies (Chen and Herrmann, 2001; Drewes et al., 2008; Walton et al., 2010). Moreover chronic pain patients display an increase in EEG power over theta frequency which also supports the neurogenic hypothesis of thalamocortical dysrhythmia (Sarnthein et al., 2006; Bjørk et al., 2009; Walton et al., 2010).

It is, however, difficult to assess how critically important are these thalamocortical changes to the onset of chronic pain symptoms, since they also occur in several non-painful neurological conditions such as epilepsy, Parkinson disease, essential tremor, tinnitus, and non-painful paraplegia (Jeanmonod et al., 2003; Hughes and Crunelli, 2005; Sarnthein and Jeanmonod, 2007; Boord et al., 2008; Kane et al., 2009). Furthermore, these human studies were based in short recording sessions, and have not taken into consideration how the disruption of the thalamocortical oscillations might affect the patient's state of vigilance, which is highly relevant since chronic pain causes fragmentation of sleep patterns (Gudbjornsson et al., 1993; Drewes et al., 1995; Jones et al., 1996; Hagen et al., 1997; Tishler et al., 1997; Morin et al., 1998) while sleep deprivation exacerbates pain perception (Moldofsky et al., 1975; Drewes et al., 1997; Lentz et al., 1999; Onen et al., 2001; Kundermann et al., 2004; Edwards et al., 2008). More importantly, the human studies cannot solve the conundrum of determining if the chronic pain is a cause or a consequence of the thalamocortical dysrhythmia.

Chronic painful conditions are commonly associated with sleep disturbances (Lautenbacher et al., 2006; Tang et al., 2007). In fact,

the relationship between pain and sleep appears to be reciprocal: while pain may interrupt or disturb sleep, poor sleep can also influence pain perception. However, the influence of sleep disturbances on pain processing is still poorly investigated. Previous neurophysiological studies describing changes in brain oscillations in animal models of chronic pain during sleep–wake cycle were commonly limited to only short periods or single sessions of recording (Andersen and Tufik, 2003; Kontinen et al., 2003; Monassi et al., 2003; Keay et al., 2004; Silva et al., 2008), and most of them were mainly focused in the changes in sleep patterns (Carli et al., 1987; Landis et al., 1988; Millecamps et al., 2005) without addressing the changes in brain activity.

On the other hand no animal studies have addressed the changes in thalamocortical dynamics after the onset of chronic pain across the sleep–wake cycle, although a few have described the changes occurring in the thalamocortical loop during acute painful stimulation or immediately following formalin injection (Wang et al., 2003, 2004; Huang et al., 2006). Therefore, our goal was to evaluate how the induction of prolonged neuropathic pain affected the thalamocortical dynamics. To pursue this goal we recorded the spontaneous neural activity of freely moving adult rats using multielectrodes chronically implanted in the primary somatosensory cortex and lateral thalamus, in long duration recording sessions – 24 h – performed before and after the induction of the spared nerve injury (SNI) – model of neuropathic pain (Decosterd and Woolf, 2000).

MATERIALS AND METHODS

ETHICS STATEMENT

All procedures and experiments adhered to the guidelines of the Committee for Research and Ethical Issues of IASP (Zimmermann, 1983), with the Ethical Guidelines for Animal Experimentation of the European Community Directive Number 86/609/ECC of 24 November of 1986, and were locally approved by national regulatory office [Direcção Geral de Veterinária (DGV), Lisboa, Portugal].

Twelve adult male *Sprague-Dawley* rats weighing between 350 and 450 g were used in this study. The rats were maintained on a 12-h light/dark cycle (light period from 7 a.m. to 7 p.m.), and given *ad libitum* access to food and water during the habituation and the recording sessions. Both habituation and recording sessions started at approximately the same time each day (7 p.m.).

SURGICAL METHODS

For the surgical implantation of the intracranial multielectrodes arrays the animals were anesthetized with a mixture of xylazine and ketamine (10 and 60 mg/kg, respectively, i.m.). Anesthesia was maintained with small additional injections of ketamine (one-third of the initial dosage). The depth of anesthesia and paralysis of the musculature was assessed by regularly testing the corneal blink, hindpaw withdrawal, and tail-pinch reflexes. After the anesthesia induction, each animal received a dose of atropine sulfate (0.02 mg/kg, s.c.), and 1 mL of serum (sucrose 2% p/v in NaCl 0.9% p/v, s.c.) every hour during the surgery. Core body temperature was measured with a rectal thermometer and maintained at 37˚C by means of a homoeothermic blanket system.

The animal's head was shaved and cleaned using a triple application of alcohol (70%, v/v) and betadine. A midline subcutaneous injection of 0.3 mL of 1% lignocaine (B Braun, Melsungen, Germany) was applied to the scalp for local analgesia. Anesthetized animals were secured in a stereotaxic frame using ear bars, and a midline incision was made caudally to the animal's eyes and ending between ears. The connective tissue was blunt-dissected from the skull, and the top of the skull was exposed and cleaned using hydrogen peroxide. After the scalp was excised, holes were drilled in the skull for microelectrode passage and for implantation of four to five screws. These screws were used for securing probes and for grounding purposes. The skull was covered by mineral oil in order to avoid dehydration during surgical procedure.

Each microelectrode array included eight filaments (1 array/area) of isonel-coated tungsten wire (35 μm diameter; California Fine Wire Company, Grover Beach, CA, USA) with impedances varying between 0.5 and 0.7 MΩ at 1 kHz, and a reference silver wire (150 μm diameter; A-M Systems Inc., WA, USA) for connection with the cranial screws. The microelectrode arrays were constructed in 4 × 2 architecture (1–2; 3–4; 5–6; 7–8 channels), interspaced 250-μm between lines and 400-μm between columns (**Figure 1A**; Silva et al., 2010). Only two of the electrodes per array (channel #3 [medial] and channel #6 [lateral]) were used for the recording of low-frequency LFPs; all eight electrodes in each array were used for recording of high frequency spike activity (data not reported here). The choice of channels was consistent across the different recording sessions for each animal. We preferred to use only LFP data because it fits better the inner characteristics of

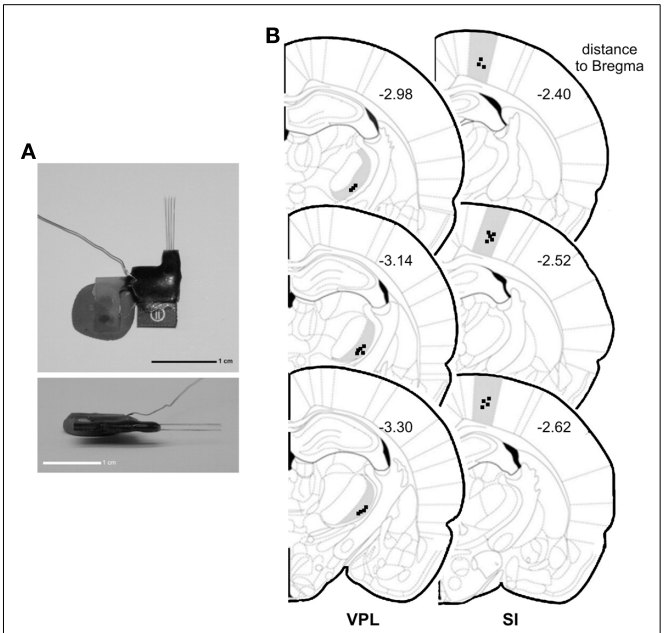

FIGURE 1 | Electrode construction and location of recordings. (A) Architecture of a microelectrode array used to record local field potentials (LFPs). **(B)** Coronal diagram illustrating the location of the LFPs recording sites (*dark squares*) in ventro-posterior-lateral thalamic nuclei (VPL) (*left side*) and in primary somatosensory cortex (SI) (*right side*). Numbers represent the rostro-caudal distance (in millimeters) relative to *bregma*.

the partial directed coherence (PDC) frequency-based methodology (see details in Partial Directed Coherence), and because LFPs reflect better the "average" neuronal activity in larger volumes of tissue which is the aim of the current study.

The arrays were oriented rostro-caudally and mounted in the holder of a hydraulic micropositioner (FHC Inc, Bowdoin, ME, USA) and subsequently slowly driven (50 μm/min) into the right primary somatosensory cortex (SI) and right ventro-posterior-lateral thalamic nucleus (VPL) after *dura mater* removal. The following coordinates in millimeters relative to bregma (Paxinos and Watson, 1998) were used to place the arrays: SI (−2.5 rostro-caudal, +2.5 medio-lateral, −1.6 dorso-ventral), and VPL (−3.1 rosto-caudal, +3.2 medio-lateral, −6.4 dorso-ventral). The location of the electrodes within SI and VPL was verified by mapping the neuronal responses elicited by tactile stimulation of the correspondent peripheral hindpaw digits receptive field. After the electrodes reached the correct position, the craniotomy was sealed with a layer of agar (4% in saline) and they were cemented to the skull screws by the use of dental acrylic. At the end of the surgery the animal was transferred to a recovery cage. The analgesic carprofen (5–10 mg/kg; Rimadyl, Pfizer Animal Health, Lisbon, Portugal) and the antibiotic amoxicillin (6 mg/kg; Clamoxyl, Pfizer Animal Health) were administered subcutaneously every 24-h during 2–3 days. Rats were allowed to recover for 1 week; after this week, animals were habituated to the recording chamber in five sessions of 90-min each in successive days. Behaviors were continuously recorded using a dedicated digital video-tracking system and synchronized with acquired neural data (CinePlex, Plexon Inc., Dallas, TX, USA).

Extracellular local field potentials (LFPs) – were recorded from the implanted microwire electrodes and processed by a 16-channel Multineuron Acquisition Processor system (16-MAP, Plexon Inc., Dallas, TX, USA). LFP signals recorded from the electrodes were pre-amplified (500×), band-pass filtered (0.5–400 Hz), and digitized at 500 Hz.

SPARED NERVE INJURY

Two animal groups were used: one group ($n = 6$) was recorded before and after the establishment of a peripheral nerve lesion (here afterward named as SNI-baseline and SNI-surgery sessions, respectively), while a second group ($n = 6$) was recorded before and after a SHAM surgery involving similar blunt dissection as the SNI-surgery but without any nerve lesion (here afterward named as SHAM-baseline and SHAM-surgery sessions, respectively). SNI and SHAM-surgery proceedings were implemented according to the published methodology (Decosterd and Woolf, 2000) in the left sciatic nerve contralateral to the hemisphere of electrodes implantation. Each recording session lasted 24-h (12/12-h in light/dark experimental conditions). The animals were placed in the recording chamber with cables connected 30-min before each 24-h session of LFPs continuous recording that were always initiated at 7 p.m. (start of dark phase). During the recording sessions the tethered animals were allowed to move freely in a 45-cm × 45-cm recording chamber with free access to food and water. Recordings were performed during two sessions in the baseline period (days -10 and -2 before surgery, pooled together as baseline recordings) and in two sessions after SHAM or SNI lesion (with recordings in day 2 and 10 after surgery. During the analysis of the experimental data it became clear that the two recordings done at 2 and 10 days after surgery (both after nerve lesion or sham surgery) did not significantly differ in any of our analysis; we have therefore used both recordings as coming from a single "post-surgery" period.

Sensory threshold for noxious stimulation was measured using von Frey filaments (Somedic, Sweden) as previously described (Chaplan et al., 1994). Von Frey testing was always performed during the light phase, 1 h before the beginning of each recording session. Testing was performed in an elevated chamber with a thin metallic mesh floor that allowed easy access to the plantar surface of the hindpaw. Filament series were run from the thinnest to the widest to detect the filament to which the animal withdraw the paw in at least 6 of 10 successive applications; we then performed another two series of 10 stimulations using the same filament (2-min intervals between sessions) and averaged the number of positive responses evoked by the three series.

STATEMAP

In order to identify wakefulness and sleep brain states of the rat circadian cycle, we used the method recently developed by Gervasoni, Lin, Ribeiro, and colleagues (Gervasoni et al., 2004; Lin et al., 2006). Briefly, this technique splits wakefulness and sleep states as distinct clusters into a two-dimensional state space map derived from two LFPs power spectral ratios. These ratios were heuristically established, and allowed for the best separation of each brain state based on their spectral features. Each point of the two-dimensional state space (example in **Figure 2A**) represents 1-s of ongoing brain activity. The density of points reflects the relative abundance of the different brain states, and the distance between two consecutive data points reflects the speed of spectral changes. Clustering was performed semi-automatically using the StateMap algorithm (Gervasoni et al., 2004). The slow-wave-sleep (SWS) cluster was always located on the upper right quadrant of the StateMap, whereas REM occupied the left quadrants, and the WK cluster occupied the lower right quadrant. The generated hypnograms (1-s bins of resolution) were used to calculate the frequency of episodes of each brain state, respective mean duration, and transitions between them (**Figure 2C**). The term "episode" was used to classify the occurrence of a brain state with duration in the hypnogram longer than 3 s.

Six different brain states were identified using the methodology described above. The WK state, characterized by theta (θ, 4–9 Hz) and gamma (γ, 30–55 Hz) LFPs spectral power (Steriade et al., 1993; Destexhe et al., 1999). During waking state the animals were involved in exploratory and stereotyped behaviors, such as locomotion, whisking, eating, drinking, etc. An additional transient waking state (WT) was characterized by synchronized rat whisker-twitching and corticothalamic LFPs oscillations at 7–12 Hz (Nicolelis et al., 1995; Fanselow and Nicolelis, 1999). These oscillations have been demonstrated to define a physiological state associated with normal sensory perception (Fanselow and Nicolelis, 1999; Wiest and Nicolelis, 2003). The REM was characterized by low cortical LFPs amplitude and high theta and gamma power state, and the animals were immobile with intermittent whisker and ear twitches (Vanderwolf, 1969; Steriade et al., 1993). In SWS state, the animals were immobile with eyes closed

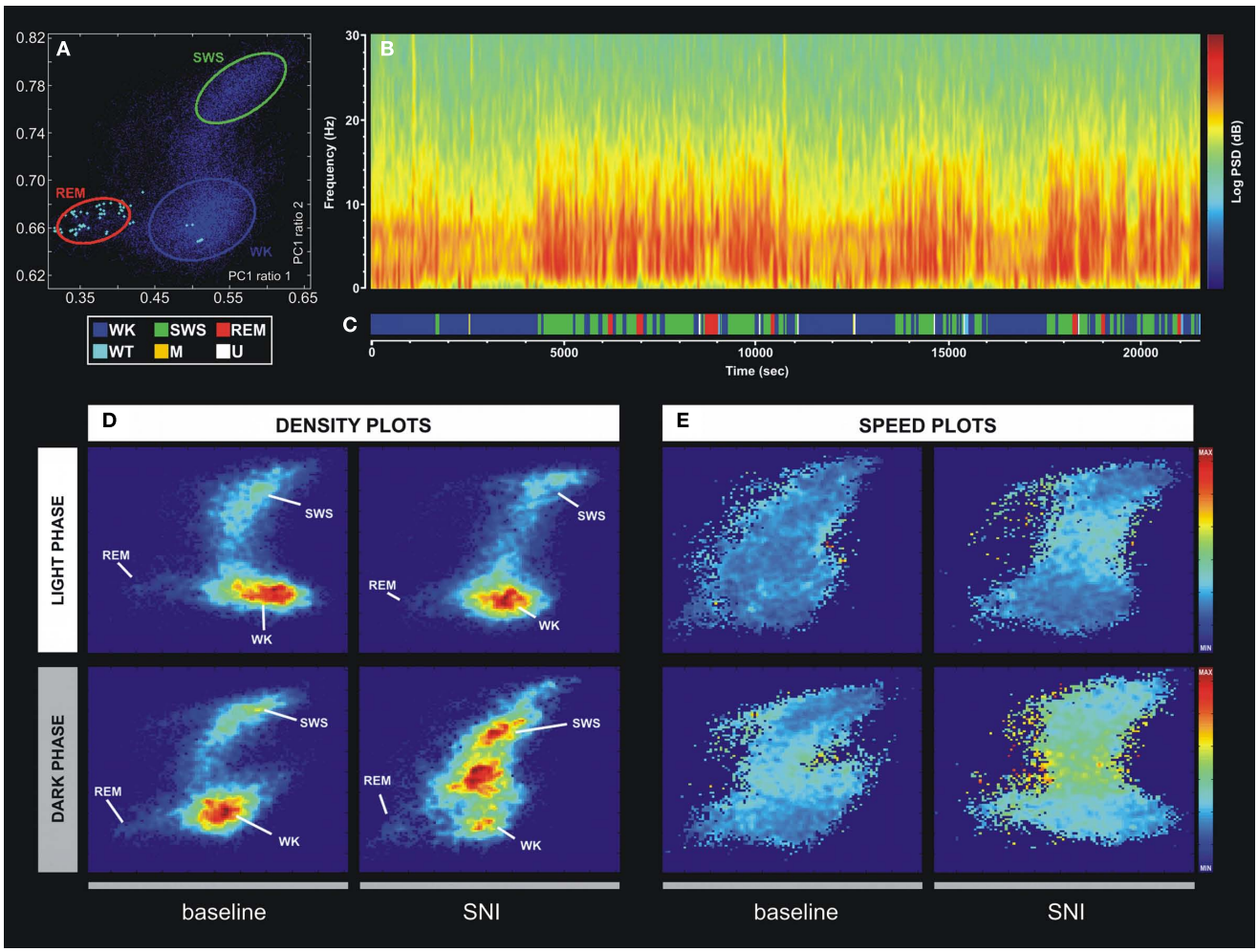

FIGURE 2 | Example of the technique used for statistical classification of oscillatory patterns according to Principal Component Analysis of the LFP signals. (A) Two-dimension brain StateMap. Three major clusters were represented corresponding to waking state (WK), slow-wave-sleep (SWS) and rapid-eye-movement (REM) states. **(B)** Power spectrogram of a SI LFP channel showing the different patterns of signal power oscillations across brain state episodes transitions. **(C)** Brain states hypnogram obtained from two-dimensional state illustrated in panel A. Six different brain states were coded: WK, SWS, REM, whisker-twitching (WT), M (undefined movement), and U (transition states). **(D)** Density plots calculated from scatter plots [e.g., **(A)**], showing the conserved cluster topography and the relative abundance of the various brain states. Scale from dark-blue (low-density) to red (high-density). **(E)** Speed plots representing the average of spontaneous trajectories within the two-dimensional StateMap. Stationarity (low speed) can be observed in the three main clusters (WK, SWS, and REM), whereas a maximum speed is reached during transitions from one clusters to another. After SNI lesion the velocity between WK and SWS state episodes increased, suggesting also an increase of WK/SWS transitions during the neuropathic pain period.

and had slow regular respiratory movements. The light SWS is characterized by sleep spindles (10–14 Hz) superimposed to delta waves (δ, 1–4 Hz), while in deep SWS the delta oscillations are more prominent (Achermann and Borbely, 1997; Destexhe et al., 1999). Furthermore, SWS state can be followed by a transient intermediate state of unstable oscillations named as U-transition state (Gottesmann, 1992; Mandile et al., 1996; Vescia et al., 1996). An additional M state was coded to include all unspecific patterns of oscillations that are exhibited by the rat. Examples of traces of the WK, SWS, and REM states are presented in **Figure A2** in Appendix. In order to confirm and validate the brain states hypnogram generated by the StateMap, two different experimenters visually identified WK, SWS, and REM episodes in the video recordings using the behavioral characteristics and associated LFP spectral features as detailed above (see also **Figure A1** in Appendix).

Rats spent more time in the awake state during the dark phase than during the light phase, and, conversely, the rat sleep states during the light phase are more frequent and longer than in the dark phase.

SPECTRAL ANALYSIS

Power spectral density and coherence

Power spectral density (PSD) of cortical and thalamic LFPs signals were calculated between 1 and 50 Hz using the Welch's method (MATLAB function), with 512-points fast Fourier transform of non-overlapping 1-s epochs (Hanning-window). Data is shown

as the percentage of total PSD within the frequency range considered (1–50 Hz). In order to determine the spectral coupling among signals from thalamocortical recorded regions, we have calculated the correlation coefficient or sometimes referred to as coherence in the signal engineering community. Coherence (C_{xy}) was measured applying the equation mathematically equivalent to $C_{xy} = |P_{xy}|^{2/}(P_xP_y)$ where the coherence from two signals, x and y, is equal to the average cross power spectral density (P_{xy}) normalized by the averaged power spectra of the two signals. Its value lies between 0 and 1, and it estimates the degree to which phases at the frequency (f) of interest are dispersed. $C_{xy} = 0$ means that phases are dispersed, and high coherence ($C_{xy} = 1$) means phases of signals x and y are identical and the two signals are totally phase-locked at this frequency. Cross power spectral density was calculated using the default MATLAB function.

Phase–coherence

Phase–coherence (ϕ_{xy}) of simultaneously recorded thalamocortical LFPs was evaluated calculating the Hilbert transform of each LFP segment. The phase angles of each signal segment were extracted and wrapped between 0° and 360° and displayed as a rose plot histogram. The whole rose plot (360°) was divided in 60 bins of resolution (6° per bin), with each bin displaying the respective population percentage. The Rayleigh test of uniformity ($P < 0.01$) was used to assess the resulting phase distributions for deviations from the circular uniform distribution. The degree of phase-locking or phase–coherence was determined calculating the concentration around the preferred phase in the circular-distribution, with its value lying between 0 and 1, where $\phi_{xy} = 0$ indicates that phase values at a particular frequency range are randomly distributed across the time interval, while $\phi_{xy} = 1$ indicates that phase values are exactly the same across the time interval. Phase–coherence values are inversely related to the Rayleigh P-value, with $\phi_{xy} = 0$ standing for uniform distribution. Circular statistics were calculated according to Fisher (1993).

Partial directed coherence

The PDC measure was used to identify and quantify the information flow interactions in the thalamocortical loop. The PDC method has been described in detail elsewhere (Sameshima and Baccalá, 1999; Baccala and Sameshima, 2001). Briefly, PDC is an alternative representation of Granger-causality involving multivariate processes to uncover direct influences in the frequency domain. The allied PDC from structure j-th to i-th at frequency λ is defined as:

$$\pi_{ij}(\lambda) = \frac{\bar{A}_{ij}(\lambda)}{\sqrt{\sum_{n=1}^{N} \bar{A}_{nj}(\lambda) \cdot \bar{A}^{*}_{nj}(\lambda)}}$$

where,

$$\overline{A}_{ij}(\lambda) = \begin{cases} 1 - \sum_{r=1}^{p} a_{ij}(r) \exp(-j2\pi\lambda r), & \text{if } i = j \\ -\sum_{r=1}^{p} a_{ij}(r) \exp(-j2\pi\lambda r), & \text{otherwise,} \end{cases}$$

a_{ij} are multivariate autoregressive coefficients and p is the model order. Nullity of PDC [$\pi_{ij}(\lambda) = 0$] can be interpreted as absence of effective connectivity from the j-th structure to the i-th structure at frequency λ and high PDC, near one, indicates strong connectivity between the structures. This can be interpreted as existence of information flow from brain area j to i.

STATISTICAL ANALYSIS

Neural activity data was processed and validated by offline analysis using NeuroExplorer 4 (NEX, Plexon Inc., Dallas, TX, USA) and exported to MatLab R14 Version 2008a (MathWorks, Natick, MA, USA) for complementary analysis. The PSD, C_{xy}, ϕ_{xy}, and PDC parameters were calculated using the same 40 LFPs signal segments of 10-s per recording session for each of the three more frequent behaviors (WK, SWS, and REM). These signal segments were randomly selected based on brain states hypnogram generated by the two-dimensional StateMap, and were verified and validated by visual inspection of behavior states in the video recordings and LFP spectral features.

In all analyses the distribution of the data was initially checked for potential deviations from normality assumptions, in order to choose the appropriate statistical test to apply. Non-parametric statistics were used when the Kolmogorov–Smirnov test (with Dallal–Wilkinson–Lilliefor corrected P-value) revealed deviations from the normal distribution ($P > 0.05$, Kolmogorov–Smirnov test). In this case, we performed non-parametric Wilcoxon signed-rank test for paired samples, or non-parametric Mann–Whitney test for unpaired samples. To compare multiple groups, we relied on the Kruskal–Wallis analysis of ranks (with *post hoc* Dunn's test), which is a non-parametric version of the classical one-way analysis of variance (ANOVA), and an extension of the Wilcoxon rank sum test to more than two groups. The level of significance was set as 5% (or $P < 0.05$).

Under normality assumptions, we used ANOVA to compare multiple groups. Statistical comparisons between frequency spectra were performed by a two-way ANOVA (groups × frequency bands) with *post hoc* Bonferroni test. In this case, and to facilitate interpretation of data, we performed separate comparisons for paired experimental groups [two-way ANOVA-repeated measures (RM); SHAM-baseline vs. SHAM-surgery and SNI-baseline vs. SNI-surgery] and for unpaired groups (two-way ANOVA non-matching; SHAM-baseline vs. SNI-baseline and SHAM-surgery vs. SNI-surgery). Thus, we are testing four separate comparisons on our dataset. We therefore need to take care in selecting our statistical significance level to account for the fact, by chance alone, we may encounter a favorable significance level simply because of the number of comparisons that we are conducting. In this case, we apply the Bonferroni correction. The Bonferroni correction states that if we test n comparisons on a set of data, then we should adjust our statistical significance level by a factor of $1/n$. Choosing a standard significance level of $P < 0.05$ for a single comparison, our Bonferroni-corrected significance level in this work is $P < 0.05/4$, or $P < 0.0125$.

The results were expressed as mean ± SEM.

HISTOLOGY

At the end of all experiments, the rats were deeply anesthetized with ketamine/xylazine mixture and the recording site was marked by injecting DC current (10–20 μA for 10–20 s) through one

microwire per matrix group, marking the area below the electrode tips. Afterward animals were perfused through the heart with 0.01 M phosphate buffer (pH = 7.2) in 0.9% saline solution followed by 4% paraformaldehyde. Brains were removed and post-fixed in 4% paraformaldehyde during 4 h and stored in 30% sucrose before freeze-sectioning into 60 μm sections, and stained for site identification under the microscope. This technique, in conjunction with careful notation of electrodes movements during implantation, allowed for localization of all recording sites (**Figure 1B**).

RESULTS

MECHANICAL STIMULATION THRESHOLDS

All SNI animals developed mechanical allodynia as indicated by the significant decrease in the mechanical withdrawal stimulus threshold in the hindpaw ipsilateral to the lesion, but not in the contralateral paw or in the SHAM-operated control group. In the SHAM group, no statistical difference was noted between the control period (SHAM-baseline) and after the surgery (SHAM-surgery; 16.6 ± 0.7 to 17.3 ± 0.8 g; NS; Wilcoxon test). In the SNI group, relative to baseline, a large decrease (83.9%) was observed in the threshold required to induce a paw response to stimulation with von Frey filaments (17.4 ± 1.2 to 2.8 ± 1.2 g; $P < 0.05$).

BRAIN STATES AND SPECTRAL CHARACTERISTICS

In order to quantitatively distinguish stable oscillatory episodes and brain states, we have used the StateMap algorithm (Gervasoni et al., 2004; Lin et al., 2006) that maps wakefulness and sleep states as distinct clusters in a two-dimensional state space derived from two LFP spectral ratios (**Figure 2A**). This technique presents the advantage of clearly distinguishing brain states that shared common spectral features, such as the theta oscillations observed during WK and REM episodes (**Figure 2B**). The three spectral clusters were clearly visible in two-dimensional state maps, corresponding to WK, SWS, and REM 1-s segments (hypnogram of **Figure 2C**).

All LFPs data segments with amplitude saturation were discarded from the working dataset (5.86 ± 0.91% of the total data per rat). The inspection of intracranial LFP activity confirmed that large-power oscillations were present during all brain states. The spontaneous spectral trajectories (distance between two consecutive points in the state map per unit of time, 1-s) that govern transitions between brain states were characterized by specific duration patterns in the state maps. The most frequent transitions occurred between WK → SWS → WK and WK → SWS → REM → WK episodes (**Figure 2C**). The speed of the spontaneous spectral trajectories on the state map can identify the regions in which little spectral variation exists (light blue area in **Figure 2E**) that coincide with the accumulation of points of the states identified by the algorithm [delimitation on blue (WK), green (SWS), and red (REM) in **Figure 2A** and density plot of **Figure 2D**], and the regions with fast spectral oscillations (yellow area in **Figure 2E**) that correspond to segments of transitions between different brain states (e.g., transitions between WK and SWS state episodes). After the nerve lesion (SNI-surgery vs. SNI-baseline) the spontaneous spectral trajectories velocity showed an increase in the WK → SWS → WK transitions during the dark phase (**Figure 2E**), whereas in the SHAM animals no differences were observed (data not presented in the figure). This increase in velocity can be associated with the increase in the number of WK–SWS transitions observed after nerve injury.

SLEEP–WAKE CHARACTERISTICS

Brain state episodes

As shown in **Table 1** (panel above), there were statistical significant differences between experimental groups in the number of brain state episodes (Kruskal–Wallis test; WK-light phase: K–W = 15.01, $P = 0.0018$, and WK-dark phase: K–W = 9.64, $P = 0.0219$; SWS-dark phase: K–W = 9.94, $P = 0.0191$; U-light phase: K–W = 10.38, $P = 0.0156$, and U-dark phase: K–W = 17.97, $P = 0.0004$). The *post hoc* comparison of the SNI-baseline group to the SNI-surgery showed a significant increase in the number of WK state episodes during the light and dark phases (291.1 ± 19.7 to 383.7 ± 22.1, and 310.3 ± 13.3 to 491.9 ± 31.7, respectively; Dunn's test, $P < 0.05$), while for SWS it was significant only during the dark phase (241.8 ± 26.2 to 376.5 ± 53.0; $P < 0.05$). In the case of U-transition state episodes, they also revealed an increase during both recording phases (258.2 ± 24.9 to 398.7 ± 16.9, and 318.4 ± 22.5 to 502.9 ± 23.3, respectively; $P < 0.05$). The *post hoc* comparison between SHAM-surgery/SNI-surgery groups revealed that the number of WK episodes in SNI-surgery was superior to SHAM-surgery during both light (383.7 ± 22.1 vs. 303.7 ± 29.9; Dunn's test, $P < 0.05$) and dark phases (491.9 ± 31.7 vs. 312.9 ± 20.9; $P < 0.05$), while the number of SWS episodes was superior in SNI group only during the dark phase (376.5 ± 28.1 vs. 254.1 ± 23.4; $P < 0.05$). A similar result was obtained for U-transition episodes during both phases (398.7 ± 16.9 vs. 286.3 ± 26.9, and 502.9 ± 23.2 vs. 312.3 ± 40.2, respectively; $P < 0.05$). In addition, *post hoc* analysis revealed no significant differences between SHAM-baseline/SHAM-surgery, and SHAM-baseline/SNI-baseline sessions.

In terms of the mean duration of each state episode (**Table 1**, panel below), there were statistical differences between experimental groups but only for the U-transition state (Kruskal–Wallis test; light phase: K–W = 18.98, $P = 0.0003$, and dark phase: K–W = 15.92, $P = 0.0012$). *Post hoc* analysis revealed a significant decrease of the U-transition state episodes mean duration for SNI-baseline/SNI-surgery (light phase: 25.4 ± 2.4 to 11.6 ± 1.3 s; and dark phase: 23.4 ± 4.2 to 8.3 ± 1.6; Dunn's test, $P < 0.05$), and SHAM-surgery/SNI-surgery comparisons (light phase: 27.8 ± 5.6 to 11.6 ± 1.3 s; and dark phase: 28.4 ± 7.9 to 8.3 ± 1.6, $P < 0.05$). In addition, *post hoc* analysis revealed no significant differences between SHAM-baseline/SHAM-surgery, or SHAM-baseline/SNI-baseline sessions.

Brain state transitions

After the SNI nerve lesion, all rats showed an increase in the number of state transitions between the more representative brain states (WK, SWS, and REM), indicating an increase of circadian pattern fragmentation in these animals (**Table 2**). ANOVA revealed significant differences between all experimental groups for WK–SWS transitions (Kruskal–Wallis test; light phase: K–W = 9.98, $P = 0.0188$, and dark phase: K–W = 9.46, $P = 0.0237$), SWS–WK (dark phase: K–W = 13.46, $P = 0.0037$), SWS–REM (light phase:

Table 1 | The number and mean duration of episodes from the different sleep states to wakefulness are shown for the light and dark phases (expressed as mean value per period of 12-h).

		SHAM		SNI	
		Baseline ($n = 6$)	**Surgery ($n = 6$)**	**Baseline ($n = 6$)**	**Surgery ($n = 6$)**
EPISODE					
WK	Light	256.3 (23.4)	303.7 (29.2) #	291.1 (19.7)	383.7 (22.1)*
	Dark	314.1 (15.2)	312.9 (20.9) #	310.3 (13.3)	491.9 (31.7)*
SWS	Light	207.8 (12.3)	199.1 (23.3)	195.5 (14.2)	177.3 (24.3)
	Dark	232.7 (14.2)	254.1 (23.4) #	241.8 (26.2)	376.5 (28.1)*
REM	Light	37.1 (7.2)	23.4 (7.2)	38.3 (6.0)	22.1 (7.2)
	Dark	56.3 (11.0)	58.0 (3.2)	59.1 (11.2)	68.2 (21.2)
WT	Light	26.0 (9.8)	15.8 (3.4)	23.4 (9.9)	18.8 (3.3)
	Dark	19.5 (5.4)	18.2 (3.7)	18.3 (5.7)	17.8 (3.1)
M	Light	11.4 (4.3)	6.7 (2.1)	13.6 (4.5)	6.8 (2.1)
	Dark	21.1 (2.4)	13.9 (0.9)	20.8 (3.7)	17.7 (3.4)
U	Light	282.2 (25.9)	286.3 (26.9) #	258.2 (24.9)	398.6 (16.9)*
	Dark	315.9 (33.7)	312.3 (40.2) #	318.4 (22.5)	502.9 (23.2)*
DURATION (S)					
WK	Light	66.4 (15.1)	59.1 (17.9)	61.1 (14.1)	58.4 (15.7)
	Dark	61.1 (24.6)	59.9 (15.6)	64.9 (17.1)	44.9 (8.9)
SWS	Light	68.8 (26.5)	66.1 (26.6)	65.2 (12.5)	74.3 (16.2)
	Dark	47.3 (23.5)	51.2 (24.5)	49.9 (15.1)	35.4 (9.8)
REM	Light	34.3 (13.2)	27.6 (14.4)	29.2 (9.8)	31.3 (11.2)
	Dark	31.0 (5.7)	28.1 (8.8)	23.1 (8.8)	26.2 (10.0)
WT	Light	6.8 (3.9)	4.0 (2.9)	3.3 (0.5)	5.8 (1.7)
	Dark	5.5 (3.7)	5.4 (1.1)	4.3 (0.9)	2.9 (0.3)
M	Light	15.2 (10.7)	9.3 (4.8)	10.7 (6.1)	5.7 (2.1)
	Dark	7.9 (2.6)	5.2 (2.7)	6.8 (2.4)	7.4 (1.8)
U	Light	23.5 (2.9)	27.8 (5.6) #	25.4 (2.4)	11.6 (1.3)*
	Dark	27.9 (3.4)	28.4 (7.9) #	23.4 (4.2)	8.3 (1.6)*

Six different brain states were considered: WK, waking state; SWS, slow-wave-sleep; REM, rapid-eye-movement sleep; WT, whisker-twitching; M, undefined movement; U, transition state. Values are expressed as mean (SEM). Statistical differences between study groups indicated by asterisks (*) for SNI-baseline/SNI-surgery and cardinal (#) for SHAM-surgery/SNI-surgery comparisons (/# $P < 0.05$).*

K–W = 9.99, $P = 0.0187$), REM–WK (light phase: K–W = 9.21, $P = 0.0266$), WK–U (light phase: K–W = 12.13, $P = 0.0070$), U–WK (light phase: K–W = 10.85, $P = 0.0125$, and dark phase: K–W = 11.57, $P = 0.0090$), and REM–U (light phase: K–W = 12.19, $P = 0.0068$).

When compared SNI-baseline group to SNI-surgery (**Table 2**, significance indicated by asterisks symbols), *post hoc* analysis revealed an increase of the WK-to-SWS transitions during the light and dark phases (100.9 ± 9.1 to 173.9 ± 10.9, and 119.2 ± 24.4 to 201.9 ± 32.6, respectively; Dunn's test, $P < 0.05$), and SWS-to-WK transitions but only during the dark phase (87.1 ± 11.9 to 168.9 ± 11.2; $P < 0.05$). Other low-frequency state transitions such as SWS-to-REM and REM-to-WK increased only during the light phase (6.5 ± 1.4 to 22.4 ± 2.9, and $7.6 \pm$ to 45.2 ± 14.1, respectively; $P < 0.05$). In addition, all SNI rats showed a significant increase in the transitions mediated by U-state and WK states. For example, the WK-to-U transitions increased during the light phase (126.3 ± 30.9 to 215.7 ± 17.1; $P < 0.05$), while U-to-WK increased during both phases (134.1 ± 19.4 vs. 211.4 ± 21.2, and 195.1 ± 29.1 vs. 272.3 ± 8.6, respectively; $P < 0.05$), and the REM-to-U transitions increased during the light phase of the recordings (8.1 ± 2.1 vs. 32.1 ± 5.2; $P < 0.05$).

Post hoc statistical analysis of the SNI-surgery/SHAM-surgery groups showed similar differences to those observed when comparing SNI-surgery/SNI-baseline (**Table 2**, significance indicated by cardinal symbols). In SNI-surgery group, the number of WK-to-SWS transitions was superior to SHAM-surgery during the light (173.9 ± 10.9 vs. 97.2 ± 18.5; Dunn's test, $P < 0.05$) and dark phases (201.9 ± 32.6 vs. 124.4 ± 19.9; $P < 0.05$), whereas for SWS-to-WK it was significant only during the dark phase (168.9 ± 11.2 vs. 88.3 ± 9.3; $P < 0.05$). Other low-frequency transitions such as SWS-to-REM and REM-to-WK increased only during light phase (22.4 ± 2.9 vs. 6.2 ± 4.4, and 45.2 ± 14.1 vs. 7.7 ± 2.3, respectively; $P < 0.05$). Transitions mediated by U-state also increased in SNI-surgery group: WK-to-U transitions during the light phase (215.21 ± 17.1 vs. 111.9 ± 22.4; $P < 0.05$); U-to-WK transitions during the light (211.4 ± 21.2 vs. 137.7 ± 14.1; $P < 0.05$) and dark phases (272.3 ± 8.6 vs. 197.4 ± 21.3; $P < 0.05$); and REM-to-U transitions during the light phase (32.1 ± 5.2 vs. 9.3 ± 2.2; $P < 0.05$).

Table 2 | The number of transitions from the different sleep states to wakefulness are shown for the light and dark phases (expressed as mean value per period of 12-h).

		SHAM		SNI	
		Baseline ($n = 6$)	**Surgery ($n = 6$)**	**Baseline ($n = 6$)**	**Surgery ($n = 6$)**
TRANSITIONS					
WK–SWS	Light	102.7 (14.7)	97.2 (18.5) #	100.9 (9.1)	173.9 (10.9)*
	Dark	125.2 (14.3)	124.4 (19.9) #	119.2 (24.4)	201.9 (32.6)*
SWS–WK	Light	118.1 (16.4)	119.1 (21.7)	121.0 (14.4)	159.8 (15.0)
	Dark	89.7 (13.4)	88.3 (9.3) #	87.1 (11.9)	168.8 (11.2)*
SWS–REM	Light	4.5 (1.1)	6.2 (4.4) #	6.5 (1.4)	22.4 (2.9)*
	Dark	16.6 (7.4)	16.1 (9.1)	14.8 (8.1)	15.5 (7.7)
REM–WK	Light	6.6 (3.9)	7.7 (2.3) #	7.6 (2.8)	45.2 (14.1)*
	Dark	18.6 (17.8)	18.9 (23.2)	15.9 (10.4)	44.8 (2.3)
WK–U	Light	122.1 (32.4)	111.9 (22.4) #	126.3 (30.9)	215.7 (17.1)*
	Dark	151.6 (37.1)	152.7 (39.2)	149.7 (55.1)	248.4 (21.9)
U–WK	Light	138.1 (25.1)	137.7 (14.1) #	134.1 (19.4)	211.4 (21.2)*
	Dark	199.7 (24.2)	197.4 (21.3) #	195.1 (29.1)	272.3 (8.6)*
SWS–U	Light	89.3 (35.4)	94.0 (29.8)	98.1 (31.3)	93.1 (15.2)
	Dark	76.4 (7.8)	74.4 (8.2)	73.5 (7.7)	135.7 (41.1)
U–SWS	Light	45.2 (33.4)	41.9 (29.1)	54.1 (23.4)	95.7 (18.3)
	Dark	106.7 (29.8)	104.1 (22.8)	104.8 (35.7)	148.3 (26.6)
REM–U	Light	7.5 (3.7)	9.3 (2.2) #	8.1 (2.1)	32.1 (5.2)*
	Dark	29.4 (27.1)	31.3 (26.1)	32.4 (16.1)	34.4 (10.2)
U–REM	Light	7.6 (6.1)	5.6 (1.9)	9.2(4.3)	29.3 (4.3)
	Dark	34.3 (21.1)	33.7 (19.4)	34.9 (17.1)	66.7 (10.2)

Values are expressed as mean (SEM). Statistical differences between study groups indicated by asterisks (*) for SNI-baseline/SNI-surgery and cardinal (#) for SHAM-surgery/SNI-surgery comparisons (/# $P < 0.05$).*

In addition, *post hoc* analysis revealed no significant differences between SHAM-baseline/SHAM-surgery, or SHAM-baseline/SNI-baseline sessions across the considered state transitions.

THALAMOCORTICAL POWER SPECTRAL DENSITY AND COHERENCE

Power spectral density analysis was employed to visualize the power spectra of LFPs of WK, SWS, and REM brain states across the studied frequency range (1–50 Hz). A qualitative comparison of PSD measurements between the thalamocortical LFPs is shown in **Figure 3A–D**, comparing both SHAM-baseline and SNI-baseline with SHAM-surgery and SNI-surgery. The inspection of PSD confirmed that characteristic power oscillations were as expected, with a prominent high-power in theta frequency band (4–9 Hz) in WK and REM episodes, and a high-power in delta band (1–4 Hz) observed during SWS episodes.

The qualitative comparison of the coherence measurements between the thalamocortical LFPs clearly showed similar values of coherence activity across selected brain states (**Figures 3E,F**). Note however that REM revealed an increase of coherence activity across gamma frequency band (30–50 Hz) that was not observed in WK or SWS episodes. We present additional data (see **Figure A3** in Appendix) of average PSD and coherence per frequency band. ANOVA (two-way ANOVA) revealed no differences in these measurements between experimental groups.

THALAMOCORTICAL PHASE–COHERENCE

As shown in **Figure 4A**, there were statistical significant differences between experimental groups in SI–VPL phase–coherence (1–50 Hz frequency range) for WK and SWS brain states (Kruskal–Wallis test; K–W = 13.28, $P = 0.0041$; and K–W = 12.08, $P = 0.0071$; respectively), and no differences for REM state (K–W = 3.47, $P = 0.3243$). When compared SNI-baseline group to SNI-surgery, *post hoc* analysis revealed a significant enhancement of SI–VPL phase–coherence after nerve lesion (WK: from 0.52 ± 0.02 to 0.65 ± 0.04; SWS: from 0.61 ± 0.02 to 0.69 ± 0.03; Dunn's test, $P < 0.05$), and also the comparison of SHAM-surgery/SNI-surgery groups (WK: from 0.55 ± 0.05 to 0.65 ± 0.04; SWS: from 0.58 ± 0.04 to 0.69 ± 0.03; $P < 0.05$; **Figure 4A**). In addition, *post hoc* analysis revealed no significant differences between SHAM-baseline/SHAM-surgery groups for WK, SWS, and REM brain states. As shown in **Figure 4B**, the rose plot histograms present a narrow range of phase–coherence in all three brain states, indicating a high degree of phase synchronization of SI–VPL LFPs activity; this suggests a broader coordination of thalamocortical activities after nerve lesion. Indeed, all phase distributions are significantly non-uniform ($P < 0.01$, Rayleigh test of uniformity).

The analyses of mean phase–coherence across frequency bands are illustrated in **Figure 4C**. In the case of WK state, the comparison of SHAM-baseline/SHAM-surgery groups

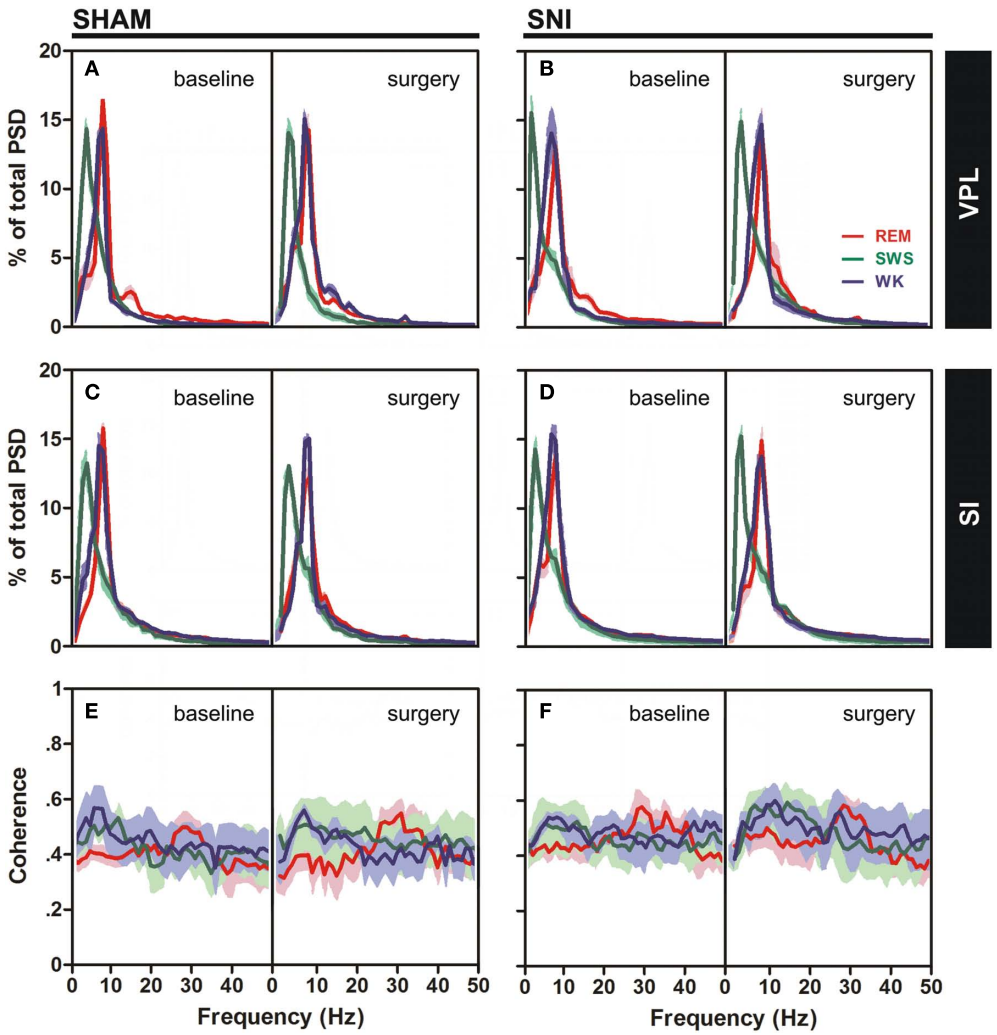

FIGURE 3 | Spectral analysis of SI–VPL LFPs channels during WK (blue), SWS (green), and REM (red) states. Data were presented comparing the baseline (left side of each panel) and respective SHAM or SNI lesion (right side). Values are expressed for all animals as mean (±SEM). **(A–D)** Power spectral density (PSD) of LFPs normalized by the percentage of total power within the frequency range analyzed (1–50 Hz) for VPL **(A,B)** and SI **(C,D)** channels. PSD showed that spectral power patterns were conserved across the experimental groups. **(E,F)** Coherence between VPL and SI LFPs showed similar levels of coherence activity across all experimental groups.

revealed no significant differences across experimental groups [two-way ANOVA-RM: $F_{(1,25)} = 1.73$, $P = 0.2182$] and interaction [groups × frequency bands; $F_{(4,25)} = 0.48$, $P = 0.7479$], and a significant effect across frequency bands [$F_{(4,25)} = 10.74$, $P < 0.0001$]. In addition, the comparison of SHAM-baseline/SNI-baseline groups revealed also no significant differences across experimental groups [two-way ANOVA: $F_{(1,50)} = 1.56$, $P = 0.2173$] and interaction [$F_{(4,50)} = 0.16$, $P = 0.9567$], and a significant effect across frequency bands [$F_{(4,50)} = 7.65$, $P < 0.0001$]. On the other hand, when comparing SNI-baseline/SNI-surgery groups significant effects were encountered across groups [two-way ANOVA-RM: $F_{(1,25)} = 19.30$, $P = 0.0002$] and frequency bands [$F_{(4,25)} = 3.15$, $P = 0.0314$], and no significant interaction effect between these two factors [$F_{(4,25)} = 1.55$, $P = 0.2180$]. *Post hoc* analysis revealed a significant increase of the mean phase–coherence across delta frequency band in the SNI-surgery group ($P < 0.0125$, Bonferroni test with corrected P-value). In the case of the comparison of SHAM-surgery/SNI-surgery groups, ANOVA revealed significant differences across experimental groups [two-way ANOVA: $F_{(1,50)} = 32.49$, $P < 0.0001$], and no differences across frequency bands [$F_{(4,50)} = 2.13$, $P = 0.0914$] and interaction effect [$F_{(4,50)} = 1.40$, $P = 0.2475$]. *Post hoc* analysis revealed a significant increase of mean phase–coherence across delta ($P < 0.0025$, Bonferroni test with corrected P-value) and theta ($P < 0.0125$) frequency bands after nerve lesion (**Figure 4C**). In the case of SWS state, the comparison of SHAM-baseline/SHAM-surgery groups revealed no significant differences across experimental groups [two-way ANOVA-RM: $F_{(1,25)} = 0.04$, $P = 0.8346$], frequency bands [$F_{(4,25)} = 1.25$, $P = 0.3191$], as well for the interaction effect [$F_{(4,25)} = 0.01$,

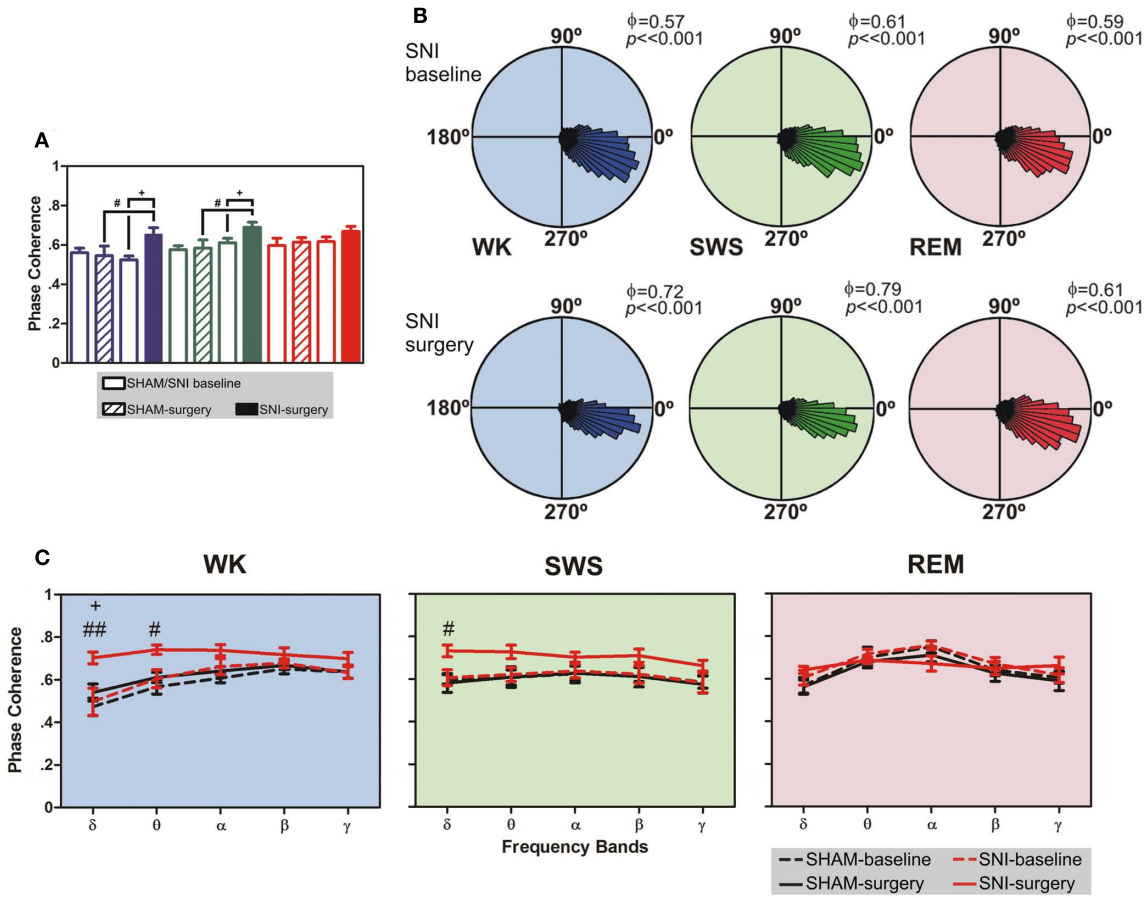

FIGURE 4 | Phase-locking of cortical and thalamic local field potentials. **(A)** Comparison of mean phase–coherence of SI–VPL LFPs segments recorded during WK, SWS, and REM states. Data was calculated for a 1- to 50-Hz frequency range. A significant increase of phase–coherence was observed for WK and SWS episodes after nerve lesion. **(B)** Examples of LFPs phase distributions during WK, SWS, and REM episodes for one rat submitted to the nerve lesion protocol. The numbers in the upper right corner of each plot shows the value of the mean phase–coherence. All circular-concentration distributions are significantly non-uniform (Rayleigh test, $P < 0.01$) indicating a high degree of thalamocortical phase synchronization. **(C)** Average phase–coherence across frequency bands analyzed during the baseline and respective SHAM or SNI lesion (surgery). Frequency bands: delta (δ, 1–4 Hz), theta (θ, 4–9 Hz), alpha (α, 9–15 Hz), beta (β, 15–30 Hz), and slow-gamma (γ, 30–50 Hz). Comparison of SNI-surgery in respect to SNI-baseline (plus symbols), and to SHAM-surgery (cardinal symbols). Values are expressed as mean ± SEM. +/# $P < 0.0125$, ++/## $P < 0.0025$, +++/### $P < 0.0002$ (Bonferroni test with corrected P-value).

$P = 0.9996$]. A similar result were obtained for the comparison of SHAM-baseline/SNI-baseline groups [two-way ANOVA: groups $F_{(1,50)} = 0.08$, $P = 0.7822$, frequency bands $F_{(4,50)} = 0.52$, $P = 0.7172$, and interaction $F_{(4,50)} = 0.02$, $P = 0.9992$]. On the other hand, when comparing SNI-baseline/SNI-surgery groups significant differences were encountered across groups [two-way ANOVA-RM: $F_{(1,25)} = 54.79$, $P < 0.0001$], and no differences across frequency bands [$F_{(4,25)} = 0.48$, $P = 0.7485$] and interaction effect [$F_{(4,25)} = 0.71$, $P = 0.5902$]. In the case of the comparison of SHAM-surgery/SNI-surgery groups, ANOVA revealed significant differences across experimental groups [two-way ANOVA: $F_{(1,50)} = 21.97$, $P < 0.0001$], and no differences across frequency bands [$F_{(4,50)} = 0.58$, $P = 0.6803$] and interaction effect [$F_{(4,50)} = 0.34$, $P = 0.8475$]. *Post hoc* analysis revealed a significant increase of mean phase–coherence across delta frequency band after nerve lesion ($P < 0.0125$, Bonferroni test with corrected P-value; **Figure 4C**).

In the case of REM state, the comparison of SHAM-baseline/ SHAM-surgery groups, SHAM-baseline/SNI-baseline, and SHAM-surgery/SNI-surgery revealed no significant differences across experimental groups [two-way ANOVA-RM: $F_{(1,25)} = 0.64$, $P = 0.4323$; and two-way ANOVA: $F_{(1,50)} = 1.04$, $P = 0.3124$; $F_{(1,50)} = 1.97$, $P = 0.1664$; respectively] and interaction effect [groups × frequency bands, two-way ANOVA-RM: $F_{(4,25)} = 0.05$, $P = 0.9952$; and two-way ANOVA: $F_{(4,50)} = 0.08$, $P = 0.9884$; $F_{(4,50)} = 1.16$, $P = 0.3378$; respectively], and a significant effect across frequency bands [two-way ANOVA-RM: $F_{(4,25)} = 9.51$, $P < 0.0001$; and two-way ANOVA: $F_{(4,50)} = 9.40$, $P < 0.0001$; $F_{(4,50)} = 2.85$, $P = 0.0330$; respectively]. In addition, when comparing SNI-baseline/SNI-surgery groups no statistical differences were encountered across experimental groups [two-way ANOVA-RM: $F_{(1,25)} = 1.13$, $P = 0.2977$], frequency bands [$F_{(4,25)} = 2.17$, $P = 0.1013$], as well for the interaction effect [$F_{(4,25)} = 1.15$, $P = 0.3024$].

THALAMOCORTICAL PARTIAL DIRECTED COHERENCE

The changes of thalamocortical information flow in SHAM and SNI animals before and after surgery were determined by PDC analysis. **Figure 5A** shows the averaged PDC between SI cortex and VPL thalamic nuclei during WK, SWS, and REM states selected using the two-dimensional cluster technique described above. The qualitative comparison of the data suggests that, in the SNI-surgery group, the amount of information flow from VPL-to-SI and from SI-to-VPL decreased in both directions indicating that less information was transmitted in the thalamocortical loop after peripheral sciatic nerve injury. In addition, the decrease in the descending direction (from cortex to thalamus) was smaller when compared to the ascending direction (from thalamus to cortex).

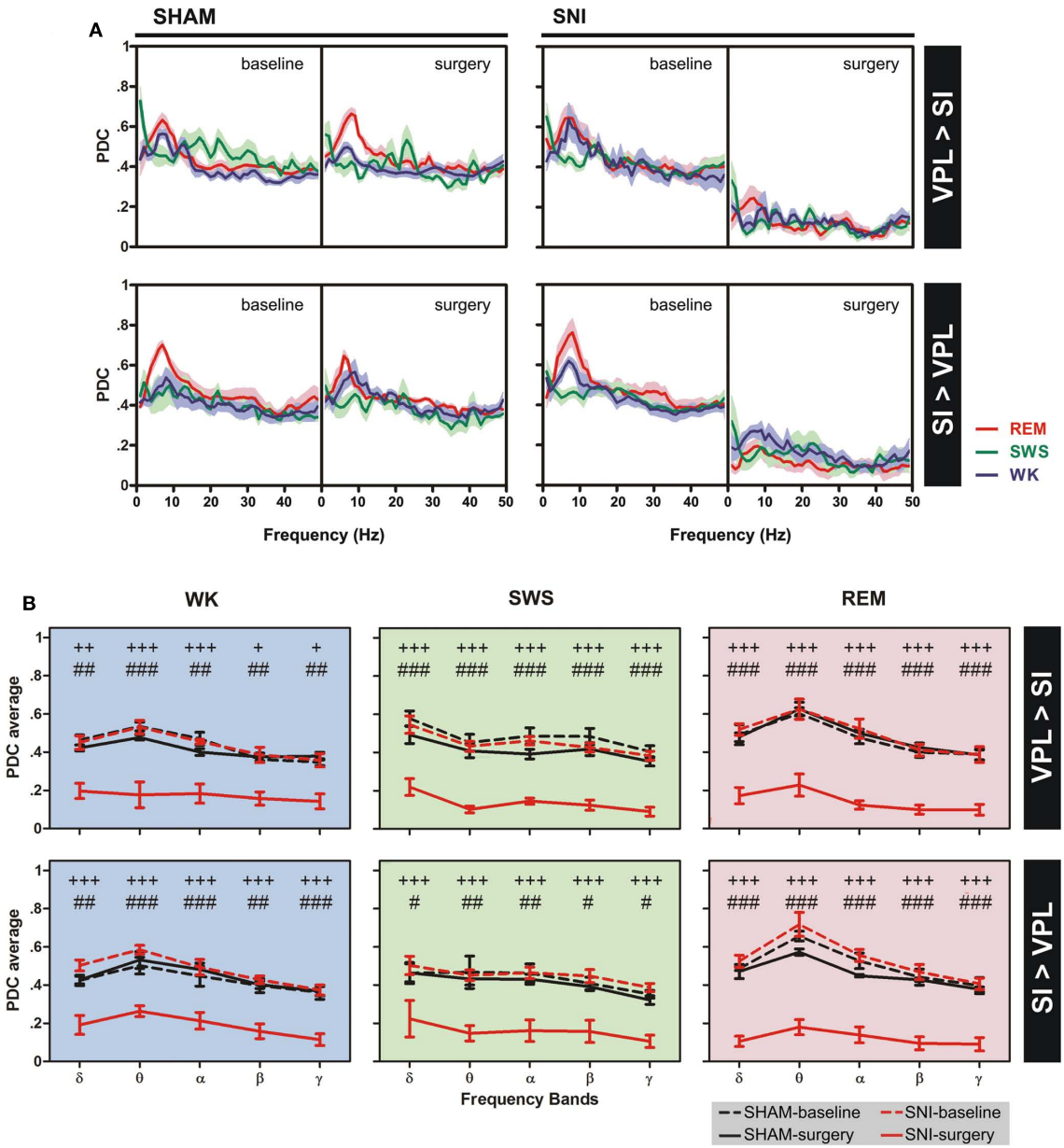

FIGURE 5 | Information flow between the two recorded regions were determined by partial directed coherence (PDC) analysis during WK (blue), SWS (green), and REM (red) states. (A) The amount of information flow in ascending (VPL-to-SI) and descending (SI-to-VPL) directions did not show significant differences for SHAM-lesion animals, while decreased significantly for SNI group after peripheral nerve lesion, indicating that less information was processed in the thalamocortical circuit after lesion. **(B)** The averaged PDC across frequency bands revealed a significant decrease of information flow for both directions at all frequency bands. Frequency bands: delta (δ, 1–4 Hz), theta (θ, 4–9 Hz), alpha (α, 9–15 Hz), beta (β, 15–30 Hz), and slow-gamma (γ, 30–50 Hz). Comparison of SNI-surgery groups in respect to SNI-baseline (plus symbols), and to SHAM-surgery (cardinal symbols). Values are expressed as mean ± SEM. +/# $P < 0.0125$, ++/## $P < 0.0025$, +++/### $P < 0.0002$ (Bonferroni test with corrected P-value).

In order to detail the thalamocortical information flow across frequency bands, we calculated the averaged PDC per range of frequencies (**Figure 5B**). ANOVA was performed to measure the differences in the averaged PDC across experimental groups. In the case of the thalamocortical ascending direction (VPL-to-SI), the comparison of SHAM-baseline/SHAM-surgery groups, and SHAM-baseline/SNI-baseline revealed no significant differences across experimental groups [two-way ANOVA-RM: WK $F_{(1,25)} = 2.65$, $P = 0.0746$; SWS $F_{(1,25)} = 2.67$, $P = 0.0691$; REM $F_{(1,25)} = 0.73$, $P = 0.4006$; and two-way ANOVA: WK $F_{(1,50)} = 0.01$, $P = 0.9706$; SWS $F_{(1,50)} = 1.94$, $P = 0.1703$; REM $F_{(1,50)} = 0.79$, $P = 0.3789$; respectively] and interaction effect [groups × frequency bands; two-way ANOVA-RM: WK $F_{(4,25)} = 2.07$, $P = 0.3442$; SWS $F_{(4,25)} = 0.50$, $P = 0.7290$; REM $F_{(4,25)} = 0.36$, $P = 0.8356$; and two-way ANOVA: WK $F_{(4,50)} = 0.17$, $P = 0.9526$; SWS $F_{(4,50)} = 0.10$, $P = 0.9817$; REM $F_{(4,50)} = 0.11$, $P = 0.9778$; respectively], and as expected a significant effect across frequency bands [two-way ANOVA-RM: WK $F_{(4,25)} = 11.87$, $P < 0.0001$; SWS $F_{(4,25)} = 24.66$, $P < 0.0001$; REM $F_{(4,25)} = 10.85$, $P < 0.0001$; and two-way ANOVA: WK $F_{(4,50)} = 12.09$, $P < 0.0001$; SWS $F_{(4,50)} = 6.07$, $P = 0.0005$; REM $F_{(4,50)} = 11.06$, $P < 0.0001$; respectively]. On the other hand, when comparing SNI-baseline/SNI-surgery groups significant differences were encountered across experimental groups [two-way ANOVA-RM; WK $F_{(1,25)} = 85.33$, $P < 0.0001$; SWS $F_{(1,25)} = 725.00$, $P < 0.0001$; REM $F_{(1,25)} = 362.60$, $P < 0.0001$], frequency bands [WK $F_{(4,25)} = 8.79$, $P < 0.0001$; SWS $F_{(4,25)} = 4.78$, $P = 0.0053$; REM $F_{(4,25)} = 4.72$, $P = 0.0056$], and no interaction effect between these two factors [WK $F_{(4,25)} = 0.73$, $P = 0.5787$; SWS $F_{(4,25)} = 0.39$, $P = 0.8168$; REM $F_{(4,25)} = 1.48$, $P = 0.2378$]. *Post hoc* analysis revealed a significant decrease of PDC activity across all frequency bands after nerve lesion [WK: delta ($P < 0.0025$), theta and alpha ($P < 0.0002$), beta and gamma ($P < 0.0125$); SWS and REM: all bands ($P < 0.0002$); Bonferroni test with corrected *P*-value; **Figure 5B**]. The comparison of SHAM-surgery/SNI-surgery groups revealed significant differences across experimental groups [two-way ANOVA; WK $F_{(1,50)} = 110.70$, $P < 0.0001$; SWS $F_{(1,50)} = 202.30$, $P < 0.0001$; REM $F_{(1,50)} = 273.50$, $P < 0.0001$] and frequency bands but only for SWS and REM state [$F_{(4,50)} = 5.17$, $P = 0.0015$; $F_{(1,50)} = 9.90$, $P < 0.0001$; respectively], and no interaction effect between these two factors. *Post hoc* analysis revealed a significant decrease of PDC activity across all frequency bands after nerve lesion [WK: theta ($P < 0.0002$), delta, alpha, beta, and gamma ($P < 0.0025$); SWS and REM: all bands ($P < 0.0002$); Bonferroni test with corrected *P*-value; **Figure 5B**].

In the case of the thalamocortical descending direction (SI-to-VPL), the comparison of SHAM-baseline/SHAM-surgery groups, and SHAM-baseline/SNI-baseline revealed no significant differences across experimental groups [two-way ANOVA-RM: WK $F_{(1,25)} = 1.12$, $P = 0.3006$; SWS $F_{(1,25)} = 0.76$, $P = 0.0620$; REM $F_{(1,25)} = 1.93$, $P = 0.1704$; and two-way ANOVA: WK $F_{(1,50)} = 2.20$, $P = 0.0701$; SWS $F_{(1,50)} = 0.51$, $P = 0.4780$; REM $F_{(1,50)} = 1.88$, $P = 0.1767$; respectively] and interaction effect [two-way ANOVA-RM: WK $F_{(4,25)} = 0.21$, $P = 0.9319$; SWS $F_{(4,25)} = 0.07$, $P = 0.9912$; REM $F_{(4,25)} = 1.03$, $P = 0.4116$; and two-way ANOVA: WK $F_{(4,50)} = 0.39$, $P = 0.8133$; SWS $F_{(4,50)} = 0.16$, $P = 0.9559$; REM $F_{(4,50)} = 0.12$, $P = 0.9731$; respectively], and a significant effect across frequency bands but only for WK and REM states [two-way ANOVA-RM: WK $F_{(4,25)} = 3.54$, $P = 0.0203$; REM $F_{(4,25)} = 7.20$, $P < 0.0001$; and two-way ANOVA: WK $F_{(4,50)} = 7.17$, $P = 0.0001$; REM $F_{(4,50)} = 16.36$, $P < 0.0001$; respectively]. On the other hand, when comparing SNI-baseline/SNI-surgery groups significant differences were encountered across experimental groups [two-way ANOVA-RM; WK $F_{(1,25)} = 257.20$, $P < 0.0001$; SWS $F_{(1,25)} = 158.90$, $P < 0.0001$; REM $F_{(1,25)} = 304.10$, $P < 0.0001$] and frequency bands but only for WK and REM state [$F_{(4,25)} = 5.98$, $P = 0.0016$, and $F_{(4,25)} = 7.54$, $P < 0.0001$, respectively], and no interaction effect between these two factors. *Post hoc* analysis revealed a significant decrease of PDC activity across all frequency bands after nerve lesion [WK, SWS, and REM: all bands ($P < 0.0002$); Bonferroni test with corrected *P*-value; **Figure 5B**]. In addition, the comparison of SHAM-surgery/SNI-surgery groups revealed significant differences across experimental groups [two-way ANOVA; WK $F_{(1,50)} = 133.60$, $P < 0.0001$; SWS $F_{(1,50)} = 66.76$, $P < 0.0001$; REM $F_{(1,50)} = 340.90$, $P < 0.0001$] and frequency bands for WK and REM states [$F_{(4,50)} = 6.01$, $P = 0.0005$, and $F_{(4,50)} = 6.79$, $P = 0.0002$, respectively], and no interaction effect. *Post hoc* analysis revealed a significant decrease of PDC activity across all frequency bands after nerve lesion [WK: delta and beta ($P < 0.0025$), theta, alpha, and gamma ($P < 0.0002$); SWS: delta, beta, and gamma ($P < 0.0125$), theta and alpha ($P < 0.0025$); REM: all bands ($P < 0.0002$); Bonferroni test with corrected *P*-value; **Figure 5B**].

DISCUSSION

In this study we report how the induction of chronic neuropathic pain affects the circadian patterns of thalamocortical oscillatory activity and the bidirectional flow of information between the cortical and thalamic somatosensory areas; for this we contrasted before- and after-pain sessions of 24 h of continuous recording of neurophysiological activity in freely moving rats chronically implanted with intracranial multielectrodes. The few previous neurophysiological studies describing changes in brain oscillations in animal models of chronic pain used whole-brain EEG scalp activity with poor spatial resolution; furthermore, they were commonly limited to only a few hours of recording (Landis et al., 1989; Palma et al., 2000; Tokunaga et al., 2007) or to a single session of 24 h of recording (Andersen and Tufik, 2003; Kontinen et al., 2003; Monassi et al., 2003; Keay et al., 2004; Silva et al., 2008). In fact, several studies dealing with pain-induced arousal changes focused on the description of behavioral alterations in the sleep cycle without any neurophysiological recording (Carli et al., 1987; Landis et al., 1988; Millecamps et al., 2005). Therefore, in contrast with the many clinical reports in humans that have used multichannel EEG, MEG, and intracranial recordings in an effort to address the spatial origins of brain oscillations (Sarnthein et al., 2006; Stern et al., 2006; Boord et al., 2008; Drewes et al., 2008; Sarnthein and Jeanmonod, 2008; Bjørk et al., 2009; Walton et al., 2010), almost no information exists from animal models on how chronic pain affects the functioning of the thalamocortical loop, since the only studies addressing this issue were limited to acute pain stimulation (Wang et al., 2003, 2004; Huang et al., 2006).

CHRONIC PAIN DISRUPTS THALAMOCORTICAL FLOW OF INFORMATION

The most significant finding in the present study is that the onset of neuropathic pain causes a rapid and dramatic decrease in the thalamocortical flow of information as measured by PDC (Sameshima and Baccalá, 1999; Baccala and Sameshima, 2001); this decrease was observed across all the brain states of the wake–sleep cycle, in spite of the lack of alterations in other thalamocortical features such as the frequency power spectrum and spectral coherence. PDC is a bidirectional frequency domain representation of the concept of Granger-Causality that measures how a time series $x(n)$ *causes* another series $y(n)$, if knowledge of $x(n)$'s past significantly improves prediction of $y(n)$. Hence, the thalamocortical PDC reflects how much of the cortical frequency space is temporally dependent on the thalamic LFP, and vice-versa.

The use of PDC analyses is growing in literature (Winterhalder et al., 2006; Sato et al., 2009); it has been validated in real neurophysiological data (Fanselow et al., 2001; Wang et al., 2003, 2004, 2008; Winterhalder et al., 2005; Huang et al., 2006) as well as in several theoretical studies using simulated data (Sameshima and Baccalá, 1999; Baccala and Sameshima, 2001; Schelter et al., 2006a,b; Takahashi et al., 2010), to demonstrate expected changes in brain networks that other less complex methods had failed to identify. As examples, PDC was able to uncover dopaminergic-dependent changes in connectivity between visual and motor areas in Parkinson patients that were undetectable by traditional spectral analysis (Tropini et al., 2011), and it was used to identify the directionality of widespread oscillatory brain interactions during visual object processing in the recognition of familiar vs. unfamiliar objects (Supp et al., 2007).

In what concerns thalamocortical processing of nociceptive information, PDCs have been calculated only in acute pain studies, in which it was shown that immediately after formalin injection the flow of information is maximal from cortex to the thalamus but that the direction of maximal information flow is reversed after 1 h (Huang et al., 2006); more recently, the same research group showed that noxious heat stimulation significantly increased the flow of information from SI cortex to ventral posterior thalamus, while in the ascending direction the flow of information decreased or remained unchanged, demonstrating for the first time that during pain processing the primary somatosensory cortex has a prominent role over the activity of thalamic neurons (Wang et al., 2007). This observation is in agreement with previous studies that have proposed that the descending corticothalamic projection could amplify noxious inputs of interest while simultaneously inhibiting other irrelevant information in order to improve input selectivity and detection (Rauschecker, 1997; Suga et al., 1997, 2000).

Our current results seem to suggest that the descending pathway remains functionally stronger than the ascending pathway raising the possibility that the cortex is still exerting an inhibitory role over the thalamus; this is in agreement with several studies indicating thalamic hypoactivity after prolonged pain conditions (Iadarola et al., 1995; Apkarian et al., 2004; Garcia-Larrea et al., 2006; Sorensen et al., 2008). Moreover, our calculation of information flow across states of the wake–sleep cycle is also in agreement with the observed disruption of default-mode network connectivity that is also observed in chronic pain patients (Baliki et al., 2008; Cauda et al., 2009).

CHRONIC PAIN CHANGES THALAMOCORTICAL PHASE–COHERENCE

Our results show that after nerve injury there was an increase in thalamocortical phase–coherence during episodes of awake – WK – and SWS, while at the same time there was a decrease in the flow of information between cortex and thalamus. Notably, all the differences that were observed at 48 h following the induction of chronic neuropathic pain were also observed in the recordings performed 10 days afterward, suggesting that these changes have fast onset and endure while the pain symptoms persist. In contrast to the change in thalamocortical phase–coherence, power spectrum, and spectral coherence were unaltered throughout all frequency bands which was not expected given that several human studies have shown an increase in spectral power and coherence in pain patients, specially at theta frequencies (Sarnthein and Jeanmonod, 2008; Ray et al., 2009; Walton et al., 2010). The most probable reason for this discrepancy between previous human studies and the present results is the fact that we have performed pre- vs. post-pain intracranial recordings of LFPs from the lateral thalamus and somatosensory cortex while similar human studies used non-invasive whole-brain recording techniques in which patients were compared to a control population. These human recordings comprise brain sources such as frontal areas that are known to be highly relevant to the increase in theta power and coherence (Sarnthein et al., 2006; Stern et al., 2006). In fact, when recorded simultaneously, the peaks of activity differ between EEG and LFPs with the EEG having maximal frequencies at the theta range and thalamic LFPs at the faster alpha range (Sarnthein and Jeanmonod, 2008). Moreover, the few human studies made with intracranial thalamic recordings are commonly based on medial areas and not on the lateral thalamus (Sarnthein et al., 2006; Sarnthein and Jeanmonod, 2008).

On the other hand, several studies have also shown evidence for not only a more desynchronized thalamic activity (Kane et al., 2009), but also reduced EEG power spectra in chronic pain patients (Boord et al., 2008). It is also interesting to note that other studies using animal models of pain have also failed to observe an increase in EEG power (Landis et al., 1989; Kontinen et al., 2003).

CHRONIC PAIN DISRUPTS THE BRAIN STATEMAPS

After the induction of the SNI model of neuropathic pain, the number of WK and SWS episodes increased whereas their mean duration remained the same; the increase in SWS occurred during both the dark and the light phases of recording, while the increase in WK episodes occurred only in the dark phase of the recording. Our observation of an increase in WK episodes is in agreement with published data from different chronic pain models that have also showed an increase in the percentage of time allocated to alertness episodes during the pain period (Carli et al., 1987; Landis et al., 1988, 1989; Andersen and Tufik, 2003; Monassi et al., 2003; Keay et al., 2004). However, our observation of an increase in SWS episodes is in contrast to previous observations that have reported either a decrease (Carli et al., 1987; Landis et al., 1988; Andersen and Tufik, 2003; Monassi et al., 2003; Silva et al., 2008), or no

alteration in SWS episodes after induction of chronic pain (Millecamps et al., 2005). We also did not observe differences in REM episodes, which is in agreement with previous findings (Monassi et al., 2003), while other reports showed either a decrease (Carli et al., 1987; Landis et al., 1989) or an increase (Andersen and Tufik, 2003; Schutz et al., 2003) in the time spent in REM.

It must be noted that our statistically based classification of brain states according to intracranial LFPs (Gervasoni et al., 2004) is inherently distinct from traditional wake–sleep EEG/EMG classification, with increased sensitivity to short duration transitional episodes and the ability to discriminate brain states based on higher frequencies than what is typically possible using scalp EEG. Therefore, direct comparison with previous studies is not entirely possible, particularly because the literature differs widely on the duration of the recording periods.

Transitions between the three more frequent states (WK, SWS, and REM) also increased after peripheral nerve injury. Our data showed an increase of WK → SWS transitions (in light phase), SWS → WK (in light and dark phases), and of low-frequency transitions such as SWS → REM and REM → WK during the light phase. In literature, similar results were published in several clinical chronic pain studies (Drewes et al., 1998; Lentz et al., 1999; Peyron et al., 2004; Lautenbacher et al., 2006). Apart the more frequent transitions, also the U-transition episodes that mediate state transitions increased after nerve lesion, namely WK → U and U → WK. These changes are probably related to the significant increase in the amount of U episodes that occurs after nerve lesion. Some studies in the literature report a similar short duration transition state called TS that was firstly described in the rat (Gottesmann, 1992; Benington et al., 1994), and sporadically observed during the transition between SWS and REM episodes. Mandile and co-workers using high temporal resolution computational methods for the EEG pattern analyses also identified this type of oscillation during the transitions between SWS → TS → WK (Mandile et al., 1996; Vescia et al., 1996), however with a longer duration compared to the transition observed between SWS → TS → REM.

A final note should be given on the inherent impossibility of teasing apart the strictly somatosensory effects from the indirect effects of pain. However, it may be argued that the non-specific effects are also intrinsic to the full neuropathic syndrome, to the extent that teasing them is almost impossible, if not senseless. Although we cannot rule out that the observed changes in sleep patterns or in thalamocortical connectivity may result from physical or motivational changes in locomotion patterns, we cannot dismiss that even those changes were triggered by the neuropathic model.

In summary, our results showed that peripheral nerve injury (SNI) induces a clear reduction of the amount of information flow and an enhancement of phase synchronization between the lateral thalamus and the primary somatosensory cortex. Our findings also demonstrate wake–sleep cycle disturbances, namely in the number, duration and transitions between brain state episodes. As previously suggested (Llinás et al., 2005; Walton et al., 2010), one possible explanation is that these changes may be caused by the unmasking of cortical descending inhibitory mechanisms that regulate the thalamic balance between continuously amplification of nociceptive information and suppression of non-nociceptive information.

ACKNOWLEDGMENTS

Special thanks to Dr. Shih-Chieh Lin for the StateMap toolbox for brain states classification. This work was supported by grants from Portuguese Foundation for Science and Technology (FCT; FCT-PTDC/SAU-NEU/100773/2008, PhD Grant FCT-SFRH/42500/2007), and BIAL Foundation (grant BIAL 126/08). The funders had no role in study design, data collection and analysis, decision to publish, or preparation of the manuscript.

REFERENCES

Achermann, P., and Borbely, A. A. (1997). Low-frequency (<1 Hz) oscillations in the human sleep electroencephalogram. *Neuroscience* 81, 213–222.

Andersen, M. L., and Tufik, S. (2003). Sleep patterns over 21-day period in rats with chronic constriction of sciatic nerve. *Brain Res.* 984, 84–92.

Apkarian, A. V., Sosa, Y., Sonty, S., Levy, R. M., Harden, R. N., Parrish, T. B., and Gitelman, D. R. (2004). Chronic back pain is associated with decreased prefrontal and thalamic gray matter density. *J. Neurosci.* 24, 10410–10415.

Baccala, L. A., and Sameshima, K. (2001). Partial directed coherence: a new concept in neural structure determination. *Biol. Cybern.* 84, 463–474.

Baliki, M. N., Geha, P. Y., Apkarian, A. V., and Chialvo, D. R. (2008). Beyond feeling: chronic pain hurts the brain, disrupting the default-mode network dynamics. *J. Neurosci.* 28, 1398–1403.

Benington, J. H., Kodali, S. K., and Heller, H. C. (1994). Scoring transitions to Rem-sleep in rats based on the Eeg phenomena of Pre-Rem sleep – an improved analysis of sleep structure. *Sleep* 17, 28–36.

Bjørk, M., Stovner, L., Engstrøm, M., Stjern, M., Hagen, K., and Sand, T. (2009). Interictal quantitative EEG in migraine: a blinded controlled study. *J. Headache Pain* 10, 331–339.

Boord, P., Siddall, P., Tran, Y., Herbert, D., Middleton, J., and Craig, A. (2008). Electroencephalographic slowing and reduced reactivity in neuropathic pain following spinal cord injury. *Spinal Cord* 46, 118–123.

Carli, G., Montesano, A., Rapezzi, S., and Paluffi, G. (1987). Differential-effects of persistent nociceptive stimulation on sleep stages. *Behav. Brain Res.* 26, 89–98.

Cauda, F., Sacco, K., Duca, S., Cocito, D., D'agata, F., Geminiani, G. C., and Canavero, S. (2009). Altered resting state in diabetic neuropathic pain. *PLoS ONE* 4, e4542. doi: 10.1371/journal.pone.0004542

Chaplan, S. R., Bach, F. W., Pogrel, J. W., Chung, J. M., and Yaksh, T. L. (1994). Quantitative assessment of tactile allodynia in the rat paw. *J. Neurosci. Methods* 53, 55–63.

Chen, A., and Herrmann, C. (2001). Perception of pain coincides with the spatial expansion of electroencephalographic dynamics in human subjects. *Neurosci. Lett.* 297, 183–186.

de Labra, C., Rivadulla, C., Grieve, K., Mariño, J., Espinosa, N., and Cudeiro, J. (2007). Changes in visual responses in the feline dLGN: selective thalamic suppression induced by transcranial magnetic stimulation of V1. *Cereb. Cortex* 17, 1376–1385.

Decosterd, I., and Woolf, C. J. (2000). Spared nerve injury: an animal model of persistent peripheral neuropathic pain. *Pain* 87, 149–158.

Destexhe, A., Contreras, D., and Steriade, M. (1999). Spatiotemporal analysis of local field potentials and unit discharges in cat cerebral cortex during natural wake and sleep states. *J. Neurosci.* 19, 4595–4608.

Drewes, A., Gratkowski, M., Sami, S., Dimcevski, G., Funch-Jensen, P., and Arendt-Nielsen, L. (2008). Is the pain in chronic pancreatitis of neuropathic origin? Support from EEG studies during experimental pain. *World J. Gastroenterol.* 14, 4020–4027.

Drewes, A. M., Gade, K., Nielsen, K. D., Bjerregard, K., Taagholt, S. J., and Svendsen, L. (1995). Clustering of sleep electroencephalographic patterns in patients with the fibromyalgia syndrome. *Br. J. Rheumatol.* 34, 1151–1156.

Drewes, A. M., Nielsen, K. D., Arendt-Nielsen, L., Birket-Smith, L., and Hansen, L. M. (1997). The effect of cutaneous and deep pain on the electroencephalogram during sleep – an experimental study. *Sleep* 20, 632–640.

Drewes, A. M., Svendsen, L., Taagholt, S. J., Bjerregard, K., Nielsen, K. D., and Hansen, B. (1998). Sleep in rheumatoid arthritis: a comparison with healthy subjects and studies of sleep/wake interactions. *Br. J. Rheumatol.* 37, 71–81.

Edwards, R., Almeida, D., Klick, B., Haythornthwaite, J., and Smith, M. (2008). Duration of sleep contributes to next-day pain report in the general population. *Pain* 137, 202–207.

Fanselow, E. E., and Nicolelis, M. A. L. (1999). Behavioral modulation of tactile responses in the rat somatosensory system. *J. Neurosci.* 19, 7603–7616.

Fanselow, E. E., Sameshima, K., Baccala, L. A., and Nicolelis, M. A. (2001). Thalamic bursting in rats during different awake behavioral states. *Proc. Natl. Acad. Sci. U.S.A.* 98, 15330–15335.

Fisher, N. I. (1993). *Statistical Analysis of Circular Data.* Cambridge: Cambridge University Press.

Garcia-Larrea, L., Maarrawi, J., Peyron, R., Costes, N., Mertens, P., Magnin, M., and Laurent, B. (2006). On the relation between sensory deafferentation, pain and thalamic activity in Wallenberg's syndrome: a PET-scan study before and after motor cortex stimulation. *Eur. J. Pain* 10, 677–688.

Gervasoni, D., Lin, S. C., Ribeiro, S., Soares, E. S., Pantoja, J., and Nicolelis, M. A. (2004). Global forebrain dynamics predict rat behavioral states and their transitions. *J. Neurosci.* 24, 11137–11147.

Gottesmann, C. (1992). Detection of 7 sleep-waking stages in the rat. *Neurosci. Biobehav. Rev.* 16, 31–38.

Gudbjornsson, B., Broman, J. E., Hetta, J., and Hallgren, R. (1993). Sleep disturbances in patients with primary Sjogrens-syndrome. *Br. J. Rheumatol.* 32, 1072–1076.

Hagen, K. B., Kvien, T. K., and Bjorndal, A. (1997). Musculoskeletal pain and quality of life in patients with noninflammatory joint pain compared to rheumatoid arthritis: a population survey. *J. Rheumatol.* 24, 1703–1709.

Huang, J., Chang, J., Woodward, D., Baccalá, L., Han, J., Wang, J., and Luo, F. (2006). Dynamic neuronal responses in cortical and thalamic areas during different phases of formalin test in rats. *Exp. Neurol.* 200, 124–134.

Hughes, S., and Crunelli, V. (2005). Thalamic mechanisms of EEG alpha rhythms and their pathological implications. *Neuroscientist.* 11, 357–372.

Iadarola, M. J., Max, M. B., Berman, K. F., Byas-Smith, M. G., Coghill, R. C., Gracely, R. H., and Bennett, G. J. (1995). Unilateral decrease in thalamic activity observed with positron emission tomography in patients with chronic neuropathic pain. *Pain* 63, 55–64.

Jeanmonod, D., Schulman, J., Ramirez, R., Cancro, R., Lanz, M., Morel, A., Magnin, M., Siegemund, M., Kronberg, E., Ribary, U., and Llinas, R. (2003). Neuropsychiatric thalamocortical dysrhythmia: surgical implications. *Neurosurg. Clin. N. Am.* 14, 251–265.

Jones, E. (2001). The thalamic matrix and thalamocortical synchrony. *Trends Neurosci.* 24, 595–601.

Jones, S. D., Koh, W. H., Steiner, A., Garret, S. L., and Calin, A. (1996). Fatigue in ankylosing spondylitis: Its prevalence and relationship to disease activity, sleep, and other factors. *J. Rheumatol.* 23, 487–490.

Kane, A., Hutchison, W., Hodaie, M., Lozano, A., and Dostrovsky, J. (2009). Enhanced synchronization of thalamic theta band local field potentials in patients with essential tremor. *Exp. Neurol.* 217, 171–176.

Keay, K. A., Monassi, C. R., Levison, D. B., and Bandler, R. (2004). Peripheral nerve injury evokes disabilities and sensory dysfunction in a subpopulation of rats: a closer model to human chronic neuropathic pain? *Neurosci. Lett.* 361, 188–191.

Kontinen, V. K., Ahnaou, A., Drinkenburg, W. H., and Meert, T. F. (2003). Sleep and EEG patterns in the chronic constriction injury model of neuropathic pain. *Physiol. Behav.* 78, 241–246.

Kundermann, B., Krieg, J. C., Schreiber, W., and Lautenbacher, S. (2004). The effect of sleep deprivation on pain. *Pain Res. Manag.* 9, 25–32.

Landis, C. A., Levine, J. D., and Robinson, C. R. (1989). Decreased slow-wave and paradoxical sleep in a rat chronic pain model. *Sleep* 12, 167–177.

Landis, C. A., Robinson, C. R., and Levine, J. D. (1988). Sleep fragmentation in the arthritic rat. *Pain* 34, 93–99.

Lautenbacher, S., Kundermann, B., and Krieg, J. C. (2006). Sleep deprivation and pain perception. *Sleep Med. Rev.* 10, 357–369.

Lentz, M. J., Landis, C. A., Rothermel, J., and Shaver, J. L. (1999). Effects of selective slow wave sleep disruption on musculoskeletal pain and fatigue in middle aged women. *J. Rheumatol.* 26, 1586–1592.

Lima, D. (2008). "Ascending pathways: anatomy and physiology," in *The Science of Pain*, eds. A. Basbaum and M. C. Bushnell (New York: Academic Press), 477–526.

Lin, S. C., Gervasoni, D., and Nicolelis, M. A. L. (2006). Fast modulation of prefrontal cortex activity by basal forebrain noncholinergic neuronal ensembles. *J. Neurophysiol.* 96, 3209–3219.

Llinás, R., Ribary, U., Jeanmonod, D., Kronberg, E., and Mitra, P. (1999). Thalamocortical dysrhythmia: a neurological and neuropsychiatric syndrome characterized by magnetoencephalography. *Proc. Natl. Acad. Sci. U.S.A.* 96, 15222–15227.

Llinás, R., Urbano, F. J., Leznik, E., Ramírez, R. R., and Van Marle, H. J. (2005). Rhythmic and dysrhythmic thalamocortical dynamics: GABA systems and the edge effect. *Trends Neurosci.* 28, 325–333.

Lumer, E., Edelman, G., and Tononi, G. (1997). Neural dynamics in a model of the thalamocortical system. II. The role of neural synchrony tested through perturbations of spike timing. *Cereb. Cortex* 7, 228–236.

Mandile, P., Vescia, S., Montagnese, P., Romano, F., and Giuditta, A. (1996). Characterization of transition sleep episodes in baseline EEG recordings of adult rats. *Physiol. Behav.* 60, 1435–1439.

Massimini, M., Boly, M., Casali, A., Rosanova, M., and Tononi, G. (2009). A perturbational approach for evaluating the brain's capacity for consciousness. *Prog. Brain Res.* 177, 201–214.

McCormick, D. A., and Bal, T. (1997). Sleep and arousal: thalamocortical mechanisms. *Annu. Rev. Neurosci.* 20, 185–215.

Meehan, S., Legon, W., and Staines, W. (2008). Paired-pulse transcranial magnetic stimulation of primary somatosensory cortex differentially modulates perception and sensorimotor transformations. *Neuroscience* 157, 424–431.

Millecamps, M., Jourdan, D., Leger, S., Etienne, M., Eschalier, A., and Ardid, D. (2005). Circadian pattern of spontaneous behavior in monarthritic rats – a novel global approach to evaluation of chronic pain and treatment effectiveness. *Arthritis Rheum.* 52, 3470–3478.

Moldofsky, H., Scarisbrick, P., England, R., and Smythe, H. (1975). Musculosketal symptoms and non-REM sleep disturbance in patients with "fibrositis syndrome" and healthy subjects. *Psychosom. Med.* 37, 341–351.

Monassi, C. R., Bandler, R., and Keay, K. A. (2003). A subpopulation of rats show social and sleep-waking changes typical of chronic neuropathic pain following peripheral nerve injury. *Eur. J. Neurosci.* 17, 1907–1920.

Morin, C. M., Gibson, D., and Wade, J. (1998). Self-reported sleep and mood disturbance in chronic pain patients. *Clin. J. Pain* 14, 311–314.

Nicolelis, M. A. L., Baccala, L. A., Lin, R. C., and Chapin, J. K. (1995). Sensorimotor encoding by synchronous neural ensemble activity at multiple levels of the somatosensory system. *Science* 268, 1353–1358.

Onen, S. H., Alloui, A., Gross, A., Eschallier, A., and Dubray, C. (2001). The effects of total sleep deprivation, selective sleep interruption and sleep recovery on pain tolerance thresholds in healthy subjects. *J. Sleep Res.* 10, 35–42.

Palma, B. D., Suchecki, D., and Tufik, S. (2000). Differential effects of acute cold and footshock on the sleep of rats. *Brain Res.* 861, 97–104.

Paxinos, G., and Watson, C. (1998). *The Rat Brain in Stereotaxic Coordinates.* San Diego: Academic Press.

Peyron, R., Schneider, F., Faillenot, I., Convers, P., Barral, F. G., Garcia-Larrea, L., and Laurent, B. (2004). An fMRI study of cortical representation of mechanical allodynia in patients with neuropathic pain. *Neurology* 63, 1838–1846.

Rauschecker, J. P. (1997). Mechanisms of compensatory plasticity in the cerebral cortex. *Brain Plast.* 73, 137–146.

Ray, N., Jenkinson, N., Kringelbach, M., Hansen, P., Pereira, E., Brittain, J., Holland, P., Holliday, I., Owen, S., Stein, J., and Aziz, T. (2009). Abnormal thalamocortical dynamics may be altered by deep brain stimulation: using magnetoencephalography to study phantom limb pain. *J. Clin. Neurosci.* 16, 32–36.

Ribary, U. (2005). Dynamics of thalamo-cortical network oscillations and human perception. *Prog. Brain Res.* 150, 127–142.

Sameshima, K., and Baccalá, L. (1999). Using partial directed coherence to describe neuronal ensemble interactions. *J. Neurosci. Methods* 94, 93–103.

Sarnthein, J., and Jeanmonod, D. (2007). High thalamocortical

theta coherence in patients with Parkinson's disease. *J. Neurosci.* 27, 124–131.

Sarnthein, J., and Jeanmonod, D. (2008). High thalamocortical theta coherence in patients with neurogenic pain. *Neuroimage* 39, 1910–1917.

Sarnthein, J., Stern, J., Aufenberg, C., Rousson, V., and Jeanmonod, D. (2006). Increased EEG power and slowed dominant frequency in patients with neurogenic pain. *Brain* 129, 55–64.

Sato, J. R., Takahashi, D. Y., Arcuri, S. M., Sameshima, K., Morettin, P. A., and Baccalá, L. A. (2009). Frequency domain connectivity identification: an application of partial directed coherence in fMRI. *Hum. Brain Mapp.* 30, 452–461.

Schelter, B., Winterhalder, M., Eichler, M., Peifer, M., Hellwig, B., Guschlbauer, B., Lücking, C. H., Dahlhaus, R., and Timmer, J. (2006a). Testing for directed influences among neural signals using partial directed coherence. *J. Neurosci. Methods* 152, 210–219.

Schelter, B., Winterhalder, M., Hellwig, B., Guschlbauer, B., Lücking, C. H., and Timmer, J. (2006b). Direct or indirect? Graphical models for neural oscillators. *J. Physiol. Paris* 99, 37–46.

Schutz, T. C. B., Andersen, M. L., and Tufik, S. (2003). Sleep alterations in an experimental orofacial pain model in rats. *Brain Res.* 993, 164–171.

Sherman, S., and Guillery, R. (2002). The role of the thalamus in the flow of information to the cortex. *Philos. Trans. R. Soc. Lond. B Biol. Sci.* 357, 1695–1708.

Silva, A., Andersen, M. L., and Tufik, S. (2008). Sleep pattern in an experimental model of osteoarthritis. *Pain* 140, 446–455.

Silva, A., Cardoso-Cruz, H., Silva, F., Galhardo, V., and Antunes, L. (2010). Comparison of anesthetic depth indexes based on thalamocortical local field potentials in rats. *Anesthesiology* 112, 355–363.

Sorensen, L., Siddall, P., Trenell, M., and Yue, D. (2008). Differences in metabolites in pain-processing brain regions in patients with diabetes and painful neuropathy. *Diabetes Care* 31, 980–981.

Steriade, M., Mccormick, D. A., and Sejnowski, T. J. (1993). Thalamocortical oscillations in the sleeping and aroused brain. *Science* 262, 679–685.

Stern, J., Jeanmonod, D., and Sarnthein, J. (2006). Persistent EEG overactivation in the cortical pain matrix of neurogenic pain patients. *Neuroimage* 31, 721–731.

Suga, N., Gao, E. Q., Zhang, Y. F., Ma, X. F., and Olsen, J. F. (2000). The corticofugal system for hearing: Recent progress. *Proc. Natl. Acad. Sci. U.S.A.* 97, 11807–11814.

Suga, N., Zhang, Y. F., and Yan, J. (1997). Sharpening of frequency tuning by inhibition in the thalamic auditory nucleus of the mustached bat. *J. Neurophysiol.* 77, 2098–2114.

Supp, G. G., Schlögl, A., Trujillo-Barreto, N., Müller, M. M., and Gruber, T. (2007). Directed cortical information flow during human object recognition: analyzing induced EEG gamma-band responses in brain's source space. *PLoS ONE* 2, e684. doi: 10.1371/journal.pone.0000684

Takahashi, D. Y., Baccala, L. A., and Sameshima, K. (2010). Frequency domain connectivity: an information theoretic perspective. *Conf. Proc. IEEE Eng. Med. Biol. Soc.* 2010, 1726–1729.

Tang, N. K., Wright, K. J., and Salkovskis, P. M. (2007). Prevalence and correlates of clinical insomnia co-occurring with chronic back pain. *J. Sleep Res.* 16, 85–95.

Tishler, M., Barak, Y., Paran, D., and Yaron, M. (1997). Sleep disturbances, fibromyalgia and primary Sjogren's syndrome. *Clin. Exp. Rheumatol.* 15, 71–74.

Tokunaga, S., Takeda, Y., Shinomiya, K., Yamamoto, W., Utsu, Y., Toide, K., and Kamei, C. (2007). Changes of sleep patterns in rats with chronic constriction injury under aversive conditions. *Biol. Pharm. Bull.* 30, 2088–2090.

Tropini, G., Chiang, J., Wang, Z. J., Ty, E., and Mckeown, M. J. (2011). Altered directional connectivity in Parkinson's disease during performance of a visually guided task. *Neuroimage* 56, 2144–2156.

Vanderwolf, C. H. (1969). Hippocampal electrical acitvity and voluntary movement in rat. *Electroencephalogr Clin. Neurophysiol.* 26, 407–418.

Vescia, S., Mandile, P., Montagnese, P., Romano, F., Cataldo, G., Cotugno, M., and Giuditta, A. (1996). Baseline transition sleep and associated sleep episodes are related to the learning ability of rats. *Physiol. and Behav.* 60, 1513–1525.

Walton, K., Dubois, M., and Llinás, R. (2010). Abnormal thalamocortical activity in patients with complex regional pain syndrome (CRPS) type I. *Pain* 150, 41–51.

Wang, J., Chang, J., Woodward, D., Baccalá, L., Han, J., and Luo, F. (2007). Corticofugal influences on thalamic neurons during nociceptive transmission in awake rats. *Synapse* 61, 335–342.

Wang, J., Luo, F., Chang, J., Woodward, D., and Han, J. (2003). Parallel pain processing in freely moving rats revealed by distributed neuron recording. *Brain Res.* 992, 263–271.

Wang, J., Zhang, H., Han, J., Chang, J., Woodward, D., and Luo, F. (2004). Differential modulation of nociceptive neural responses in medial and lateral pain pathways by peripheral electrical stimulation: a multichannel recording study. *Brain Res.* 1014, 197–208.

Wang, J. Y., Zhang, H. T., Chang, J. Y., Woodward, D. J., Baccalá, L. A., and Luo, F. (2008). Anticipation of pain enhances the nociceptive transmission and functional connectivity within pain network in rats. *Mol. Pain* 4, 34.

Wiest, M. C., and Nicolelis, M. A. L. (2003). Behavioral detection of tactile stimuli during 7-12 Hz cortical oscillations in awake rats. *Nat. Neurosci.* 6, 913–914.

Willis, W. J. (2007). The somatosensory system, with emphasis on structures important for pain. *Brain Res. Rev.* 55, 297–313.

Winterhalder, M., Schelter, B., Hesse, W., Schwab, K., Leistritz, L., Klan, D., Bauer, R., Timmer, J., and Witte, H. (2005). Comparison of linear signal processing techniques to infer directed interactions in multivariate neural systems. *Signal Processing* 85, 2137–2160.

Winterhalder, M., Schelter, B., Hesse, W., Schwab, K., Leistritz, L., Timmer, J., and Witte, H. (2006). Detection of directed information flow in biosignals. *Biomed. Tech. (Berl.)* 51, 281–287. doi: 10.1515/bmt.2006.058, 01/12/2006

Zimmermann, M. (1983). Ethical guidelines for investigations of experimental pain in conscious animals. *Pain* 16, 109–110.

Conflict of Interest Statement: The authors declare that the research was conducted in the absence of any commercial or financial relationships that could be construed as a potential conflict of interest.

Received: 02 June 2011; accepted: 04 August 2011; published online: 23 August 2011.

*Citation: Cardoso-Cruz H, Sameshima K, Lima D and Galhardo V (2011) Dynamics of circadian thalamocortical flow of information during a peripheral neuropathic pain condition. Front. Integr. Neurosci. **5**:43. doi: 10.3389/fnint.2011.00043*

APPENDIX

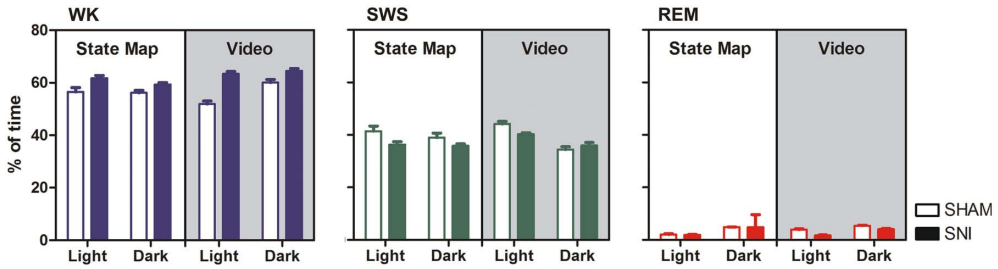

FIGURE A1 | Comparison of the efficiency in states detection between the StateMap algorithm selection vs. visual inspection of the video recordings and spectral bands. Brain states are expressed as percentage of the total recording time during the light and dark phases in the SNI group (filled bars) and in the SHAM-group plotted for waking state (WK, blue), slow-wave-sleep (SWS, green), and rapid-eye-movement (REM, red). No statistical differences were encountered between both methodologies of detection (Mann–Whitney test, $P < 0.05$). The determinations are expressed for all animals as mean (±SEM).

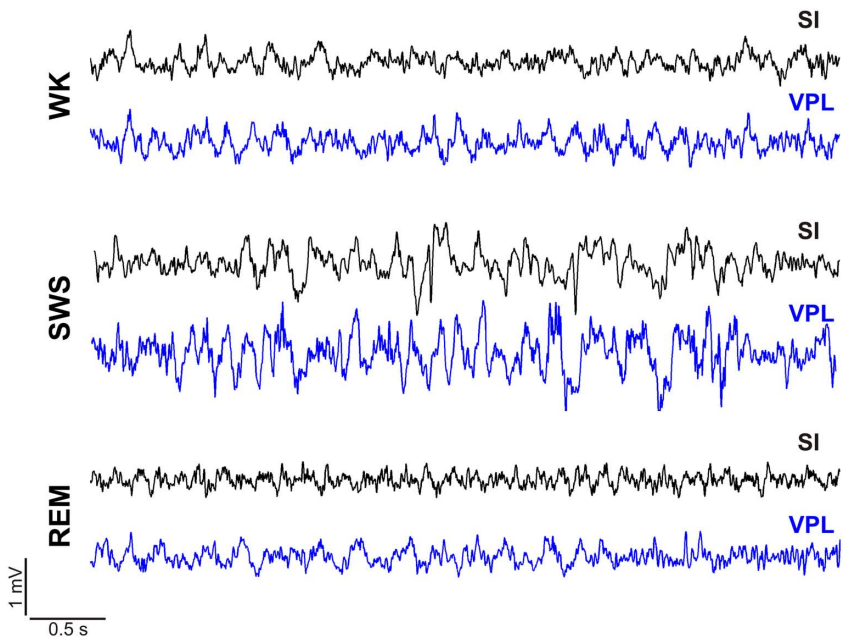

FIGURE A2 | Oscillations on intracranial local field potentials (LFPs) recorded in one session during the dark phase (SHAM-baseline period) simultaneously in the primary somatosensory cortex (SI, *black trace*) and in the ventro-posterior-lateral thalamic nuclei (VPL, *blue trace*). Raw recordings representing 5-s of ongoing LFP activity recorded during a waking state (WK) episode, slow-wave-sleep (SWS), and rapid-eye-movement (REM) states.

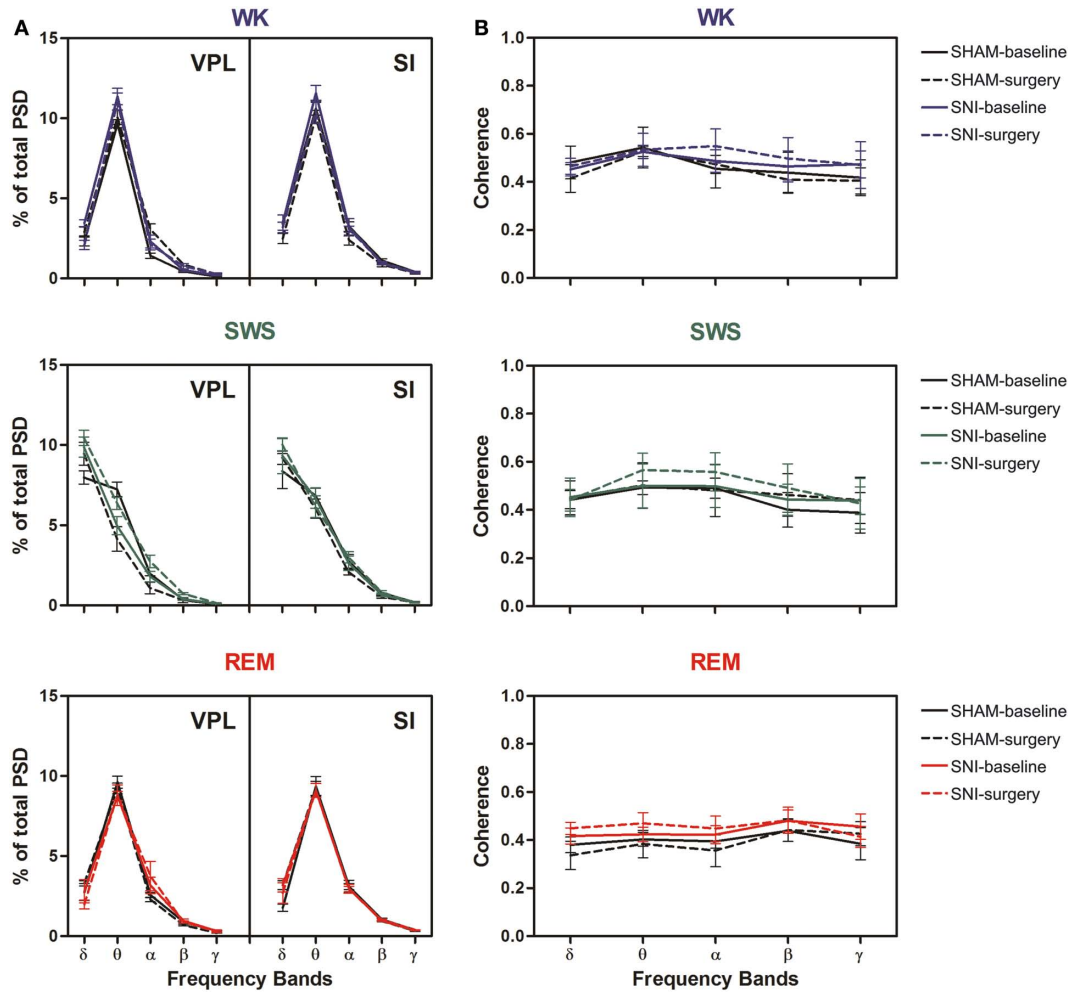

FIGURE A3 | Spectral analysis of SI–VPL LFPs channels during WK (blue), SWS (green), and REM (red) state episodes across frequency bands. Frequency bands: delta (δ, 1–4 Hz), theta (θ, 4–9 Hz), alpha (α, 9–15 Hz), beta (β, 15–30 Hz), and slow-gamma (γ, 30–50 Hz). Each point represents the mean value within the frequency band. Experimental groups were represented: SHAM-baseline (continuous black line), SHAM-surgery (black line-dotted), SNI-baseline (continuous color line: WK (blue), SWS (green), and REM (red), and SNI-surgery (color line-dotted). **(A)** Left column represents the power spectra density (PSD) measurements across frequency bands for the two recorded areas (ventro-posterior-lateral thalamic nuclei, VPL and primary somatosensory cortex – SI). Analysis of variance revealed no differences across experimental groups [(SHAM-baseline/SHAM-surgery) – VPL: WK $F_{(1,25)} = 1.61$, $P = 0.1874$, SWS $F_{(1,25)} = 0.27$, $P = 0.6081$, REM $F_{(1,25)} = 0.41$, $P = 0.5271$; and SI: WK $F_{(1,25)} = 3.71$, $P = 0.0538$, SWS $F_{(1,25)} = 3.04$, $P = 0.0934$, REM $F_{(1,25)} = 1.34$, $P = 0.2588$; (SHAM-baseline/SNI-baseline) – VPL: WK $F_{(1,50)} = 2.24$, $P = 0.0989$, SWS $F_{(1,50)} = 0.10$, $P = 0.7552$, REM $F_{(1,50)} = 0.02$, $P = 0.8800$; and SI: WK $F_{(1,50)} = 0.46$, $P = 0.4993$, SWS $F_{(1,50)} = 0.19$, $P = 0.6683$, REM $F_{(1,50)} = 0.76$, $P = 0.3900$; (SNI-baseline/SNI-surgery) – VPL: WK $F_{(1,25)} = 1.86$, $P = 0.4147$, SWS $F_{(1,25)} = 0.25$, $P = 0.6237$, REM $F_{(1,25)} = 0.08$, $P = 0.7753$; and SI: WK $F_{(1,25)} = 1.53$, $P = 0.2281$, SWS $F_{(1,25)} = 1.72$, $P = 0.4266$, REM $F_{(1,25)} = 0.21$, $P = 0.6500$; (SHAM-surgery/SNI-surgery) – VPL: WK $F_{(1,50)} = 0.76$, $P = 0.3880$, SWS $F_{(1,50)} = 3.43$, $P = 0.0698$, REM $F_{(1,50)} = 0.01$, $P = 0.9999$; and SI: WK $F_{(1,50)} = 3.35$, $P = 0.0732$, SWS $F_{(1,50)} = 1.58$, $P = 0.6673$, REM $F_{(1,50)} = 0.40$, $P = 0.5288$] and interaction [(SHAM-baseline/SHAM-surgery) – VPL: WK $F_{(4,25)} = 2.74$, $P = 0.0510$, SWS $F_{(4,25)} = 0.75$, $P = 0.5652$, REM $F_{(4,25)} = 1.29$, $P = 0.3009$; and SI: WK $F_{(4,25)} = 0.69$, $P = 0.6073$, SWS $F_{(4,25)} = 074$, $P = 0.5693$, REM $F_{(4,25)} = 2.42$, $P = 0.0750$; (SHAM-baseline/SNI-baseline) – VPL: WK $F_{(4,50)} = 2.66$, $P = 0.0701$, SWS $F_{(4,50)} = 0.33$, $P = 0.8566$, REM $F_{(4,50)} = 1.04$, $P = 0.3979$; and SI: WK $F_{(4,50)} = 0.80$, $P = 0.5339$, SWS $F_{(4,50)} = 0.88$, $P = 0.5407$, REM $F_{(4,50)} = 2.44$, $P = 0.0590$; (SNI-baseline/SNI-surgery) – VPL: WK $F_{(4,25)} = 1.93$, $P = 0.3969$, SWS $F_{(4,25)} = 0.60$, $P = 0.6686$, REM $F_{(4,25)} = 1.15$, $P = 0.3561$; and SI: WK $F_{(4,25)} = 0.81$, $P = 0.5322$, SWS $F_{(4,25)} = 1.97$, $P = 0.1294$, REM $F_{(4,25)} = 0.34$, $P = 0.8449$; (SHAM-surgery/SNI-surgery) – VPL: WK $F_{(4,50)} = 2.23$, $P = 0.1003$, SWS $F_{(4,50)} = 0.69$, $P = 0.5992$, REM $F_{(4,50)} = 1.45$, $P = 0.2703$; and SI: WK $F_{(4,50)} = 0.45$, $P = 0.7730$, SWS $F_{(4,50)} = 2.20$, $P = 0.0823$, REM $F_{(4,50)} = 0.26$, $P = 0.9030$], and as expected an effect across frequency bands [(SHAM-baseline/SHAM-surgery) – VPL: WK $F_{(4,25)} = 459.20$, $P < 0.0001$, SWS $F_{(4,25)} = 185.40$, $P < 0.0001$, REM $F_{(4,25)} = 381.80$, $P < 0.0001$; and SI: WK $F_{(4,25)} = 337.10$, $P < 0.0001$, SWS $F_{(4,25)} = 239.10$, $P < 0.0001$, REM $F_{(4,25)} = 293.80$, $P < 0.0001$; (SHAM-baseline/SNI-baseline) – VPL: WK $F_{(4,50)} = 542.90$, $P < 0.0001$, SWS $F_{(4,50)} = 83.05$, $P < 0.0001$, REM $F_{(4,50)} = 183.30$, $P < 0.0001$; and SI: WK $F_{(4,50)} = 274.40$, $P < 0.0001$, SWS $F_{(4,50)} = 244.50$, $P < 0.0001$, REM $F_{(4,50)} = 255.60$, $P < 0.0001$; (SNI-baseline/SNI-surgery) – VPL: WK $F_{(4,25)} = 272.80$, $P < 0.0001$, SWS $F_{(4,25)} = 91.82$, $P < 0.0001$, REM $F_{(4,25)} = 67.83$, $P < 0.0001$; and SI: WK $F_{(4,25)} = 270.40$, $P < 0.0001$, SWS $F_{(4,25)} = 172.50$, $P < 0.0001$, REM $F_{(4,25)} = 165.10$, $P < 0.0001$; (SHAM-surgery/SNI-surgery) – VPL: WK $F_{(4,50)} = 358.20$, $P < 0.0001$, SWS $F_{(4,50)} = 246.40$, $P < 0.0001$, REM $F_{(4,50)} = 163.10$, $P < 0.0001$; and SI: WK $F_{(4,50)} = 296.80$, $P < 0.0001$, SWS $F_{(4,50)} = 189.80$, $P < 0.0001$, REM $F_{(4,50)} = 244.40$, $P < 0.0001$].

(*Continued*)

FIGURE A3 | (Continued)
(B) Right column represents the thalamocortical VPL–SI coherence activity. Analysis of variance revealed no significant differences across experimental groups [(SHAM-baseline/SHAM-surgery): WK $F_{(1,25)} = 0.21$, $P = 0.6524$, SWS $F_{(1,25)} = 0.25$, $P = 0.6202$, REM $F_{(1,25)} = 0.12$, $P = 0.7314$; (SHAM-baseline/SNI-baseline): WK $F_{(1,50)} = 0.11$, $P = 0.7419$, SWS $F_{(1,50)} = 0.31$, $P = 0.5815$, REM $F_{(1,50)} = 2.26$, $P = 0.1388$; (SNI-baseline/SNI-surgery): WK $F_{(1,25)} = 0.62$, $P = 0.4378$, SWS $F_{(1,25)} = 0.50$, $P = 0.4882$, REM $F_{(1,25)} = 0.20$, $P = 0.6553$; (SHAM-surgery/SNI-surgery): WK $F_{(1,50)} = 2.11$, $P = 0.1530$, SWS $F_{(1,50)} = 0.27$, $P = 0.6026$, REM $F_{(1,50)} = 3.87$, $P = 0.0544$], frequency bands [(SHAM-baseline/SHAM-surgery): WK $F_{(4,25)} = 1{,}64$, $P = 0.1956$, SWS $F_{(4,25)} = 0.43$, $P = 0.7844$, REM $F_{(4,25)} = 0.90$, $P = 0.4783$; (SHAM-baseline/SNI-baseline): WK $F_{(4,50)} = 0.58$, $P = 0.6721$, SWS $F_{(4,50)} = 0.66$, $P = 0.6208$, REM $F_{(4,50)} = 0.63$, $P = 0.6431$; (SNI-baseline/SNI-surgery): WK $F_{(4,25)} = 0.32$, $P = 0.8626$, SWS $F_{(4,25)} = 0.51$, $P = 0.7284$, REM $F_{(4,25)} = 0.46$, $P = 0.7675$; (SHAM-surgery/SNI-surgery): WK $F_{(4,50)} = 0.97$, $P = 0.4346$, SWS $F_{(4,50)} = 0.51$, $P = 0.7293$, REM $F_{(4,50)} = 0.55$, $P = 0.7006$], and interaction effect [groups × frequency bands; (SHAM-baseline/SHAM-surgery): WK $F_{(4,25)} = 0.09$, $P = 0.9851$, SWS $F_{(4,25)} = 0.08$, $P = 0.9879$, REM $F_{(4,25)} = 0.21$, $P = 0.9295$; (SHAM-baseline/SNI-baseline): WK $F_{(4,50)} = 0.15$, $P = 0.9613$, SWS $F_{(4,50)} = 0.05$, $P = 0.9956$, REM $F_{(4,50)} = 0.11$, $P = 0.9784$; (SNI-baseline/SNI-surgery): WK $F_{(4,25)} = 0.16$, $P = 0.9560$, SWS $F_{(4,25)} = 0.17$, $P = 0.9508$, REM $F_{(4,25)} = 0.32$, $P = 0.8607$; (SHAM-surgery/SNI-surgery): WK $F_{(4,50)} = 0.13$, $P = 0.9718$, SWS $F_{(4,50)} = 0.11$, $P = 0.9779$, REM $F_{(4,50)} = 0.48$, $P = 0.7508$]. The determinations are expressed for all animals as mean (±SEM).

PUBLICAÇÃO 2

Anesthesiology 2010; 112:355–63

Comparison of Anesthetic Depth Indexes Based on Thalamocortical Local Field Potentials in Rats

Aura Silva, D.V.M., M.Sc.,* Hélder Cardoso-Cruz, M.Sc.,† Francisco Silva, M.Sc.,‡ Vasco Galhardo, Ph.D.,§ Luís Antunes, Ph.D.,‖

ABSTRACT

Background: Local field potentials may allow a more precise analysis of the brain electrical activity than the electroencephalogram. In this study, local field potentials were recorded in the thalamocortical axis of rats to (i) compare the performance of several indexes of anesthetic depth and (ii) investigate the existence of thalamocortical correlated or disrupted activity during isoflurane steady-state anesthesia.

Methods: Five rats chronically implanted with microelectrodes were used to record local field potentials in the primary somatosensory cortex and ventroposterolateral thalamic nuclei at six periods: before induction of anesthesia; in the last 5 min of randomized 20-min steady-state end-tidal 0.8, 1.1, 1.4, and 1.7% isoflurane concentrations; and after recovery. The approximate entropy, the index of consciousness, the spectral edge frequency, and the permutation entropy were estimated using epochs of 8 s. A correction factor for burst suppression was applied to the spectral edge frequency and to the permutation entropy. The correlation between the derived indexes and the end-tidal isoflurane was calculated and compared for the two studied brain regions indexes. Coherence analysis was also performed.

Results: The burst suppression–corrected permutation entropy showed the highest correlation with the end-tidal isoflurane concentration, and a high coherence was obtained between the two studied areas.

Conclusions: The permutation entropy corrected with the classic burst suppression ratio is a promising alternative to other indexes of anesthetic depth. Furthermore, high coherence level of activity exists between the somatosensory cortical and thalamic regions, even at deep isoflurane stages.

What We Already Know about This Topic

- Surface electroencephalographic analysis of anesthetic depth reflects overlapping activity
- Analysis of intracranial local field potentials may improve understanding and advancement of electroencephalographic analysis

What This Article Tells Us That Is New

- In rats, there was high coherence between cortical and thalamic activity during steady-state anesthesia
- Permutation entropy corrected with classic burst suppression was noted as a promising new index of anesthetic state

THERE are several indexes of anesthetic depth developed to translate the information of the complex electroencephalogram signal into a number. However, the electroencephalogram reflects noisy overlapping of activity from different brain regions[1] and only its lower frequency components (below 30 Hz) are normally analyzed because of potential electromyographic activity interferences.[2] Intracranial techniques, such as the local field potentials (LFPs), are not contaminated by electromyographic activity and allow the analysis of higher frequencies, such as the γ-band. Thus, the effect of anesthetics on the brain could be more accurately reflected on the LFPs than on the electroencephalogram, allowing a more precise analysis of the performance of anesthetic depth indexes.

LFPs represent the extracellular low-frequency summed postsynaptic potentials from local cell groups and have been applied in neurophysiology studies to record the electric signal from specific brain areas.[3–5] By recording thalamocortical LFPs, it is possible to compare the activity in the cortical and thalamic neurons and answer the controversy regarding which region is responsible for anesthetic-induced unconsciousness, the cortex[6,7] or the thalamus.[8,9] These structures are densely and reciprocally interconnected,[10–13] even during quiet physiologic sleep,[10] but it is not known whether this connection is interrupted by anesthetics.[14] The use of electroencephalogram-derived indexes to analyze LFPs is a strong tool to address these questions. The most recently investigated indexes of anesthetic depth are the approximate entropy (AE), the permutation entropy (PE),[15–17] and other commercial monitors such as the most recently introduced

* Ph.D. Student, ‖ Associate Professor of Veterinary Anesthesiology and Researcher, Centro de Ciência Animal e Veterinária (CECAV), Universidade de Trás-os-Montes e Alto Douro (UTAD), Vila Real, and Instituto de Biologia Molecular e Celular (IBMC), Universidade do Porto. † Ph.D. Student, Insituto de Histologia e Embriologia, Faculdade de Medicina and IBMC, ‡ Research Student, Departmento de Física, Faculdade de Ciências, § Associate Professor, Instituto de Histologia e Embriologia, Faculdade de Medicina and Principal Investigator at IBMC, Universidade do Porto.

Received from Centro de Ciência Animal e Veterinária, Universidade de Trás-os-Montes e Alto Douro, Vila Real, Portugal; and Instituto de Biologia Molecular e Celular, Universidade do Porto, Porto, Portugal. Submitted for publication May 28, 2009. Accepted for publication October 30, 2009. Supported by the Foundation for Science and Technology, Lisbon, Portugal, for projects POCTI/CVT/59056/2004, PTDC/EEA-ACR/69288/2006, PTDC/SAU-NEU/100773/2008, PhD Grant FCT SFRH/42500/2007 and Project Grant BIAL 126/08.

Address correspondence to Dr. Silva: Rua do Campo Alegre, 823, 4150-180 Porto, Portugal. asilva@ibmc.up.pt.

index of consciousness (IoC).[18] On the other hand, classic spectral edge frequency (SEF) is mathematically simpler and has been suggested to adequately reflect depth of anesthesia from the electroencephalogram of rats, when corrected for the burst suppression (BS) ratio.[19]

In this study, LFPs were recorded in isoflurane-anesthetized rats with two main objectives: (i) to compare the performance of the more recently introduced indexes of anesthetic depth and (ii) to investigate the existence of thalamocortical correlated or disrupted activity during isoflurane steady-state anesthesia.

Materials and Methods

Subjects

Five adult male Sprague-Dawley rats weighing between 350 and 400 g were used in this study. The rats were maintained on a 12-h light and dark cycle, with *ad libitum* access to food and water. All procedures and experiments were conducted in compliance with the Ethical Guidelines for Animal Experimentation and Animal Care Committee imposed by the European Community Directive Number 86/609/ECC, November 24, 1986, and approved by the national regulatory office (Direcção Geral de Veterinária—DGV, Lisboa, Portugal) under the title "Melhorias das técnicas anestésicas e analgésicas em animais de laboratório de 21 de Outubro de 2003," and the project was approved by the Foundation for Science and Technology with the number POCI/CVT/59056/2004 and the same name.

Surgery

At least 7 days before the experiment, the rats were anesthetized with an intramuscular injection of a mixture of xylazine and ketamine (10 and 60 mg/kg, respectively). Anesthesia was maintained with additional injections of ketamine (one-third of the initial doses). A fresh gas supply of oxygen was delivered during the procedure by a facemask. Depth of anesthesia was assessed by regularly testing the corneal blink, hind paw withdrawal, and tail-pinch reflexes. Core body temperature was measured with a rectal thermometer and maintained at 37°C by a homeothermic blanket system. Animal heads were shaved and cleaned by using a triple application of alcohol (70% v/v) and betadine. A midline subcutaneous injection of 0.3 ml of 1% lignocaine (B Braun, Melsungen, Germany) was applied to the scalp for local analgesia. Anesthetized animals were secured in a stereotaxic frame using ear bars, and a midline incision was made caudally to the animal's eyes and ending between ears. The connective tissue was blunt dissected from skull, and the top of the skull was exposed and cleaned by using hydrogen peroxide. After the scalp was excised, holes were bored in the skull for four to five screws and for two microelectrode arrays (4 × 4-mm portion). These screws were used for securing probes and for grounding purposes. The skull was covered with mineral oil. Just before the implantation, microelectrode array filaments were cut to the ideal length, using a sharp pair of scissors, and then soaked in a saturated solution of sucrose. Each microelectrode array included eight filaments (one array per area) and isonel-coated tungsten wire (35 μm in diameter) (California Fine Wire Company, Grover Beach, CA) with impedances varying between 0.5 and 0.7 M[Omega] at 1 KHz. The microelectrode arrays were constructed in 4 × 2 architecture (1–2; 3–4; 5–6; 7–8 channels), interspaced 250 μm between lines and 450 μm between columns (fig. 1A). The arrays were oriented rostrocaudally and mounted in the holder of a hydraulic micropositioner (FHC Inc., Bowdoin, ME) and subsequently slowly driven (50 μm/min) into the primary somatosensory cortex (SI) and ventroposterolateral (VPL) after dura mater removal. The following coordinates in millimeters relative to Bregma[20] were used to center the arrays: SI (−2.5 rostro-caudal, +2.5 mediolateral, and −1.6 dorsoventral) and VPL (−3.1 rostrocaudal, +3.2 mediolateral, and −6.4 dorsoventral). The location of the electrodes within SI and VPL was verified by mapping the neuronal responses elicited by tactile stimulation of the correspondent peripheral hind paw receptive field. After electrodes were placed in the correct position, the craniotomy was sealed with a layer of agar (4% in saline), and they were cemented to skull screws by the use of dental acrylic.[21] In the end of the implantation, the animal was transferred to a recovery cage. The analgesic carprofene (5–10 mg/kg) (Rimadyl; Pfizer Animal Health, Lisboa, Portugal) and the antibiotic amoxiciline (6 mg/kg) (Clamoxyl; Pfizer Animal Health) were administered subcutaneously every 24 h during 2 or 3 days. Rats were allowed to recover for 1 week before the recording sessions began.

Histology

After the end of all experiments, the rats were deeply anesthetized with ketamine and xylazine mixture, and the recording site was marked by injecting direct current (10–20 μA for 10–20 s) through one microwire per matrix group, marking the area below the electrode tips. After this step, the animals were perfused through the heart with 0.01 M phosphate buffer (pH = 7.2) in 0.9% saline solution followed by 4% paraformaldehyde. The brains were removed and post-fixed in 4% paraformaldehyde during 4 h and then stored in 30% sucrose before they were frozen and sectioned into 60-μm slices. The sections were stained to identify the recording site under the microscope. This technique, in conjunction with careful notation of electrode movements during implantation surgery, allowed localization of all recording sites (fig. 1B).

Isoflurane Anesthesia Studies

To reduce stress during induction, animals were placed in the induction chamber, connected to the data recording cables, and oxygen was administered several days before the experiment. This allowed animals' acclimatization to the induction chamber and instrumentation. On the testing day, neuronal recording started 5 min before induction of anesthesia. Anesthetic induction was performed with 4% isoflurane (isoflu-

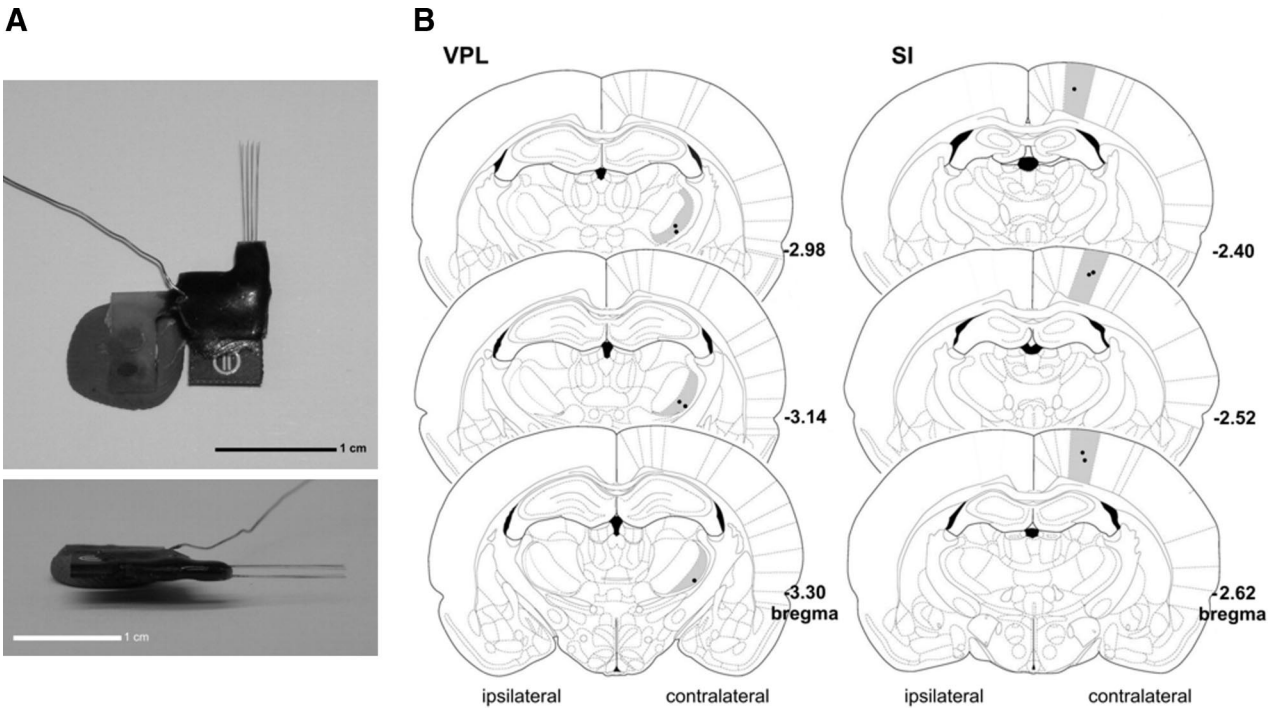

Fig. 1. (*A*) Architecture of a microelectrode array used to record local field potentials (LFP). (*B*) Coronal diagram illustrating the location in ventroposterolateral thalamic nuclei (VPL) (*left*) and primary somatosensory cortex (SI) (*right*) of the LFP recording sites (*dark dots*). Numbers represent the distance (in millimeters) relative to bregma.[20]

rane; Abbott, Amadora, Portugal) in 5 l/min of 100% oxygen. After loss of the righting reflex and evaluation of changes in respiratory rate, the animal was transferred to a smaller chamber placed above an homeothermic blanket (Harvard Apparatus, Edenbridge, Kent, United Kingdom), which also recorded the animal's temperature by a rectal probe. A purpose-built hole in the chamber allowed the passage of the LFP signals recording cable. A gas sensor, connected to an anesthetic agent monitor (Capnomac II; Datex Ohmeda, Helsinki, Finland) was placed inside the chamber at the level of the rat's nose. The animal was positioned with the head turned to the inflow port in ventral recumbence. The end-tidal isoflurane (etISO) concentration was stabilized at 0.8, 1.1, 1.4, and 1.7% concentrations for 20 min to allow equilibration between inspired and end-tidal concentration, according to a predetermined randomized sequence for each animal. These concentration stages were named as 0.8, 1.1, 1.4, and 1.7.

During the experiments, the animals breathed spontaneously, and the respiratory frequency was monitored every 5 min. In the end of the last isoflurane concentration stage, the animal was transferred to the induction chamber, where oxygen was delivered, and the recording continued for 5 min after the animal recovered its righting reflex.

LFP Recording and Processing

LFPs represent the extracellular low-frequency current flow that reflects the linearly summed postsynaptic potentials from local cell groups around the microelectrode. This type of neural signal has a temporal structure mainly in the frequency of 0–100 Hz. Extracellular LFP activity was recorded from the implanted microwires and processed by using a 16-channel Multineuron Acquisition Processor (Plexon Inc., Dallas, TX). LFP signals recorded from electrodes were preamplified (500×), filtered (0.5–400 Hz), and digitized at 1,000 Hz using a Digital Acquisition card (NIDAQ; National Instruments, Austin, TX) and sent to the 16-channel Multineuron Acquisition Processor system. Only two LFP channels per array per area were recorded and considered for posterior analysis (channel 3 [medial] and channel 6 [lateral]). The LFP frequencies analyzed ranged from 1 to 100 Hz.

Data were validated by offline analysis using NeuroExplorer 4 (Plexon Inc.) and exported to MatLab R14 (Version 2008a) for complementary analysis (MathWorks, Natick, MA).

Calculation of AE, PE, SEF, and BS Ratio. The LFP sampling frequency was first decreased to 250 Hz. All four parameters were derived from epochs of 8 s from the mean of the two cortical channels and the mean of the two thalamic channels.

The AE and the PE were computed according to the published algorithms.[15,22] The AE measures the predictability of a time series. There are three essential parameters on its calculation: the embedding dimension (m) that refers to the number of points used for prediction, the number of samples considered for each calculation (N), and a noise threshold (r). These parameters and the AE algorithm are explained in more detail in the literature.[15,22] Studies carried out by Bruhn *et al.*[22] showed that the AE yielded the highest pre-

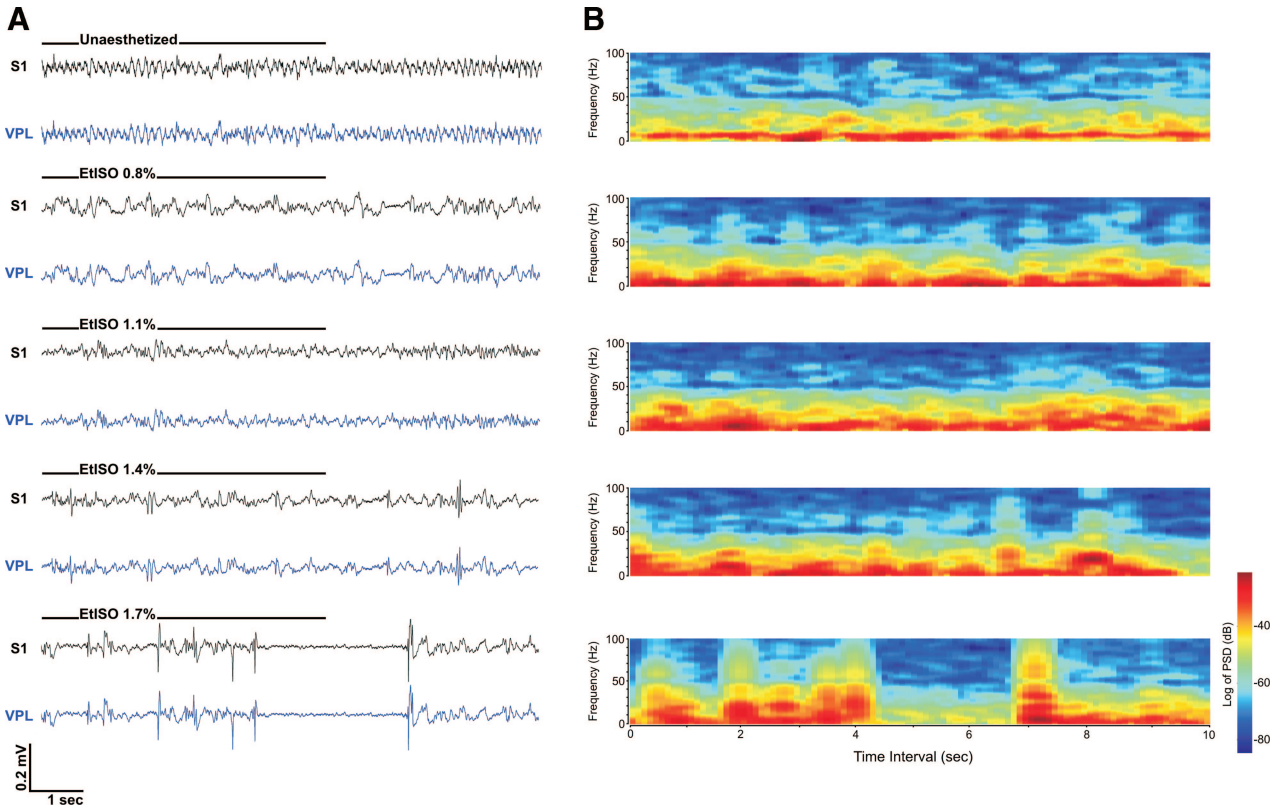

Fig. 2. Effects of isoflurane on intracranial local field potentials (LFPs) recorded simultaneously in the primary somatosensory cortex (SI, *black trace*) and in the ventroposterolateral thalamic nuclei (VPL, *blue trace*). (*A*) Raw LFP recordings representing a sample of 10 s of ongoing LFP activity recorded during the last 5 min before anesthesia induction (unaesthetized period) and during the last 5 min of each isoflurane concentration (0.8, 1.1, 1.4, and 1.7%). Visual inspection of the LFP traces revealed similar patterns of signal amplitude oscillations developed by the two recorded areas across the anesthesia stages. (*B*) Correspondent power spectrogram of each SI trace from *A*. Spectrograms showed the different patterns of signal power across the frequency range analyzed, with the appearance of alternating periods of quiescence and high-frequency activity, at higher anesthetic depths. This is compatible with the burst suppression pattern observed on the LFP correspondent traces (*A*).

diction probability with desflurane effect site concentration using m = 2, r = 0.2, and an epoch length equal or higher than 1.024 points. N = 2,000, m = 2, and r = 0.2 were selected in our study for AE calculation.

The PE is a method for ordinal time series analysis. It analyzes consecutive subvectors of constant length (m) in the analyzed signal interval (length, N). Then, it orders the samples in every subvector according to their amplitude and defines permutations of order m (m!). The parameter value is given by the resultant normalized probability distribution of the obtained permutations, using the Shannon entropy formula. In this study, we used m = 3 and N = 2,000. A more detailed description of the PE calculation can be found in the published works.[15–17]

The SEF that consists of the power spectrum in the 95% quantile was also calculated and was corrected for the presence of BS patterns according to the correction factor proposed by Rampil[23] for human electroencephalogram studies. The same correction factor was applied to PE, calculated as follows: BS-corrected PE = PE × (1 − BS/100), where the BS is defined as the epoch length in which the LFP voltage did not exceed 50 μV.

Calculation of the IoC. The IoC was derived from the signal using an executable file provided by the manufacturer (Aircraft Medical, Barcelona, Spain). Its calculation is based on the symbolic dynamics method that transforms a time series into a symbol sequence that can reveal the nonlinear characteristics of the electroencephalogram. It also integrates the β-ratio (frequency range between 11 and 42 Hz) during superficial anesthesia and the amount of suppression of the electroencephalogram (equivalent to the BS). Similar to entropy methods, this method also expresses the complexity of the signal that makes it a correlate to the depth of anesthesia. In humans, decreasing values of IoC correspond to a gradual loss of consciousness and a deepening of the level of anesthesia. In a unitless scale from 99 to 0, an index of 99 indicates an awake patient and an index of 0 indicates a flat electroencephalogram. More details on its calculation were recently published.[18]

Spectral Analysis. Spectrogram analysis was used to visualize LFP power at different frequency bands as a function of time for each etISO concentration (fig. 2). LFP spectrograms were computed in NeuroExplorer (Version 4, Plexon Inc.), with a 0.5-Hz spectral resolution and a 100-ms temporal

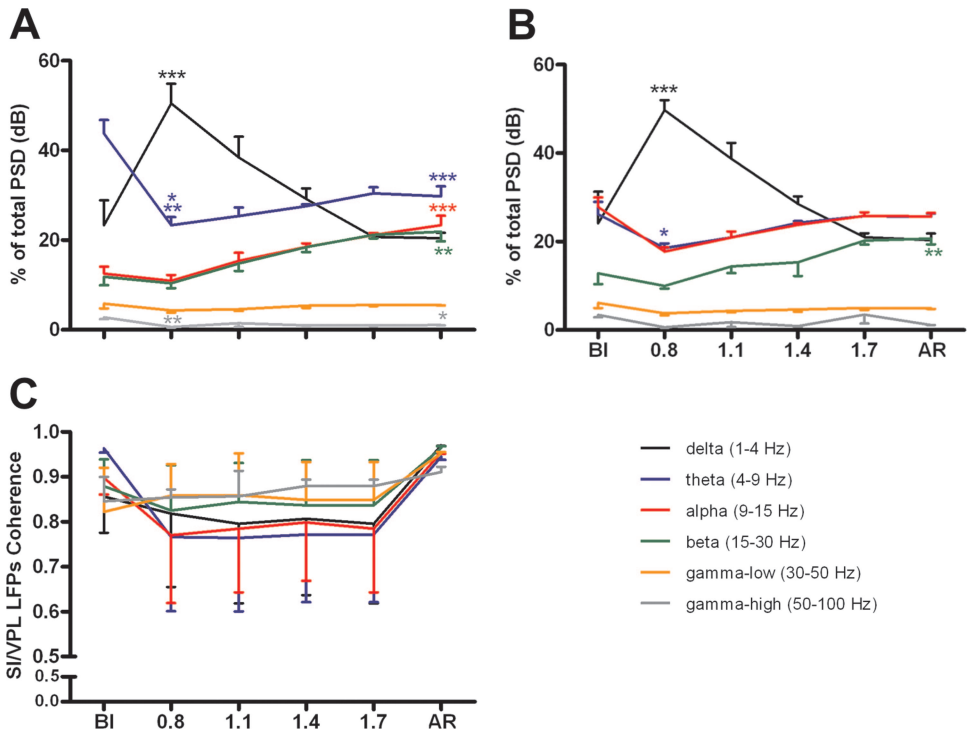

Fig. 3. Normalized power spectral density calculated using the average of all primary somatosensory cortex (SI) (*A*) and ventroposterolateral thalamic nuclei (VPL). (*B*) Local field potentials (LFP) channels illustrating the changes in spectral power across awake (before induction [BI]), isoflurane anesthetic concentrations (0.8, 1.1, 1.4, and 1.7), and after recovery (AR). (*C*) SI-VPL LFP coherence measurements illustrating a stronger level of coherence of simultaneously recorded channels of LFPs across the frequency bands considered at the different study periods BI, isoflurane concentrations (0.8, 1.1, 1.4, and 1.7%), and AR. Frequency bands: δ (1–4 Hz), θ (4–9 Hz), α (9–15 Hz), β (15–30 Hz), γ-low (30–50 Hz), and γ-high (50–100 Hz). Values are means ± SE. Comparisons based on two-way analysis of variance test, followed by Bonferroni *post hoc* test. $^{*}P < 0.05$; $^{**}P < 0.01$, and $^{***}P < 0.001$. Color version of this figure is available at www.anesthesiology.org.

resolution, using a 512-point fast Fourier transform and a 50-ms Hanning window. The power was normalized by the logarithm of the power spectral density (in decibel) and a smoothing was applied (Gaussian filter, width = 3).

The power spectra of cortical (P_{xx}) and thalamic (P_{yy}) LFP signals were calculated between 1 and 100 Hz by fast Fourier transform (512 point) of nonoverlapping 1-s epochs (Hanning window). Data are shown as the percentage of total power spectral density within each considered frequency band: δ (1–4 Hz), θ (4–9 Hz), α (9–15 Hz), β (15–30 Hz), γ-low (30–50 Hz), and γ-high (50–100 Hz) (figs. 3A and B).

Coherence $K_{xy} = (P_{xy}{}^2/(P_{xx}\,P_{yy})$ for two signals, *x* and *y*, is equal to the average cross power spectrum (P_{xy}) normalized by the averaged power spectra of the signals. This technique was used to measure the strength of the linear relationship at every frequency band[24] between the cortical and thalamic LFP signals across each etISO concentration (fig. 3C). Its value lies between 0 and 1, where $K_{xy} = 0$ means phases are eventually dispersed, and high coherence ($K_{xy} = 1$) means phases of signals *x* and *y* are identical.

Intervals of 5 min were used to calculate signal power spectral density and coherence (K_{xy}). Isoflurane stages were calculated during the last 5 min, 5 min before anesthesia induction, and 5 min after anesthesia recovery.

Statistical Analysis

Data resultant from the LFP processing were exported from MatLlab to Graphpad Prism (Version 5; GraphPad Software Inc., San Diego, CA) for statistical analysis. The Kolmogorov-Smirnov test was used to determine whether datasets were normally distributed. The correlation between the studied indexes AE, IoC, SEF, PE, BS-corrected SEF, BS-corrected PE, and the etISO was calculated using the Spearman rank correlation coefficient (r), with data from all animals. Statistical comparisons for the derived indexes, between animals and between SI and VPL channels (including comparisons of the r values) were made using the Mann–Whitney and the Wilcoxon matched-pairs tests, respectively. One-way repeated-measures ANOVA with Bonferroni *post hoc* was used to address the existence of significant differences in the spectral frequency bands of the LFP signal at the different study periods.

Results

Spontaneous intracranial LFP activity was recorded from the SI and VPL of awake and anesthetized rats (n = 5).

Six indexes of anesthetic depth were derived from the SI and VPL recordings: the AE, the IoC, the SEF, the PE, the BS-corrected SEF, and the BS-corrected PE. The values of the indexes, at each study period, for the five rats are pre-

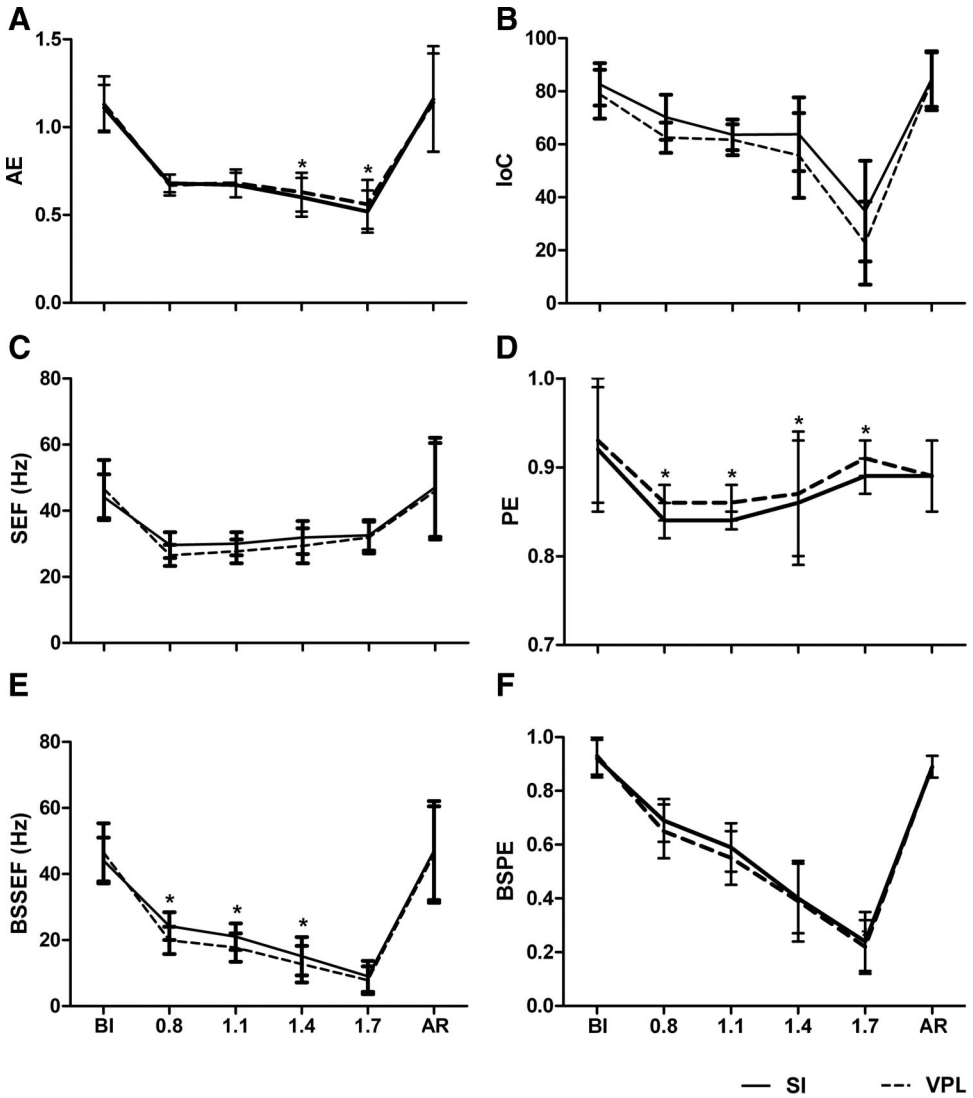

Fig. 4. Indexes derived from the signal recorded on the somatosensory cortex (SI) and in the ventroposterothalamic nuclei (VPL) at different study periods: before induction (BI) of anesthesia at steady-state end-tidal isoflurane concentrations of 0.8, 1.1, 1.4, and 1.7% (0.8, 1.1, 1.4, and 1.7) and after recovery (AR). The following indexes are presented: (*A*) approximate entropy (AE), (*B*) index of consciousness (IoC), (*C*) spectral edge frequency 95% (SEF), (*D*) permutation entropy (PE), (*E*) burst suppression–corrected SEF (BSSEF), and (*F*) burst suppression–corrected PE (BSPE).The mean and SD are presented (n = 5; *$P < 0.05$).

sented in figure 4. The Spearman rank correlation coefficient (r) between the indexes and the etISO concentration was calculated for the indexes derived from the SI and the VPL and compared (table 1).

The indexes tended to decrease similarly with increasing concentrations of etISO, except the SEF and PE. Both SEF and PE decreased from the period before induction to the period 0.8 but increased paradoxically with higher etISO concentrations, as shown in figures 4C and D. When the correction factor for BS was applied, both parameters decreased monotonically with increasing etISO concentrations (figs. 4E and F).

Comparisons between the SI and VPL revealed significant differences only in the AE (1.4 and 1.7; $P < 0.05$), PE (0.8, 1.1, 1.4, and 1.7; $P < 0.05$), and BS-corrected SEF (0.8, 1.1, and 1.4; $P = 0.0025$). No significant differences were found between the r values of the SI- and VPL-derived indexes ($P = 0.089$), although the indexes derived from the SI tended to have higher r values with the etISO (table 1). A correlation was found between AE and BS ($r = -0.73$; $P < 0.001$).

Data obtained from a representative recording are given in figure 2. The visual inspection of the raw LFPs confirmed that large signal amplitude oscillations were developed simultaneously in both recording areas during all anesthesia concentrations (fig. 2A). In addition, anesthetic induced changes in the signal power in the frequency range considered (1–100 Hz) (fig. 2B).

The LFP signal power spectral density over all experimental conditions is shown in figures 3A and B. The statistical comparison of the signal power of each considered frequency band between the two recorded areas revealed that no differences were present for δ ($F(5,40) = 0.0136$, $P = 0.99$),

Table 1. Correlation Coefficients (Spearman Rank r) with End-tidal Isoflurane Concentration for the Studied Parameters

	Spearman Rank (r)	
	SI	VPL
AE	−0.89	−0.87
IoC	−0.85	−0.83
PE	NS	NS
BSPE	−0.97	−0.95
SEF	−0.42	−0.41
BSSEF	−0.94	−0.93

Correlation coefficients (Spearman rank r) for the studied parameters: approximate entropy (AE), index of consciousness (IoC), permutation entropy (PE), burst suppression–corrected permutation entropy (BSPE), spectral edge frequency 95% (SEF), and burst suppression corrected spectral edge frequency (BSSEF). The r values calculated from pooled data of all rats indexes derived from the primary somatosensory cortex (SI) and ventroposterolateral thalamic nuclei (VPL) are presented. Correlations were considered statistically significant with $P < 0.05$; correlation was not statistically significant (NS) at the 0.05 level.

γ-low (30–50 Hz) ($F(5,40) = 0.3789$, $P = 0.8692$), and γ-high (50–100 Hz) ($F(5,40) = 0.8445$, $P = 0.5264$) bands. However, analysis of variance showed differences for θ ($F(5,40) = 6.033$, $P = 0.0003$), α (9–15 Hz) ($F(5,40) = 3.698$, $P = 0.0076$), and 32 β (15–30 Hz) ($F(5,40) = 3.124$, $P = 0.0179$) bands, with the signal power on the θ and β bands being higher on the SI and the signal power of the α band higher on the VPL.

ANOVA in the case of SI recordings data showed that signal power changed across the increase of the anesthetic (δ, $F(5,24) = 10.78$, $P < 0.0001$; θ, $F(5,24) = 13.69$, $P < 0.0001$; α, $F(5,24) = 11.47$, $P < 0.0001$; and γ-high, $F(5,24) = 4.356$, $P = 0.0058$). The exception was encountered for γ-low frequency band (30–50 Hz) ($F(5,24) = 1.213$, $P = 0.333$). In addition, *post hoc* analysis showed that δ increased and θ and γ-high power decreased between the period before induction and 0.8% etISO states (Bonferroni, $P < 0.001$, $P < 0.001$, and $P < 0.05$).

On the other hand, in the case of VPL recordings, data showed that the power of δ ($F(5,24) = 10.88$, $P < 0.0001$), θ ($F(5,24) = 4.761$, $P = 0.0037$), α ($F(5,24) = 9.062$, $P < 0.0001$), β ($F(5,24) = 5.055$, $P = 0.0026$) frequency bands changed with the increase of the anesthetic. However, no differences were encountered for γ band (γ-low, $F(5,24) = 1.885$, $P = 0.1345$; γ-high, $F(5,24) = 1.760$, $P = 0.15$). *Post hoc* analysis showed that δ power increased after anesthesia induction and θ decreased (Bonferroni, $P < 0.01$ and $P < 0.05$, respectively).

Coherence measurements between simultaneously recorded SI-VPL channels clearly showed high values of coherence activity across all the frequency bands analyzed (fig. 3C). Moreover, analysis of variance revealed no significant differences in SI-VPL activity coherence between unanesthetized and anesthesia periods (δ, $F(5,24) = 0.7585$, $P = 0.5900$; θ, $F(5,24) = 1.302$, $P = 0.3027$; α, $F(5,24) = 1.233$, $P = 0.3306$; β, $F(5,24) = 1.433$, $P = 0.2557$; γ-low, $F(5.24) = 1.226$, $P = 0.3336$; γ-high, $F(5,24) = 0.7522$, $P = 0.5943$).

Discussion

LFPs may allow a more precise analysis of the brain electrical activity than the electroencephalogram. In this study, LFPs were recorded in the thalamocortical axis of rats to (i) compare the performance of several indexes of anesthetic depth and (ii) investigate the existence of thalamocortical correlated or disrupted activity during isoflurane steady-state anesthesia. The use of electroencephalogram-derived indexes to analyze LFPs was a strong help for the interpretation of the results obtained for the second objective.

Two main results were obtained with this study: (i) the BS-corrected PE had the best correlation with steady-state etISO concentration and (ii) high coherence activity exists between the cortical and thalamic regions during steady-state anesthesia, even at deeper stages.

Both the SEF and the PE values decreased from the awake state to 0.8% isoflurane etISO concentration but paradoxically increased when higher concentrations were used. This phenomenon is well described for the SEF in electroencephalographic signals and is assumed to be caused by the appearance of the BS pattern.[23,25] This paradoxical increase was also seen in the spectral analysis, with increasing spectral power on the θ, α, and β bands with increasing etISO concentration. A similar paradoxical increase occurred in PE in humans anesthetized with sevoflurane.[15,17] The inclusion of a BS component in the PE would, therefore, contribute to the improvement of the parameter,[15] and the correction applied in this study seems appropriate to adapt the PE for deeper anesthetic states.

There was no correction necessary to achieve an adequate association between AE and etISO concentration. This parameter seems to correctly classify the BS pattern, which is in accordance to previous findings in humans[26] and rats.[19] However, AE has the drawback of being very sensitive to artifacts. In the study by Ihmsen *et al.*, higher etISO concentrations were achieved (a maximum of 2.1%) and the AE did not decrease to values lower than 0.4, whereas in this study lower values were achieved with etISO concentration of 1.7%. This may be due to the presence of residual noise during BS pattern in the study by Ihmsen *et al.*, which could have been classified as brain activity by AE. In our study, with a cleaner signal from intracranial recordings this situation could be avoided. The IoC[18] had an acceptable performance in detecting the effects of different isoflurane concentrations in the LFPs. It is a proprietary monitor and its exact calculation algorithm is not published. However, it is known that, as other commercial monitors, it has a BS component. The lower correlation value obtained with the IoC, when compared with BS-corrected PE, BS-corrected SEF, and AE, could be related to the fact that its algorithm is adjusted for the human electroencephalogram and the BS limit might

need an adaptation for this type of signal to achieve a better performance. Its major drawback is being proprietary, which makes it impossible to adapt the algorithm to the type of signal and species. On the other hand, the other three parameters (AE, SEF, and PE) have a greater advantage of having published algorithms thereby allowing its continuous improvement. The calculation of the SEF is very simple relying only on frequency changes. Its major problems are the sensitivity to artifacts and the need for a correction for BS. With this correction, it seems to be able to classify different anesthetic depths, with a correlation with the anesthetic concentration even better than the AE in this study.

The type of signal analyzed here represents a relevant difference to previous studies comparing anesthetic depth indexes. No artifact-filtering systems were applied before deriving the indexes and only a 50-Hz notch filter was applied because, contrary to the electroencephalogram, the LFPs do not suffer interference from the electromyographic activity. This way, the γ-band oscillations could be preserved, which are known to be important markers of the conscious state.[2] In this study, the γ-band power decreased from the awake to the anesthetized state, but this decrease was only significant in the SI. This may be due to the association of the γ oscillations to cortical conscious activity[2] and may be the reason for the higher correlation coefficients with the etISO concentration obtained with the SI indexes. Significant differences between the two areas were found for the θ, α, and β bands. This could also be related to the different origins of these rhythms: while the spindle activity (14 Hz) is generated on the thalamus[10] and may increase the power in the α band (9–15 Hz), the β rhythms (15–30 Hz) generated by corticocortical interactions caused higher power on the SI.[14]

The BS pattern simultaneously appeared in the SI and VPL and was highly synchronized, as previously suggested.[27]

Although there was a tendency for the correlation coefficients from the SI indexes to be higher than those from the VPL indexes, the difference was not statistically significant. It could be expected that the SI indexes had a better correlation with the anesthetic concentration, because they were developed to analyze the electroencephalogram that reflects mainly the cortical activity, contrary to previous findings with neuroimaging techniques in humans.[28] But this result together with the high coherence obtained between the two areas may indicate that the cortical and thalamic neurons remain connected to some extent during steady-state anesthesia. Our results support the existence of a "permanent corticothalamic dialogue" during steady-state anesthesia, as has been suggested for quiet physiologic sleep.[10] However, the existence of a separate role of the cortex[6,7] or the thalamus,[8,9] as targets of anesthetic effects, cannot be clarified with the present results because the dynamic phases of anesthesia were not studied but only steady-state effects. These results are in accordance with the ideas that loss of consciousness may not necessarily require that talamocortical neurons are inactivated[10,11] and that anesthesia causes a drop in γ-frequency power.[2,11] According to the information or integration theory proposed by Alkire *et al.*,[11] anesthetic-induced unconsciousness presupposes two mechanisms: (1) a loss of information capacity reflected by reduction in the number of electrophysiological patterns with increasing anesthetic depth and (2) a loss of integration capacity reflected by an interruption in the interactions between brain structures. Although this study does not reveal a disruption in the thalamocortical interactions, it may support the loss of information idea, because a decrease in the electrophysiological patterns was observed, shrinking to the stereotypic BS pattern at deeper stages.

Meanwhile, these results do not guarantee the existence of equal activity in both areas, because output neuronal activity is not contemplated on the LFPs, but only slower postsynaptic activity. Nevertheless, this animal preparation is a promising method for future investigations on the mechanisms of anesthetic action, especially by analyzing the dynamic phases of anesthesia, at induction and recovery and including other recording techniques such as multiunit recordings. Also, by knowing how the SI and VPL neurons interact during steady-state anesthesia, it will be easier to draw conclusions on the effects of intraoperative noxious stimuli and analgesic administration on pain processing by the somatosensory system, with the same animal preparation.[29]

LFP recordings performed in this study resulted in two main conclusions: (i) the PE corrected with the classic BS ratio is a promising alternative to other indexes of anesthetic depth and (ii) data showed high coherence level of activity between cortical and thalamic regions, even at deep isoflurane stages.

References

1. Nunez P, Srinivasan R: Electric Fields of the Brain: The Neurophysics of EEG, 2nd edition. Oxford, Oxford University Press, 2006
2. Sleigh JW, Steyn-Ross DA, Steyn-Ross ML, Williams ML, Smith P: Comparison of changes in electroencephalographic measures during induction of general anaesthesia: Influence of the gamma frequency band and electromyogram signal. Br J Anaesth 2001; 86:50–8
3. Gervasoni D, Lin SC, Ribeiro S, Soares ES, Pantoja J, Nicolelis MA: Global forebrain dynamics predict rat behavioral states and their transitions. J Neurosci 2004; 24: 11137–47
4. Juergens E, Guettler A, Eckhorn R: Visual stimulation elicits locked and induced gamma oscillations in monkey intracortical and EEG-potentials, but not in human. Exp Brain Res 1999; 129:247–59
5. Legatt AD, Arezzo J, Vaughan HG Jr: Averaged multiple unit activity as an estimate of phasic changes in local neuronal activity: Effects of volume-conducted potentials. J Neurosci Methods 1980; 2:203–17
6. Velly LJ, Rey MF, Bruder NJ, Gouvitsos FA, Witjas T, Regis JM, Peragut JC, Gouin FM: Differential dynamic of action on cortical and subcortical structures of anesthetic agents during induction of anesthesia. ANESTHESIOLOGY 2007; 107: 202–12
7. Hentschke H, Schwarz C, Antkowiak B: Neocortex is the major target of sedative concentrations of volatile anaesthetics: Strong depression of firing rates and increase of GABAA receptor-mediated inhibition. Eur J Neurosci 2005; 21:93–102

8. Alkire MT, McReynolds JR, Hahn EL, Trivedi AN: Thalamic microinjection of nicotine reverses sevoflurane-induced loss of righting reflex in the rat. ANESTHESIOLOGY 2007; 107:264–72
9. Alkire MT, Haier RJ, Fallon JH: Toward a unified theory of narcosis: Brain imaging evidence for a thalamocortical switch as the neurophysiologic basis of anesthetic-induced unconsciousness. Conscious Cogn 2000; 9:370–86
10. Amzica F, Steriade M: Integration of low-frequency sleep oscillations in corticothalamic networks. Acta Neurobiol Exp (Wars) 2000; 60:229–45
11. Alkire MT, Hudetz AG, Tononi G: Consciousness and anesthesia. Science 2008; 322:876–80
12. Jones EG: The thalamic matrix and thalamocortical synchrony. Trends Neurosci 2001; 24:595–601
13. Steriade M: The GABAergic reticular nucleus: A preferential target of corticothalamic projections. Proc Natl Acad Sci USA 2001; 98:3625–7
14. Schneider G, Kochs EF: The search for structures and mechanisms controlling anesthesia-induced unconsciousness. ANESTHESIOLOGY 2007; 107:195–8
15. Li X, Cui S, Voss LJ: Using permutation entropy to measure the electroencephalographic effects of sevoflurane. ANESTHESIOLOGY 2008; 109:448–56
16. Jordan D, Stockmanns G, Kochs EF, Pilge S, Schneider G: Electroencephalographic order pattern analysis for the separation of consciousness and unconsciousness: An analysis of approximate entropy, permutation entropy, recurrence rate, and phase coupling of order recurrence plots. ANESTHESIOLOGY 2008; 109:1014–22
17. Olofsen E, Sleigh JW, Dahan A: Permutation entropy of the electroencephalogram: A measure of anaesthetic drug effect. Br J Anaesth 2008; 101:810–21
18. Revuelta M, Paniagua P, Campos JM, Fernandez JA, Martinez A, Jospin M, Litvan H: Validation of the index of consciousness during sevoflurane and remifentanil anaesthesia: A comparison with the bispectral index and the cerebral state index. Br J Anaesth 2008; 101:53–8
19. Ihmsen H, Schywalsky M, Plettke R, Priller M, Walz F, Schwilden H: Concentration-effect relations, prediction probabilities (Pk), and signal-to-noise ratios of different electroencephalographic parameters during administration of desflurane, isoflurane, and sevoflurane in rats. ANESTHESIOLOGY 2008; 108:276–85
20. Paxinos G, Watson C: The Rat Brain in Stereotaxic Coordinates, 4th edition. San Diego, Academic Press, 1998
21. Nicolelis MA, Ghazanfar AA, Faggin BM, Votaw S, Oliveira LM: Reconstructing the engram: Simultaneous, multisite, many single neuron recordings. Neuron 1997; 18:529–37
22. Bruhn J, Ropcke H, Hoeft A: Approximate entropy as an electroencephalographic measure of anesthetic drug effect during desflurane anesthesia. ANESTHESIOLOGY 2000; 92:715–26
23. Rampil IJ: A primer for EEG signal processing in anesthesia. ANESTHESIOLOGY 1998; 89:980–1002
24. Achermann P, Borbely AA: Temporal evolution of coherence and power in the human sleep electroencephalogram. J Sleep Res 1998; 7(suppl 1):36–41
25. Antunes LM, Golledge HD, Roughan JV, Flecknell PA: Comparison of electroencephalogram activity and auditory evoked responses during isoflurane and halothane anaesthesia in the rat. Vet Anaesth Analg 2003; 30:15–23
26. Bruhn J, Ropcke H, Rehberg B, Bouillon T, Hoeft A: Electroencephalogram approximate entropy correctly classifies the occurrence of burst suppression pattern as increasing anesthetic drug effect. ANESTHESIOLOGY 2000; 93: 981–5
27. Detsch O, Kochs E, Siemers M, Bromm B, Vahle-Hinz C: Increased responsiveness of cortical neurons in contrast to thalamic neurons during isoflurane-induced EEG bursts in rats. Neurosci Lett 2002; 317:9–12
28. White NS, Alkire MT: Impaired thalamocortical connectivity in humans during general-anesthetic-induced unconsciousness. Neuroimage 2003; 19:402–11
29. Cardoso-Cruz H, Lima D, Galhardo V: Thalamocortical pain processing in freely behaving rats: A study based on chronic extracellular multichannel recordings. Eur J Pain 2006; 10:S54–5

PUBLICAÇÃO 3

EJN fens EUROPEAN JOURNAL OF NEUROSCIENCE

European Journal of Neuroscience, Vol. 33, pp. 2255–2264, 2011 doi:10.1111/j.1460-9568.2011.07721.x

NEUROSYSTEMS

Instability of spatial encoding by CA1 hippocampal place cells after peripheral nerve injury

Helder Cardoso-Cruz,[1,2] Deolinda Lima[1,2] and Vasco Galhardo[1,2]
[1]Instituto de Biologia Molecular e Celular (IBMC), Grupo de Morfofisiologia do Sistema Somatosensitivo, Universidade do Porto, 4150-180 Porto, Portugal
[2]Departamento de Biologia Experimental, Faculdade de Medicina, Universidade do Porto, Porto, Portugal

Keywords: multichannel recording, neuropathy, pain, rat

Abstract

Several authors have shown that the hippocampus responds to painful stimulation and suggested that prolonged painful conditions could lead to abnormal hippocampal functioning. The aim of the present study was to evaluate whether the induction of persistent peripheral neuropathic pain would affect basic hippocampal processing such as the spatial encoding performed by CA1 place cells. These place cells fire preferentially in a certain spatial position in the environment, and this spatial mapping remains stable across multiple experimental sessions even when the animal is removed from the testing environment. To address the effect of prolonged pain on the stability of place cell encoding, we chronically implanted arrays of electrodes in the CA1 hippocampal region of adult rats and recorded the multichannel neuronal activity during a simple food-reinforced alternation task in a U-shaped runway. The activity of place cells was followed over a 3-week period before and after the establishment of an animal model of neuropathy, spared nerve injury. Our results show that the nerve injury increased the number of place fields encoded per cell and the mapping size of the place fields. In addition, there was an increase in in-field coherence while the amount of spatial information content that a single spike conveyed about the animal location decreased over time. Other measures of spatial tuning (in-field firing rate, firing peak and number of spikes) were unchanged between the experimental groups. These results demonstrate that the functioning of spatial place cells is altered during neuropathic pain conditions.

Introduction

It has long been known that the hippocampus is crucial for learning and memory. One special feature of pyramidal complex-spike neurons found in CA1 and CA3 areas of the hippocampus is that they encode the animal location in the environment (Fox & Ranck, 1981). These place cells increase their firing rate when an animal is in a particular position within its environment (place field; O' Keefe & Dostrovsky, 1971; O' Keefe & Nadel, 1978), and this place field is usually stable across repeated visits to the same environment, even when the animal is removed from it for extended time periods (Muller *et al.*, 1987; Thompson & Best, 1990). Several studies have shown that changes in the spatial features or motivational content of the testing environment may disrupt the place field stability (Kobayashi *et al.*, 1997; Markus *et al.*, 1995; Moita *et al.*, 2004; Muller & Kubie, 1987; Wood *et al.*, 2000). On the other hand it has been shown that place field instability could also result from pharmacological manipulations of hippocampal functioning (Dragoi *et al.*, 2003; Kentros *et al.*, 1998; Rotenberg *et al.*, 2000) or from direct lesioning of the hippocampus or hippocampal-connected areas (Leutgeb & Mizumori, 1999; Liu *et al.*, 2003; McNaughton *et al.*, 1989; Mizumori *et al.*, 1994; Muir & Bilkey, 2001).

In addition to spatial information, the hippocampus has repeatedly been described as being involved in the regulation of several behavioural aspects of the adaptation to aversive situations, including pain (Khanna, 1997; Khanna & Sinclair, 1992; Soleimannejad *et al.*, 2006). Hippocampal neurons respond to noxious stimulation (Delgado, 1955; Halgren *et al.*, 1978; Khanna, 1997; Soleimannejad *et al.*, 2006; Tai *et al.*, 2006; Wei *et al.*, 2000; Zheng & Khanna, 2008), and human imaging studies have shown its activation by acute noxious stimulation (Bingel *et al.*, 2002; Ploghaus *et al.*, 2001, 2000). Moreover, partial hippocampectomy has been used (albeit with moderated success) as a treatment for human chronic pain syndromes (Gol & Faibish, 1967), while the inactivation of hippocampal synaptic transmission attenuated nociceptive behaviour in the rat formalin model (Khanna, 1997; McKenna & Melzack, 1992, 2001).

Despite all the knowledge gathered on how the hippocampus affects pain processing, little is known about how pain affects hippocampal functioning. It has been shown that chronic pain changes c-fos expression (Carter *et al.*, 2011; Ceccarelli *et al.*, 2003) and long-term potentiation (Kodama *et al.*, 2007; Ren *et al.*, 2011), and causes changes in hippocampal volume (Lutz *et al.*, 2008; Younger *et al.*, 2010), but it is still unknown whether pain affects crucial hippocampal functions such as the generation of spatial maps. Therefore, our goal

Correspondence: Vasco Galhardo, [1]Instituto de Biologia Molecular e Celular (IBMC), as above.
E-mail: galhardo@med.up.pt

Received 2 February 2011, revised 13 March 2011, accepted 5 April 2011

was to verify whether long-term neuropathic pain disrupts the stability of CA1 hippocampal place fields in the absence of spatial or motivational changes introduced in the familiar testing environment, or alterations in the performance capability of the animal. We recorded neuronal activity of freely moving rats in a simple spatial alternation task, performed before and after the induction of the spared nerve injury (SNI) model of neuropathic pain (Decosterd & Woolf, 2000).

Materials and methods

Subjects

Twelve adult male Sprague–Dawley rats weighing between 275 and 325 g were used in this study. The rats were maintained on a 12-h light–dark cycle, and both training and recording sessions ran at approximately the same time each day, during the light portion of the cycle. All procedures and experiments adhered to the guidelines of the Committee for Research and Ethical Issues of IASP (Zimmermann, 1983) and with the Ethical Guidelines for Animal Experimentation of the European Community Directive Number 86/609/ECC of 24 November of 1986, and were approved by national and local boards.

Behavioral arena

The testing environment consisted of a U-shaped arena with three sections that were 72 cm long and 15 cm wide, and with opaque walls 30 cm high (Fig. 1); this arena was similar to an elevated runway previously used in a place cell stability study (Tropp *et al.*, 2005). Rats were trained to run an alternation schedule on the arena to receive food reinforcements at both ends of the runway; one chocolate-flavoured pellet was automatically delivered by a pellet dispenser (Coulbourn Instruments, Whitehall, PA, USA), depending on previous visit to the opposite end of the runway. Control of pellet dispensers was fully automated using the OpenControl software adapted to this particular task (Aguiar *et al.*, 2007). We preferred the use of this simple task in a linear runway instead of a more complex bifurcating arena that requires navigational decision-making because pain is known to affect both decision-making and spatial navigation in working memory-dependent tasks (Pais-Vieira *et al.*, 2009a; Hu *et al.*, 2010; our own unpublished results), and any perturbations of the navigational performance of the animals may lead to spontaneous place field remapping.

Experimental schedule

During the training period, the rats were given two 15-min sessions per day to learn the alternation schedule until they performed 80 correct runway alternations within a period of 4 consecutive days (Tropp *et al.*, 2005). After reaching this performance criterion the animals were surgically implanted unilaterally with a multielectrode array for single-unit recording (see details below).

After 7 days of recovery from the implantation surgery, 12 animals ($n = 6$ in both sham and nerve-lesioned groups) were recorded over 4 consecutive days (hereafter named baseline or control period) while performing the runway alternation task in two daily sessions of 15 min. The detailed results from this control period sessions are presented in Table S1 as Supporting Information. On the following day the animals were briefly anesthetized and either surgically subjected to the SNI model of neuropathic pain (Decosterd & Woolf, 2000) or to a sham intervention with the same extent of skin incision and muscle dissection, performed in the left hindpaw contralateral to the location of the intracranial recording electrodes. Both groups of animals were then recorded for a period of 3 weeks (with recordings performed on days 1, 2, 3, 7, 10, 15 and 21 after SNI or sham intervention). The sensory threshold for noxious stimulation was measured using von Frey filaments (Somedic, Sweden) as previously described (Chaplan *et al.*, 1994). Von Frey testing was always performed after the second recording session of the day (with at least a minimum interval of 1 h after replacing the animals in their home cage). Testing was performed in an elevated chamber with a thin metallic mesh floor that allowed easy access to the plantar surface of the left hindpaw; filament series were run from the thinnest to the widest to detect the filament to which the animal withdrew the paw in at least six of 10 successive applications; we then performed another two series of 10 stimulations using the same filament (2-min intervals between sessions) and averaged the number of positive responses evoked by the three series.

Multielectrode implantation

For the surgical implantation of the intracranial multielectrode array the animals were anesthetized with an intramuscular injection of a mixture of xylazine and ketamine (10 and 60 mg/kg, respectively). Anesthesia was maintained with small additional injections of ketamine (one-third of the initial dosage). Oxygen was supplied during the procedure via a face mask. The depth of anesthesia and paralysis of the musculature was assessed by regularly testing the corneal blink, hindpaw withdrawal and tail-pinch reflexes. After the anesthesia induction, each animal received a single dose of atropine sulphate (0.02 mg/kg, subcutaneous) and 1 mL of serum (sucrose 2% w/v in NaCl 0.9% w/v, subcutaneous) every hour throughout the surgery. Core body temperature was measured with a rectal thermometer and maintained at 37 °C by means of a homeothermic blanket system. The animal's head was shaved and cleaned using a triple application of alcohol (70%, v/v) and Betadine. A midline subcutaneous injection of 0.3 mL of 1% lignocaine (B Braun, Melsungen, Germany) was applied to the scalp for local analgesia. Anesthetized animals were secured in a stereotaxic frame using ear bars, and a midline incision was made caudally to the animal's eyes and ending between ears. The connective tissue was blunt-dissected, and the top of the skull was exposed and cleaned using hydrogen peroxide. After exposure of the scalp, holes were bored for fixation of four screws used for securing the array and for grounding. One craniotomy (3×3 mm) was made for implantation of the multielectrode.

Each multielectrode array consisted of eight filaments of isonel-coated tungsten wire (35 μm diameter; California Fine Wire Company, Grover Beach, CA, USA) with impedances varying between 0.5 and 0.7 MΩ at 1 kHz. The multielectrode arrays were built in a 4×2 architecture, interspaced with 250 μm between rows and 400 μm between columns (Silva *et al.*, 2010). The arrays were rostrocaudally oriented and mounted in the holder of a hydraulic micropositioner (FHC Inc, Bowdoin, ME, USA) and slowly driven (50 μm/min) into the right hippocampal CA1 region after *dura mater* removal, while monitoring the neuronal activity. The following coordinates in mm relative to bregma (Paxinos & Watson, 1998) were used to center the arrays: −3.2 rostrocaudal, +2.2 mediolateral and −2.6 dorsoventral. After the electrodes were advanced to the correct position, the craniotomy was sealed with a layer of agar (4% in saline) and the array was cemented to the skull screws using dental acrylic. At the end of the implantation the animal was transferred to a recovery cage. The analgesic carprofen (7.5 mg/kg; Rimadyl, Pfizer Animal Health, Lisbon, Portugal) and the antibiotic amoxicillin (6 mg/kg; Clamoxyl, Pfizer Animal Health,

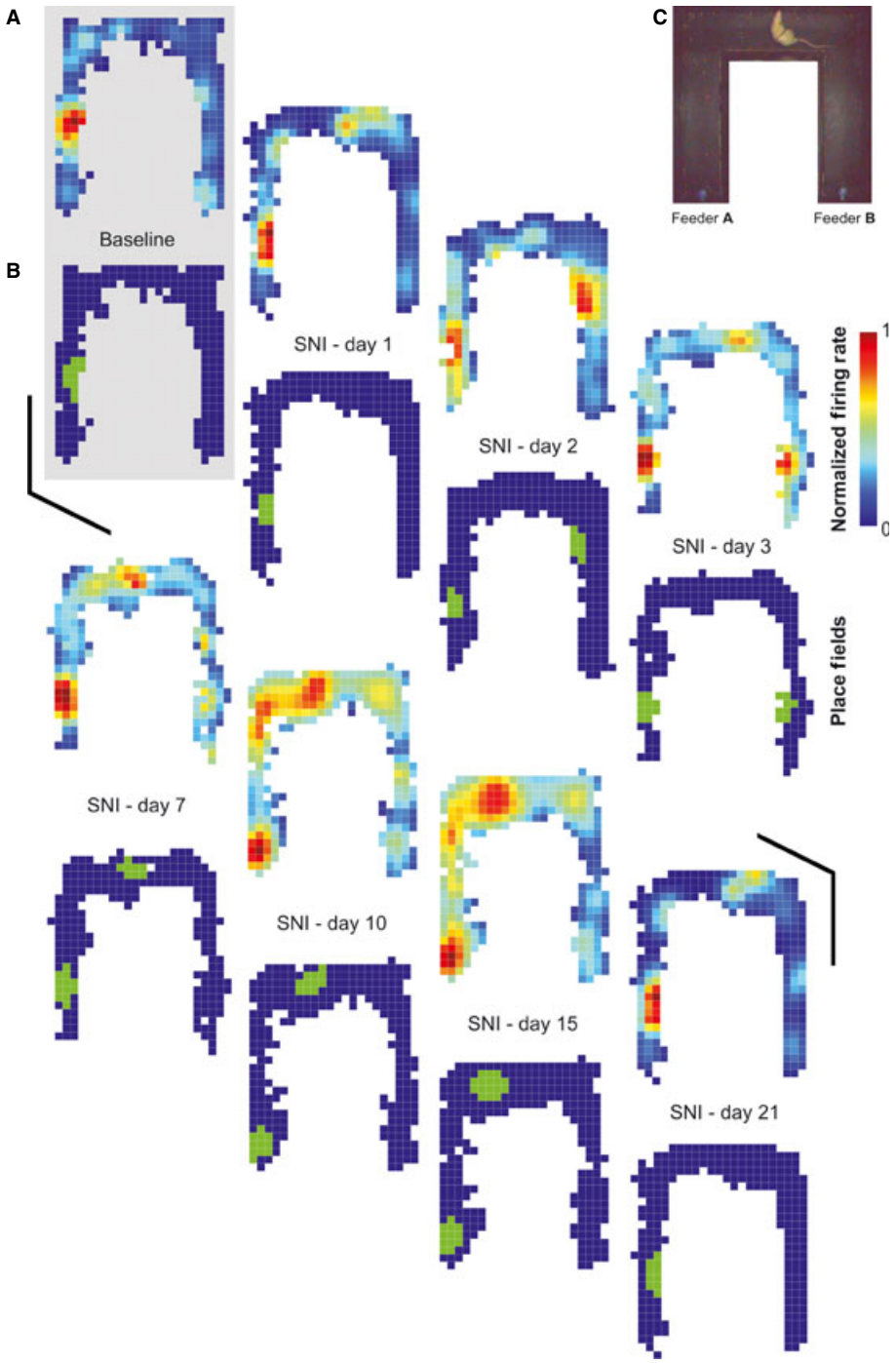

FIG. 1. Illustration of activity of a place cell during the testing environment navigation before (baseline) and after nerve injury (SNI). (A) Normalized firing rate maps. The bright red pixels correspond to regions where the cell fired at a higher rate, and the dark blue to a lower rate. (B) Correspondent encoded place fields (green pixels). (C) Photograph of the U-shaped testing environment. The rats were trained to alternate between feeders A and B in the maze for food reinforcement dispensed by pellet feeders located one at the end of each arm. The feeders dispensed a single food pellet when the animal performed a correct alternation.

Lisbon, Portugal) was administered subcutaneously every 24 h for 3 days while the animal recovered from surgery. Rats were allowed to recover for 1 week before the task re-training sessions began.

Neural recordings

All neural activity signals from the implanted microelectrodes were recorded and processed using a Multineuron Acquisition Processor system (16-MAP; Plexon Inc., Dallas, TX, USA). Voltage–time threshold windows were used to identify single-unit waveforms. The differentiated neural signals were preamplified (10 000–25 000 ×), and digitized at 40 kHz. Up to two neuronal action potentials per recording channel were sorted online (SortClient 2008; Plexon Inc.) and validated by offline analysis (Offline Sorter 2.8.; Plexon Inc.) according to the following cumulative criteria: voltage thresholds > 2 SD of amplitude distributions; signal-to-noise ratio > 3; fewer than 1% of interspike intervals > 1.2 ms; and stability of the waveform shape as determined by a waveform matching template

algorithm and principal component analysis. In addition, the Waveform Tracker software (Plexon Inc.) was used to verify that the recorded units were stable across experimental sessions. This software ensures that the same neuron is recorded in consecutive sessions through the analysis of the projection of the waveform of each recorded unit onto its three-dimensional principal components analysis space. An overhead video tracking system (CinePlex; Plexon Inc.) was used to provide information about the animal location on the runway and synchronize the video recordings with the acquired neuronal data.

Data analysis

Neural ensemble data were processed offline using NeuroExplorer 4 (NEX; Plexon Inc.) and exported to our own MatLab R14 routines for additional analysis (MathWorks, Natick, MA, USA). Statistical comparisons of the experimental groups were performed by repeated-measures two-way ANOVA and, when appropriate, a *post hoc* analysis was carried out using the Bonferroni test (Prism 5.0; GraphPad, San Diego, CA, USA). The level of significance was set as at 5%. Results are expressed as mean ± SEM.

Classification of cells

Putative pyramidal complex-spike 'place cells' were classified as such if they had a spike width (peak-to-trough) > 450 μs and a signal-to-noise ratio $> 3 : 1$. These cells were characterized by complex bursts wherein they often fired two to five spikes with an interspike interval of approximately 5 ms. Complex bursts were identified with an autocorrelation function (Neuroexplorer; Plexon Inc.) that calculated the time between all spike pairs and distinguished between the firing patterns of place cells and those of theta cells (putative interneurons; Markus *et al.*, 1994). Data from recorded theta cells were not included in the present study. Place cells recorded in the testing environment typically presented a mean firing rate < 5 Hz and a maximal in-field firing rate < 30 Hz. Because most of the examined parameters are affected by low firing rates, cells that had firing rates < 0.1 Hz were not analyzed. Furthermore, because it was important to ensure that the same unit was being recorded in repeated sessions, only units that exhibited stable spike amplitudes and consistent waveforms within and between recording sessions were included in this study.

Firing properties

Firing rate maps were prepared for each cell by dividing the recording environment into a 32×32-bin array, each bin corresponding to 20×20 pixels of video resolution. Average firing rate for each bin was calculated for each neuron by dividing the number of recorded spikes by the time spent in that bin. Place fields were designated as an area of 5–20 bins sharing adjacent edges, with a firing rate > 2 SD above of the average cell firing rate over the entire arena (Muller & Kubie, 1989). Place field size was defined as the number of bins sharing adjacent edges that comprised the place field.

Basic firing properties were calculated: (i) the average firing rate of the unit on testing environment; (ii) the average firing rate within the place field; (iii) the maximum peak of firing rate within the place field; (iv) spatial discrimination capability, the ratio between the mean firing rate inside the place field and the mean firing rate outside the place field; and (v) the coherence of the firing inside the place field, this coherence measure being a computed autocorrelation between the rate for each bin of the place field and the average rate of all in-field bins (Neuroexplorer; Plexon Inc.).

In order to provide a measure of spatial firing that does not require characterization of the place field, the data obtained from the recording sessions were analyzed using a measure of spatial information content measure (I, or specificity; Skaggs & McNaughton, 1996; Skaggs *et al.*, 1993). Specificity of the place field was calculated in terms of the amount of spatial information content (in bits) that a single spike conveyed about the animal's location and was calculated using the equation $I = \Sigma\ P_i\ (R_i/R).\log_2(R_i/R)$, where i is the bin number, P_i is the probability for occupancy of bin i, R_i is the mean firing rate for bin i and R is the overall mean firing rate. A value of 0 indicates that no spatial information is conveyed, while a typical place cell generates a value close to 1 bit of information per spike.

The averaged position of a place field on the runway was defined by calculating the centre of mass (centroid) of the firing rate distribution within the place field boundaries (Mehta *et al.*, 1997). To assess place field expansion we calculated the size (in bins) of each field. In addition, to assess shifts in the place field position, we calculated the linear distance (in pixels) between field centroids of the current and previous recording sessions.

Histology

At the end of all experiments, the rats were deeply anesthetized with a mixture of ketamine and xylazine, and the recording site was marked by injecting DC current (10–20 μA for 10–20 s) through one microelectrode, marking the area below the electrode tips. Afterwards animals were perfused through the heart with 0.01 M phosphate buffer (pH = 7.2) in 0.9% saline solution, followed by 4% paraformaldehyde. Brains were removed and post-fixed in 4% paraformaldehyde for 4 h and stored in 30% sucrose before they were frozen and sectioned into 60-μm slices. Sections were stained with Cresyl violet for microscopic identification of the recording site (shown in Supporting Information Fig. S1).

Results

Mechanical hypersensitivity after SNI

All SNI animals developed mechanical allodynia as indicated by the significant decrease in the mechanical force needed to evoke paw withdrawal to Von Frey stimulation in the hindpaw ipsilateral to the lesion, but not in the contralateral hindpaw (Bonferroni, $P < 0.001$). In the SHAM group, no statistical differences were noted between before and after surgery sessions (Fig. 2A).

Behavioral task activity

No evident variation was found in rat activity across training sessions, and no signs of satiation were observed in the 15-min duration of each session. ANOVA revealed no significant differences in the number of correct alternations (from feeder A to feeder B) between SNI and SHAM animals (ANOVA-RM, $F_{7,70} = 1.33$, $P = 0.2421$; Fig. 2B). However, there was a within-group time effect across pre- and post-surgery recording sessions (ANOVA-RM, $F_{7,70} = 8.33$, $P < 0.0001$), probably due to the decrease in correct alternations that occurred in both groups in the first 3 days after surgery.

These results show that the induction of chronic pain did not cause a significant change in task performance between control and pain groups; this is technically crucial for establishing that eventual alterations in hippocampal spatial encoding did not result from

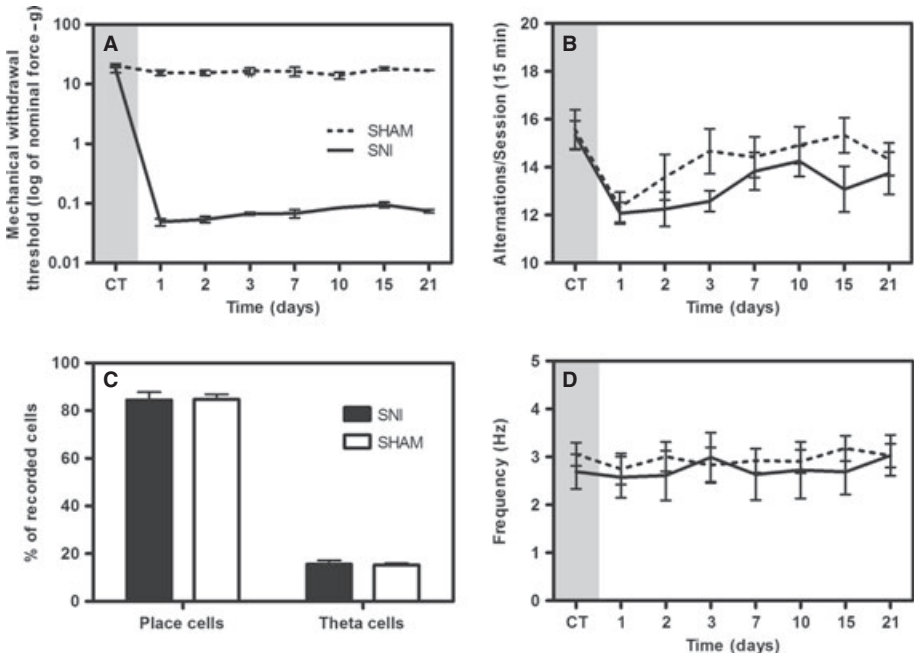

FIG. 2. Behavioural performance in the runway alternation task. (A) Level of sensitivity to mechanical stimulation evaluated using von Frey filaments. A large decrease was observed in the threshold required to induce a paw response in the SNI group. (B) Number of correct alternations on the U-shaped maze. Similar levels of behavioural task activity were observed for the two experimental groups. (C) The proportion of recorded neurons that were classified as place cells showed a similar distribution in the two experimental groups. Note that only neurons classified as place cells were considered in the analyses of the present study. (D) Average firing rate per place cell during the entire session remained unchanged after surgery. SNI, nerve lesion group; SHAM, control group. Values are mean ± SEM. Shaded area on the left of each graph represents the baseline control period (CT); the baseline plotted value is the collapsed average of the recording sessions in the 4 days before the nerve lesion, although it should be noted that in all statistical comparisons the values of the control days were used without any averaging. Comparisons between control and after surgery recording sessions based on two-way repeated-measures ANOVA, followed by Bonferroni's *post hoc* test.

changes in either locomotion or reward motivation, which are known to induce place cell instability by themselves.

Neuronal activity during task performance

We used the Waveform Tracker software (Plexon Inc.) to ensure that individual neural recordings were correctly identified across experiments; only place cells that remained stable throughout the recording sessions in terms of waveform shape were considered in the present study (Supporting Information Fig. S1). Therefore, a total of 117 validated neurons were recorded from the CA1 region in six nerve-injured rats (SNI; $n = 58$ cells) and six control SHAM rats ($n = 59$ cells). Some cells were excluded from the final analysis because they did not exhibit the criterion properties of pyramidal complex cells described earlier (18 neurons, presumably theta cells). Consequently, 49/58 (84.48%) of cells from the SNI group and 50/59 (84.75%) cells from the SHAM group were determined to be place cells (Fig. 2C).

The mean firing rate was calculated for each place cell for the duration of the behavioural task. A two-factor repeated-measures ANOVA was used to compare the firing rates of cells from SNI and SHAM animals in pre- and post-surgery recording sessions (Fig. 2D), and revealed no significant differences in mean firing rate between the two experimental groups (ANOVA-RM, $F_{7,70} = 0.99$, $P = 0.4466$) and across the recording sessions (ANOVA-RM, $F_{7,70} = 1.03$, $P = 0.4225$).

Encoding of place fields

CA1 pyramidal cells of the SNI group showed a significant increase in the number of encoded place fields. This increase was observed on a cell-by-cell basis and did not affect all cells simultaneously recorded in the same animal (Fig. 3). Repeated-measures ANOVA revealed that there were differences between the two groups ($F_{7,70} = 5.87$, $P < 0.0001$) and across time ($F_{7,70} = 3.27$, $P = 0.0460$). Moreover, *post hoc* analysis showed that the number of place fields in the SNI group was larger than in SHAM control animals (Bonferroni, $P < 0.01$ for day 7 after SNI and $P < 0.001$ for day 10 after SNI; Fig. 4A).

A two-factor repeated-measures ANOVA was used to compare the in-field firing activity of cells from SHAM and lesion animals in pre- and post-surgery recording sessions. There was no significant group effect for the place cells' in-field mean firing rate ($F_{7,70} = 1.03$, $P = 0.4201$) or in-field peak of firing ($F_{7,70} = 0.66$, $P = 0.7059$; Fig. 4B and C). However, over the recording sessions there was a significant effect of time in the in-field mean firing rate ($F_{7,70} = 6.99$, $P < 0.0001$) and in-field peak of firing ($F_{7,70} = 4.26$, $P = 0.0006$).

The recordings in the SNI and SHAM groups show that the internal place field coherence of place cells was affected after peripheral nerve injury with a significant increase after 7 days of lesion (Fig. 4D). Analysis revealed that there were differences between groups (ANOVA-RM, $F_{7,70} = 5.45$, $P < 0.0001$) and across the recording sessions (ANOVA-RM, $F_{7,70} = 4.74$, $P = 0.0002$). *Post hoc* analysis showed that values of field coherence after nerve injury were greater than those observed in the SHAM group (days 7 and 10; Bonferroni, $P < 0.05$).

There were also differences in the field size between the two experimental groups (ANOVA-RM, $F_{7,70} = 3.57$, $P = 0.0025$) and across the recording sessions (ANOVA-RM, $F_{7,70} = 2.63$, $P = 0.0179$; Fig. 4E). *Post hoc* analysis of field size revealed a significant increase for SNI group after nerve injury. However, no group interaction was found for field centroid movement (ANOVA-RM, $F_{7,70} = 1.38$,

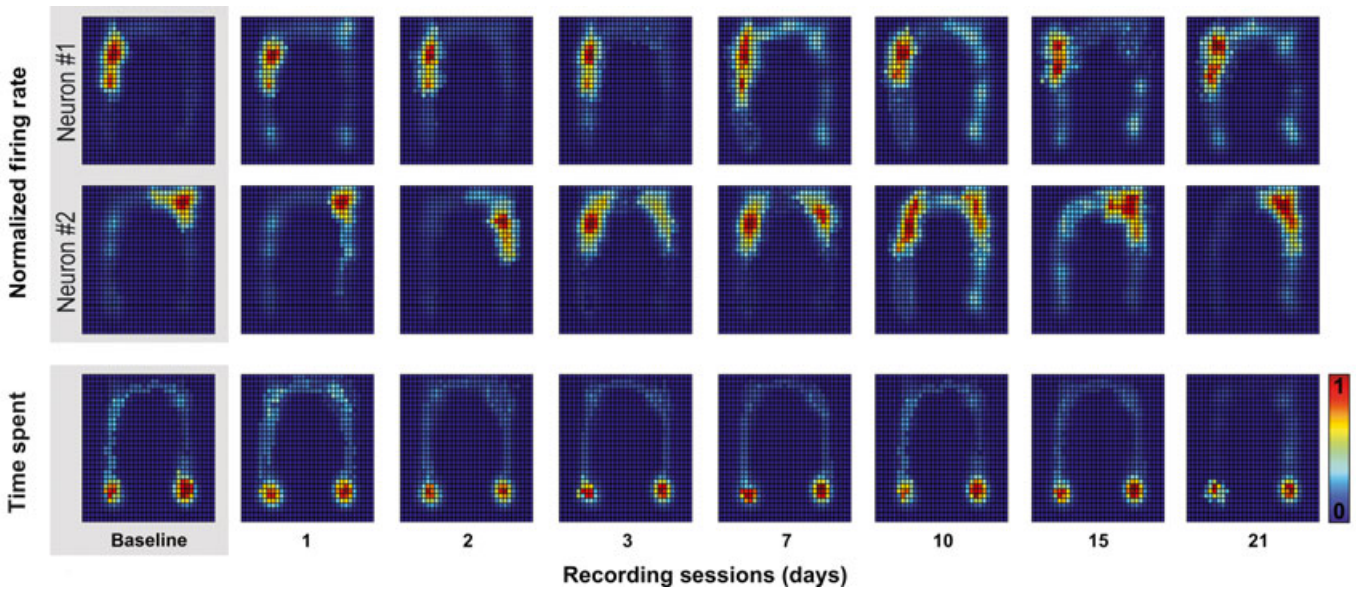

FIG. 3. Differential effect of pain over the remapping of place fields. The top two rows show the normalized firing rate per bin of two simultaneously recorded hippocampal place cells during the alternation task in the U-shaped runway. Note the similarity in the spatial firing activity of neuron 1 across recording sessions, and the encoding instability of neuron 2 in the days following the nerve lesion. The bottom row shows the time spent in each bin during the entire recording session, and demonstrates that the place field locations are commonly unrelated to the movement of the animal. Bright red represents bins with higher firing rate (top two rows) or where the animal spent more time (bottom row), and dark blue represent bins with lower firing rates (top two rows) or where the animal spent less time during the session (bottom row). The shaded plot on the left of each row represents the baseline control period; the baseline plotted values are the collapsed average of the activity in the 4 days before the nerve lesion.

$P = 0.2275$), although both groups presented changes over time (ANOVA-RM, $F_{7,70} = 13.10$, $P < 0.0001$; Fig. 4F).

Spatial information content

The information content (bits/spike) of cells recorded from peripheral nerve injury animals (SNI group) was significantly lower than that of cells from SHAM control animals (Fig. 4G). ANOVA-RM analysis revealed there was a difference between groups ($F_{7,70} = 16.06$, $P < 0.0001$) and across the recording sessions ($F_{7,70} = 10.44$, $P < 0.0001$). *Post hoc* analysis revealed a significant decrease in information content encoded by the cells of the SNI group 10 days after nerve injury when compared with SHAM group (Bonferroni, $P < 0.05$).

Spatial discrimination capability

Spatial discrimination capability, or the ratio between the mean firing rate inside the place field and the mean firing rate outside the place field, is shown in Fig. 4H. The results indicate that spatial discrimination did not differ between experimental groups (ANOVA-RM, $F_{7,70} = 1.13$, $P = 0.3565$) or over recording sessions (ANOVA-RM, $F_{7,70} = 1.79$, $P = 0.1037$).

Discussion

The aim of the present study was to address for the first time whether the onset of an animal model of the chronic neuropathic pain condition affects the spatial encoding properties of hippocampal CA1 pyramidal cells. This type of cell is considered to be crucial for the continuously updated representation of space and individual position. However, this dynamic information is only one of several features stored in the hippocampal network (Eichenbaum *et al.*, 1999; Leutgeb *et al.*, 2005), and for this reason it is of primary interest to determine what factors, including pain, may contribute to disruption of the stability of place cells.

Our results show that pain causes instability in hippocampal place field encoding in the absence of changes in overall task performance. As intended, the onset of the pain model caused a transient reduction in task performance only in the days immediately following the surgery and this effect was equally observed in both control and pain animals. We specifically used this simple alternation task because it is not cognitively challenging and our results are in agreement with previous reports showing that pain has no impact on performance in simple spatial and nonspatial memory tasks (Apkarian *et al.*, 2004; LaBuda & Fuchs, 2000; Leite-Almeida *et al.*, 2009), although pain-related memory deficits may be observed in more complex memory tasks (Dick & Rashiq, 2007; Millecamps *et al.*, 2004; Leite-Almeida *et al.*, 2009). Moreover, the transient effect in performance (Fig. 2B) is not temporally correlated with the peak of place field instability (Fig. 4A), suggesting that the late onset instability of CA1 place fields is not caused by motor impairment or reduced motivation for task completion.

It is important to note that, although the task used in this study is not strictly hippocampus-dependent, several single-unit recording studies have also used tasks which are not hippocampus-dependent, such as forced-choice tasks, to examine place field characteristics, showing that place cells present environment re-mapping even on nonhippocampal tasks (Markus *et al.*, 1995; Muller & Kubie, 1987; Ranck, 1973).

Chronic pain changed CA1 place cell activity

Basic firing properties of CA1 place cells remained stable after peripheral nerve lesion. These properties included mean firing rate

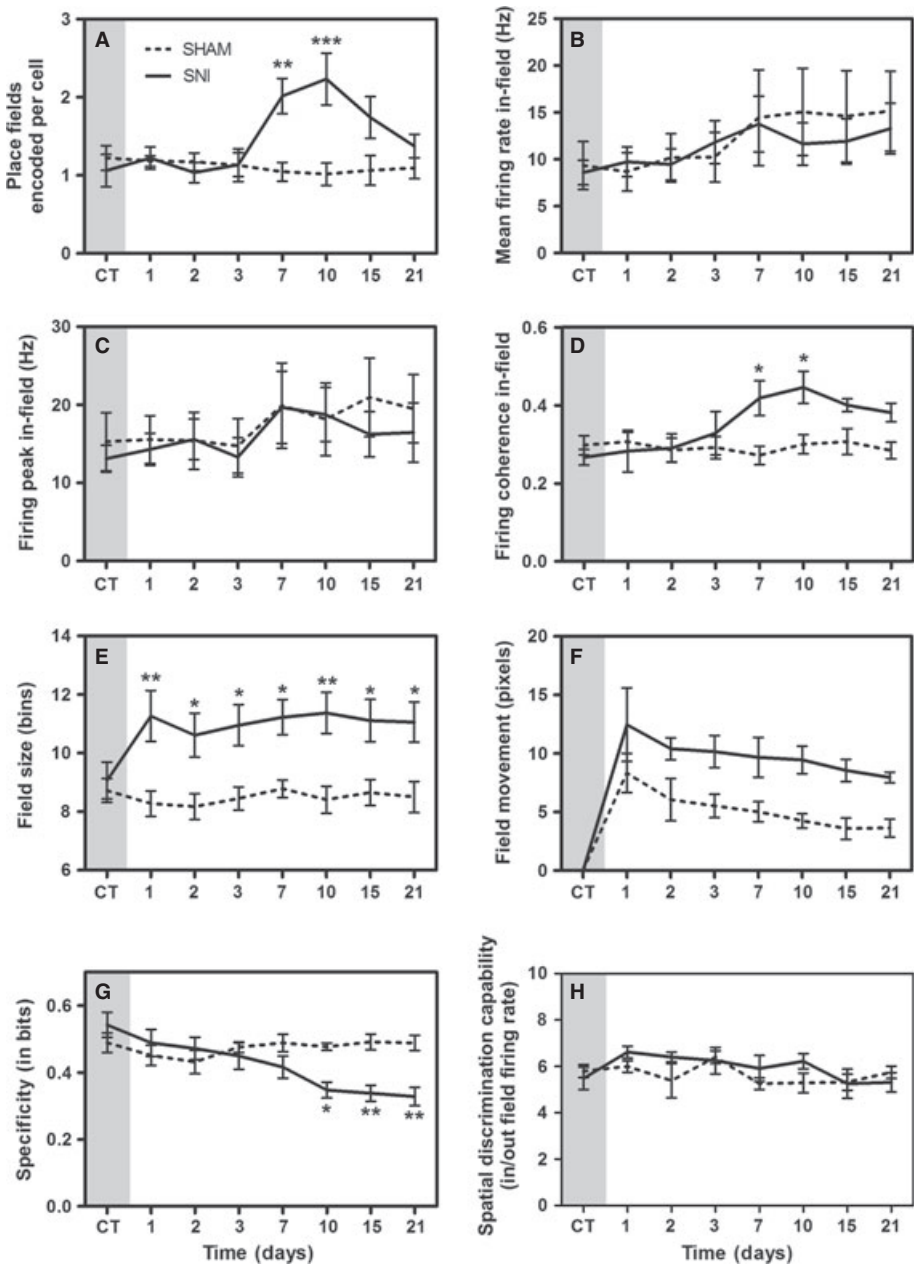

FIG. 4. Spatial place field properties across recording sessions. (A) Number of place fields encoded per recorded place cell. (B) Place field firing coherence. (C) Average in-field firing rate. (D) maximum firing rate for in-field peak. (E) Average size, in bins, of the place fields. (F) Place field shifts of centroid location, in pixels. (G) Specificity, or spatial content information (in bits), conveyed per spike of place cells. (H) Spatial discrimination capability (in-field/out-field firing ratio) between groups. SNI, nerve lesion group; SHAM, control group. Values are mean ± SEM. Shaded area on the left of each graph represents the baseline control period (CT); the baseline plotted value is the collapsed average of the recording sessions in the 4 days before the nerve lesion, although it should be noted that in all statistical comparisons the values of the control days were used without any averaging. Comparisons between control and after surgery recording sessions based on two-way repeated-measures ANOVA, followed by Bonferroni's *post hoc* test. $*P < 0.05$; $**P < 0.01$, and $***P < 0.001$.

activity and spatial discrimination capability. Indeed, the fact that the spatial discrimination was similar across the two groups implies a proportional firing activity in both experimental conditions. However, the analysis of spatial information content, or specificity (Skaggs *et al.*, 1993), a measure of spatial firing that does not require that a particular region be defined as a place field, revealed significantly lower values in the neurons recorded from nerve-lesioned rats, indicating that the activity of these neurons provided less information about spatial location. It should also be noted that the spatial information content is only minimally affected by proportional changes in the firing rate.

Chronic pain disrupted place field stability

Spatial tuning characteristics such as number of place fields encoded per cell and in-field firing coherence changed after nerve lesion, with a peak effect observed 7 days after the lesion, of two place fields encoded per cell. Interestingly, 21 days after nerve lesion the majority of the cells returned to the baseline encoding of only one place field in average. A possible hypothesis to explain this transient effect is a reduction in pain threshold associated with nerve-injured animals; however, no statistically significant differences in data were encountered between days 15 and 21 in the von Frey test. In addition, it is

important to note that the second place field occupied a location which was not adjacent to the first one; this suggests that pain-induced field remapping and field expansion are different phenomena. It has been reported that place fields may be modified during a single recording session, and this may represent the within-session continuous acquisition of novel spatial information (Mehta *et al.*, 1997, 2000). This hypothesis does not apply to our results because we only started the control recording sessions after several training sessions, and during all control recording sessions the properties of place field remained stable (see Supporting Information Table S1).

Mechanisms of place field instability

Apart from studies involving lesioning of the hippocampus or hippocampus-connected areas (McNaughton *et al.*, 1989; Muir & Bilkey, 2001), to our best knowledge no previous studies have shown disruption of place fields in the absence of changes to the testing environment. Stressful stimuli were shown to alter the in-field firing rate stability of place cells but not the stability of the field's location within a familiar environment (Kim *et al.*, 2007), although the data presented by the authors suggest a shift in pre- vs. post-stress location. A similar study has shown that the stability of place fields in a familiar environment does not change across the estrous cycle (Tropp *et al.*, 2005).

Several studies have shown that place field instability is accompanied by an overall increase in the size of preexisting place fields, and it has been reported that this size expansion is diminished in aged rats (Barnes *et al.*, 1997; Shen *et al.*, 1997) and abolished by selective blockade of NMDA receptors (Ekstrom *et al.*, 2001). Moreover, NMDA-dependent long-term potentiation processes are important for maintaining the stability of place fields (Kentros *et al.*, 1998; Shapiro & Eichenbaum, 1999).

Only incomplete and sometimes conflicting data exist on the molecular mechanisms of interplay between pain and hippocampal plasticity; it has been shown that chronic neuropathy reduces CA1 long-term potentiation (Kodama *et al.*, 2007; Ren *et al.*, 2011) while the opposite effect has been described after acute peripheral injection of formalin (Zhao *et al.*, 2009). In addition, recent studies have shown that chronic pain reduces the hippocampal levels of BDNF (Duric & McCarson, 2005; Hu *et al.*, 2010; Al-Amin *et al.*, 2011), which is known to be a key regulator of hippocampal synaptic plasticity (Minichiello, 2009). It must be noted that to our best knowledge no direct connection has been demonstrated between neurotrophin levels in the hippocampus and the stability of place cells, but it is expected that the modulation of molecules important for synaptic plasticity also leads to changes in the circuitry of hippocampal spatial encoding.

Finally, it has been proposed that hippocampal remapping may result from memory interference between concurrent sets of experiences (Colgin *et al.*, 2008). This is in agreement with the idea that evoked or spontaneous pain perception causes an interference with ongoing cognitive functions (Seminowicz & Davis, 2007; Moriarty *et al.*, 2011), disrupting the attentional processes that are crucial for learning and memory (Boyette-Davis *et al.*, 2008; Pais-Vieira *et al.*, 2009b).

Conclusion

In summary, our data suggest that peripheral nerve injury (SNI) induces a relative instability of hippocampal CA1 place cells' spatial features. The present data indicate that nerve lesion induces a clear reduction in the speciality measure, indicating that place cells provided less information about spatial location after lesion. Our findings also demonstrate place field disturbances, namely in the number, size and in-field firing coherence. These changes are probably caused by hippocampal structural adaptive mechanisms that occur during the onset of the painful condition, which may disturb the mnemonic processes that rely on the integration and consolidation of spatial reference memory.

Supporting Information

Additional supporting information may be found in the online version of this article:

Fig. S1. Stability of waveform shapes of two hippocampal place cells simultaneously recorded from the same channel (yellow and green) across experimental sessions (A). Note that the waveform shape of each place cell remained stable throughout the recording sessions. Only units with a $> 3:1$ signal to noise rate were considered. (B) Illustration of the Unit A firing activity recorded from a rat running on the U-shaped task encoding a spatial place field (area with peak of firing). Maximum firing rate is indicated by red and occupancy with no firing by blue. (C) Offline analysis of 3-D PC cluster stability from the channel shown across the whole recording sessions using the WaveTracker software (Plexon Inc., Dallas, TX, USA). In this view (D), 2-D PC clusters are projected as function of time (*Z*-axis). Stability across time and absence of overlap between units isolated from the same channel were used as extra-selection criteria. (E) Location of implanted multielectrode arrays for nine rats used in this study. The black dots indicate the location of the centre of the array in CA1 region.

Table S1. Statistical summary for SHAM and SNI-group comparison across all measurements during the eight recording sessions of the control period.

Please note: As a service to our authors and readers, this journal provides supporting information supplied by the authors. Such materials are peer-reviewed and may be re-organized for online delivery, but are not copy-edited or typeset by Wiley-Blackwell. Technical support issues arising from supporting information (other than missing files) should be addressed to the authors.

Acknowledgements

This work was supported by grants from the Portuguese Foundation for Science and Technology – FCT: FCT SFRH/42500/2007, FCT PTDC/SAU-NEU/100733/2008; and BIAL Foundation: BIAL Project 126/08.

Abbreviations

SNI, spared nerve injury.

Conflict of interest

The authors do not have any conflicts of interest.

References

Aguiar, P., Mendonça, L. & Galhardo, V. (2007) OpenControl: a free opensource software for video tracking and automated control of behavioral mazes. *J. Neurosci. Methods*, **166**, 66–72.

Al-Amin, H., Sarkis, R., Atweh, S., Jabbur, S. & Saadé, N. (2011) Chronic dizocilpine or apomorphine and development of neuropathy in two animal

models II: effects on brain cytokines and neurotrophins. *Exp. Neurol.*, **228**, 30–40.
Apkarian, A.V., Sosa, Y., Krauss, B.R., Thomas, P.S., Fredrickson, B.E., Levy, R.E., Harden, R.N. & Chialvo, D.R. (2004) Chronic pain patients are impaired on an emotional decision-making task. *Pain*, **108**, 129–136.
Barnes, C.A., Suster, M.S., Shen, J.M. & McNaughton, B.L. (1997) Multistability of cognitive maps in the hippocampus of old rats. *Nature*, **388**, 272–275.
Bingel, U., Quante, M., Knab, R., Bromm, B., Weiller, C. & Buchel, C. (2002) Subcortical structures involved in pain processing: evidence from single-trial fMR1. *Pain*, **99**, 313–321.
Boyette-Davis, J.A., Thompson, C.D. & Fuchs, P.N. (2008) Alterations in attentional mechanisms in response to acute inflammatory pain and morphine administration. *Neuroscience*, **151**, 558–563.
Carter, J.L., Lubahn, C., Lorton, D., Osredkar, T., Der, T.C., Schaller, J., Evelsizer, S., Flowers, S., Ruff, N., Reese, B. & Bellinger, D.L. (2011) Adjuvant-induced arthritis induces c-Fos chronically in neurons in the hippocampus. *J. Neuroimmunol.*, **230**, 85–94.
Ceccarelli, I., Scaramuzzino, A., Massafra, C. & Aloisi, A.M. (2003) The behavioral and neuronal effects induced by repetitive nociceptive stimulation are affected by gonadal hormones in male rats. *Pain*, **104**, 35–47.
Chaplan, S.R., Bach, F.W., Pogrel, J.W., Chung, J.M. & Yaksh, T.L. (1994) Quantitative assessment of tactile allodynia in the rat paw. *J. Neurosci. Methods*, **53**, 55–63.
Colgin, L.L., Moser, E.I. & Moser, M.B. (2008) Understanding memory through hippocampal remapping. *Trends Neurosci.*, **31**, 469–477.
Decosterd, I. & Woolf, C.J. (2000) Spared nerve injury: an animal model of persistent peripheral neuropathic pain. *Pain*, **87**, 149–158.
Delgado, J.M.R. (1955) Cerebral structures involved in transmission and elaboration of noxious stimulation. *J. Neurophysiol.*, **18**, 261–275.
Dick, B.D. & Rashiq, S. (2007) Disruption of attention and working memory traces in individuals with chronic pain. *Anesth. Analg.*, **104**, 1223–1229.
Dragoi, G., Harris, K.D. & Buzsaki, G. (2003) Place representation within hippocampal networks is modified by long-term potentiation. *Neuron*, **39**, 843–853.
Duric, V. & McCarson, K.E. (2005) Hippocampal neurokinin-1 receptor and brain-derived neurotrophic factor gene expression is decreased in rat models of pain and stress. *Neuroscience*, **133**, 999–1006.
Eichenbaum, H., Dudchenko, P., Wood, E., Shapiro, M. & Tanila, H. (1999) The hippocampus, memory, and place cells: is it spatial memory or a memory space? *Neuron*, **23**, 209–226.
Ekstrom, A.D., Meltzer, J., McNaughton, B.L. & Barnes, C.A. (2001) NMDA receptor antagonism blocks experience-dependent expansion of hippocampal "place fields". *Neuron*, **31**, 631–638.
Fox, S.E. & Ranck, J.B. Jr (1981) Electrophysiological characteristics of hippocampal complex-spike cells and theta cells. *Exp. Brain Res.*, **41**, 399–410.
Gol, A. & Faibish, G.M. (1967) Effects of human hippocampal ablation. *J. Neurosurg.*, **26**, 390–398.
Halgren, E., Walter, R.D., Cherlow, D.G. & Crandall, P.H. (1978) Mental phenomena evoked by electrical-stimulation of human hippocampal formation and amygdala. *Brain*, **101**, 83–117.
Hu, Y., Yang, J., Hu, Y., Wang, Y. & Li, W. (2010) Amitriptyline rather than lornoxicam ameliorates neuropathic pain-induced deficits in abilities of spatial learning and memory. *Eur. J. Anaesthesiol.*, **27**, 162–168.
Kentros, C., Hargreaves, E., Hawkins, R.D., Kandel, E.R., Shapiro, M. & Muller, R.V. (1998) Abolition of long-term stability of new hippocampal place cell maps by NMDA receptor blockade. *Science*, **280**, 2121–2126.
Khanna, S. (1997) Dorsal hippocampus field CA1 pyramidal cell responses to a persistent versus an acute nociceptive stimulus and their septal modulation. *Neuroscience*, **77**, 713–721.
Khanna, S. & Sinclair, J. (1992) Responses in the CA1 region of the rat hippocampus to a noxious stimulus. *Exp. Neurol.*, **117**, 28–35.
Kim, J., Lee, H., Welday, A., Song, E., Cho, J., Sharp, P., Jung, M. & Blair, H. (2007) Stress-induced alterations in hippocampal plasticity, place cells, and spatial memory. *Proc. Natl. Acad. Sci. USA*, **104**, 18297–18302.
Kobayashi, T., Nishijo, H., Fukuda, M., Bures, J. & Ono, T. (1997) Task-dependent representations in rat hippocampal place neurons. *J. Neurophysiol.*, **78**, 597–613.
Kodama, D., Ono, H. & Tanabe, M. (2007) Altered hippocampal long-term potentiation after peripheral nerve injury in mice. *Eur. J. Pharmacol.*, **574**, 127–132.
LaBuda, C.J. & Fuchs, P.N. (2000) A behavioral test paradigm to measure the aversive quality of inflammatory and neuropathic pain in rats. *Exp. Neurol.*, **163**, 490–494.
Leite-Almeida, H., Almeida-Torres, L., Mesquita, A.R., Pertovaara, A., Sousa, N., Cerqueira, J.J. & Almeida, A. (2009) The impact of age on emotional and cognitive behaviours triggered by experimental neuropathy in rats. *Pain*, **144**, 57–65.
Leutgeb, S. & Mizumori, S.J.Y. (1999) Excitotoxic septal lesions result in spatial memory deficits and altered flexibility of hippocampal single-unit representations. *J. Neurosci.*, **19**, 6661–6672.
Leutgeb, S., Letugeb, J.K., Barnes, C.A., Moser, E.I., McNaughton, B.L. & Moser, M.B. (2005) Independent codes for spatial and episodic memory in hippocampal neuronal ensembles. *Science*, **309**, 619–623.
Liu, X., Muller, R.U., Huang, L.T., Kubie, J.L., Rotenberg, A., Rivard, B., Cilio, M.R. & Holmes, G.L. (2003) Seizure-induced changes in place cell physiology: relationship to spatial memory. *J. Neurosci.*, **23**, 11505–11515.
Lutz, J., Jager, L., de Quervain, D., Krauseneck, T., Padberg, F., Wichnalek, M., Beyer, A., Stahl, R., Zirngibl, B., Morhard, D., Reiser, M. & Schelling, G. (2008) White and gray matter abnormalities in the brain of patients with fibromyalgia: a diffusion-tensor and volumetric imaging study. *Arthritis Rheum.*, **58**, 3960–3969.
Markus, E.J., Barnes, C.A., McNaughton, B.L., Gladden, V.L. & Skaggs, W.E. (1994) Spatial information content and reliability of hippocampal CA1 neurons: effects of visual input. *Hippocampus*, **4**, 410–421.
Markus, E.J., Qin, Y.L., Leonard, B., Skaggs, W.E., McNaughton, B.L. & Barnes, C.A. (1995) Interactions between location and task affect the spatial and directional firing of hippocampal neurons. *J. Neurosci.*, **15**, 7079–7094.
McKenna, J.E. & Melzack, R. (1992) Analgesia produced by lidocaine microinjection into the dentate gyrus. *Pain*, **49**, 105–112.
McKenna, J.E. & Melzack, R. (2001) Blocking NMDA receptors in the hippocampal dentate gyrus with AP5 produces analgesia in the formalin pain test. *Exp. Neurol.*, **172**, 92–99.
McNaughton, B.L., Barnes, C.A., Meltzer, J. & Sutherland, R.J. (1989) Hippocampal granule cells are necessary for normal spatial learning but not for spatially-selective pyramidal cell discharge. *Exp. Brain Res.*, **76**, 485–496.
Mehta, M.R., Barnes, C.A. & McNaughton, B.L. (1997) Experience-dependent, asymmetric expansion of hippocampal place fields. *Proc. Natl. Acad. Sci. U S A*, **94**, 8918–8921.
Mehta, M.R., Quirk, M.C. & Wilson, M.A. (2000) Experience-dependent asymmetric shape of hippocampal receptive fields. *Neuron*, **25**, 707–715.
Millecamps, M., Etienne, M., Jourdan, D., Eschalier, A. & Ardid, D. (2004) Decrease in non-selective, non-sustained attention induced by a chronic visceral inflammatory state as a new pain evaluation in rats. *Pain*, **109**, 214–224.
Minichiello, L. (2009) TrkB signalling pathways in LTP and learning. *Nat. Rev. Neurosci.*, **10**, 850–860.
Mizumori, S., Miya, D. & Ward, K. (1994) Reversible inactivation of the lateral dorsal thalamus disrupts hippocampal place representation and impairs spatial learning. *Brain Res.*, **644**, 168–174.
Moita, M.A., Rosis, S., Zhou, Y., LeDoux, J.E. & Blair, H.T. (2004) Putting fear in its place: remapping of hippocampal place cells during fear conditioning. *J. Neurosci.*, **24**, 7015–7023.
Moriarty, O., McGuireb, B.E. & Finn, D.P. (2011) The effect of pain on cognitive function: a review of clinical and preclinical research. *Prog. Neurobiol.*, **93**, 385–404.
Muir, G. & Bilkey, D. (2001) Instability in the place field location of hippocampal place cells after lesions centered on the perirhinal cortex. *J. Neurosci.*, **21**, 4016–4025.
Muller, R.U. & Kubie, J.L. (1987) The effects of changes in the environment on the spatial firing of hippocampal complex-spike cells. *J. Neurosci.*, **7**, 1951–1968.
Muller, R.U. & Kubie, J.L. (1989) The firing of hippocampal place cells predicts the future position of freely moving rats. *J. Neurosci.*, **9**, 4101–4110.
Muller, R.U., Kubie, J.L. & Ranck, J.B. Jr (1987) Spatial firing patterns of hippocampal complex-spike cells in a fixed environment. *J. Neurosci.*, **7**, 1935–1950.
O' Keefe, J. & Dostrovsky, J. (1971) Hippocampus as a spatial map – preliminary evidence from unit activity in freely-moving rat. *Brain Res.*, **34**, 5.
O' Keefe, J. & Nadel, L. (1978) *The hippocampus as a cognitive map*. Clarendon, Oxford.
Pais-Vieira, M., Mendes-Pinto, M.M., Lima, D. & Galhardo, V. (2009a) Cognitive impairment of prefrontal-dependent decision-making in rats after the onset of chronic pain. *Neuroscience*, **161**, 671–679.
Pais-Vieira, M., Lima, D. & Galhardo, V. (2009b) Sustained attention deficits in rats with chronic inflammatory pain. *Neurosci. Lett.*, **463**, 98–102.

Paxinos, G. & Watson, C. (1998) *The Rat Brain in Stereotaxic Coordinates*. Academic Press, San Diego.

Ploghaus, A., Tracey, I., Clare, S., Gati, J.S., Rawlins, J.N.P. & Matthews, P.M. (2000) Learning about pain: the neural substrate of the prediction error for aversive events. *Proc. Natl Acad. Sci. USA*, **97**, 9281–9286.

Ploghaus, A., Narain, C., Beckmann, C.F., Clare, S., Bantick, S., Wise, R., Matthews, P.M., Rawlins, J.N.P. & Tracey, I. (2001) Exacerbation of pain by anxiety is associated with activity in a hippocampal network. *J. Neurosci.*, **21**, 9896–9903.

Ranck, J.B. Jr (1973) Studies on single neurons in dorsal hippocampal formation and septum in unrestrained rats. I. Behavioral correlates and firing repertoires. *Exp. Neurol.*, **41**, 461–531.

Ren, W.J., Liu, Y., Zhou, L.J., Li, W., Zhong, Y., Pang, R.P., Xin, W.J., Wei, X.H., Wang, J., Zhu, H.Q., Wu, C.Y., Qin, Z.H., Liu, G. & Liu, X.G. (2011) Peripheral nerve injury leads to working memory deficits and dysfunction of the hippocampus by upregulation of TNF-α in rodents. *Neuropsychopharmacology*, **36**, 979–992.

Rotenberg, A., Abel, T., Hawkins, R.D., Kandel, E.R. & Muller, R.U. (2000) Parallel instabilities of long-term potentiation, place cells, and learning caused by decreased protein kinase A activity. *J. Neurosci.*, **20**, 8096–8102.

Seminowicz, D.A. & Davis, K.D. (2007) Interactions of pain intensity and cognitive load: the brain stays on task. *Cereb. Cortex*, **17**, 1412–1422.

Shapiro, M.L. & Eichenbaum, H. (1999) Hippocampus as a memory map: synaptic plasticity and memory encoding by hippocampal neurons. *Hippocampus*, **9**, 365–384.

Shen, J., Barnes, C.A., McNaughton, B.L., Skaggs, W.E. & Weaver, K.L. (1997) The effect of aging on experience-dependent plasticity of hippocampal place cells. *J. Neurosci.*, **17**, 6769–6782.

Silva, A., Cardoso-Cruz, H., Silva, F., Galhardo, V. & Antunes, L. (2010) Comparison of anesthetic depth indexes based on thalamocortical local field potentials in rats. *Anesthesiology*, **112**, 355–363.

Skaggs, W.E. & McNaughton, B.L. (1996) Replay of neuronal firing sequences in rat hippocampus during sleep following spatial experience. *Science*, **271**, 1870–1873.

Skaggs, W.E., McNaughton, B.L., Gothard, K.M. & Markus, E.J. (1993) An Information-theoretic approach to deciphering the hippocampal code. In Hanson, S.J., Cowan, J.D. & Giles, C.L. (Eds), *Advances in neural information processing*. Morgan Kaufmann, San Mateo, pp. 1030–1037.

Soleimannejad, E., Semnanian, S., Fathollahi, Y. & Naghdi, N. (2006) Microinjection of ritanserin into the dorsal hippocampal CA1 and dentate gyrus decrease nociceptive behavior in adult male rat. *Behav. Brain Res.*, **168**, 221–225.

Tai, S.K., Huang, F.D., Moochhala, S. & Khanna, S. (2006) Hippocampal theta state in relation to formalin nociception. *Pain*, **121**, 29–42.

Thompson, L.T. & Best, P.J. (1990) Long-term stability of the place-field activity of single units recorded from the dorsal hippocampus of freely behaving rats. *Brain Res.*, **509**, 299–308.

Tropp, J., Figueiredo, C.M. & Markus, E.J. (2005) Stability of hippocampal place cell activity across the rat estrous cycle. *Hippocampus*, **15**, 154–165.

Wei, F., Xu, Z.C., Qu, Z., Milbrandt, J. & Zhuo, M. (2000) Role of EGR1 in hippocampal synaptic enhancement induced by tetanic stimulation and amputation. *J. Cell Biol.*, **149**, 1325–1333.

Wood, E.R., Dudchenko, P.A., Robitsek, R.J. & Eichenbaum, H. (2000) Hippocampal neurons encode information about different types of memory episodes occurring in the same location. *Neuron*, **27**, 623–633.

Younger, J.W., Shen, Y.F., Goddard, G. & Mackey, S.C. (2010) Chronic myofascial temporomandibular pain is associated with neural abnormalities in the trigeminal and limbic systems. *Pain*, **149**, 222–228.

Zhao, X.Y., Liu, M.G., Yuan, D.L., Wang, Y., He, Y., Wang, D.D., Chen, X.F., Zhang, F.K., Li, H., He, X.S. & Chen, J. (2009) Nociception-induced spatial and temporal plasticity of synaptic connection and function in the hippocampal formation of rats: a multi-electrode array recording. *Mol. Pain*, **5**, 55.

Zheng, F. & Khanna, S. (2008) Intra-hippocampal tonic inhibition influences formalin pain-induced pyramidal cell suppression, but not excitation in dorsal field CA1 of rat. *Brain Res. Bull.*, **77**, 374–381.

Zimmermann, M. (1983) Ethical guidelines for investigations of experimental pain in conscious animals. *Pain*, **16**, 109–110.

Supporting Information

Figure S1.

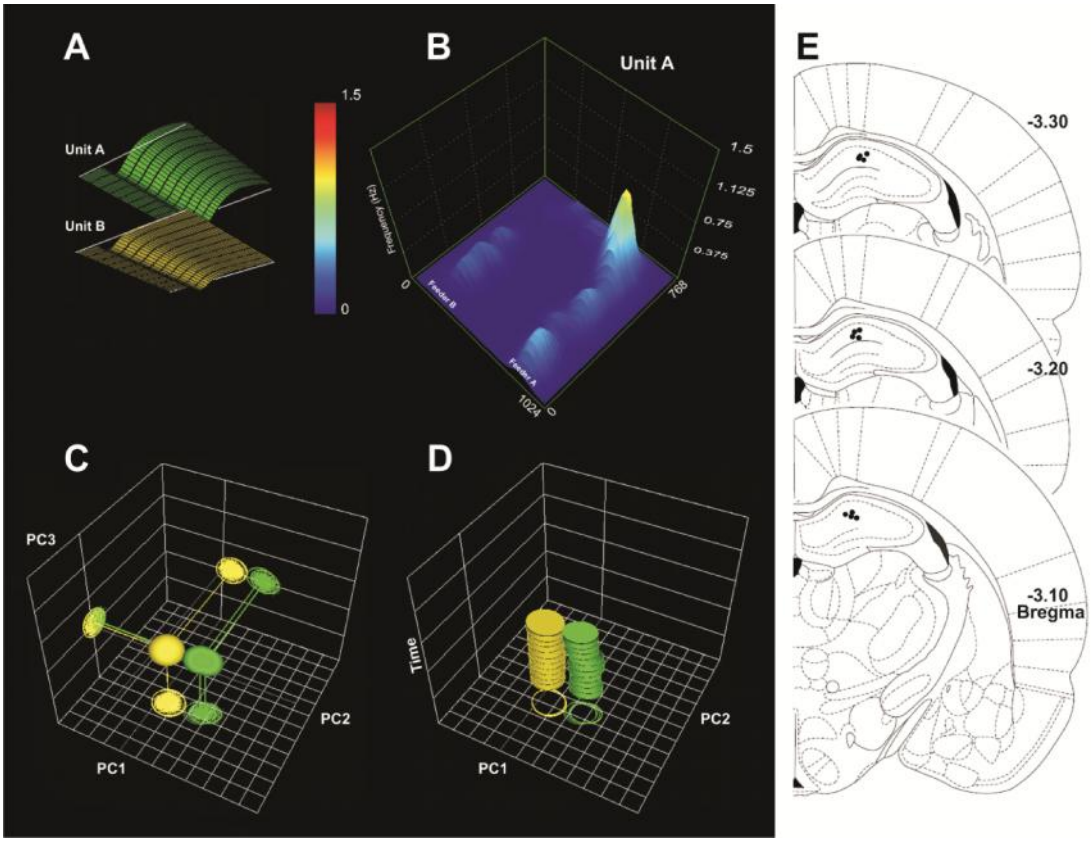

Stability of waveform shapes of two hippocampal place cells simultaneously recorded from the same channel (yellow and green) across experimental sessions **(A).** Note that the waveform shape of each place cell remained stable throughout the recording sessions. Only units with a greater than 3:1 signal to noise rate were considered. **(B)** Illustration of the Unit A firing activity recorded from a rat running on the U-shaped task encoding a spatial place field (area with peak of firing). Maximum firing rate is indicated by red and occupancy with no firing by blue. **(C)** Offline analysis of 3-D PC cluster stability from the channel shown across the whole recording sessions using the WaveTracker software (Plexon Inc., Dallas, TX, USA). In this view **(D)**, 2-D PC clusters are projected as function of time (Z-axis). Stability across time and absence of overlap between units isolated from the same channel were used as extra-selection criteria. **(E)** Location of implanted multielectrode arrays for nine rats used in this study. The black dots indicate the location of the centre of the array in CA1 region.

Table S1.

Statistical summary for SHAM and SNI-group comparison across all measurements during the 8 recording sessions of the control period.

Measurement		*Comparison*	*Statistics*	*Degrees of freedom*	*P*
Mechanical stimulation	2-way repeated measures ANOVA	Factor 1 – Time (SHAM x SNI)	F=0.1689	3, 30	0.9530
		Factor 2 – Groups (SHAM x SNI)	F=1.5600	1, 30	0.2402
		Interaction (F1 x F2)	F=0.1041	3, 30	0.9804
Correct alternations per trial	2-way repeated measures ANOVA	Factor 1 – Time (SHAM x SNI)	F=2.188	7, 70	0.0878
		Factor 2 – Groups (SHAM x SNI)	F=0.0776	1, 70	0.7862
		Interaction (F1 x F2)	F=0.6929	7, 70	0.6012
Mean firing rate (Hz)	2-way repeated measures ANOVA	Factor 1 – Time (SHAM x SNI)	F=0.1261	7, 70	0.9722
		Factor 2 – Groups (SHAM x SNI)	F=0.1823	1, 70	0.6784
		Interaction (F1 x F2)	F=0.3308	7, 70	0.8556
Specificity (in bits)	2-way repeated measures ANOVA	Factor 1 – Time (SHAM x SNI)	F=1.255	7, 70	0.1169
		Factor 2 – Groups (SHAM x SNI)	F=0.0001	1, 70	0.9945
		Interaction (F1 x F2)	F=1.975	7, 70	0.3036
Spatial discrimination capability	2-way repeated measures ANOVA	Factor 1 – Time (SHAM x SNI)	F= 1.760	7, 70	0.1561
		Factor 2 – Groups (SHAM x SNI)	F=0.5245	1, 70	0.4855
		Interaction (F1 x F2)	F=1.975	7, 70	0.9339
Place fields encoded per cell	2-way repeated measures ANOVA	Factor 1 – Time (SHAM x SNI)	F=0.1210	7, 70	0.9742
		Factor 2 – Groups (SHAM x SNI)	F=0.0731	1, 70	0.7924
		Interaction (F1 x F2)	F=0.6885	7, 70	0.6042

Firing coherence in-field	2-way repeated measures ANOVA	Factor 1 – Time (SHAM x SNI)	F=2.279	7, 70	0.0776
		Factor 2 – Groups (SHAM x SNI)	F=5.015	1, 70	0.0512
		Interaction (F1 x F2)	F=0.8711	7, 70	0.4897
Mean firing rate in-field (Hz)	2-way repeated measures ANOVA	Factor 1 – Time (SHAM x SNI)	F=1.322	7, 70	0.2783
		Factor 2 – Groups (SHAM x SNI)	F=0.0212	1, 70	0.8870
		Interaction (F1 x F2)	F=0.1834	7, 70	0.9457
Firing peak in-field (Hz)	2-way repeated measures ANOVA	Factor 1 – Time (SHAM x SNI)	F=1.963	7, 70	0.1187
		Factor 2 – Groups (SHAM x SNI)	F=0.1539	1, 70	0.7031
		Interaction (F1 x F2)	F=0.7105	7, 70	0.5896
Field size (bins)	2-way repeated measures ANOVA	Factor 1 – Time (SHAM x SNI)	F=0.7374	7, 70	0.5720
		Factor 2 – Groups (SHAM x SNI)	F=0.0908	1, 70	0.7693
		Interaction (F1 x F2)	F=0.7135	7, 70	0.5876
Field movement (pixels)	2-way repeated measures ANOVA	Factor 1 – Time (SHAM x SNI)	F=1.855	7, 70	0.1585
		Factor 2 – Groups (SHAM x SNI)	F=0.6696	1, 70	0.4323
		Interaction (F1 x F2)	F=1.169	7, 70	0.3379

The data presented in this table serves to demonstrate the stability of place fields and related properties during the 8 recording sessions made before the induction of the neuropathic injury. No differences were found across time, as well as between experimental groups during the control period. Given the stability of these measurements we have used the average value of these 8 sessions throughout the manuscript.

PUBLICAÇÃO 4

REDUCED HIPPOCAMPAL-PREFRONTAL CORTEX CONNECTIVITY IN NEUROPATHIC PAIN RATS PERFORMING AN SPATIAL NAVIGATION TASK

Helder Cardoso-Cruz, Deolinda Lima, Vasco Galhardo

ABSTRACT

Chronic pain patients commonly complain of working memory deficits, but the mechanisms and brain areas underlying this cognitive impairment remain elusive. The neuronal populations of the medial prefrontal cortex and dorsal hippocampal CA1 are well known to form an interconnected neural circuit that is crucial for correct performance in spatial memory dependent tasks. In this paper, we investigated whether the functional connectivity between these two areas is affected by the onset of an animal model of peripheral neuropathic pain. To address this issue, we chronically implanted two multichannel arrays of electrodes in the frontal cortex and dorsal hippocampus of adult rats and recorded the neuronal activity during a food-reinforced spatial working memory task in a figure-eight shaped maze. Recordings were performed for three weeks, before and after the establishment of the spared nerve injury (SNI) model of neuropathy. Our results show that the nerve lesion caused a clear impairment of working memory performance that is temporally correlated with a decrease in single neuron activity in the mPFC. Moreover, the activity of both frontal and hippocampal neuronal populations after the nerve injury increased their phase-locking in respect to hippocampal theta rhythm. Finally, our data revealed that chronic pain induces a reduction in the overall amount of information flowing in the frontohippocampal circuit, that is well correlated with the correct or incorrect performance of the animal on a trial-by-trial basis. The present results demonstrate that functional disturbances in the mPFC-CA1 connectivity are certainly a relevant cause for pain-induced working memory deficits.

INTRODUCTION

Evidence from both animal neurophysiological recordings and human brain imaging studies show that the neural activity of medial prefrontal cortex (mPFC) and hippocampus correlates with the retention of information over a brief temporal scale, a function that is crucial for a wide range of cognitive tasks (Floresco *et al.*, 1997; Jung *et al.*, 1998; Rainer *et al.*, 1999; Stern *et al.*, 2001; Pesaran *et al.*, 2002; Baeg *et al.*, 2003; Schon *et al.*, 2005). Important memory performance-related mPFC-hippocampal interactions occur via coherent oscillations in the theta frequency range (Jones & Wilson, 2005b; Siapas *et al.*, 2005), during which the mPFC neurons alternate between phase and non-phase firing patterns depending on the behavioural context (Hyman *et al.*, 2005). These interactions were greatest just before a correct mnemonic decision was made (Jones & Wilson, 2005a), and are evidence of a functional connection between both regions.

Impaired working memory is observed in several clinical conditions, such as traumatic brain injury (McDowell *et al.*, 1997), mental retardation (Vallar & Papagno, 1993), schizophrenia (Green, 2006), attention-deficit hyperativity disorder (Frank *et al.*, 1996), and chronic pain (Ling *et al.*, 2007; Luerding *et al.*, 2008a). Indeed, it is commonly assumed that chronic pain may lead to learning dysfunctions in patients (Kim *et al.*, 2011). This clinical observation is corroborated by neuroimaging studies during noxious stimulation that have demonstrated an activation of brain areas that are particularly involved in memory and learning processes (Peyron *et al.*, 1998; Ploghaus *et al.*, 2000; Ducreux *et al.*, 2006; Schweinhardt *et al.*, 2006; Apkarian *et al.*, 2011). Recent studies in animals pain models have also demonstrated that pain induces reduced working memory performance (Leite-Almeida *et al.*, 2009; Hu *et al.*, 2010), and poor attentional performance (Millecamps *et al.*, 2004; Pais-Vieira *et al.*, 2009; Legrain *et al.*, 2011).

However, little is known about how pain affects the mPFC–hippocampal circuit. It has been shown that mPFC region have important key role in pain-modulatory process (Seifert *et al.*, 2009; Devoize *et al.*, 2011); and that morphological and functional reorganization of mPFC region can be in celular basis for cognitive impairments under neuropathic pain condition (Metz *et al.*, 2009). Additionally, chronic pain has been associated to working memory deficits due to hippocampal LTP inhibition (Ren *et al.*, 2011), and disturbances in the spatial reference memory integration (Cardoso-Cruz *et al.*, 2011a). Despite all the knowledge gathered in recent years it remains unclear how pain affects the share, maintenance, and processing of information that are crucial for spatial mnemonic processes. Therefore, our interest was to study how the mPFC-hippocampal connectivity is affected by a prolonged neuropathic pain condition. We recorded neuronal activity and local-field-potentials of freely moving rats in a spatial alternation task,

performed before and after the induction of the Spared Nerve Injury model – SNI (Decosterd & Woolf, 2000).

MATERIALS AND METHODS

Animal model and ethical statement

Ten adult male Sprague-Dawley rats weighing between 275 and 320 g were used in this study. The rats were maintained on a 12-h light/dark cycle, and both training and recording sessions run at approximately the same time each day during the light portion of the cycle. All animals were food deprived to 90-95% of their *ad libitum* body weights during the course of these experiments. All procedures and experiments adhered to the guidelines of the Committee for Research and Ethical Issues of IASP (Zimmermann, 1983), with the Ethical Guidelines for Animal Experimentation of the European Community Directive Number 86/609/ECC of 24 November of 1986, and were approved by national and local boards.

Maze and training procedure

The behavioral task consisted of a food-reinforced spatial alternation task on a figure-eight shaped maze, similar to the maze used in studies of episodic memory (Baeg *et al.*, 2003; Ji & Wilson, 2007). The total dimension of the arena was 90 x 60 cm, with plexiglass corridors 15 cm wide and opaque walls 30 cm high with intramaze cues (Fig. 1A). Starting from the center of the maze (C), the rats were trained to alternately visit two reward sites (R) to obtain one chocolate-flavored pellet (45 mg) that was automatically delivered by a pellet dispenser (Coulbourn Instruments, Whitehall, PA, USA). After visiting one of the reward locations, the animal had to continue forward and cross again the central corridor before visiting the opposite reward site; food rewards were not dispensed if the animal failed to cross the central corridor immediately before arriving at the reward sites or if the animal made two consecutive visits to the same reward site (arrows in Fig. 1A illustrate the pattern of correct maze navigation). Control of pellet dispensers was fully automated using the OpenControl software adapted to this particular task (Aguiar *et al.*, 2007). In all the analysis of this study we have considered three different zones in the behavioral arena: the “reward-zones” are the 15x15 cm corner areas where the animal receives a pellet upon a correct alternation; the “delay-zones” comprise the area between the reward-zones and the central corridor; finally, the “choice-zone” is the area preceding the reward-zones and immediately following the central corridor (Fig. 1A).

The testing room was moderately illuminated and rich in visual cues distant from the maze. During the training period, the rats were given three daily 10-min sessions to learn the

alternation schedule until they reached at least 80% of correct maze alternations (Fig. 1B). An error was defined by a consecutive visit to the same reward site or when the return route was the same from the approach route. Errors were not reinforced. After reaching this performance criterion the animals were surgically implanted with two arrays two arrays of 8 isonel-insulated tungsten filaments of 35-microns in diameter, for recording of extracellular single-unit and local field potentials (LFPs) (see details below).

After 7 days of recovery from the implantation surgery, ten animals (n = 5 in both sham and nerve-lesioned groups) were re-trained and recorded during 5 consecutive days (hereafter named baseline or control period) while performing the maze alternation task in 2 daily sessions of 10 minutes with 4 hours of interval between sessions. In the following day the animals were briefly anesthetized and either surgically subjected to the Spared Nerve Injury (SNI) - model of neuropathic pain (Decosterd & Woolf, 2000) or to a sham intervention with the same extent of skin incision and muscle dissection. Both interventions are implemented in the contralateral side to recording probes implantation. Both groups of animals were then recorded for a period of three weeks (with recordings performed at days 1, 3, 5, 7, 10, 15 and 21 after SNI or sham intervention). Sensory threshold for noxious stimulation was assessed 1 hour after the end of the second daily recording session by placing the animals in a cage with a metal mesh floor and touching the plantar surface of the paw with von Frey filaments (Somedic, Sweden) as previously described (Chaplan *et al.*, 1994; Cardoso-Cruz *et al.*, 2011a).

Electrodes implantation

The procedure for the surgical implantation of intracranial multielectrode arrays has been previously described in detail elsewhere (Cardoso-Cruz *et al.*, 2011a). The multielectrodes arrays were oriented rostrocaudally and driven to the medial prefrontal cortex (mPFC) and dorsal hippocampal CA1-field (CA1). The following coordinates in millimeters relative to Bregma (Paxinos & Watson, 1998) were used to place the arrays: mPFC (-2.2 rostro-caudal, 1.0 medio-lateral, 3.2 dorso-ventral), and CA1 (+3.2 rostro-caudal, 2.2 medio-lateral, 2.7 dorso-ventral). After surgery, rats were allowed to recover for 1 week before the task re-training sessions began.

Neural recordings

All neural activity signals from the implanted microelectrodes were recorded and processed using a Multineuron Acquisition Processor system (16-MAP, Plexon Inc., Dallas, TX, USA). Voltage-time threshold windows were used to identify single-units waveforms. Neural

signals were pre-amplified (10000-25000X) and digitized at 40 kHz. Up to two neuronal action potentials per recording channel were sorted online (SortClient 2.6., Plexon Inc., Dallas, TX, USA) and validated by offline analysis (Offline Sorter 2.8., Plexon Inc., Dallas, TX, USA) according to the following cumulative criteria: voltage threshold greater than two standard deviations of the amplitude distribution; signal-to-noise ratio larger than 3; less than 1% of inter-spike intervals smaller than 1.2 msec; and stability of the waveform shape as determined by a waveform matching template algorithm and principal component analysis. In addition, the Waveform Tracker software (Plexon Inc., Dallas, TX, USA) was used to verify that the recorded units were stable across experimental sessions. Extracellular LFPs were simultaneously recorded from the same implanted microwires by low-frequency (0.5-200 Hz) filtering of the raw signals. LFPs were pre-amplified and digitized at 500 Hz. An overhead video tracking system (CinePlex 2, Plexon Inc., Dallas, TX, USA) was used to provide information about the animal position on the maze, and synchronize the video-recordings with the acquired neuronal data.

Data analysis

Neural data were processed offline using NeuroExplorer 4 (NEX, Plexon Inc., Dallas TX, USA) and exported to our own MatLab R14 routines for additional analysis (MathWorks, Natick, MA, USA). In all analyses the distribution of the data was initially checked for potential deviations from normality assumptions (Prism 5.0, GraphPad, San Diego, CA, USA), in order to choose the appropriate statistical test to apply. Parametric statistics were used when the Kolmogorov-Smirnov test (with Dallal-Wilkinson-Lilliefor corrected *P*-value) revealed no deviations from the normal distribution ($P<0.05$, Kolmogorov-Smirnov test). Analyses of variance between experimental groups were performed by two-factor ANOVA – repeated measures (ANOVA-RM; group x recording days and/or group x frequency bands), and when appropriate a *Post hoc* analysis was carried out using the Bonferroni test. The level of significance was set as 5%. Results are expressed as mean ± standard error of the mean (SEM). All results were averaged per recording days.

Spiking activity

Average firing rate activity for the mPFC and CA1 neurons were examined across maze navigation zones, comparing SNI and SHAM animals in pre- and post-surgery recording sessions.

In order to analyze firing activity response for correct versus error alternations during each recording session, individual perievent time decision histograms were computed for each recorded neuron and plotted in a 2-sec range centered at the time of the transition between the

delay and the choice navigation zones (50-msec per bin). A Kolmogorov-Smirnov test (KS, $P<0.05$) was used to test differences in the firing distribution of each neuron. The units were classified based in their increased, decreased, or unchanged firing rate. All recording sessions selected for comparisons of neuronal activity for correct vs. error alternations have at least 5% of incorrect alternations.

Additionally, to examine which neurons displayed elevated activity in the delay-zone navigation, we compared in each alternation the average firing rate of the last second spent in the delay-zone versus the global firing rate of the session (paired *t*-test, $P<0.05$). Neurons whose average delay-zone firing rate was <1 Hz were excluded from analysis because these provided too few spikes to be analyzed (mPFC – SHAM: 3 neurons, SNI: 6 neurons; CA1 – SHAM: 11 neurons, SNI: 9 neurons).

To characterize the temporal structure of the spiking activity in respect to the theta cycle, the raw hippocampal LFPs were filtered in the theta range (4-9 Hz) using a zero-phase forward and reverse digital 4-pole Butterworth band-pass filter to yield the signal LFP_{ϑ}. The relationship between temporal structure of mPFC and CA1 neuronal spiking activity and hippocampal ongoing theta rhythm was calculated using standard cross-correlograms (Neuroexplorer 4, Plexon Inc., Dallas, TX, USA). Correlations were computed using CA1 LFP_{θ} as reference with a temporal resolution of 2-msec per bin, and the rate histograms for both mPFC and CA1 spiking activity were calculated individually for each cell, and represented in function of the populational activity across navigation zones. Given the complexity of the analysis we compared the signals from the control period versus the signals from only one post-surgery session and selected day 10 because the nerve lesioned animals reach stable levels of pain at this time point. The comparison of phase distributions was performed using a two-sample KS test ($P<0.05$).

Spectral analysis

Global spectral characteristics of mPFC-CA1 LFPs signals were presented in function of maze navigation zone. The power spectral density (PSD) of mPFC (P_{xx}) and CA1 (P_{yy}) LFPs signals were calculated between 1 and 50 Hz using the Welch's method (MatLab native function), with 512-points fast Fourier transform of non-overlapping 1-sec epochs (Hanning-window). Data are presented as the percentage of total PSD within the 1-50 Hz frequency range. Five frequency bands were considered: 1-4 Hz (δ, delta), 4-9 Hz (θ, theta), 9-15 Hz (α, alpha), 15-30 Hz (β, beta), and 30-50 Hz (γ, gamma). In order to determine the spectral coupling among signals from recorded regions, we calculated the correlation coefficient or coherence. Coherence (C_{xy}) was

measured applying the equation mathematically equivalent to $C_{xy} = |P_{xy}|^2 / (P_x P_y)$ where the coherence for two signals, *x* and *y*, is equal to the average cross power spectrum (P_{xy}) normalized by the averaged power spectra of the two signals. Its value lies between 0 and 1, and it estimates for a given frequency the level to which phases are dispersed. $C_{xy} = 0$ means that phases are dispersed, and high coherence ($C_{xy} = 1$) means phases of signals *x* and *y* are identical and the two signals are totally phase-locked at this frequency.

The statistical method of partial directed coherence (PDC) was used to quantify the information flow within the mPFC-CA1 circuit. The PDC method has been described in detail elsewhere (Sameshima & Baccalá, 1999; Baccala & Sameshima, 2001; Cardoso-Cruz *et al.*, 2011b). Briefly, PDC is an alternative representation of multivariate processes involving Granger-causality to uncover frequency-domains of direct influence, which allows for assessing interactions between brain regions and revealing their directionality. Its value lies between 0 and 1. PDC = 0 can be interpreted as absence of functional connectivity from the first structure (*j*) to the second structure (*i*) at a particular frequency-window, while high PDC values indicate strong connectivity between the structures. This can be interpreted as existence of information flow from brain structure *j* to *i*.

Histology

After the end of all experiments, the rats were deeply anesthetized with ketamine/xylazine mixture and the recording site was marked by injecting DC current (10-20 µA for 10-20 sec) through one microwire per array, marking the area below the electrode tips. After this step the animals were perfused through the heart with 0.01 M phosphate buffer (pH=7.2) in a 0.9% saline solution followed by 4% paraformaldehyde. Brains were removed and post-fixed in 4% paraformaldehyde during 4 hours and stored in 30% sucrose before they were frozen and sectioned into 60 µm slices. Sections were Nissl counterstained to help visualize the electrode tracks under the microscope.

RESULTS

Behavior

Rats were trained to optimal performance prior to electrode implantation, and all animals performed the task at levels higher than 80% of correct choices after 10 days of training (3 daily sessions of 10 minutes per animal) (Fig. 1B). Fig. 1C shows two examples of cumulative animal trajectories in early day 2 and late day 10 of training period. As shown, the animal

frequently made more navigation errors in the early days of training (see for example the direct trajectories between the reward locations in the top diagram of Fig. 1C).

Mechanical stimulation thresholds

All SNI animals developed mechanical allodynia as indicated by the significant decrease in the mechanical force needed to evoke paw withdrawal to Von Frey filaments stimulation in the hindpaw ipsilateral to the lesion (Fig. 1D). In the SHAM group, no statistical differences were noted in respect to pre-operation period (control period). A two-factor ANOVA-RM was used to compare responses from SHAM and SNI animals. Significant statistical differences were observed between experimental groups ($F_{(1,56)}$=432.7, P<0.0001), across recording days ($F_{(7,56)}$=19.24, P<0.0001), and interaction effect (group x time; $F_{(7,56)}$=7.61, P<0.0001).

Performance during recording sessions

The performance in SNI rats with mechanical allodynia was significantly worse than those in SHAM group (Fig. 1E). Analysis of variance revealed statistical differences in the rat's performance between experimental groups (two-factor ANOVA-RM; $F_{(1,56)}$=12.97, P=0.0006), and across recording sessions ($F_{(7,56)}$=2.17, P=0.0482). No interaction effect between factors was observed (group x time; $F_{(7,56)}$=0.67, P=0.6936). *Post hoc* analysis revealed a significant performance decrease in the SNI group at day 3 after nerve lesion (Bonferroni, P<0.05). Additionally, a decrease in the running velocity was observed after lesion in both experimental groups; both groups fully recovered to normal values of running speed 7 days after the surgery (Fig. 1F). Analysis of variance showed significant differences between experimental groups (two-factor ANOVA-RM; $F_{(1,56)}$=2.34, P=0.0341) and recording days ($F_{(7,56)}$=10.97, P<0.0001). No significant statistical differences for the factor-interaction effect (groups x time; $F_{(7,56)}$=1.28, P=0.2743). *Post hoc* analysis revealed a decrease of the running velocity for SNI group at day 5 after lesion (Bonferroni, P<0.05).

An essential issue of alternation tasks is the temporal gap between trajectory decisions, in which the animal should maintain a retrospective memory of the previous visited food cup in order to choose correctly in the next left/right decision point. Our results show that after the nerve lesion, the SNI animals spent more time navigating in the delay-zone of the behavioral test (Fig. 1G). Analysis of variance showed a significant statistical difference between experimental groups (two-factor ANOVA-RM; $F_{(1,56)}$=12.15, P=0.0009), and no effects across recording days ($F_{(7,56)}$=1.69, P=0.1284) and factor-interaction (groups x time; $F_{(7,56)}$=1.37, P=0.2327). *Post hoc* analysis revealed an increase of the time of navigation in the delay-zone for the SNI group at day 3 after lesion (Bonferroni, P<0.05). The average interval of time that mediated two consecutive

correct choices increased significantly for the SNI animals (Fig. 1H); analysis of variance revealed a significant effect between experimental groups (two-factor ANOVA-RM, $F_{(1,56)}$=44.87, *P*<0.0001), and across the recording sessions after lesion ($F_{(7,56)}$=3.60, *P*=0.0025). However, no factor-interaction effect was observed for these two factors (groups x time; $F_{(7,56)}$=1.58, *P*=0.1591). *Post hoc* analysis revealed an increase of the average interval between correct choices for SNI-group between day 7 and 21 after lesion (Bonferroni test; days 7, 10, and 21, *P*<0.05; day 15, *P*<0.01).

Neuronal activity

In the present study, a total of 175 neurons were recorded (mPFC - SHAM: 44, SNI: 46; CA1 - SHAM: 42, SNI: 43 neurons). The Waveform Tracker Software (Plexon Inc., Dallas, TX, USA) was used to ensure that individual neural recordings were correctly identified across recording sessions (Fig. 2). Only neurons that remained stable throughout the recording sessions in terms of waveform shape were considered in the analysis.

Population spiking activity

Fig. 2E-F presents the average neuronal firing rate calculated for each zone of the maze for both brain areas. Although there were no statistical differences in the pre-surgery firing rates, there was a visible increase in the firing rate of mPFC neurons when the animal was navigating the delay-zone versus the other two zones (Fig. 2E).

The nerve lesion did not affect the pre-surgery firing rates of mPFC neurons: no significant statistical effects were observed between experimental groups (two-factor ANOVA-RM; reward-zone: $F_{(1,56)}$=0.44, *P*=0.5255; delay-zone: $F_{(1,56)}$=1.63, *P*=0.2372; and choice-zone: $F_{(1,56)}$=3.07, *P*=0.1177), recording sessions (reward-zone: $F_{(7,56)}$=0.63, *P*=0.7238; delay-zone: $F_{(7,56)}$=0.98, *P*=0.4548; and choice-zone: $F_{(7,56)}$=0.53, *P*=0.8088), and no factor-interaction effect was observed (groups x time; reward-zone: $F_{(7,56)}$=0.64, *P*=0.7198; delay-zone: $F_{(7,56)}$=0.83, *P*=0.5635; and choice-zone: $F_{(7,56)}$=0.67, *P*=0.6973). It may be noted that the firing rate increase during navigation in the delay-zone is lower in SNI animals when compared to SHAM animals.

In contrast, the nerve injury caused an increase in the firing rate of hippocampal CA1 neurons when the animal was in the reward-zone and choice-zone, but not during navigation in the delay-zone, when compared to the pre-surgery firing rates (Fig. 2F). We found statistical differences across time (reward-zone: $F_{(7,56)}$=3.36, *P*=0.0046; and choice-zone: $F_{(7,56)}$=4.06, *P*=0.0012), and in factor-interaction effect (reward-zone: $F_{(7,56)}$=2.74, *P*=0.0163; and choice-zone: $F_{(7,56)}$=3.59, *P*=0.0029). *Post hoc* analysis revealed an increase of the average firing rate for SNI

group at day 5 for reward-zone (P<0.05), and at day 7 for choice-zone (Bonferroni, P<0.05). In respect to delay-zone no significant differences were encountered in average firing rate across experimental groups and recording days (delay-zone: groups – $F_{(7,56)}$=1.63, P=0.2372, time – $F_{(7,56)}$=0.98, P=0.4548, and factor-interaction – $F_{(7,56)}$=0.83, P=0.5635). No overall statistical differences were observed between experimental groups for reward and choice-zones (reward-zone: $F_{(1,56)}$=2.42, P=0.1587; and choice-zone: $F_{(1,56)}$=4.67, P=0.0626).

Firing activity of correct and error alternations

In order to analyze if the firing activity was affected when the animal approached the decision point of left/right alternation temporal vicinity, we have calculated for each neuron the respective perievent time decision histogram of firing activity for either correct or error trials (marked as green and red vertical lines in Fig. 3A respectively). The Fig. 3A presents examples of mPFC and CA1 neurons with different activity patterns. The majority of the mPFC neurons increase their firing activity after the rat performed a correct direction choice (Fig. 3B, above panel). In contrast, the activity of CA1 neurons commonly decreased across error alternations (Fig. 3C, below panel).

The analysis of firing patterns revealed no significant differences in the percentage of neurons that increased their activity, decreased, or remained unchanged at the decision point after nerve lesion (Fig. 3 B-C). In the case of correct alternations, no statistical differences were encountered in the percentage of neurons that increased their firing activity (two-factor ANOVA-RM; mPFC: groups $F_{(1,56)}$=1.18, P=0.3094, time $F_{(7,56)}$=1.27, P=0.2831, interaction $F_{(7,56)}$=1.32, P=0.2567; CA1: groups $F_{(1,56)}$=0.23, P=0.6448, time $F_{(7,56)}$=0.17, P=0.9789, interaction $F_{(7,56)}$=0.18, P=0.9890), decreased (mPFC: groups $F_{(1,56)}$=0.24, P=0.6356, time $F_{(7,56)}$=1.76, P=0.1134, interaction $F_{(7,56)}$=1.34, P=0.2478; CA1: groups $F_{(1,56)}$=0.15, P=0.7116, time $F_{(7,56)}$=0.20, P=0.9684, interaction $F_{(7,56)}$=0.21, P=0.9538), or remained unchanged (mPFC: groups $F_{(1,56)}$=0.52, P=0.4902, time $F_{(7,56)}$=0.36, P=0.9239, interaction $F_{(7,56)}$=0.38, P=0.9092; CA1: groups $F_{(1,56)}$=0.02, P=0.8948, time $F_{(7,56)}$=0.42, P=0.2848, interaction $F_{(7,56)}$=0.38, P=0.2914) (Fig. 3B). In the case of error alternations, no statistical differences were encountered in the percentage of neurons that increased their firing activity (mPFC: groups $F_{(1,56)}$=0.96, P=0.3558, time $F_{(7,56)}$=0.43, P=0.8791, interaction $F_{(7,56)}$=0.43, P=0.8791; CA1: groups $F_{(1,56)}$=1.10, P=0.3259, time $F_{(7,56)}$=0.9761, P=0.23, interaction $F_{(7,56)}$=0.24, P=0.0.9676), decreased (mPFC: groups $F_{(1,56)}$=0.95, P=0.3590, time $F_{(7,56)}$=0.51, P=0.8261, interaction $F_{(7,56)}$=0.73, P=0.6500; CA1: groups $F_{(1,56)}$=0.02, P=0.8801, time $F_{(7,56)}$=0.82, P=0.5688, interaction $F_{(7,56)}$=0.84, P=0.5477), or remained unchanged (mPFC: groups

$F_{(1,56)}$=1.80, *P*=0.2172, time $F_{(7,56)}$=0.12, *P*=0.9966, interaction $F_{(7,56)}$=0.44, *P*=0.8752; CA1: groups $F_{(1,56)}$=0.57, *P*=0.4736, time $F_{(7,56)}$=0.01, *P*=0.9999, interaction $F_{(7,56)}$=0.01, *P*=0.9999) (Fig. 3C).

Spiking activity during the navigation on the delay-zone

We calculated the percentage of neurons that elevated their average firing rate during the delay-zone navigation in respect to the whole recording session. Note that only the activity recorded in correct trials were selected for this analysis, so that direct comparisons could be done. In the case of mPFC neurons, significant differences were encountered between experimental groups (two-factor ANOVA-RM; $F_{(1,56)}$=8.76, *P*=0.0182), and no differences across recording days ($F_{(7,56)}$=1.46, *P*=0.1991) and factor-interaction effect (groups x time; $F_{(7,56)}$= 1.20, *P*=0.3198) (Fig. 3D, above panel). *Post hoc* analysis revealed a decrease in the percentage of mPFC neurons that elevated their average firing rate within the delay-zone at days 1, 7 and 10 after nerve lesion (Bonferroni, *P*<0.05). In the case of CA1 neurons, no significant statistical differences were encountered between experimental groups ($F_{(1,56)}$=1.52, *P*=0.2532), recording sessions ($F_{(7,56)}$=1.33, *P*=0.2535), and in factor-interaction effect (groups x time; $F_{(7,56)}$=0.99, *P*=0.4417) (Fig. 3D, below panel).

Changes in the hippocampal-theta rhythm

The relationship between the temporal structure of populational neuronal spiking activity and ongoing theta cycle of hippocampal LFPs was calculated for the pre-surgery period versus day 10 after SHAM or SNI surgery. As illustrated in Fig. 4, different temporal activity patterns were encountered for mPFC and CA1 recorded areas across environment testing zones after peripheral nerve lesion. In the case of mPFC, no differences were observed after nerve lesion during the reward-zone navigation between experimental groups (CT/SNI: KS=0.04, *P*=0.9217, and SHAM/SNI: KS=0.08, *P*=0.6864; two-sample KS test). In respect to delay and choice-zones, the mPFC neurons after lesion increased their firing precision in relation to theta rhythm (delay-zone: CT/SNI: KS=0.28, *P*=0.0459, and SHAM/SNI: KS=0.25, *P*=0.0257; choice-zone: CT/SNI: KS=0.26, *P*=0.0389, and SHAM/SNI: KS=0.26, *P*=0.0291) (Fig. 4A and 4B). In the case of CA1, no differences in the timing of spiking activity were observed between groups for reward (CT/SNI: KS=0.09, *P*=0.5912, and SHAM/SNI: KS=0.08, *P*=0.6151) and choice-zones (CT/SNI: KS=0.11, *P*=0.4987, and SHAM/SNI: KS=0.11, *P*=0.4591), while for delay-zone after lesion the spiking activity was phase-locked in respect to theta cycle (CT/SNI: KS=0.24, *P*=0.0289, and SHAM/SNI: KS=0.26, *P*=0.0311) (Fig. 4C and 4D). No significant differences were observed when compared control period (CT) to SHAM group (mPFC - reward-zone: KS=0.05, *P*=0.9102; delay-

zone: KS=0.06, *P*=0.8744; choice-zone: KS=0.09, *P*=0.7423; and CA1 – reward-zone: KS=0.05, *P*=0.9044; delay-zone: KS=0.12, *P*=0.6422; choice-zone: KS=0.10, *P*=0.7231).

SPECTRAL ANALYSIS

Changes in Power Spectral Densities

A qualitative comparison of power spectral density (PSD) values for mPFC and hippocampal dorsal CA1 LFPs is shown in Fig. 5A and 5C, comparing SHAM and SNI groups across recording sessions and maze navigation zones. The inspection of PSD confirmed that characteristic power oscillations were as expected, with a high-power in the theta frequency band (4-9 Hz) shared by both recorded areas as has been previously described (Buzsaki, 2002; Lörincz *et al.*, 2007). Analysis of variance revealed no statistical differences between experimental groups (two-factor ANOVA-RM; mPFC - reward-zone: $F_{(1,30)}$=0.02, *P*=0.9821; delay-zone: $F_{(1,30)}$=0.01, *P*=0.9999; choice-zone: $F_{(1,30)}$=0.01, *P*=0.9266; CA1 - reward-zone: $F_{(1,30)}$=0.01, *P*=0.9999; delay-zone: $F_{(1,30)}$=0.01, *P*=0.9998; choice-zone: $F_{(1,30)}$=0.01, *P*=0.9964) and factor-interaction effect (groups x frequency bands; mPFC - reward-zone: $F_{(4,30)}$=0.51, *P*=0.7314; delay-zone: $F_{(4,30)}$=0.90, *P*=0.4747; choice-zone: $F_{(4,30)}$=1.85, *P*=0.1452; CA1 - reward-zone: $F_{(4,30)}$=0.94, *P*=0.4527; delay-zone: $F_{(4,30)}$=1.50, *P*=0.2274; choice-zone: $F_{(4,30)}$=1.05, *P*=0.4005), but as expected a significant effect was encountered across frequency bands (mPFC - reward-zone: $F_{(4,30)}$=139.6, *P*<0.0001; delay-zone: $F_{(4,30)}$=152.40, *P*<0.0001; choice-zone: $F_{(4,30)}$=371.30, *P*<0.0001; CA1 - reward-zone: $F_{(4,30)}$=139.90, *P*<0.0001; delay-zone: $F_{(4,30)}$=89.40, *P*<0.0001; and choice-zone: $F_{(4,30)}$=164.10, *P*<0.0001; respectively) (Fig. 5B and 5D, respectively).

Coherence Analysis

A qualitative comparison of the coherence measurements between the mPFC-CA1 circuit LFPs across recording days and testing environment navigation zones were illustrated in Fig. 6A. The global levels of mPFC-CA1 coherence after nerve lesion changed across recordings sessions, but not across frequency bands. Analysis of variance revealed no significant differences after nerve lesion between experimental groups in the reward locations (two-factor ANOVA-RM; $F_{(1,56)}$=0.04, *P*=0.8541), but there were significant differences across recording sessions ($F_{(7,56)}$=17.93, *P*<0.0001), as well as a factor-interaction effect (groups x time; $F_{(7,56)}$=9.03, *P*<0.0001). *Post hoc* analysis revealed differences between experimental groups at days 1 and 21 after lesion (Bonferroni, *P*<0.001) (Fig. 6B, left panel). In the case of the delay-zone, analysis of variance revealed no differences between groups ($F_{(1,56)}$=0.23, *P*=0.6428), but there were significant differences across recording days ($F_{(7,56)}$=10.33, *P*<0.0001) and a factor-interaction

effect ($F_{(7,56)}$=9.16, *P*<0.0001). *Post hoc* analysis revealed differences between SHAM and SNI-groups during the first (*P*<0.05) and last two recording sessions performed after nerve lesion (*P*<0.01, and 0.05, respectively) (Fig. 6B, center panel). No differences were encountered in the choice-zone between experimental groups ($F_{(1,56)}$=0.07, *P*=0.7996), but differences were found across recording days ($F_{(7,56)}$=10.52, *P*<0.0001), as well as a factor-interaction effect ($F_{(7,56)}$=9.16, *P*<0.0001). *Post hoc* analysis revealed significant differences in coherence between experimental groups across days 1, 3 (*P*<0.01), and 21 (*P*<0.001) after lesion (Fig. 6B, right panel).

We calculated the averaged mPFC-CA1 circuit coherence per range of frequencies (Fig. 6C). No differences were encountered between groups (reward-zone: $F_{(1,30)}$=0.02, *P*=0.9536; delay-zone: $F_{(1,30)}$=0.02, *P*=0.8827; choice-zone: $F_{(1,30)}$=0.04, *P*=0.8474), frequency bands (reward-zone: $F_{(4,30)}$=1.23, *P*=0.3199; delay-zone: $F_{(4,30)}$=2.02, *P*=0.1170; choice-zone: $F_{(4,30)}$= 1.13, *P*=0.3621), or in the factor-interaction effect (reward-zone: $F_{(4,30)}$=0.08, *P*=0.9879; delay-zone: $F_{(4,30)}$=0.25, *P*=0.9097; choice-zone: $F_{(4,30)}$= 0.76, *P*=0.5625).

Partial directed coherence

The changes of mPFC-CA1 circuit information flow in SHAM and SNI animals were determined by PDC analysis. Fig. 7 illustrates the PDC activity across recording days and testing environment navigation zones. In the case of the direction from CA1 to mPFC (Fig. 7A), the qualitative analysis confirmed strong PDC values at the theta frequency band (4-9 Hz) in the choice and also delay navigation zones, which is lost after peripheral nerve lesion. In the opposite direction - from mPFC to CA1 – high PDC values at the theta band are also visible in the choice-zone, and they are also lost after the nerve injury (Fig. 7B).

Detailed analysis of averaged PDC values across the 1-50 Hz frequencies for each recording session showed that the levels of information flow decreased significantly after nerve lesion. The global PDC level is particularly decreased in the reward-zone, for both circuit directions, and in the choice-zone in the CA1 to mPFC direction of information. In the case of CA1>mPFC direction, analysis of variance for reward location revealed significant differences between experimental groups (two-factor ANOVA-RM; $F_{(1,56)}$=21.17, *P*=0.0066), and no effects across recording days ($F_{(7,56)}$=1.12, *P*=0.3612) and a factor-interaction (group x time; $F_{(7,56)}$=1.51, *P*=0.1821). *Post hoc* analysis revealed a significant decrease of PDC level for SNI animals at days 1, 7 and 15 after lesion (Bonferroni, *P*<0.01) (Fig. 8A, left panel). For the delay-zone, no differences were found between experimental groups ($F_{(1,56)}$=3.55, *P*=0.0961), but a significant effect was found for time ($F_{(7,56)}$=4.57, *P*=0.0004) and factor-interaction ($F_{(7,56)}$=2.42, *P*=0.0309). *Post hoc* analysis revealed a significant decrease of the PDC levels in the SNI-group at day 15

after lesion (P<0.001) (Fig. 8A, center panel). In respect to choice-zone, statistical differences were encountered between groups ($F_{(1,56)}$=197.60, P<0.0001), time ($F_{(7,56)}$=8.50, P<0.0001), as well as a factor-interaction effect ($F_{(7,56)}$=3.32, P=0.0050). *Post hoc* analysis revealed that the PDC level decreased dramatically for SNI group after lesion (P<0.001) (Fig. 8A, right panel). In the case of the direction from mPFC to CA1, a significant effect was observed between experimental groups when the animal was in the reward-zone (two-factor ANOVA-RM: $F_{(1,56)}$=113.4, P<0.0001), but no effect across recording sessions ($F_{(7,56)}$=0.91, P=0.5042) or factor-interaction (groups x time; $F_{(7,56)}$=0.72, P=0.6537). *Post hoc* analysis revealed that after the lesion the PDC level decreased significantly in the SNI-group (at days 1, 3, and 7 (P<0.05); at days 5 and 21 (P<0.01); and at days 10 and 15 (P<0.001)) (Fig. 8C, left panel). In the delay-zone, analysis of variance revealed no differences between groups ($F_{(1,56)}$=0.17, P=0.6916), but there was a significant effect across time ($F_{(7,56)}$=2.20, P=0.0481) and a factor-interaction ($F_{(7,56)}$=3.49, P=0.0035) (Fig. 8C, center panel). In respect to choice-zone no significant differences were registered between experimental groups ($F_{(1,56)}$=3.56, P=0.0961), but a significant effect was observed across recording sessions ($F_{(7,56)}$=3.76, P=0.0021) as well as a factor-interaction ($F_{(7,56)}$=5.28, P<0.0001). *Post hoc* analysis revealed that at day 3 after lesion the PDC was significantly lower in the SNI group in comparison to the SHAM group (P<0.05) (Fig. 8C, right panel).

In order to detail the mPFC-CA1 information flow across frequency bands, we calculated the averaged PDC per range of frequencies (Fig. 8B). A two-way ANOVA-RM was performed to assess the differences in the averaged PDC between the SHAM and SNI groups. In the case of the CA1>mPFC direction there was a significant difference between experimental groups (two-factor ANOVA-RM; reward-zone: $F_{(1,30)}$=87.34, P<0.0001; delay-zone: $F_{(1,30)}$=20.08, P<0.0001; and choice-zone: $F_{(1,30)}$=326.89, P<0.0001), between frequency bands (reward-zone: $F_{(4,30)}$=13.16, P<0.0001; delay-zone: $F_{(4,30)}$=21.10, P<0.0001; and choice-zone: $F_{(4,30)}$=39.86, P<0.0001), as well a factor-interaction effect (groups x frequency bands; reward-zone: $F_{(4,30)}$=2.69, P=0.0395; delay-zone: $F_{(4,30)}$=3.37, P=0.0148; and choice-zone: $F_{(1,30)}$=7.20, P<0.0001). *Post hoc* analysis revealed that after the nerve lesion the PDC level decrease at all frequency bands in the choice zone and in the reward-zone, with the exception of the reward-zone delta band (Bonferroni, P<0.001). In the delay-zone, we found only a significant decrease at the theta frequency band (P<0.001). In the case of the mPFC>CA1 direction there was a significant difference between experimental groups at the reward and choice-zones ($F_{(1,30)}$=363.50, P<0.0001; and $F_{(1,30)}$=26.61, P<0.0001; respectively), between frequency bands (reward-zone: $F_{(4,30)}$=8.59, P<0.0001; delay-zone: $F_{(4,30)}$=4.32, P=0.0039; and choice-zone: $F_{(4,30)}$=81.91, P<0.0001), as well as a factor-interaction

effect at the reward and choice-zones ($F_{(4,30)}$=4.57, *P*=0.0028; and $F_{(4,30)}$=15.73, *P*<0.0001; respectively) (Fig. 8D). *Post hoc* analyses revealed that after the nerve lesion the PDC level decrease in all frequency bands at the reward-zone (*P*<0.001), and decreased in theta and alpha bands at the choice-zone. No significant differences were encountered for the delay-zone.

Information flow activity in correct and error alternations

We expanded the analysis of the lesion-induced changes in perievent time decision of neuronal activity by comparing the PDC values of the local field potentials signals for the same transition periods, and again separated the transition periods of correct alternations from the incorrect alternations. Different patterns of PDC activity were observed across correct and error alternations for both directions of the circuit (Fig. 9A).

The quantitative analysis of the averaged PDC in the 1-50 Hz frequency range showed that the global levels of information flow decreased significantly after nerve lesion (Fig. 9B). These changes were observed for both directions of the mPFC-CA1 circuit in both correct and error alternations. In the case of CA1>mPFC direction, for correct alternations statistical differences were encountered for experimental groups (two-factor ANOVA-RM; $F_{(1,56)}$=17.77, *P*=0.0029), but not across recording sessions ($F_{(7,56)}$=1.73, *P*=0.1210) and factor-interaction (groups x recording sessions, $F_{(7,56)}$=1.73, *P*=0.1362). *Post hoc* analysis revealed a significant increase of the PDC level across the day 21 after SNI lesion (Bonferroni, *P*<0.01). For error alternations, significant effects were observed across groups ($F_{(1,56)}$=57.34, *P*<0.0001) and recording sessions ($F_{(7,56)}$=4.35, *P*=0.0007), but not a factor-interaction effect between these factors ($F_{(7,56)}$=1.53, *P*=0.1765). *Post hoc* analysis revealed a significant decrease of the PDC activity across the day 1 and 5 after nerve lesion (Bonferroni, *P*<0.05). In the case of mPFC>CA1 direction, for correct alternations statistical differences were encountered for experimental groups ($F_{(1,56)}$=21.74, *P*=0.0016), but not across recording sessions ($F_{(7,56)}$=1.48, *P*=0.1920) and factor-interaction ($F_{(7,56)}$=1.23, *P*=0.3002). *Post hoc* analysis revealed a significant decrease of the PDC activity across the day 1 and 21 after SNI lesion (Bonferroni, *P*<0.05 and *P*<0.01, respectively). For error alternations, statistical differences were observed across groups ($F_{(1,56)}$=60.86, *P*<0.0001), recording sessions ($F_{(7,56)}$=4.47, *P*=0.0005), as well for the factor-interaction effect ($F_{(7,56)}$=2.90, *P*=0.0118). *Post hoc* analysis revealed a significant decrease of the PDC level across the day 1, 3, 5, and 21 after nerve lesion (Bonferroni, *P*<0.001, *P*<0.001, *P*<0.05, and *P*<0.001; respectively).

In what concerns the frequency bands (Fig. 9C), the global PDC level were particularly decreased across theta, alpha, and delta frequency bands for correct and error alternations. One exception was encountered across correct alternations, for the CA1 to mPFC direction, which

decreased across theta and increased for gamma frequency band after nerve lesion. In the CA1>mPFC direction during correct alternations we found significant differences between experimental groups (two-factor ANOVA-RM; $F_{(1,30)}$=4.83, *P*=0.0319), frequency bands ($F_{(4,30)}$=41.96, *P*<0.0001), as well as a factor-interaction effect (groups x frequency bands, $F_{(4,30)}$=7.96, *P*<0.0001). *Post hoc* analysis revealed a significant decrease of PDC activity after SNI lesion in the theta frequency band (Bonferroni, *P*<0.01), and an increase in the gamma frequency band (*P*<0.01). During error alternations, statistical differences were found between groups ($F_{(1,30)}$=30.42, *P*<0.0001) and frequency bands ($F_{(4,30)}$=11.49, *P*<0.0001), but not a factor-interaction effect (groups x frequency bands, $F_{(4,30)}$=1.43, *P*=0.2357). *Post hoc* analysis revealed a significant decrease of the PDC level for theta (Bonferroni, *P*<0.01), alpha (*P*<0.01), and beta (*P*<0.05) frequency bands after nerve lesion. In the case of mPFC>CA1 direction, for correct alternations significant differences were encountered between experimental groups ($F_{(1,30)}$=41.38, *P*<0.0001) and across frequency bands ($F_{(4,30)}$=18.14, *P*<0.0001), but not a factor-interaction effect between these factors ($F_{(4,30)}$=1.02, *P*=0.4026). *Post hoc* analysis revealed a significant decrease of the PDC activity for SNI group across theta (Bonferroni, *P*<0.001), alpha (*P*<0.01), and beta (*P*<0.05) frequency bands. For error alternations, statistical differences were encountered across groups ($F_{(1,30)}$=59.87, *P*<0.0001) and frequency bands ($F_{(4,30)}$=9.31, *P*<0.0001), but no interaction effect between these factors ($F_{(4,30)}$=1.35, *P*=0.2621). *Post hoc* analysis revealed a significant decrease of the information flow across theta (Bonferroni, *P*<0.001), alpha (*P*<0.001), and beta (*P*<0.05) frequency bands for SNI group.

DISCUSSION

In this study we report how the induction of chronic neuropathic pain affects the mPFC-hippocampal functional connectivity by examining the temporal structure in spiking and LFPs activity while rats performed a spatial alternation task. The behavioral task used in the present study is a classical spatial working memory task, where the animals need to remember the route previously used in order to correctly alternate between reward sites.

We report that the pain-inducing SNI lesion impaired the spatial memory performance in these animals. These results are in accordance with recent studies using animal models of neuropathic pain that have also showed a reduction in spatial memory (Leite-Almeida *et al.*, 2009; Hu *et al.*, 2010; Ren *et al.*, 2011), and with clinical reports that chronic pain patients commonly present working memory impairments (Ling *et al.*, 2007; Luerding *et al.*, 2008b). Similar memory impairments has been reported following prefrontal (Kyd & Bilkey, 2003) or

hippocampal lesions (Gaskin *et al.*, 2009a; Gaskin *et al.*, 2009b), and during the inhibition of the mPFC-hippocampal circuit by lidocaine (Floresco *et al.*, 1997) or muscimol infusions (Wang & Cai, 2006; Yoon *et al.*, 2008).

Previous reports have shown an increase in firing rate of mPFC neurons firing activity during the delay period in delayed-choice tasks (Miller *et al.*, 1996; Fuster, 1997; Rainer *et al.*, 1999), and this led to the suggestion that working memory processing may be dependent on increased activity of mPFC neurons. Our results show that the nerve lesion reduced the number of mPFC and CA1 neurons with increased firing rates in the delay-zone versus the other zones of the maze. This decrease in mPFC activity during the delay period is in agreement with the suggestion that mPFC instability may play a crucial role in pain-induced memory dysfunction (Metz *et al.*, 2009; Apkarian *et al.*, 2011). In contrast, the nerve lesion marginally affected the overall neuronal firing rate of the CA1 in which we observed an increase in the populational activity during navigation in the reward and choice zones. In addition, our data showed that the majority of the mPFC neurons increased their firing activity in the decision point when the rat performed a correct alternation, while the activity of CA1 neurons decreased during error alternations. More importantly, these firing patterns remain unchanged after peripheral nerve lesion.

Recordings from awake animals have shown that hippocampal neurons fire at phase-locked to the theta oscillation of the hippocampal field potential (Fox & Ranck, 1981; Skaggs *et al.*, 1996), in which the supramammillary nucleus have an important role in its generation (Ruan *et al.*, 2010). The robust hippocampal theta frequency band has also been reported to be responsible for theta phase-locked firing patterns of mPFC neurons (Hyman *et al.*, 2005; Jones & Wilson, 2005a; Siapas *et al.*, 2005; Sirota *et al.*, 2008), and these phase-interactions were greatest when the animal made a decision (Jones & Wilson, 2005a; b). Hyman et al. (2010) using a two level delayed non-match to sample task (DNMS) reported that during error trials the mPFC neurons loose the theta-entrainment that occurs via theta range interactions between mPFC and hippocampus, in agreement with human studies showing strong mPFC-hippocampal theta coherence during working memory tasks (Tesche & Karhu, 2000; Onton *et al.*, 2005). In fact, half of the mPFC neuronal population recorded by Hyman et al. (2010) presented theta-entrainment across the correct trials, while only a limited number of mPFC neurons presented theta-entrainment for the error trials. Moreover, the authors found that almost all of the mPFC neurons had a similar pattern of activity across correct and error trials.

Despite the differences between both behavioral tasks, we found that after nerve lesion the spiking oscillatory activity of mPFC and CA1 neurons increased their level of correlation in

respect to the hippocampal theta rhythm. This change was particularly evident for both recorded areas during delay-zone navigation, suggesting a disturbance of the mPFC-hippocampal circuit synchronization.

Although the LFPs activity did not present changes in power spectrum, both recorded brain regions shared a prominent theta power band as previously been described in other research reports (Buzsaki, 2002; Lörincz *et al.*, 2007). An intensification of theta-range coherence across frontal and hippocampal regions has been described during the execution of working memory tasks using human EEG recordings (Onton *et al.*, 2005) (Tesche & Karhu, 2000). More recently, an elevation of mPFC gamma-range power has been associated to the maintenance of working memory processes (Izaki & Akema, 2008; Klimesch *et al.*, 2008; Sirota *et al.*, 2008; Colgin *et al.*, 2009). In fact, it has been suggested that working memory is coordinated by oscillatory processes shared simultaneously by the theta and gamma frequency bands (see for review, Lisman, 2010). In our study the mPFC-hippocampal LFPs coherence changed across groups and recording sessions; however no significant differences were encountered across frequency bands.

The most significant finding in the present study is that the onset of neuropathic pain causes a decrease in mPFC-hippocampal flow of information as measured by partial directed coherence – PDC (Sameshima & Baccalá, 1999; Baccala & Sameshima, 2001); this decrease was observed in both directions of the circuit across reward and choice navigation zones, in spite of the lack of alteration in the mPFC-hippocampal power spectrum. More importantly, the amount of information flow from mPFC to CA1 during delay-zone navigation remained partially conserved across frequency bands; and from CA1 to mPFC the PDC level decreased specifically in the theta-range. In terms of the nature of the information conveyed in correct and error alternations, the analysis of PDC activity revealed that the activity in theta, alpha, and beta frequency bands were decreased. This decrease occurred for both correct and error alternations in the case of the mPFC to CA1 direction and for error alternations in the case of the CA1 to mPFC direction, while for the correct alternations in the CA1 to mPFC direction there was a decrease only at the theta band together with an increase in the PDC activity at the gamma frequency.

Several authors have suggested that pain is one of the leading factors that can induce disruptions of spontaneous oscillations at different cortico-subcortical circuits (Corbetta & Shulman, 2002; Mouraux *et al.*, 2003; Ohara *et al.*, 2004), including the inhibition or potentiation of oscillatory rhythms (Backonja *et al.*, 1991; Chang *et al.*, 2002; Ploner *et al.*, 2004). Oscillatory interactions across the different brain circuits reflect a global functional state of the system, and

are used as an alert mechanism to find normal functional state perturbations (Ploner *et al.*, 2006). In what concerns processing of nociceptive information, an example of these perturbations was recently been reported in the rat thalamocortical circuit using the same chronic pain model applied to this study (Cardoso-Cruz *et al.*, 2011b).

It should be noted that the reduction in task performance could result from pain-induced motor impairment of the animals; indeed both groups experienced a reduction of the navigation velocity following the sham or SNI surgery, which resolved after 7 days for pre-surgery levels of movement. However, we believe that this motor impairment is not the leading cause for the performance difference between groups because it similarly affected both sham and nerve-lesioned animals and because the video-tracking measurement of instantaneous speed showed similar running speeds in both groups (Fig. 1F). Moreover, the observed difference between groups in alternation duration is caused by the longer trajectories and frequent pauses at transition points done by the nerve-lesioned animals; this increase in the average time of navigation also leads to longer delays between alternations which results in more challenging tasks (Lee & Kesner, 2003).

In summary, our data suggest that peripheral nerve injury (SNI) causes impairment in spatial working memory performance. In terms of the temporal structure of spiking and LFPs activity in the mPFC-CA1 circuit, both populations of neurons increased their spiking phase-precision in respect to hippocampal theta rhythm after nerve lesion. In addition, our data showed a clear reduction of the amount of information shared by this circuit, which occurs at different frequency bands depending on whether the rat performs a correct or error alternation. These changes are probably caused by adaptive mechanisms that occur during the onset of painful condition, which may disturb the mnemonic processes that rely on the integration and consolidation of spatial working memory.

Acknowledgments:

This work was supported by grants from the Portuguese Foundation for Science and Technology – FCT: PhD grant SFRH/42500/2007; Project PTDC/SAU-NEU/100773/2008; and BIAL Foundation: BIAL Project 126/08.

Conflict of interest:

The authors do not have any conflicts of interest.

LEGEND OF FIGURES

FIGURE 1. Apparatus and behavioral performance.

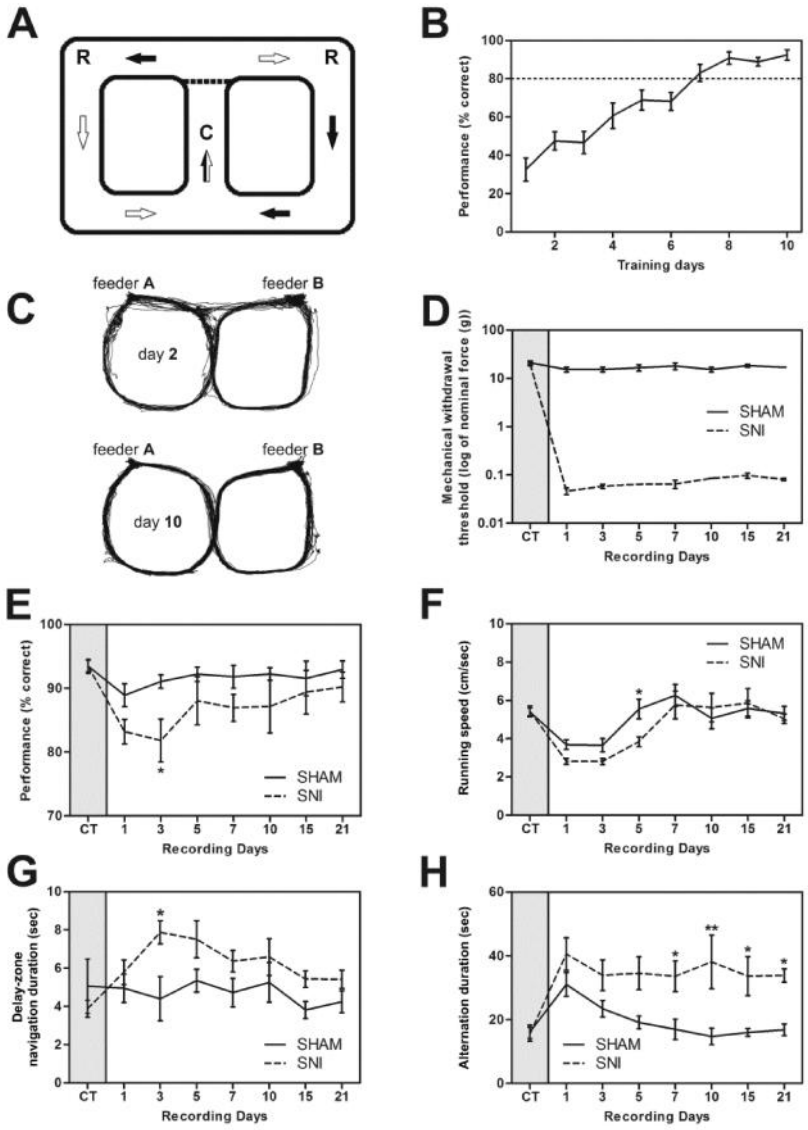

(A) Figure-eight maze, spatial alternation working memory task. Starting from the center of the maze (C), the animal had to alternately visit two reward sites (R) (feeder A and B) to obtain chocolate-flavored pellets. The animal was required to come back to the center from a given reward site before visiting the other reward site. The arrows indicate the direction of travel when going to the left and right goals. **(B)** Training period performance for the spatial working-memory task. Only rats that reach at least the threshold of 80% of correct alternations from feeder A to feeder B according to the task imposed rules were selected to be candidates to receive the surgery for electrodes implantation. **(C)** Movement map of a rat across the day 2 and 10 of the training period. As shown, the rat frequently made more navigation errors in early days of training (see for example the direct trajectories between reward locations across day 2). **(D)** Level of sensibility to mechanical stimulation evaluated using von Frey filaments. A large decrease was observed in the threshold required to induce a paw response in the SNI-group. **(E)**

Recording period performance for the spatial working-memory task. A significant decrease in performance level and running velocity **(F)** was observed in the SNI-group after nerve lesion. **(G)** The SNI animals spent more time navigating in the delay-zone of the behavioral test after lesion. **(H)** Also a significant increase of the average interval between correct alternations was observed in this experimental group. Values are presented as mean ± SEM. Comparisons between control (CT) and after surgery recording sessions based on two-factor ANOVA - repeated measures, followed by *Post hoc* Bonferroni test. **P*<0.05, and ***P*<0.01.

FIGURE 2. Stability of two cells simultaneously recorded in the same animal across experimental sessions and firing activity during task navigation.

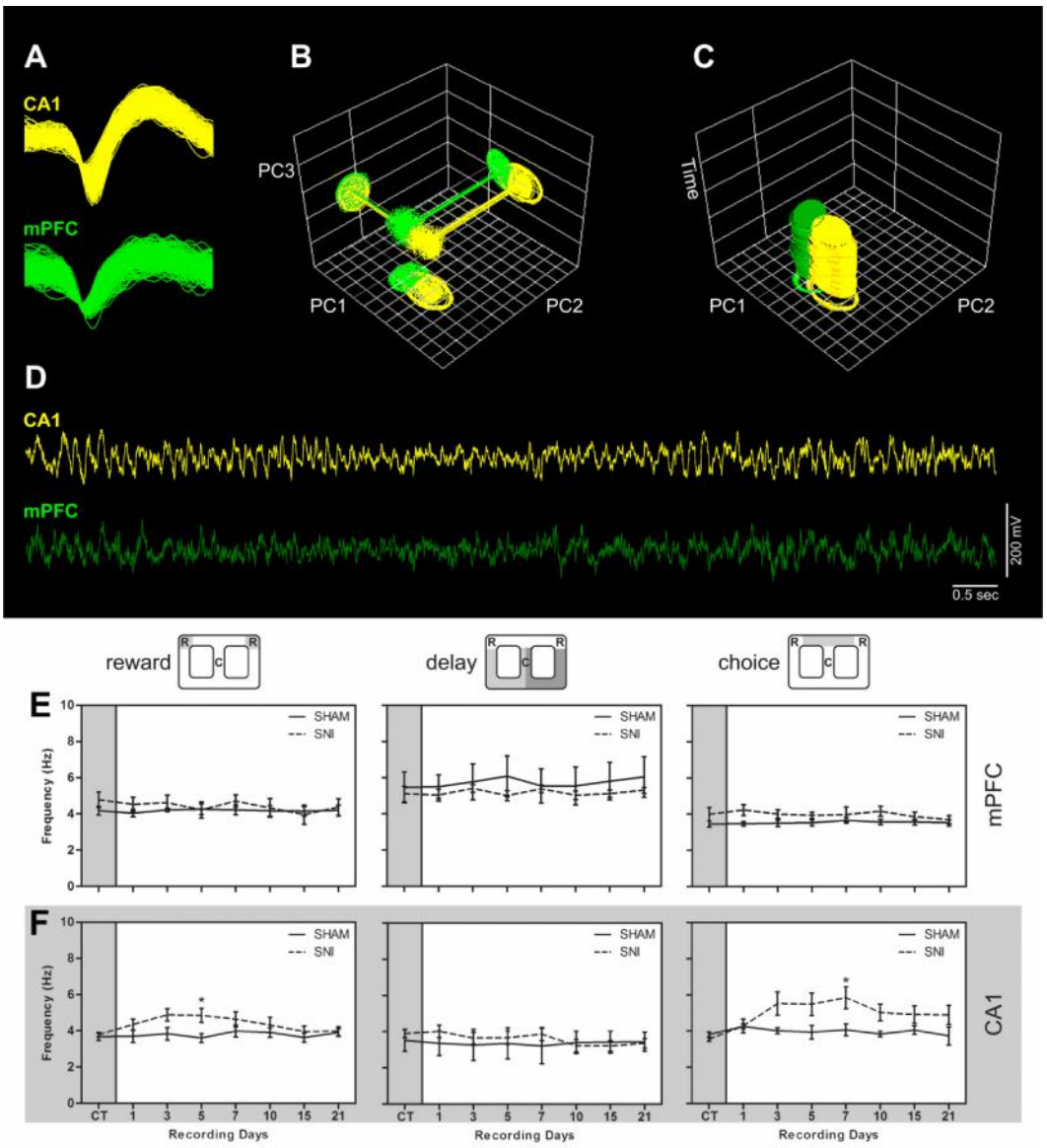

(A) Illustration of the waveform shape of a hippocampal CA1 cell (yellow) and a mPFC cell (green). Only units with a greater than 3:1 signal to noise rate were considered. **(B)** Offline analysis of 3-D PC cluster stability from each channel shown across the whole recording sessions using the WaveTracker software (Plexon Inc., Dallas, TX, USA). In this view **(C)**, 2-D PC clusters are projected as function of time (Z-axis). Stability across time of the units isolated was used as extra-selection criteria. **(D)** Correspondent oscillations of intracranial LFP channels. Raw recordings representing 10-sec of ongoing LFP activity. Average firing rate activity for mPFC **(E)** and CA1 **(F)** neurons when the animals ran the eight-figure task. Data were presented individually across the three considered navigation zones of the behavioral task. No significant differences were encountered in mPFC neurons; note however in this case that the average firing rate was significantly higher during the navigation in the delay-zone when compared to reward and choice-zones. In the case of CA1 an increase of the average firing rate was observed during reward and choice-zones navigation after nerve lesion. Values are presented as mean ±

SEM. Comparisons between control (CT) and after surgery recording sessions based on two-factor ANOVA - repeated measures, followed by *Post hoc* Bonferroni test. *P<0.05.

FIGURE 3. Typical neuronal responses for correct and error alternations.

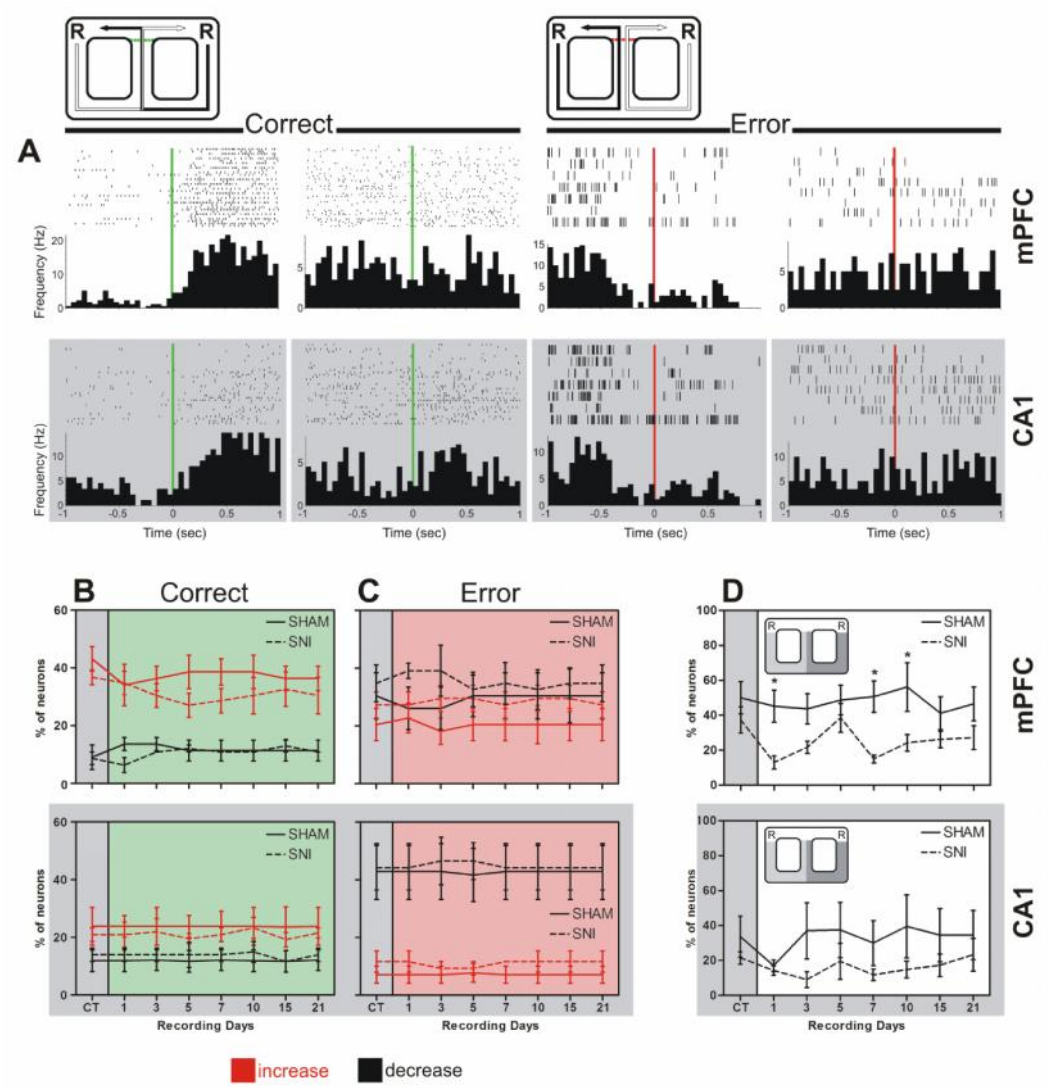

(A) Perievent time decision histograms illustrate the averaged firing rate of four mPFC and four CA1 representative neurons around the decision limit (bin resolution of 50-msec). Time = 0 on the x-axis corresponded to the time of decision of direction turn in order to yield the reward location. Across both recorded regions, some neurons changed their spiking activity and others remain unchanged in respect to correct and error alternations after the decision of direction (from left to right, mPFC: KS=0.32, *P*=0.0001; KS=0.07, *P*=0.8200; KS=0.24, *P*=0.0282; and KS=0.10, *P*=0.6725; from left to right CA1: KS=0.29, *P*=0.0003; KS=0.15 *P*=0.1349; KS=0.25, *P*=0.0026; and KS=0.13, *P*=0.4973; respectively). The majority of mPFC neurons elevated their average firing activity when the rat performed a correct alternation **(B)**, and CA1 neurons decreased their firing activity across error alternations **(C)**. In both cases, no differences were encountered between experimental groups. **(D)** The percentage of neurons that elevated their average firing rate during the delay-zone navigation in respect to whole recording session decreased significantly after nerve lesion in the case of mPFC neurons. Values are presented as mean ± SEM. Comparisons between control (CT) and after surgery recording sessions based on two-factors ANOVA - repeated measures, followed by Bonferroni *Post hoc* test. **P*<0.05.

FIGURE 4. Correlation between hippocampal theta oscillations and spiking activity.

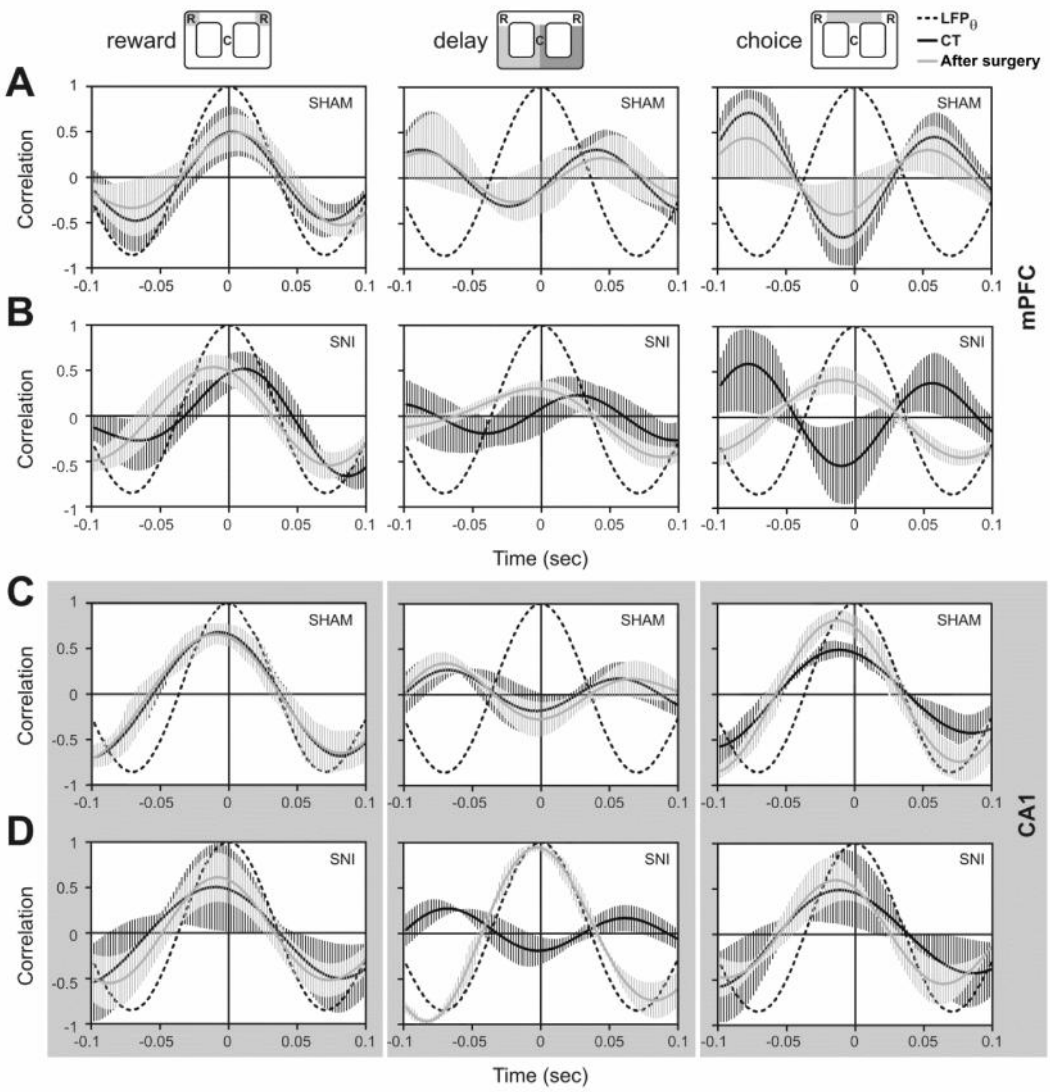

The relationship between temporal structure of population neuronal spiking activity and ongoing theta cycle of hippocampal LFPs (black dotted line) as calculated for pre-operation period and day 10 after SHAM or SNI surgery. The black dotted line represents the phase histogram of the 4-9 Hz hippocampal local field potential (LFP_θ). The panel **(A)** illustrate the populational mPFC activity before (CT, control period) and after SHAM surgery, and the panel **(B)** the activity before (CT) and after SNI surgery. The mPFC neurons increased their firing precision in respect to theta rhythms after nerve lesion during the navigation across delay and choice-zones (two-sample Kolmogorov-Smirnov test; delay-zone: CT/SNI: KS=0.24, *P*=0.0459; SHAM/SNI: KS=0.25, *P*=0.0257; choice-zone: CT/SNI: KS=0.26, *P*=0.0389; SHAM/SNI: KS=0.28, *P*=0.0291). The panel **(C)** Illustrate the populational CA1 activity before (CT) and after SHAM surgery, and the panel **(D)** the activity before (CT) and after SNI surgery. The CA1 conserved their temporal structure of activity across reward and choice-zones, but across delay-zone increased their firing precision (CT/SNI: KS=0.24, *P*=0.0289, and SHAM/SNI: KS=0.26, *P*=0.0311). Values are means $\pm$ SEM.

FIGURE 5. Spectral analysis of mPFC-CA1 LFPs channels.

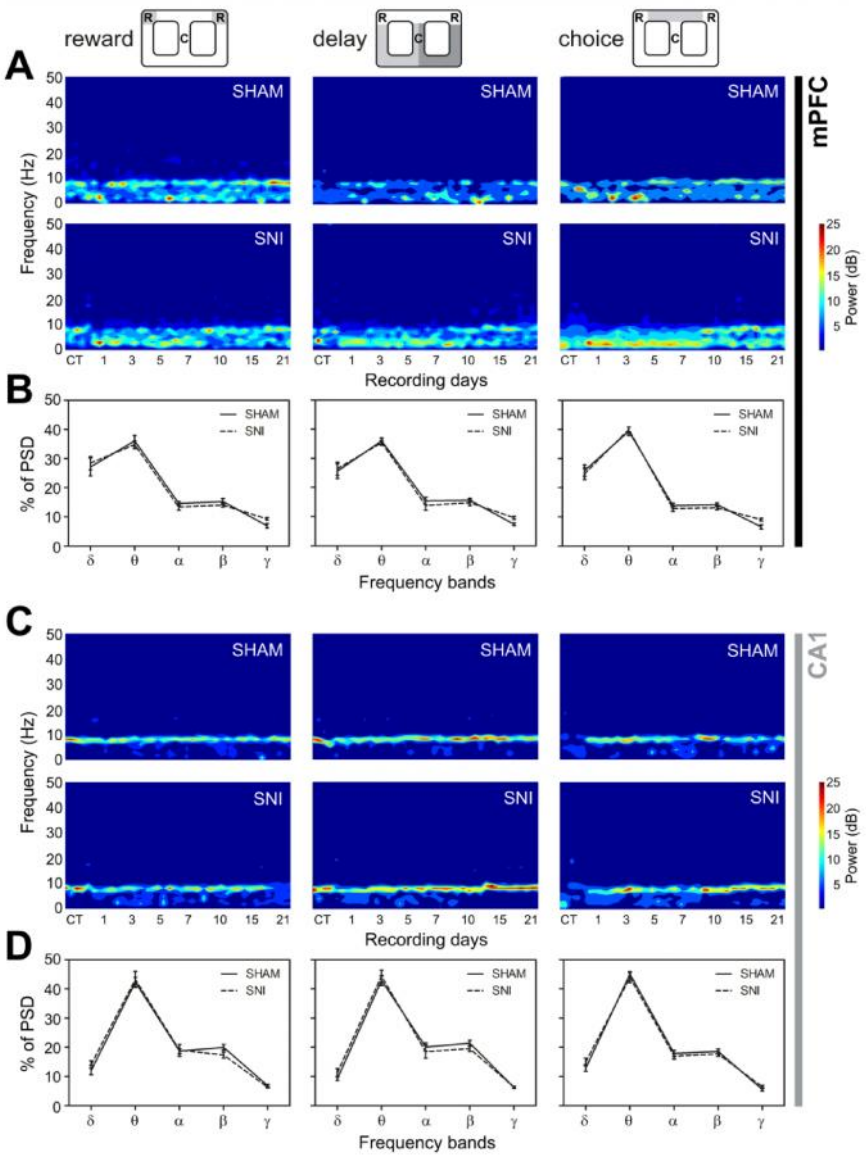

Power spectral density (PSD) of LFPs normalized by the percentage of total power within the frequency range analyzed (1-50 Hz) for mPFC and CA1 channels **(A, C)**, comparing the control period (CT) and SHAM or SNI recording sessions after surgery. PSD showed that spectral power patterns were partially conserved across the experimental groups. The averaged % of PSD across frequency bands revealed as expected that significant differences between frequency bands, however no significant differences were found between experimental groups **(B, D)**. Values are expressed for all animals as mean ±SEM. Frequency bands: delta (δ, 1-4 Hz), theta (θ, 4-9 Hz), alpha (α, 9-15 Hz), beta (β, 15-30 Hz), and slow-gamma (γ, 30-50 Hz). Comparisons between control SHAM and SNI groups after surgery recording sessions based on two-factor ANOVA - repeated measures, followed by *Post hoc* Bonferroni test.

FIGURE 6. Spectral coherence.

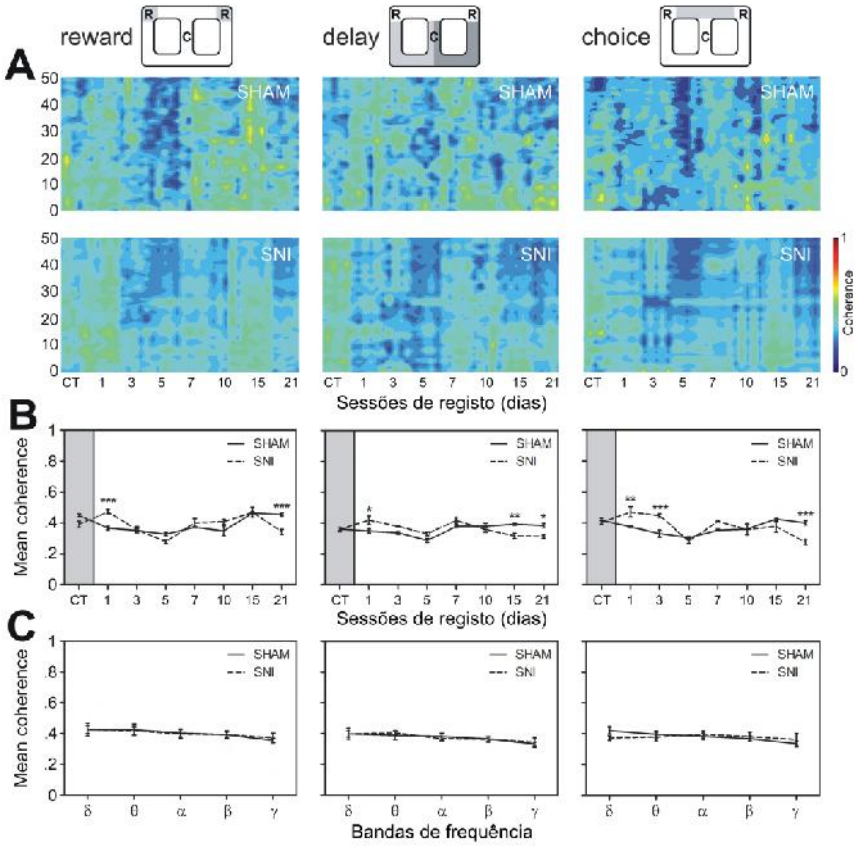

Spectral coherence between simultaneously mPFC and CA1 LFPs recorded channels showed similar global levels of coherence activity across navigation zones for experimental groups **(A)**. The averaged coherence (in 1-50 Hz frequency range) across recording sessions indicate no significant differences between experimental groups, however significant differences were found across recording sessions particularly during the early recording sessions after lesion. **(C)** The averaged coherence within frequency bands showed no differences for reward and choice-zones, but for delay-zone the coherence activity across frequency bands were different between experimental groups. Frequency bands: delta (δ, 1-4 Hz), theta (θ, 4-9 Hz), alpha (α, 9-15 Hz), beta (β, 15-30 Hz), and slow-gamma (γ, 30-50 Hz). Values are presented as mean ± SEM. Comparisons between control (CT) and after surgery recording sessions based on two-factor ANOVA - repeated measures, followed by *Post hoc* Bonferroni test. **P*<0.05, ***P*<0.01; and ****P*<0.001.

FIGURE 7. The oscillations of information flow between the two recorded regions were determined by partial directed coherence (PDC) analysis.

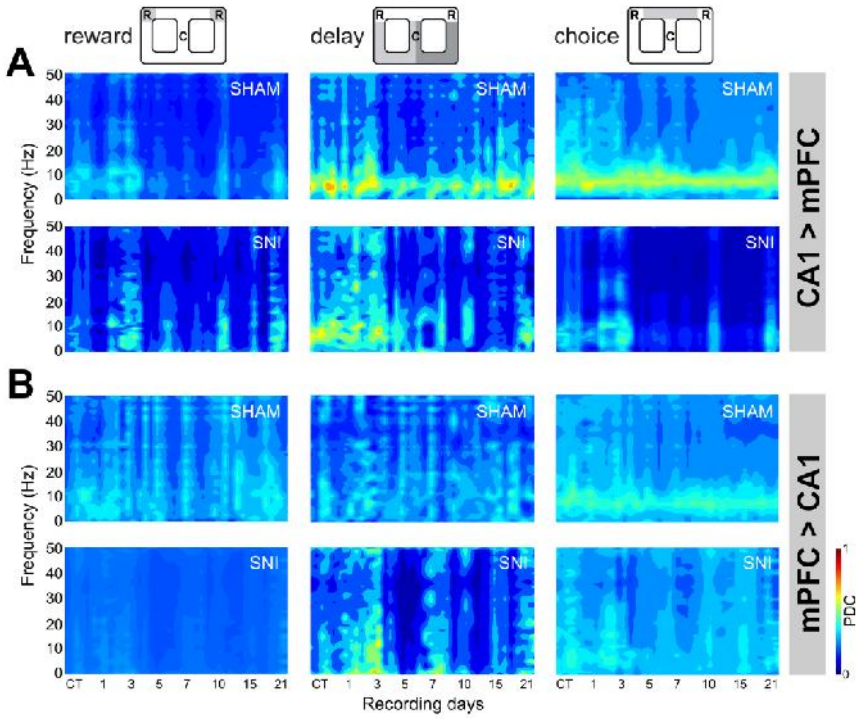

Data were presented individually across the three considered navigation zones of the behavioral task. The amount of information flow from dorsal hippocampal CA1-to-mPFC **(A)** after peripheral nerve lesion decreased dramatically across choice-zone navigation, and from mPFC-to-CA1 **(B)** across reward-zone, indicating that less information was processed in the mPFC-CA1 circuit after peripheral nerve lesion.

FIGURE 8. PDC activity across recording days and frequency bands.

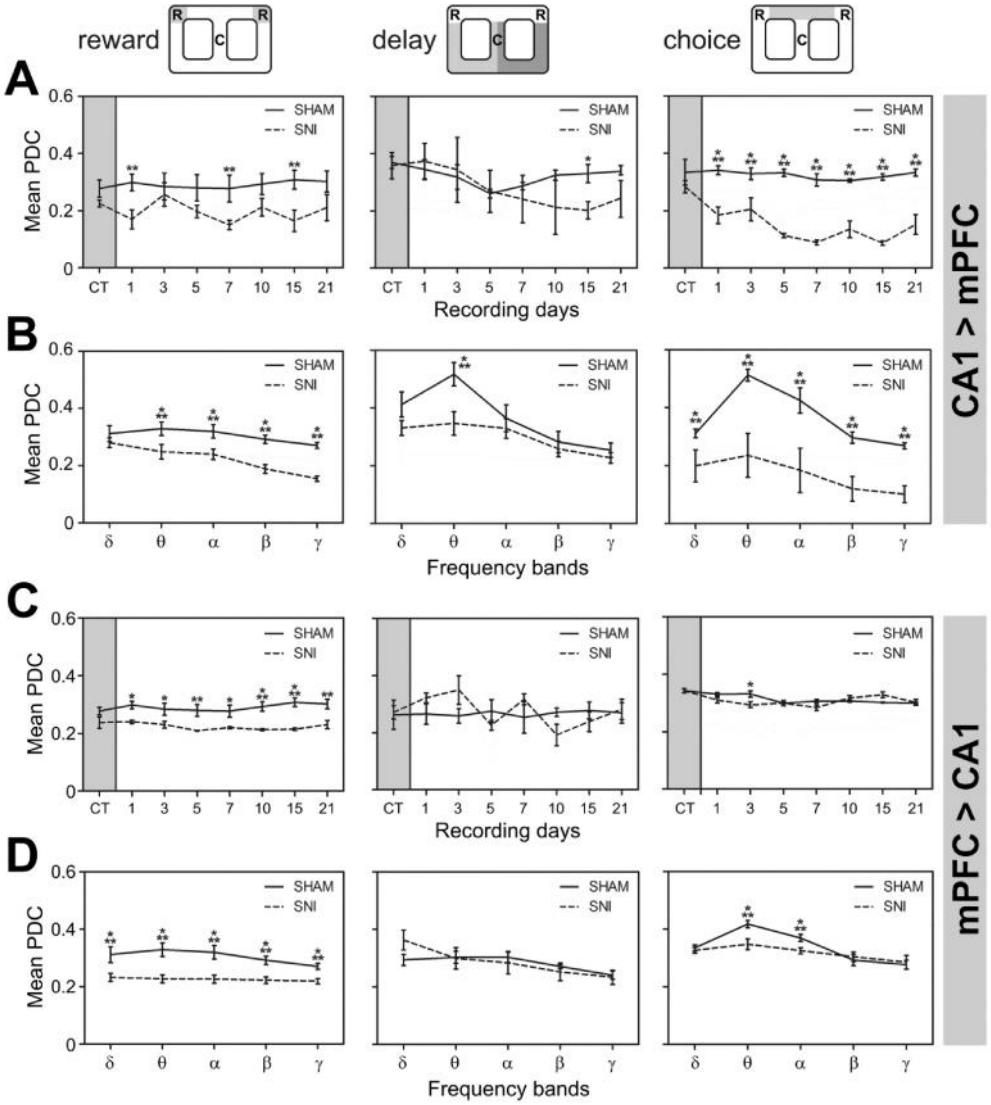

The averaged PDC level in 1-50 Hz frequency range across recording sessions indicate that less information were transmitted from CA1-to-mPFC after peripheral nerve lesion **(A)**, and across frequency bands for reward (in all frequency bands except in delta) and choice (in all frequency bands) navigation zones **(B)**. Note however that PDC activity were particularly conserved across delay-zone, and that only the theta frequency showed a decreased after lesion. In the mPFC-to-CA1 direction, the averaged PDC level decreased for reward-zone across recording days **(C)**, and across frequency bands for reward (in all frequency bands) and choice (in theta and alpha bands) zones **(D)**. No significant differences were encountered for delay-zone across frequency bands. Frequency bands: delta (δ, 1-4 Hz), theta (θ, 4-9 Hz), alpha (α, 9-15 Hz), beta (β, 15-30 Hz), and slow-gamma (γ, 30-50 Hz). Values are presented as mean ± SEM. Comparisons between control (CT) and after surgery recording sessions based on two-factor ANOVA - repeated measures, followed by *Post hoc* Bonferroni test. **P*<0.05, ***P*<0.01; and ****P*<0.001.

FIGURE 9. Patterns of information flow activity for correct and error alternations.

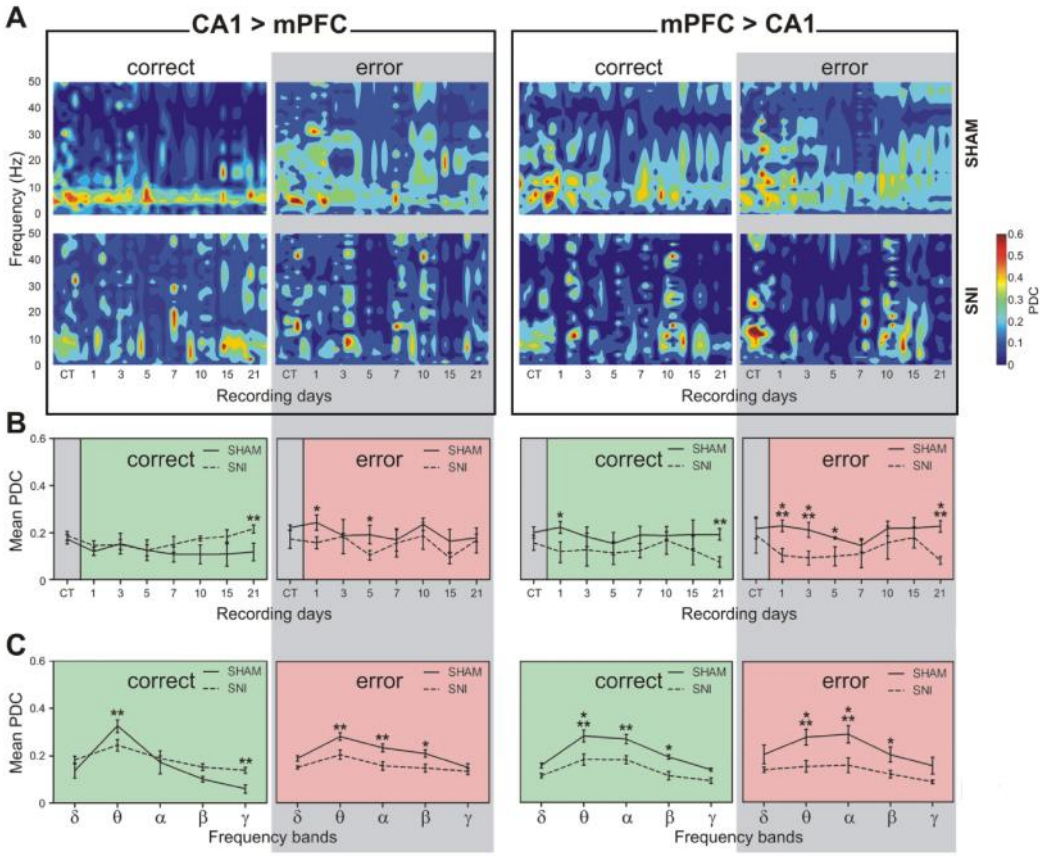

Different patterns of PDC activity were observed across correct and error alternations **(A)**. Note for example a strong theta band activity during correct alternations for CA1>mPFC direction, which is altered after peripheral nerve lesion. In terms of recording sessions, the averaged PDC activity (in 1-50 Hz frequency range) indicates that significant differences were encountered between experimental groups **(B)**. In terms of frequency bands, the PDC activity showed that less information were processed in both directions of the circuit across theta, alpha, and beta frequency bands for correct and error alternations after nerve lesion **(C)**. Frequency bands: delta (δ, 1-4 Hz), theta (θ, 4-9 Hz), alpha (α, 9-15 Hz), beta (β, 15-30 Hz), and slow-gamma (γ, 30-50 Hz). Values are presented as mean ± SEM. Comparisons between control (CT) and after surgery (SHAM or SNI) recording sessions based on two-factors ANOVA - repeated measures, followed by Bonferroni *Post hoc* test. **P*<0.05, ***P*<0.01; and ****P*<0.001.

REFERENCES

Aguiar P, Mendonça L, Galhardo V (2007) OpenControl: A free opensource software for video tracking and automated control of behavioral mazes. J Neurosci Methods 166:66-72.

Apkarian AV, Hashmi JA, Baliki MN (2011) Pain and the brain: specificity and plasticity of the brain in clinical chronic pain. Pain 152:S49-64.

Baccala LA, Sameshima K (2001) Partial directed coherence: a new concept in neural structure determination. Biol Cybern 84:463-474.

Backonja M, Howland EW, Wang J, Smith J, Salinsky M, Cleeland CS (1991) Tonic changes in alpha power during immersion of the hand in cold water. Electroencephalogr Clin Neurophysiol 79:192-203.

Baeg EH, Kim YB, Huh K, Mook-Jung I, Kim HT, Jung MW (2003) Dynamics of population code for working memory in the prefrontal cortex. Neuron 40:177-188.

Buzsaki G (2002) Theta Oscillations in the Hippocampus. Neuron 33(3):325-40.

Cardoso-Cruz H, Lima D, Galhardo V (2011a) Instability of spatial encoding by CA1 hippocampal place cells after peripheral nerve injury. Eur J Neurosci 33:2255-2264.

Cardoso-Cruz H, Sameshima K, Lima D, Galhardo V (2011b) Dynamics of circadian thalamocortical flow of information during a peripheral neuropathic pain condition. Front Integr Neurosci 5:43.

Chang PF, Arendt-Nielsen L, Chen AC (2002) Differential cerebral responses to aversive auditory arousal versus muscle pain: specific EEG patterns are associated with human pain processing. Exp Brain Res 147:387-393.

Chaplan SR, Bach FW, Pogrel JW, Chung JM, Yaksh TL (1994) Quantitative assessment of tactile allodynia in the rat paw. J Neurosci Methods 53:55-63.

Colgin LL, Denninger T, Fyhn M, Hafting T, Bonnevie T, Jensen O, Moser M-B, Moser EI (2009) Frequency of gamma oscillations routes flow of information in the hippocampus. Nature 462(7271):353-7.

Corbetta M, Shulman GL (2002) Control of goal-directed and stimulus-driven attention in the brain. Nat Rev Neurosci 3:201-215.

Decosterd I, Woolf CJ (2000) Spared nerve injury: an animal model of persistent peripheral neuropathic pain. Pain 87:149-158.

Devoize L, Alvarez P, Monconduit L, Dallel R (2011) Representation of dynamic mechanical allodynia in the ventral medial prefrontal cortex of trigeminal neuropathic rats. Eur J Pain 15(7):676-82.

Ducreux D, Attal N, Parker F, Bouhassira D (2006) Mechanisms of central neuropathic pain: a combined psychophysical and fMRI study in syringomyelia. Brain 129:963-976.

Floresco SB, Seamans JK, Phillips AG (1997) Selective roles for hippocampal, prefrontal cortical, and ventral striatal circuits in radial-arm maze tasks with or without a delay. J Neurosci 17:1880-1890.

Fox SE, Ranck JB, Jr. (1981) Electrophysiological characteristics of hippocampal complex-spike cells and theta cells. Exp Brain Res 41:399-410.

Frank Y, Seiden J, Napolitano B (1996) Visual event related potentials and reaction time in normal adults, normal children, and children with attention deficit hyperactivity disorder: differences in short-term memory processing. Int J Neurosci 88:109-124.

Fuster JM (1997) Network memory. Trends Neurosci 20:451-459.

Gaskin S, Tardif M, Mumby DG (2009a) Patterns of retrograde amnesia for recent and remote incidental spatial learning in rats. Hippocampus 19:1212-1221.

Gaskin S, Gamliel A, Tardif M, Cole E, Mumby DG (2009b) Incidental (unreinforced) and reinforced spatial learning in rats with ventral and dorsal lesions of the hippocampus. Behav Brain Res 202:64-70.

Green MF (2006) Cognitive impairment and functional outcome in schizophrenia and bipolar disorder. J Clin Psychiatry 67:e12.

Hu Y, Yang J, Wang Y, Li W (2010) Amitriptyline rather than lornoxicam ameliorates neuropathic pain-induced deficits in abilities of spatial learning and memory. Eur J Anaesthesiol 27:162-168.

Hyman JM, Zilli EA, Paley AM, Hasselmo ME (2005) Medial prefrontal cortex cells show dynamic modulation with the hippocampal theta rhythm dependent on behavior. Hippocampus 15:739-749.

Hyman JM, Zilli EA, Paley AM, Hasselmo ME (2010) Working memory performance correlates with prefrontal-hippocampal theta interactions but not with prefrontal neuron firing rates. Front Int Neurosci 4:2.

Izaki Y, Akema T (2008) Gamma-band power elevation of prefrontal local field potential after posterior dorsal hippocampus-prefrontal long-term potentiation induction in anesthetized rats. Exp Brain Res 184(2):249-53.

Ji D, Wilson MA (2007) Coordinated memory replay in the visual cortex and hippocampus during sleep. Nat Neurosci 10:100-107.

Jones MW, Wilson MA (2005a) Theta rhythms coordinate hippocampal-prefrontal interactions in a spatial memory task. PLoS Biol 3:e402.

Jones MW, Wilson MA (2005b) Phase precession of medial prefrontal cortical activity relative to the hippocampal theta rhythm. Hippocampus 15:867-873.

Jung MW, Qin Y, McNaughton BL, Barnes CA (1998) Firing characteristics of deep layer neurons in prefrontal cortex in rats performing spatial working memory tasks. Cereb Cortex 8:437-450.

Kim SH, Kim SK, Nam EJ, Han SW, Lee SJ (2011) Spatial versus verbal memory impairments in patients with fibromyalgia. Rheumatol Int (Online: DOI: 10.1007/s00296-010-1762-1)

Klimesch W, Freunberger R, Sauseng P, Gruber W (2008) A short review of slow phase synchronization and memory: evidence for control processes in different memory systems? Brain Res 1235:31-44

Kyd RJ, Bilkey DK (2003) Prefrontal cortex lesions modify the spatial properties of hippocampal place cells. Cereb Cortex 13:444-451.

Lee I, Kesner RP (2003) Time-dependent relationship between the dorsal hippocampus and the prefrontal cortex in spatial memory. J Neurosci 23:1517-1523.

Legrain V, Crombez G, Mouraux A (2011) Controlling attention to nociceptive stimuli with working memory. PLoS One 6:e20926.

Leite-Almeida H, Almeida-Torres L, Mesquita AR, Pertovaara A, Sousa N, Cerqueira JJ, Almeida A (2009) The impact of age on emotional and cognitive behaviours triggered by experimental neuropathy in rats. Pain 144:57-65.

Ling J, Campbell C, Heffernan TM, Greenough CG (2007) Short-term prospective memory deficits in chronic back pain patients. Psychosom Med 69:144-148.

Lisman J (2010) Working memory: the importance of theta and gamma oscillations. Curr Biol 20:R490-492.

Luerding R, Weigand T, Bogdahn U, Schmidt-Wilcke T (2008) Working memory performance is correlated with local brain morphology in the medial frontal and anterior cingulate cortex in fibromyalgia patients: structural correlates of pain-cognition interaction. Brain 131:3222-3231.

Lörincz M, Oláh M, Baracskay P, Szilágyi N, Juhász G (2007) Propagation of spike and wave activity to the medial prefrontal cortex and dorsal raphe nucleus of WAG/Rij rats. Physiol Behav 90:318-324.

McDowell S, Whyte J, D'Esposito M (1997) Working memory impairments in traumatic brain injury: evidence from a dual-task paradigm. Neuropsychologia 35:1341-1353.

Metz AE, Yau HJ, Centeno MV, Apkarian AV, Martina M (2009) Morphological and functional reorganization of rat medial prefrontal cortex in neuropathic pain. Proc Natl Acad Sci USA 106:2423-2428.

Millecamps M, Etienne M, Jourdan D, Eschalier A, Ardid D (2004) Decrease in non-selective, non-sustained attention induced by a chronic visceral inflammatory state as a new pain evaluation in rats. Pain 109:214-224.

Miller EK, Erickson CA, Desimone R (1996) Neural mechanisms of visual working memory in prefrontal cortex of the macaque. J Neurosci 16:5154-5167.

Mouraux A, Guérit JM, Plaghki L (2003) Non-phase locked electroencephalogram (EEG) responses to CO2 laser skin stimulations may reflect central interactions between A partial partial differential- and C-fibre afferent volleys. Clin Neurophysiol 114:710-722.

Ohara S, Crone NE, Weiss N, Lenz FA (2004) Attention to a painful cutaneous laser stimulus modulates electrocorticographic event-related desynchronization in humans. Clin Neurophysiol 115:1641-1652.

Onton J, Delorme A, Makeig S (2005) Frontal midline EEG dynamics during working memory. Neuroimage 27:341-356.

Pais-Vieira M, Lima D, Galhardo V (2009) Sustained attention deficits in rats with chronic inflammatory pain. Neurosci Lett 463:98-102.

Paxinos G, Watson C (1998) The Rat Brain in Stereotaxic Coordinates. San Diego: Academic Press.

Pesaran B, Pezaris JS, Sahani M, Mitra PP, Andersen RA (2002) Temporal structure in neuronal activity during working memory in macaque parietal cortex. Nat Neurosci 5:805-811.

Peyron R, García-Larrea L, Grégoire MC, Convers P, Lavenne F, Veyre L, Froment JC, Mauguière F, Michel D, Laurent B (1998) Allodynia after lateral-medullary (Wallenberg) infarct. A PET study. Brain 121:345-356.

Ploghaus A, Tracey I, Clare S, Gati JS, Rawlins JNP, Matthews PM (2000) Learning about pain: The neural substrate of the prediction error for aversive events. Proc Natl Acad Sci USA 97:9281-9286.

Ploner M, Pollok B, Schnitzler A (2004) Pain facilitates tactile processing in human somatosensory cortices. J Neurophysiol 92:1825-1829.

Ploner M, Gross J, Timmermann L, Pollok B, Schnitzler A (2006) Pain suppresses spontaneous brain rhythms. Cereb Cortex 16:537-540.

Rainer G, Rao SC, Miller EK (1999) Prospective coding for objects in primate prefrontal cortex. J Neurosci 19:5493-5505.

Ren WJ, Liu Y, Zhou LJ, Li W, Zhong Y, Pang RP, Xin WJ, Wei XH, Wang J, Zhu HQ, Wu CY, Qin ZH, Liu G, Liu XG (2011) Peripheral Nerve Injury Leads to Working Memory Deficits and Dysfunction of the Hippocampus by Upregulation of TNF-α in Rodents. Neuropsychopharmacology 36(5):979-992.

Ruan M, Young CK, McNaughton N (2010) Minimal driving of hippocampal theta by the supramammillary nucleus during water maze learning. Hippocampus 21(10):1074-1081.

Sameshima K, Baccalá L (1999) Using partial directed coherence to describe neuronal ensemble interactions. J Neurosci Methods 94:93-103.

Schon K, Atri A, Hasselmo ME, Tricarico MD, LoPresti ML, Stern CE (2005) Scopolamine reduces persistent activity related to long-term encoding in the parahippocampal gyrus during delayed matching in humans. J Neurosci 25:9112-9123.

Schweinhardt P, Glynn C, Brooks J, McQuay H, Jack T, Chessell I, Bountra C, Tracey I (2006) An fMRI study of cerebral processing of brush-evoked allodynia in neuropathic pain patients. Neuroimage 32:256-265.

Seifert F, Bschorer K, De Col R, Filitz J, Peltz E, Koppert W, Maihöfner C (2009) Medial prefrontal cortex activity is predictive for hyperalgesia and pharmacological antihyperalgesia. J Neurosci 29:6167-6175.

Siapas AG, Lubenov EV, Wilson MA (2005) Prefrontal phase locking to hippocampal theta oscillations. Neuron 46:141-151.

Sirota A, Montgomery S, Fujisawa S, Isomura Y, Zugaro M, Buzsáki G (2008) Entrainment of neocortical neurons and gamma oscillations by the hippocampal theta rhythm. Neuron 60:683-697.

Skaggs WE, McNaughton BL, Wilson MA, Barnes CA (1996) Theta phase precession in hippocampal neuronal populations and the compression of temporal sequences. Hippocampus 6:149-172.

Stern CE, Sherman SJ, Kirchhoff BA, Hasselmo ME (2001) Medial temporal and prefrontal contributions to working memory tasks with novel and familiar stimuli. Hippocampus 11:337-346.

Tesche CD, Karhu J (2000) Theta oscillations index human hippocampal activation during a working memory task. Proc Natl Acad Sci USA 97:919-924.

Vallar G, Papagno C (1993) Preserved vocabulary acquisition in Down's syndrome: the role of phonological short-term memory. Cortex 29:467-483.

Wang GW, Cai JX (2006) Disconnection of the hippocampal-prefrontal cortical circuits impairs spatial working memory performance in rats. Behav Brain Res 175:329-336.

Yoon T, Okada J, Jung MW, Kim JJ (2008) Prefrontal cortex and hippocampus subserve different components of working memory in rats. Learn Mem 15:97-105.

Zimmermann M (1983) Ethical guidelines for investigations of experimental pain in conscious animals. Pain 16:109-110.

PUBLICAÇÃO 5

UNCOVERING INFORMATION INTERACTIONS BETWEEN MEDIAL PREFRONTAL CORTEX AND MEDIODORSAL THALAMUS IN RATS PERFORMING A SPATIAL WORKING MEMORY TASK UNDER A CHRONIC PAIN CONDITION

Helder Cardoso-Cruz, Mafalda Sousa, Joana Vieira, Deolinda Lima, and Vasco Galhardo

Abstract

The medial prefrontal cortex (mPFC) and the mediodorsal thalamus (MD) form interconnected neural circuits that underlie aspects of spatial cognition and memory. In this paper, we investigated the effect of prolonged pain on the functional interaction between these areas in rats during the performance of a food reinforced spatial delayed alternation task for working memory test. Recordings of local-field potentials (LFPs) in the mPFC and MD were performed over a three week period before and after the establishment of an animal model of inflammatory pain. Our results showed a clear decrease in performance during the chronic pain period. The most relevant finding of the present study is that the onset of chronic pain condition caused a global decrease in mPFC-MD flow of information as measured by partial directed coherence – PDC – analysis. This decrease is observed in both directions of the circuit, but is more evident from MD-to-mPFC direction in a wide frequency range. In addition, spectral analysis of LFPs revealed significant oscillations of power spectral density across frequency bands, namely with a strong theta-range component that oscillates across pain condition onset. Moreover, mPFC-MD LFPs revealed a higher level of coherence, which is partially conserved across frequency bands. The results demonstrate that inflammatory pain leads to disturbances in the functional mPFC-MD connectivity, and that can be in the basis of impairments of spatial working memory.

Manuscript

Evidence from recording and brain imaging studies found neural activity of ventral regions of the medial prefrontal cortex (mPFC) were correlated with working memory (WM) process [3, 13, 22, 35, 48]. Anatomically, mPFC share interconnections indirectly through the mediodorsal thalamus (MD) to the dorsal hippocampal CA1-field [53], that are particularly engaged in spatial information processing [31], which is disturbed during the onset of a neuropathic pain condition [6]. By its turn, it has been shown that the mPFC region have important key role in pain-modulatory process [10, 42]; and that morphological and functional reorganization of mPFC region can be in celular basis for cognitive impairments under neuropathic pain condition [28].

A crucial key in the mPFC-hippocampal network is the MD thalamus, damage to this strucuture has been reported to induce spatial memory deficits [18], and amnesia [29, 30]. More importantly, the MD share large projections to the anterior cingulate cortex (ACC) [8, 54], that are particuarly envolved affective-motivational aspects of pain [36, 44, 52, 56]. Despite all the knowledge in remains unclear several aspects how pain affects the spatial working memory process, and particularly which is contribution of this pathway on pain information processing. Therefore, our interest was study the contribution of a long-term chronic pain condition on the neural activity of mPFC-MD circuit functioning. We recorded local-field-potentials (LFPs) activity of freely moving rats in a spatial WM task, performed before and after the induction of the complete Freund's adjuvant (*CFA*) injection – model of inflammatory pain [5].

Six adult male *Sprague-Dawley* rats (275-325 g) were used in this study. The rats were maintained on a 12-h light/dark cycle, and training and the recording sessions run at approximately the same time each day during the light portion of the cycle. All animals were food deprived to 90-95% of their *ad libitum* body weights only during training sessions. All procedures and experiments adhered to the guidelines of the Committee for Research and Ethical Issues of IASP [61], with the Ethical Guidelines for Animal Experimentation of the European Community Directive Number 86/609/ECC of 24 November of 1986, and approved by local boards.

The behavioral task consisted of a food-reinforced spatial alternation task on a figure-eight shaped maze, similar to the maze used in studies of episodic memory [19].The total dimension of the arena was 90 x 60 cm, with plexiglass corridors 15 cm

wide and opaque walls 30 cm high with intramaze cues (Fig. 1A). Starting from the center of the maze (C), the rats were trained to alternately visit two reward sites (R) to obtain one chocolate-flavored pellet (45 mg) that was automatically delivered by a pellet dispenser (Coulbourn Instruments, Whitehall, PA, USA). After visiting one of the reward locations, the animal had to continue forward and cross again the central corridor before visiting the opposite reward site; food rewards were not dispensed if the animal failed to cross the central corridor immediately before arriving at the reward sites or if the animal made two consecutive visits to the same reward site (arrows in Fig. 1A illustrate the pattern of correct maze navigation). Control of pellet dispensers was fully automated using the OpenControl software adapted to this particular task [1]. In all the analysis of this study we have considered three different zones in the behavioral arena: the “reward-zones” are the 15x15 cm corner areas where the animal receives a pellet upon a correct alternation; the “delay-zones” comprise the area between the reward-zones and the central corridor; finally, the “choice-zone” is the area preceding the reward-zones and immediately following the central corridor (Fig. 1A). The testing room was sound-attenuating, moderately illuminated and rich in visual cues. During the training period, the rats were given three daily 10-min sessions to learn the alternation schedule until they reach at least 80% of correct runway alternations. An error was defined by a consecutive visit to the same reward site or the return route was the same from the approach route. Errors were not reinforced. After reaching this performance criterion the animals were surgically implanted with two arrays of electrodes for extracellular single-unit recording.

Surgical procedures and electrode specifications were the same in our previous studies [6, 46], except for the intracranial multielectrodes arrays placement. After reaching the criterion levels of task performance (see details above), the animals received surgical implantation of two multielectrode arrays for local-field-potentials activity (LFPs) recordings. The arrays were oriented rostrocaudally and driven to the medial prefrontal cortex (mPFC) and mediodorsal thalamus (MD). The following coordinates in millimeters relative to Bregma [33] were used to place the arrays: mPFC (+2.2 rostro-caudal, 1.0 medio-lateral, -3.2 dorso-ventral), and MD (-2.3 rostro-caudal, 0.8 medio-lateral, -4.7 dorso-ventral).

After 7 days of recovery from the implantation surgery, six animals (n = 6, hereafter referred as CFA animals) were re-trained and after recorded during 5 consecutive days (hereafter named control period) while performing the runway alternation task in 2 daily sessions of 10 minutes. In the following day the animals were briefly anesthetized and subjected to induction of the complete Freund's adjuvant (*CFA*) injection – model of inflammatory pain [5]. The intervention is implemented in knee articulation, in the contralateral side to recording probes implantation. Animals were then recorded for a period of 16 days (with recordings performed at days 4, 5, 6, 7, 11 and 16 after CFA injection). Sensory threshold for noxious stimulation was assessed by placing the animals in cages with a metal mesh floor and touching the plantar surface of the paw with von Frey filaments (Somedic, Sweden) as previously described [9]. These measurements were done 1 hour after the end each neural recording session.

Extracellular local field potentials - LFPs – were recorded from the implanted microwire electrodes and processed by a sixteen-channel Multi-neuron acquisition processor (16-MAP, Plexon Inc., Dallas, TX). LFP signals recorded from electrodes were pre-amplified (500x), band-pass filtered (0.5-200 Hz), and digitized at 500 Hz. An overhead video tracking system was used to provide information about the rat's location on testing environment (CinePlex, Plexon Inc., Dallas, TX, USA), and to synchronize the behaviour video-recordings with the acquired neural data. After the end of all experiments, the rats were deeply anesthetized and brains were removed to recording sites identification under the microscope.

Computational procedures for measurements of the power spectral density (PSD) and coherence of mPFC and MD thalamus LFPs signals were described in detail elsewhere [7, 46]. The statistical method called by partial directed coherence (PDC) was used to identify and quantify the information flow interactions among the mPFC-MD circuit. The PDC method has been described in detail elsewhere [2, 38]. Briefly, PDC is an alternative representation of multivariate processes involving Granger-causality to uncover frequency-domains of direct influence. Its value lies between 0 and 1, and it estimates the degree of functional connectivity from a structure to another at a particular frequency range. Zero PDC can be interpreted as absence of functional connectivity and high PDC, near one, indicates strong connectivity between the structures. This can be interpreted as existence of information flow from brain area

source to target. Five frequency band intervals were considered: 1-4 Hz (δ, *delta*), 4-9 Hz (θ, *theta*), 9-15 Hz (α, *alpha*), 15-30 Hz (β, *beta*), and 30-50 Hz (γ, *gamma*).

Statistical comparisons between control period (CT) and post injection of CFA were performed by a one or two-factor analysis of variance – repeated measures (ANOVA-RM), and when appropriate a *post hoc* analysis was carried out using the Bonferroni test. The level of significance was set as at 5%. The results were expressed as mean ± standard error of the mean (SEM). All measures were averaged per recording days, except control period that were represented by the average of total recording sessions within this period (see details above).

Our present results show that all animals developed mechanical allodynia as indicated by the significant decrease in the mechanical force needed to evoke paw withdrawal to Von Frey filaments stimulation in the hindpaw ipsilateral to the CFA injection (ANOVA-RM; $F_{(6,30)}$=49.82, P<0.0001) (Fig. 1B). As shown in Fig. 1C the induction of chronic pain cause a significant impairment of the performance level in respect to control period (ANOVA-RM; $F_{(6,30)}$=23.93, P<0.0001). *Post hoc* analysis revealed a significant decrease during the recording sessions of day 4 and 5 (P<0.001) after CFA injection (Bonferroni test). Additionally, a decrease in the running velocity was observed after injection (ANOVA-RM; $F_{(6,30)}$=8.71, P<0.0001), returning to baseline levels in later recording days (Bonferroni; day 4 , P<0.001; 5, 6, and 7, P<0.01) (Fig. 1D).

An essential issue of delayed alternation tasks of working memory is the temporal gap between responses, where the animal should maintain a retrospective memory of the previous response in order to planning a future response. The data shows that after CFA injection, the animals spent more time navigating in the delay-zone of the testing environment (Fig. 1E). Analysis of variance revealed significant statistical differences across recording days (ANOVA-RM; $F_{(6,30)}$=7.26, P<0.0001). An additional *post hoc* analysis demonstrated an increase of the mean time of navigation in the delay-zone during the recording sessions of day 4 after injection (Bonferroni, P<0.01). Another import measure was the mean interval that mediates two consecutive correct alternations (or trials), giving us an idea of the level of improvement in the performance of the animals (Fig. 1F). Analysis of variance revealed a significant effect across recording days ($F_{(6,30)}$=4.47, P=0.0024), that was particularly increased during day 4 (Bonferroni, P<0.01).

Fig. 2 illustrates the mPFC and MD thalamus LFPs power spectral across recording days during the execution of the spatial WM task. Data were calculated separately for the three navigation zones as described previously. In the case of mPFC, significant differences were encountered across frequency bands (ANOVA-RM; reward-zone: $F_{(4,150)}$=320.10, *P*<0.0001; delay-zone: $F_{(4,150)}$=419.60, *P*<0.0001; choice-zone: $F_{(4,150)}$=146.00, *P*<0.0001), recording sessions but only for reward-zone ($F_{(6,150)}$=5.25, *P*<0.0001), as well an interaction factor effect (frequency x time; reward-zone: $F_{(24,150)}$=7.62, *P*<0.0001; delay-zone: $F_{(24,150)}$=6.99, *P*<0.0001; choice-zone: $F_{(24,150)}$=9.47, *P*<0.0001) (Fig. 2C). An additional *post hoc* analysis revealed an increase of PSD of *delta* (days 11, *P*<0.05; and 16, *P*<0.001) and *theta* (day 16, *P*<0.001) frequency bands for reward- zone; a decrease for *theta* band (days 4, 5, and 11, *P*<0.001) and an increase for *alpha* band (day 11, *P*<0.01) for delay-zone; and an increase across *theta* band for choice-zone (day 5, *P*<0.01; and *P*<0.001 for the remaining days). In the case of MD thalamus, significant differences were encountered across frequency bands (ANOVA-RM; reward-zone: $F_{(4,150)}$=247.20, *P*<0.0001; delay-zone: $F_{(4,150)}$=265.10, *P*<0.0001; choice-zone: $F_{(4,150)}$=57.27, *P*<0.0001), recording sessions for reward and choice-zones ($F_{(6,150)}$=2.32, *P*=0.0361; and $F_{(6,150)}$=2.64, *P*=0.0184; respectively); as well an interaction factor effect (frequency bands x time; reward-zone: $F_{(24,150)}$=5.86, *P*<0.0001; delay-zone: $F_{(24,150)}$=9.13, *P*<0.0001; and choice-zone: $F_{(24,150)}$=3.39, *P*<0.0001) (Fig. 2D). *Post hoc* analysis revealed an increase of *theta* band power for reward-zone (day 6, *P*<0.05; day 7, *P*<0.001; day 11, *P*<0.05; and day 16, *P*<0.001); a decrease for *theta* (day 4, *P*<0.001; day 5, *P*<0.001; and day 11, *P*<0.001) and an increase for *alpha* band (day 11, *P*<0.05) for delay-zone; and an increase across day 5 (*P*<0.001) and a decrease across day 11 (*P*<0.05) for *theta* band during the navigation across choice-zone after CFA injection.

Coherence activity of simultaneously mPFC-MD LFPs recorded channels were illustrated in Fig. 3A. Statistical differences were observed across frequency bands (ANOVA-RM; reward-zone: $F_{(4,150)}$=5.83, *P*=0.0019; delay-zone: $F_{(4,150)}$=13.54, *P*<0.0001; choice-zone: $F_{(4,150)}$=19.46, *P*<0.0001) and recording days (reward-zone: $F_{(6,150)}$=15.71, *P*<0.0001; delay-zone: $F_{(6,150)}$=9.33, *P*<0.0001; choice-zone: $F_{(6,150)}$=2.50, *P*=0.0246); however no interaction factor effect was found (frequency bands x time, reward-zone: $F_{(24,150)}$=1.44, *P*=0.0978; delay-zone: $F_{(24,150)}$=0.97; *P*=0.5122; choice-zone: $F_{(24,150)}$=0.49, *P*=0.9793). In addition, in comparison to control period *post hoc* analysis revealed an

increase of coherence activity for *delta* frequency band during day 7 post-injection (reward and delay-zones; Bonferroni, $P<0.01$); and a decrease for *alpha* and *beta* bands across days 11 (both bands, $P<0.05$) and 16 ($P<0.01$ and $P<0.001$, respectively) for reward-zone (Fig. 3B).

The changes of mPFC-MD circuit information flow during the execution of the spatial WM task were determined by PDC analysis (Fig. 3 C-D). In the case of MD-to-mPFC direction, statistical differences were observed across frequency bands (ANOVA-RM; reward-zone: $F_{(4,150)}=4.34$, $P=0.0084$; delay-zone: $F_{(4,150)}=6.15$, $P=0.0014$; choice-zone: $F_{(4,150)}=36.61$, $P<0.0001$), recordings days (reward-zone: $F_{(6,150)}=141.50$, $P<0.0001$; delay-zone: $F_{(6,150)}=47.66$, $P<0.0001$; choice-zone: $F_{(6,150)}=162.6$, $P<0.0001$), as well an interaction factor effect (frequency bands x time; reward-zone: $F_{(24,150)}=1.71$, $P=0.0283$; delay-zone: $F_{(24,150)}=1.91$, $P=0.0105$; choice-zone: $F_{(24,150)}=7.14$, $P<0.0001$). *Post hoc* analysis revealed that PDC level after CFA injection decreased in respect to control period in all considered frequency bands for reward-zone (Bonferroni, $P<0.001$, and $P<0.01$ for *beta* band at day 11); for delay-zone (from *theta* to *gamma* band across all recorded days, and for *delta* band across days 6 and 7; $P<0.001$); and for choice-zone (all bands, $P<0.001$) (Fig. 3E).

In the case of mPFC-to-MD direction, statistical differences were observed across frequency bands (ANOVA-RM; reward-zone: $F_{(4,150)}=9.29$, $P<0.0001$; delay-zone: $F_{(4,150)}=66.66$, $P<0.0001$; choice-zone: $F_{(4,150)}=134.60$, $P<0.0001$), recording days (reward-zone: $F_{(6,150)}=22.71$, $P<0.0001$; delay-zone: $F_{(6,150)}=10.37$, $P<0.0001$; choice-zone: $F_{(6,150)}=29.21$, $P<0.0001$), as well an interaction factor effect (frequency bands x time; reward-zone: $F_{(24,150)}=2.15$, $P=0.0030$; delay-zone: $F_{(24,150)}=8.33$, $P<0.0001$; choice-zone: $F_{(24,150)}=6.42$, $P<0.0001$). In addition, *post hoc* analysis revealed that PDC level in the case of reward-zone after CFA injection increased in *alpha* band at day 4 post-injection (Bonferroni, $P<0.01$), and decreased in all considered frequency bands during 16 (*delta*: $P<0.01$, *theta*: $P<0.05$, *alpha*: $P<0.01$, *beta*: $P<0.01$, and *gamma*: $P<0.05$). In what concerns to delay-zone significant differences were observed across *theta* and *alpha* bands with a decrease of the PDC level in respect to control period. For choice-zone, PDC level decrease for alpha, beta, and gamma bands across all recording session; for delta band only across day 4; and for theta only during day 11 and 16 after injection (Fig.

3F). Taking together these data, after lesion the obtained the PDC levels indicate that less information were transmitted in mPFC-MD circuit during WM task execution.

In this study we report how the induction of chronic pain affects the patterns of mPFC-MD activity by examining the LFPs activity while rats performed a spatial alternation WM task. The behavioral task used in the present study is a classical spatial WM task, where the animals should remember the spatial location of a reward. Our behavioral data showed a clear impairment of spatial memory performance in the rats after the induction of the inflammatory chronic pain model. These results are in accordance with clinical studies of chronic pain patients have WM impairment [26, 27], and recent reports using models of neuropathic pain that have suggested a spatial memory reduction after nerve lesion [15, 24, 37]. Recently, we have also reported an instability of spatial properties of the dorsal hippocampal CA1 place cells after the onset of a neuropathic pain condition [6], which may disturb the mnemonic process that rely on the integration and consolidation of spatial reference memory.

Our data showed that spectral oscillatory mPFC and MD LFPs activity changed after induction of the chronic pain condition. The most relevant finding of the present study is that the onset of chronic pain condition caused a global decrease in mPFC-MD flow of information as measured by partial directed coherence – PDC [2, 38]. This decrease is observed in both directions of the circuit, and is more evident from MD-to-mPFC direction in a wide frequency range. On the other hand, from mPFC-to-MD direction, the amount of information flow changed differently across frequency bands and maze navigation zones. For instance, across delay-zone the main decrease of the PDC level was observed across *theta* (4-9 Hz) and *alpha* (9-15 Hz) frequency bands, and remains unchanged across other bands. In contrast, across choice-zone data illustrate a strong *theta*-range that is not affected during the onset of chronic pain condition. In this zone, the principal reduction of information flow occurs in faster frequency ranges. The use of PDC analyses is growing in literature [39, 60]; it has been validated in real neurophysiological data [12, 16, 56-59] as well as in several theoretical studies using simulated data [2, 38, 40, 41, 49], to demonstrate expected changes in brain networks that other less complex methods had failed to identify.

What concerns to LFPs spectral power, we found that mPFC and MD shared similar patterns. In both cases, a strong *theta*-range component was present during

execution of the behavioral task which oscillates across pain condition onset, being particularly visible during the navigation in delay and choice zones. In addition, the mPFC-MD LFPs showed higher levels of coherence that are partially conserved across the frequency range studied (1-50 Hz) after chronic pain condition induction. An intensification of *theta*-range coherence across frontal brain regions has been described during the execution of WM tasks using human EEG recordings [32], and across hippocampal formation [50]. These *theta* rhythms are believed to be responsive to orchestrate spatial memory process. Moreover, the robust hippocampal theta frequency band coordination has been reported to be responsive for phase firing patterns of mPFC neurons [17, 21, 45, 47], that were greatest when the demand for spatial WM increases.

It has been previously reported that alterations to functional connectivity of mPFC-MD-hippocampal circuit can translate implications in memory processing [13, 29, 30, 55]. More recently, this circuit has been referred to have an important key role in pain-modulatory process [4, 8, 10, 20, 42, 43]; and that morphological and functional changes can be in the basis for cognitive impairments under chronic pain conditions [23, 28, 37]. At the network level, mPFC and dorsal hippocampal shared connections throughout the MD thalamus, and this pathway is mainly involved in spatial reference memory processing. However, studies on the supraspinal projection of the spinothalamic pathways suggest that the MD thalamus is a relay in medial pain system and plays an important role in the affective and motivational aspects of pain processing [25]. It has been report that the neurons of MD respond to noxious stimulation [11], increasing the level of c-Fos expression [34, 51]; and the stimulation of MD region evokes unit and field responses in the ACC [14], that are particularly involved in nociceptive information processing. By this way, beyond the important role in the mPFC and hippocampal interconnection for spatial reference memory integration, the MD thalamus also plays in parallel an important role in the integration of nociceptive information. More importantly, the main disturbances in the information balance occurs in the way from MD-to-mPFC, suggesting the idea that the information that reaches the mPFC from MD present a different quality than in the absence of pain or are integrated deficiently by the mPFC. On the other hand, is important to note that in the way from mPFC-to-MD less changes in PDC level were observed, and that surprisingly they are

more prominent at slow frequencies for delay zone were animal should conserve the spatial location of the reward; and at fast frequencies for choice zone.

In summary, we can hypothesize that disturbances in the mPFC-MD network during the working memory demand can be a reflex of different quality or deficiently integration of the spatial reference information, probably due to the parallel nociceptive information processing.

Conflict of interest

The authors do not have any conflicts of interest.

Acknowledgments

This work was supported by grants from the Portuguese Foundation for Science and Technology – FCT: PhD grant SFRH/42500/2007; Project PTDC/SAU-NEU/100773/2008; and BIAL Foundation: BIAL Project 126/08.

FIGURES AND LEGENDS

FIGURE 1. Apparatus and behavioral performance.

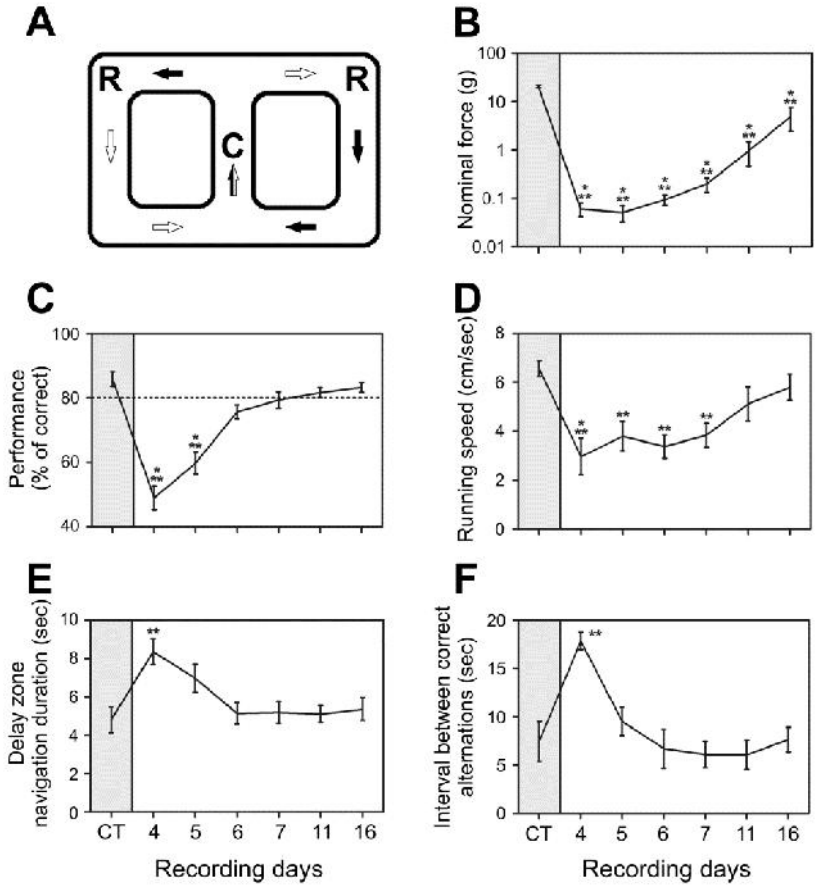

(A) Figure-eight maze, spatial alternation WM task. Starting from the center of the maze (C), the animal had to alternately visit two reward sites (R) (feeder A and B) to obtain chocolate-flavored pellets. The animal was required to come back to the center from a given reward site before visiting the other reward site. The arrows indicate the direction of travel when going to the left and right goals. **(B)** Level of sensibility to mechanical stimulation evaluated using von Frey filaments. A large decrease was observed in the threshold required to induce a paw response after CFA injection. **(C)** Recording period performance for the spatial WM task. A significant decrease in performance level and running velocity **(D)** was observed after CFA injection. **(E)** The animals spent more time navigating in the delay-zone of the behavioral test after CFA injection, and **(F)** also increased their mean interval between correct alternations. Values are means ± SEM. Comparisons between control (CT) and after surgery recording sessions based on one-factor ANOVA repeated measures, followed by Bonferroni *post hoc* test. ***P*<0.01, and ****P*<0.001.

FIGURE 2. Spectral properties.

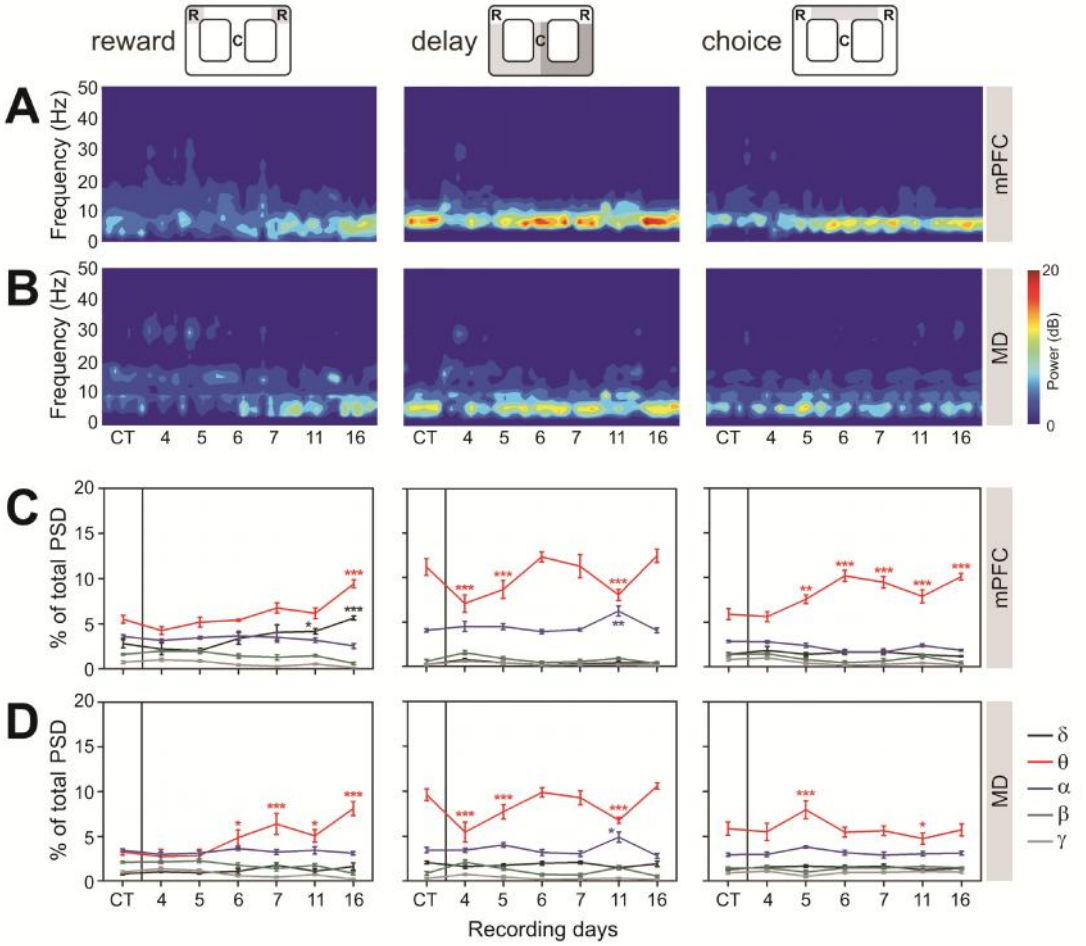

Power spectral density (PSD) of LFPs normalized by the percentage of total power within the frequency range analyzed (1-50 Hz) for mPFC **(A)** and MD **(B)** LFPs signals, comparing the control period (CT) and after CFA injection. Data were presented individually across the three considered navigation zones of the behavioral task. The inspection of PSD revealed a strong *theta*-range component that was present during execution of the behavioral task, which oscillates across pain condition onset. In terms of frequency bands, after CFA injection significant differences were encountered, namely across *delta*, *theta* and *alpha* bands for mPFC **(C)** and MD thalamus **(D)**. Values are expressed for all animals as mean (±SEM). Comparisons between control (CT) and after surgery recording sessions based on two-factors ANOVA repeated measures (frequency bands x recording days), followed by Bonferroni *post hoc* test. **P*<0.05, ***P*<0.01, and ****P*<0.001.

FIGURE 3. Spectral coherence and PDC of simultaneously mPFC and MD LFPs signals.

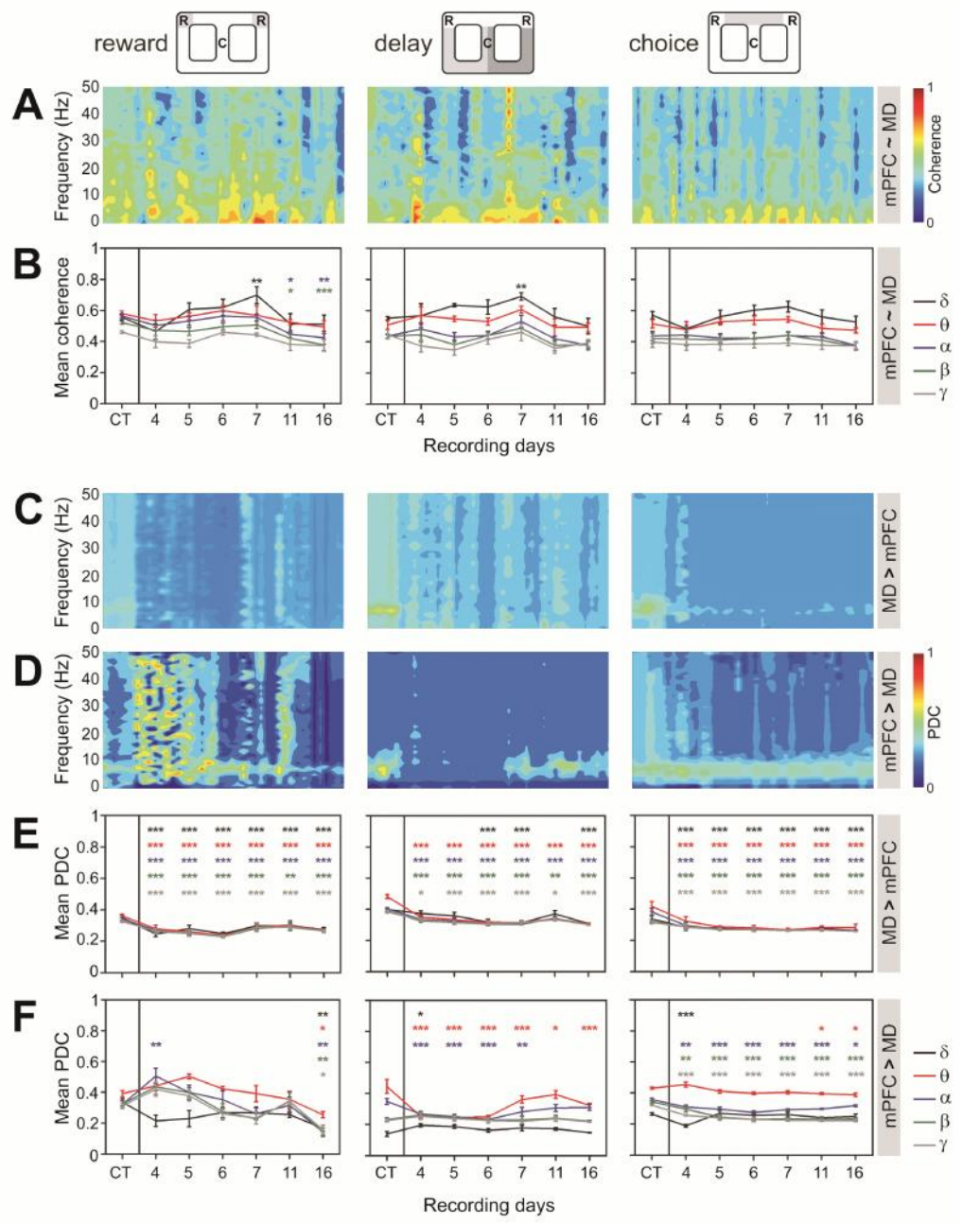

Data were presented individually across the three considered navigation zones of the behavioral task. The mPFC-MD LFPs showed higher levels of coherence activity during considered navigation zones **(A)**, which are partially conserved across frequency bands **(B)**. The oscillations of information flow between the two recorded regions were determined by partial directed coherence (PDC) analysis. Panel **(C)** shows the PDC level from MD-to-mPFC, and panel **(D)** from mPFC-to-MD. A global decrease of the information flow was observed after the induction of the inflammatory pain model. The main disturbances across frequency bands occurs in the way from MD-to-mPFC **(E)**, and from mPFC-to-MD less changes in PDC level were observed **(F)**. Comparisons between control (CT) and after surgery recording sessions based on two-factors ANOVA repeated measures (frequency bands x recording days), followed by Bonferroni *post hoc* test. **P*<0.05, ***P*<0.01, and ****P*<0.001.

REFERENCES

[1] P. Aguiar, L. Mendonça, V. Galhardo, OpenControl: A free opensource software for video tracking and automated control of behavioral mazes, Journal of Neuroscience Methods 166 (2007) 66-72.

[2] L.A. Baccala, K. Sameshima, Partial directed coherence: a new concept in neural structure determination, Biological Cybernetics 84 (2001) 463-474.

[3] E.H. Baeg, Y.B. Kim, K. Huh, I. Mook-Jung, H.T. Kim, M.W. Jung, Dynamics of population code for working memory in the prefrontal cortex., Neuron 40 (2003) 177-188.

[4] M.N. Baliki, P.Y. Geha, A.V. Apkarian, D.R. Chialvo, Beyond feeling: chronic pain hurts the brain, disrupting the default-mode network dynamics, The Journal of Neuroscience 28 (2008) 1398-1403.

[5] S.H. Butler, F. Godefroy, J.M. Besson, J. Weil-Fugazza, A limited arthritic model for chronic pain studies in the rat, Pain 48 (1992) 73-81.

[6] H. Cardoso-Cruz, D. Lima, V. Galhardo, Instability of spatial encoding by CA1 hippocampal place cells after peripheral nerve injury, Eur J Neurosci (2011).

[7] H. Cardoso-Cruz, K. Sameshima, D. Lima, V. Galhardo, Dynamics of circadian thalamocortical flow of information during a peripheral neuropathic pain condition. *Front. Integr. Neurosci.*, 2011.

[8] S.C. Chai, J.C. Kung, B.C. Shyu, Roles of the anterior cingulate cortex and medial thalamus in short-term and long-term aversive information processing., Mol Pain 6 (2010) 42.

[9] S.R. Chaplan, F.W. Bach, J.W. Pogrel, J.M. Chung, T.L. Yaksh, Quantitative assessment of tactile allodynia in the rat paw, Journal of Neuroscience Methods 53 (1994) 55-63.

[10] L. Devoize, P. Alvarez, L. Monconduit, R. Dallel, Representation of dynamic mechanical allodynia in the ventral medial prefrontal cortex of trigeminal neuropathic rats., Eur J Pain (2011).

[11] J.O. Dostrovsky, G. Guilbaud, Nociceptive responses in medial thalamus of the normal and arthritic rat., Pain 40 (1990) 93-104.

[12] E.E. Fanselow, K. Sameshima, L.A. Baccala, M.A. Nicolelis, Thalamic bursting in rats during different awake behavioral states., Proc. Natl. Acad. Sci. U. S. A. 98 (2001) 15330-15335.

[13] S.B. Floresco, J.K. Seamans, A.G. Phillips, Selective roles for hippocampal, prefrontal cortical, and ventral striatal circuits in radial-arm maze tasks with or without a delay., J Neurosci 17 (1997) 1880-1890.

[14] M.M. Hsu, B.C. Shyu, Electrophysiological study of the connection between medial thalamus and anterior cingulate cortex in the rat, NeuroReport 8 (1997) 2701-2707.

[15] Y. Hu, J. Yang, Y. Wang, W. Li, Amitriptyline rather than lornoxicam ameliorates neuropathic pain-induced deficits in abilities of spatial learning and memory., Eur J Anaesthesiol 27 (2010) 162-168.

[16] J. Huang, J. Chang, D. Woodward, L. Baccalá, J. Han, J. Wang, F. Luo, Dynamic neuronal responses in cortical and thalamic areas during different phases of formalin test in rats., Exp. Neurol. 200 (2006) 124-134.

[17] J.M. Hyman, E.A. Zilli, A.M. Paley, M.E. Hasselmo, Medial prefrontal cortex cells show dynamic modulation with the hippocampal theta rhythm dependent on behavior., Hippocampus 15 (2005) 739-749.

[18] A. Isseroff, H.E. Rosvold, T.W. Galkin, P.S. Goldman-Rakic, Spatial memory impairments following damage to the mediodorsal nucleus of the thalamus in rhesus monkeys., Brain Res 232 (1982) 97-113.

[19] D. Ji, M.A. Wilson, Coordinated memory replay in the visual cortex and hippocampus during sleep., Nat Neurosci 10 (2007) 100-107.

[20] G. Ji, H. Sun, Y. Fu, Z. Li, M. Pais-Vieira, V. Galhardo, V. Neugebauer, Cognitive impairment in pain through amygdala-driven prefrontal cortical deactivation, J Neurosci 30 (2010) 5451-5464.

[21] M.W. Jones, M.A. Wilson, Theta rhythms coordinate hippocampal-prefrontal interactions in a spatial memory task., PLoS Biol 3 (2005) e402.

[22] M.W. Jung, Y. Qin, B.L. McNaughton, C.A. Barnes, Firing characteristics of deep layer neurons in prefrontal cortex in rats performing spatial working memory tasks., Cereb Cortex 8 (1998) 437-450.

[23] D. Kodama, H. Ono, M. Tanabe, Altered hippocampal long-term potentiation after peripheral nerve injury in mice., Eur J Pharmacol 574 (2007) 127-132.

[24] H. Leite-Almeida, L. Almeida-Torres, A.R. Mesquita, A. Pertovaara, N. Sousa, J.J. Cerqueira, A. Almeida, The impact of age on emotional and cognitive behaviours triggered by experimental neuropathy in rats, Pain 144 (2009) 57-65.

[25] D. Lima, Ascending Pathways: Anatomy and Physiology. In: A. Basbaum, M.C. Bushnell (Eds.), The Science of Pain, Academic Press, New York, 2008, pp. 477-526.

[26] J. Ling, C. Campbell, T.M. Heffernan, C.G. Greenough, Short-term prospective memory deficits in chronic back pain patients., Psychosom Med 69 (2007) 144-148.

[27] R. Luerding, T. Weigand, U. Bogdahn, T. Schmidt-Wilcke, Working memory performance is correlated with local brain morphology in the medial frontal and anterior cingulate cortex in fibromyalgia patients: structural correlates of pain-cognition interaction., Brain 131 (2008) 3222-3231.

[28] A.E. Metz, H.J. Yau, M.V. Centeno, A.V. Apkarian, M. Martina, Morphological and functional reorganization of rat medial prefrontal cortex in neuropathic pain, Proc.Natl.Acad.Sci.U.S.A 106 (2009) 2423-2428.

[29] A.S. Mitchell, P.G. Browning, C.R. Wilson, M.G. Baxter, D. Gaffan, Dissociable roles for cortical and subcortical structures in memory retrieval and acquisition., J Neurosci 28 (2008) 8387-8396.

[30] A.S. Mitchell, J.C. Dalrymple-Alford, Dissociable memory effects after medial thalamus lesions in the rat., Eur J Neurosci 22 (2005) 973-985.

[31] E. Moser, M.B. Moser, P. Andersen, Spatial learning impairment parallels the magnitude of dorsal hippocampal lesions, but is hardly present following ventral lesions, The Journal of Neuroscience 13 (1993) 3916-3925.

[32] J. Onton, A. Delorme, S. Makeig, Frontal midline EEG dynamics during working memory., Neuroimage 27 (2005) 341-356.

[33] G. Paxinos, C. Watson, The Rat Brain in Stereotaxic Coordinates, Vol. 4th, Academic Press, San Diego, 1998.

[34] D.D. Pearse, G. Bushell, J.D. Leah, Jun, Fos and Krox in the thalamus after C-fiber stimulation: coincident-input-dependent expression, expression across somatotopic boundaries, and nucleolar translocation., Neuroscience 107 (2001) 143-159.

[35] G. Rainer, S.C. Rao, E.K. Miller, Prospective coding for objects in primate prefrontal cortex., J Neurosci 19 (1999) 5493-5505.

[36] P. Rainville, G.H. Duncan, D.D. Price, B. Carrier, M.C. Bushnell, Pain affect encoded in human anterior cingulate but not somatosensory cortex., Science 277 (1997) 968-971.

[37] W.J. Ren, Y. Liu, L.J. Zhou, W. Li, Y. Zhong, R.P. Pang, W.J. Xin, X.H. Wei, J. Wang, H.Q. Zhu, C.Y. Wu, Z.H. Qin, G. Liu, X.G. Liu, Peripheral Nerve Injury Leads to Working Memory Deficits and Dysfunction of the Hippocampus by Upregulation of TNF-α in Rodents., Neuropsychopharmacology (2011).

[38] K. Sameshima, L. Baccalá, Using partial directed coherence to describe neuronal ensemble interactions., J. Neurosci. Methods 94 (1999) 93-103.

[39] J.R. Sato, D.Y. Takahashi, S.M. Arcuri, K. Sameshima, P.A. Morettin, L.A. Baccalá, Frequency domain connectivity identification: an application of partial directed coherence in fMRI., Hum. Brain Mapp. 30 (2009) 452-461.

[40] B. Schelter, M. Winterhalder, M. Eichler, M. Peifer, B. Hellwig, B. Guschlbauer, C.H. Lücking, R. Dahlhaus, J. Timmer, Testing for directed influences among neural signals using partial directed coherence., J. Neurosci. Methods 152 (2006) 210-219.

[41] B. Schelter, M. Winterhalder, B. Hellwig, B. Guschlbauer, C.H. Lücking, J. Timmer, Direct or indirect? Graphical models for neural oscillators., J. Physiol. Paris 99 (2006) 37-46.

[42] F. Seifert, K. Bschorer, R. De Col, J. Filitz, E. Peltz, W. Koppert, C. Maihöfner, Medial prefrontal cortex activity is predictive for hyperalgesia and pharmacological antihyperalgesia., J Neurosci 29 (2009) 6167-6175.

[43] F. Seifert, C. Maihofner, Central mechanisms of experimental and chronic neuropathic pain: findings from functional imaging studies, Cell Mol.Life Sci. 66 (2009) 375-390.

[44] B.C. Shyu, R.W. Sikes, L.J. Vogt, B.A. Vogt, Nociceptive processing by anterior cingulate pyramidal neurons., J Neurophysiol 103 (2010) 3287-3301.

[45] A.G. Siapas, E.V. Lubenov, M.A. Wilson, Prefrontal phase locking to hippocampal theta oscillations., Neuron 46 (2005) 141-151.

[46] A. Silva, H. Cardoso-Cruz, F. Silva, V. Galhardo, L. Antunes, Comparison of anesthetic depth indexes based on thalamocortical local field potentials in rats., Anesthesiology 112 (2010) 355-363.
[47] A. Sirota, S. Montgomery, S. Fujisawa, Y. Isomura, M. Zugaro, G. Buzsáki, Entrainment of neocortical neurons and gamma oscillations by the hippocampal theta rhythm., Neuron 60 (2008) 683-697.
[48] C.E. Stern, S.J. Sherman, B.A. Kirchhoff, M.E. Hasselmo, Medial temporal and prefrontal contributions to working memory tasks with novel and familiar stimuli., Hippocampus 11 (2001) 337-346.
[49] D.Y. Takahashi, L.A. Baccala, K. Sameshima, Frequency domain connectivity: an information theoretic perspective., Conf. Proc. IEEE Eng. Med. Biol. Soc. 2010 (2010) 1726-1729.
[50] C.D. Tesche, J. Karhu, Theta oscillations index human hippocampal activation during a working memory task., Proc Natl Acad Sci U S A 97 (2000) 919-924.
[51] R.J. Traub, E. Silva, G.F. Gebhart, A. Solodkin, Noxious colorectal distention induced-c-Fos protein in limbic brain structures in the rat., Neurosci Lett 215 (1996) 165-168.
[52] R.D. Treede, D.R. Kenshalo, Jr., R.H. Gracely, A.K.P. Jones, The cortical representation of pain, Pain 79 (1999) 105-111.
[53] R.P. Vertes, Interactions among the medial prefrontal cortex, hippocampus and midline thalamus in emotional and cognitive processing in the rat., Neuroscience 142 (2006) 1-20.
[54] C.C. Wang, B.C. Shyu, Differential projections from the mediodorsal and centrolateral thalamic nuclei to the frontal cortex in rats., Brain Res 995 (2004) 226-235.
[55] G.W. Wang, J.X. Cai, Disconnection of the hippocampal-prefrontal cortical circuits impairs spatial working memory performance in rats., Behav Brain Res 175 (2006) 329-336.
[56] J. Wang, F. Luo, J. Chang, D. Woodward, J. Han, Parallel pain processing in freely moving rats revealed by distributed neuron recording., Brain Res. 992 (2003) 263-271.
[57] J. Wang, H. Zhang, J. Han, J. Chang, D. Woodward, F. Luo, Differential modulation of nociceptive neural responses in medial and lateral pain pathways by peripheral electrical stimulation: a multichannel recording study., Brain Res. 1014 (2004) 197-208.
[58] J.Y. Wang, H.T. Zhang, J.Y. Chang, D.J. Woodward, L.A. Baccalá, F. Luo, Anticipation of pain enhances the nociceptive transmission and functional connectivity within pain network in rats., Mol. Pain 4 (2008) 34.
[59] M. Winterhalder, B. Schelter, W. Hesse, K. Schwab, L. Leistritz, D. Klan, R. Bauer, J. Timmer, H. Witte, Comparison of linear signal processing techniques to infer directed interactions in multivariate neural systems, Signal Processing 85 (2005) 2137-2160.
[60] M. Winterhalder, B. Schelter, W. Hesse, K. Schwab, L. Leistritz, J. Timmer, H. Witte, Detection of directed information flow in biosignals., Biomed. Tech. (Berl) 51 (2006) 281-287.
[61] M. Zimmermann, Ethical guidelines for investigations of experimental pain in conscious animals, Pain 16 (1983) 109-110.

CONSIDERAÇÕES FINAIS III

CONSIDERAÇÕES FINAIS

A complexidade da dor deve ser compreendida como o resultado da integração de várias dimensões sensoriais, desde a que reflecte os eventos directamente associados a lesões em tecido, até à dor que é gerada na ausência de qualquer "*input*" periférico. O presente trabalho de tese pretendeu elucidar alguns destes aspectos ao nível de circuitos do cérebro afectos à componente sensorial e funções cognitivas, e de que forma estes circuitos podem alterar o seu regime de actividade na experiência da dor.

Tendo em conta as discussões parcelares elaboradas nas cinco publicações incluídas na dissertação, estas considerações finais deter-se-ão em aspectos referentes ao conjunto de resultados, no que respeita (i) ao papel do eixo tálamo-cortical na integração da informação sensorial (***Publicação I e II***), (ii) e ao papel do circuito fronto-hipocampal na interacção da experiência da dor com funções cognitivas associadas à integração da informação (***Publicação III***) ou memória espacial (***Publicação IV e V***).

A INTEGRAÇÃO E PROCESSAMENTO DA INFORMAÇÃO SENSORIAL PELO CIRCUITO TÁLAMO-CORTICAL

A actividade eléctrica é essencial para a comunicação neuronal. Ao longo dos últimos anos, os registos multi-eléctrodo *in vivo* revelaram que a actividade eléctrica de cada neurónio não é independente da actividade dos restantes. Os neurónios tendem a exibir uma actividade de disparo coordenada dentro da rede neuronal onde se encontram inseridos. Esta actividade, quando quantificada nos sinais de electroencefalografia (EEG) ou de potencial de campo local (LFP), resulta em padrões de actividade oscilatórios complexos, os quais reflectem o grau de sincronismo dos potenciais sinápticos na rede local (Lopes da Silva, 1991). A actividade eléctrica cerebral apresenta diferentes padrões de acordo com a actividade comportamental ou com os estados de vigília-sono – descritos primeiro em modelos animais e mais tarde em humanos (ver revisão, Karbowski, 1994) -, mostrando que os mesmos circuitos podem suportar regimes diferentes de actividade. As oscilações tálamo-corticais são exemplo disso, pois para além de serem um indicador clássico das transições dos estados de vigília para sono, desempenham também uma importante função na percepção de

estímulos sensoriais (Jones, 2001; Ribary, 2005). Estudos recentes demonstraram que distúrbios na actividade oscilatória tálamo-cortical estão associados a alterações dos níveis de atenção, processamento de informação sensorial ou memória de experiências sensoriais (Lumer et al., 1997; Ray et al., 2009). No que diz respeito à percepção da dor, um dos modelos mais explorados e que está na base da geração dos processos associados à dor neurogénica, assenta precisamente na existência de uma disritmia tálamo-cortical (DTC) (Llinás et al., 1999; Ribary, 2005).

No entanto, ainda é escasso o universo de estudos que abordam a dinâmica tálamo-cortical durante a dor. Partindo dessa premissa, o primeiro estudo desta dissertação teve por objectivo principal avaliar o efeito da instalação de uma condição de dor crónica neuropática nos diferentes regimes oscilatórios circadianos exibidos pelo circuito tálamo-cortical. A actividade do circuito foi avaliada pela primeira vez através de registos de LFPs de longa duração (com sessões continuas de 24 horas abrangendo um ciclo vigília-sono completo) em animais implantados cronicamente com matrizes de multi-eléctrodos no tálamo lateral e córtex somatosensitivo primário – antes e após o estabelecimento de um modelo de dor neuropática (***Publicação I***).

Ao nível comportamental, a lesão neuropática alterou a frequência dos episódios do estado de vigília e de sono *slow-wave-sleep* (SWS), aumentando de forma significativa o número total de transições entre ambos (***Publicação I***). Os dados obtidos neste estudo vão ao encontro de outras observações obtidas noutros modelos de dor neuropática (Andersen and Tufik, 2003; Kontinen et al., 2003; Monassi et al., 2003; Keay et al., 2004) e inflamatória (Carli et al., 1987; Landis et al., 1989; Andersen and Tufik, 2000), que mostraram igualmente a existência de uma fragmentação dos padrões circadianos e um incremento do tempo alocado aos episódios de alerta.

A análise da Coerência Direccionada Parcial (*partial directed coherence* - PDC) das oscilações tálamo-corticais revelou que, para os animais com neuropatia, a quantidade de informação conduzida bidireccionalmente entre o córtex e o tálamo diminuiu significativamente em todos os estados de vigília-sono, embora a diminuição seja menos expressiva no sentido descendente do circuito, sugerindo a existência de uma redução no grau de conectividade efectiva do circuito (***Publicação I***). É importante referir que esta diminuição ocorre de forma rápida logo após a lesão do nervo e que perdura com a persistência dos sintomas de dor, mas não é acompanhada por alterações ao nível de

outras propriedades espectrais do sinal como, a potência em frequência e coerência quadrática entre ambas as áreas registadas.

Os resultados apresentados na ***Publicação I*** são especialmente importantes porque demonstraram, pela primeira vez, que o córtex somatosensitivo apresenta um papel proeminente sobre a actividade dos neurónios talâmicos durante o processamento de estímulos dolorosos. Esta hipótese é apoiada por estudos recentes que demonstraram que durante a aplicação periférica de estímulos dolorosos existe um aumento significativo da actividade entre o córtex SI e o tálamo ventro-posterior, enquanto na direcção ascendente diminui ou permanece inalterada (Huang et al., 2006; Wang et al., 2007), e por estudos que propõem que a projecção descendente cortico-talâmica possa estar intrinsecamente mais envolvida na amplificação de estímulos nociceptivos, enquanto simultaneamente promove a inibição de outra informação irrelevante, aumentando desta forma a sua capacidade de selecção e detecção de estímulos (Rauschecker, 1997; Suga et al., 1997; Suga et al., 2000). Da mesma forma, os resultados da ***Publicação I*** demonstram que a via descendente, embora diminuída, permanece funcionalmente mais activa que a via ascendente, o que apoia a possibilidade do córtex somatossensitivo estar a exercer um efeito inibitório sobre o tálamo lateral. Este efeito explica em parte a redução do fluxo de informação no circuito e poderá ser o resultado do desmascarar dos mecanismos descendentes de origem cortical, que desencadeiam uma amplificação contínua da informação nociceptiva e promovem em simultâneo uma supressão da informação não-nociceptiva (Llinás et al., 2005; Walton et al., 2010). Esta hipótese é também reforçada por estudos clínicos que indicam existir uma hipoactividade talâmica (Iadarola et al., 1995; Apkarian et al., 2004a; Garcia-Larrea et al., 2006; Sorensen et al., 2008) e uma perturbação da conectividade nativa das redes corticais e subcorticais do cérebro em pacientes com dor crónica (Baliki et al., 2008; Cauda et al., 2009).

No segundo estudo que realizei nesta dissertação, utilizei as mesmas metodologias para observar as modificações que ocorrem no eixo cortico-talâmico durante a perda de consciência induzida por anestésicos, uma vez que este circuito tem sido apontado como fundamental para o suporte instrumental dos mecanismos da consciência (Llinás et al., 1998). A perda de consciência induzida por anestésicos ocorre

pela perturbação da comunicação entre os diversos circuitos do cérebro, através uma redução gradual da sua capacidade de integração de informação (Tononi, 2004; Alkire et al., 2008). O eixo cortico-talâmico é por excelência um circuito envolvido na integração e distribuição de informação para outras regiões (Contreras et al., 1996; Castro-Alamancos, 2004), e alguns investigadores defendem que durante a transição para a inconsciência ocorre uma interrupção da transferência de informação neste circuito (Alkire et al., 2007; Velly et al., 2007; Zhou et al., 2011). Todavia, não se sabe ainda qual das duas regiões é determinante na perda de consciência, nem de que forma a conexão entre ambas as regiões é afectada pelos anestésicos (Detsch et al., 2002; Hentschke et al., 2005; Schneider and Kochs, 2007; Tu et al., 2011).

Assim, no segundo trabalho que apresento nesta dissertação, tive como objectivo principal avaliar a dinâmica da actividade no circuito TC em função de diferentes concentrações de um anestésico volátil; e aplicar essa actividade eléctrica para comparar a performance de índices de monitorização da profundidade da anestesia (***Publicação II***).

A actividade do circuito foi avaliada através de registos de LFPs em animais implantados cronicamente com matrizes de multi-eléctrodos ao nível do tálamo lateral e córtex somatosensitivo primário, ao longo de diferentes concentrações do anestésico volátil isoflurano. Os resultados demonstraram que para este anestésico o índice de BS "*burst suppression*" com correcção por permutação entrópica (PE) apresentou a melhor performance na avaliação da correlação entre a concentração e a profundidade da anestesia, apresentando-se como uma alternativa promissora a outros índices comerciais (***Publicação II***). É importante referir que um dos problemas dos índices de monitorização da profundidade da anestesia reside no facto de poderem apresentar diferentes performances, e que essa diferença é mais expressiva durante a aplicação de veículos voláteis (Schneider and Kochs, 2007). Por outro lado, o sinal de EEG que está na base da construção dos diversos índices anestésicos habitualmente utilizados, apresenta também algumas desvantagens: em primeiro lugar, possui pouca especificidade espacial uma vez que o sinal obtido provém da sobreposição de actividade de grandes porções do cérebro (Legatt et al., 1980), e em segundo lugar é um sinal muito atenuado, o que leva a que as frequências superiores a 30 Hz tenham pouca potência e são muito vulneráveis a interferências causadas pelo potencial electromiográfico (Sleigh et al.,

2001). As fontes de sinal intracraniano, como os LFPs, apresentam uma melhor razão sinal/ruído e possibilitam a preservação de frequências mais rápidas na banda *gamma* (superior a 30 Hz), o que nos permitiu realizar neste estudo uma análise mais detalhada dos padrões oscilatórios associados à indução de anestesia, que foi um parâmetro crucial para o ajuste dos índices de monitorização da profundidade anestésica.

Dados de análises realizadas posteriormente à publicações destes resultados, utilizando a técnica PDC de análise espectral já acima referida, mostraram existir um desequilíbrio na conectividade do circuito cortico-talâmico que se traduz numa redução do fluxo de informação nas frequências mais lentas (*delta, theta e gamma*) e um aumento nas bandas de frequência *alpha* e *gamma*-alta (50-100 Hz) dependente da concentração de anestésico (Cardoso-Cruz *et al*., em preparação). Em conjunto, estas observações sugerem que os neurónios de ambas as regiões mantêm uma conectividade funcional mesmo durante a anestesia, o que suporta a ideia da existência de um "diálogo cortico-talâmico" contínuo e que a perda de consciência não passa necessariamente pela inactivação das populações de neurónios deste eixo sensorial (Alkire et al., 2008).

A INFORMAÇÃO E MEMÓRIA ESPACIAL DURANTE A DOR CRÓNICA

No terceiro estudo que apresento nesta dissertação, analisei as propriedades de codificação da informação espacial pelos neurónios piramidais da área dorsal da região CA1 do hipocampo (***Publicação III***), também denominados por *place cells*. Este tipo de neurónios tem um papel crucial na integração e actualização da informação espacial. No entanto, este tipo de informação é apenas uma das várias características armazenadas e processadas nessa rede hipocampal (Eichenbaum et al., 1999; Leutgeb et al., 2005). Por esta razão é especialmente relevante determinar quais os factores, incluindo a dor, que poderão contribuir para a perturbação da estabilidade funcional da actividade destes neurónios.

Os nossos dados mostraram que a actividade das *place cells* – medida pela frequência de potenciais de acção - permaneceram estáveis após a lesão periférica do nervo. Em contraste o índice de especificidade/informação de Skaggs (1993), uma medida de avaliação da actividade espacial de disparo que não requer que uma região específica seja definida como campo espacial, revelou uma diminuição significativa no

grupo de animais com neuropatia, indicando que a actividade dos neurónios deste grupo experimental codifica menos informação sobre a localização espacial após a instalação da condição de dor (***Publicação III***). No que diz respeito à codificação de campos espaciais o seu número aumentou após a lesão, passando em média a ser codificados dois campos por neurónio, o que leva a que a estimulação dolorosa tenha um efeito semelhante à exposição de animais a arenas não familiares (Renaudineau et al., 2009; Korotkova et al., 2010). Em paralelo, os nossos dados revelaram ainda que o acréscimo do número de campos espaciais é acompanhado por um aumento do seu tamanho individual e respectiva coerência de disparo a nível interno. É também importante referir que o segundo campo codificado ocupa uma localização não adjacente ao primário, o que descarta a possibilidade de esse resultar de uma expansão do primário, sugerindo que o re-mapeamento induzido pela dor e a expansão de campo são fenómenos diferentes (Mehta et al., 1997; 2000). Da literatura, é conhecido que o fenómeno de expansão dos campos espaciais hipocampais não é influenciado por flutuações hormonais (Tropp et al., 2005), mas é potenciado por condições de stress (Kim et al., 2007) e está reduzido em animais de idade avançada (Barnes et al., 1997; Shen et al., 1997; Sava and Markus, 2008). A evolução da experiência adquirida durante o processo de habituação/exposição do animal também é fundamental para a ocorrência desse re-mapeamento numa fase inicial, estabilizando numa fase posterior (Kobayashi et al., 1997; Kentros et al., 1998; Ainge et al., 2007; Korotkova et al., 2010). Por último, esse re-mapeamento pode também ser reflexo de interferências entre experiências concorrentes (Colgin et al., 2008), o que explica em parte o facto da condição de dor poder perturbar os mecanismos cognitivos de referência espacial (Seminowicz and Davis, 2007; Moriarty et al., 2011), alterando os processos de atenção que são cruciais na aprendizagem e memória (Boyette-Davis et al., 2008; Pais-Vieira et al., 2009).

Em resumo, os nossos dados demonstraram que os mecanismos hipocampais responsáveis pela integração e processamento da informação de referência espacial são perturbados pela instalação da condição de dor crónica.

Na tarefa comportamental de alternação simples em ambiente familiar que foi utilizada na ***Publicação III***, os animais apresentaram apenas uma pequena redução

temporária nos dias subsequentes à cirurgia de indução do modelo de dor, sendo que este efeito foi partilhado por ambos os grupos experimentais. Estes resultados vão ao encontro de dados publicados em outros estudos com modelos de dor crónica, nos quais é demonstrado que não existem alterações na performance de tarefas espaciais simples ou em tarefas não espaciais de memória (LaBuda and Fuchs, 2000; Apkarian et al., 2004b; Leite-Almeida et al., 2009), encontrando-se apenas défices comportamentais em tarefas mais complexas que envolvam manutenção prolongada de memória (Millecamps et al., 2004; Dick and Rashiq, 2007). Com efeito, a queixa de falta de memória é o problema cognitivo mais habitualmente auto-reportado por pacientes com síndromes de dor crónica; no entanto é actualmente reconhecido que isso não constitui uma situação de perda de memória generalizada, mas antes um problema circunscrito aos processos de memória de curto prazo com grau médio de complexidade cognitiva (Park et al., 2001; Buhle and Wager, 2010; Schmidt-Wilcke et al., 2010; Apkarian et al., 2011). As explicações mais habituais para o aparecimento de perturbações de memória são, por um lado, o facto de os pacientes terem muitas vezes regimes medicamentosos prolongados e com drogas de actuação central (Choi et al., 2007), e por outro lado a possibilidade de que os episódios súbitos de dor perturbem os mecanismos normais de aprendizagem levando a perdas temporárias de atenção (Dick et al., 2002). No entanto, nenhuma destas hipóteses permite explicar a especificidade de perdas sobre memórias de curto prazo e memórias declarativas retrospectivas, ou o facto de muitas das perturbações cognitivas provocadas por dor crónica se observarem igualmente em modelos animais na ausência de qualquer manipulação farmacológica.

A memória de curto prazo, também denominada por w*orking memory* (WM) ou memória de trabalho, está intrinsecamente correlacionada com a capacidade de performance de um leque muito variado de tarefas cognitivas (Conway et al., 2003). Esta capacidade é vista como um processo contínuo, que pode ser melhorado através do treino repetido e pelas rotinas de adaptativas obtidas na execução da tarefa em causa (Klingberg, 2010). A experiência adquirida com o treino da tarefa está associada a alterações na actividade do cérebro ao nível do córtex frontal, parietal e gânglios da base (Todd and Marois, 2004; McNab and Klingberg, 2008), e também associada a alterações na densidade de receptores de dopamina no córtex pré-frontal (McNab et al., 2009; Söderqvist et al., 2011). A transferência da experiência de treino adquirida numa

tarefa para outras tarefas de WM não treinadas, é consistente com a noção de que essa experiência é importante para o desenvolvimento de fenómenos de plasticidade nos circuitos neuronais de WM (Rainer and Miller, 2000), e que o treino repetido pode funcionar como um método para remediar factores limitativos na capacidade de WM. Partindo das anteriores premissas, no quarto e quinto estudos da presente dissertação, o objectivo principal foi avaliar as alterações na conectividade funcional do circuito fronto-hipocampal, na via que está estreitamente associada à integração da memória de referência espacial, e de que forma o regime de actividade desse circuito é afectado por dor crónica, aplicando um modelo de dor neuropática (***Publicação IV***) e um modelo de dor inflamatória (***Publicação V***).

Ao nível comportamental, os nossos resultados demonstraram que os grupos experimentais expostos à dor exibem uma redução significativa da sua performance na execução da tarefa de memória espacial. Esta redução de performance é mais evidente durante os primeiros dias após a implementação dos modelos de dor (***Publicação IV e V***), sendo que o modelo de dor inflamatória induz uma redução de performance superior ao modelo neuropático (***Publicação V***).

Em termos da actividade básica de disparo no circuito fronto-hipocampal, os neurónios das regiões CA1 dorsal do hipocampo (dCA1) e córtex préfrontal medial (mPFC) apresentam regimes de actividade diferentes após a lesão do nervo, em especial durante a navegação pela zona da tarefa na qual o animal deve reter em memória o percurso efectuado de forma a alcançar a subsequente zona de recompensa, com um aumento da actividade de disparo dos neurónios do mPFC nas alternações correctas, e com uma diminuição para os neurónios da área dCA1 nas alternações incorrectas. É também importante assinalar que após a lesão, os neurónios de ambas as regiões alteraram o seu grau de sincronismo em relação às oscilações *theta* hipocampais, sendo particularmente evidente esse efeito na zona de navegação associada à retenção em memória da resposta precedente (***Publicação IV***). Durante os processos de WM, as oscilações hipocampais em *theta* são conhecidas por estarem associadas a padrões sincronizados em relação aos neurónios préfrontais (Hyman et al., 2005; Jones and Wilson, 2005; Siapas et al., 2005; Sirota et al., 2008), mas também já foram identificados sincronismos *theta* na interacção do hipocampo com outras estruturas, tal como a amígdala durante episódios de ansiedade (Adhikari et al., 2010) ou o estriado durante

episódios de aprendizagem (DeCoteau et al., 2007). Esta preponderância das oscilações *theta* no sincronismo entre múltiplas áreas cerebrais sugere a sua importância como mecanismo primordial pelo qual é transmitida a informação entre hipocampo e essas estruturas.

Estas alterações no sincronismo da actividade dos neurónios foram também acompanhadas por uma redução da conectividade funcional do circuito mPFC-dCA1; essa redução ocorre em particular durante a navegação pela zona de recompensa e de decisão da tarefa, mas não é acompanhada por alterações nas propriedades espectrais da potência e coerência dos sinais das duas regiões. É também importante assinalar que o fluxo de informação no sentido de mPFC para dCA1 está parcialmente conservado na zona de retenção de memória e que de dCA1 para mPFC diminui apenas na banda *theta*. Em termos da natureza dos padrões de informação das respostas correctas e incorrectas, os nossos dados revelaram uma diminuição da actividade em *theta*, *alpha* e *beta* na zona de decisão da localização da recompensa após a lesão do nervo. Curiosamente, essa diminuição não difere consoante o tipo de resposta no caso do sentido de mPFC para dCA1, e está também presente nas respostas incorrectas no caso do sentido de dCA1 para mPFC, que para as respostas correctas apresentou uma diminuição em *theta* e um aumento em *gamma* (***Publicação IV***).

Com o objectivo de aprofundar o detalhe de conhecimento deste circuito, realizei uma série final de experiências em que registei a actividade neuronal em simultâneo no tálamo médio-dorsal (MD) e no mPFC durante a execução da mesma tarefa de memória espacial, mas neste caso antes e após a indução de um modelo de dor inflamatória (***Publicação V***). A nível anatómico, a região mPFC partilha conexões indirectas com a área dorsal da região CA1 do hipocampo através do tálamo MD (Vertes, 2006). O tálamo MD é um dos pontos chave do circuito fronto-hipocampal, projectando para regiões da via medial de processamento da dor, como o córtex cingulado, amígdala e outras áreas préfrontais; e está envolvido nas respostas a estímulos nociceptivos e mecanismos de memória (Markowitsch, 1982; Sikes and Vogt, 1992; Yang et al., 2006; Chai et al., 2010). A lesão desta região provou estar associada a uma redução da performance em tarefas espaciais do tipo *delayed* em primatas (Isseroff et al., 1982), bem como tarefas de condicionamento (Olton and Isaacson, 1967; Smith et al., 2002) e de memória espacial em ratos (Mitchell and Dalrymple-Alford, 2005). De forma análoga

aos dados anteriores (***Publicação IV***), o circuito mPFC-MD apresentou uma redução bidireccional da sua conectividade após a instalação do modelo de dor, acompanhada de uma redução significativa de performance na tarefa de memória espacial (***Publicação V***). É importante referir que essa redução é mais evidente no sentido de MD para mPFC e numa banda mais larga de frequências, o que sugere a hipótese da informação poder estar a chegar ao mPFC com uma qualidade diferente após a condição de dor. No caso do sentido inverso, os dados demonstraram existir uma redução confinada apenas às frequências mais lentas durante o período de navegação associada à retenção de memória, e às frequências mais rápidas durante a navegação na zona de decisão (***Publicação V***). Em conjunto, os dois estudos sugerem a existência de uma perturbação na forma como o circuito fronto-hipocampal processa e distribui a informação durante a execução da tarefa de memória espacial, o que poderá ser reflexo da competição entre experiências cognitivas concorrentes (Munoz and Esteve, 2005; Awh et al., 2006; Moriarty et al., 2011).

Em conclusão, os dados reunidos na dissertação detalham o papel das oscilações tálamo-corticais no processamento da informação sensorial e como o equilíbrio nessas oscilações é afectado durante a integração da informação nociceptiva e durante os processos de redução de consciência. Os resultados obtidos mostram ainda que condições de dor prolongada afectam a estabilidade da codificação da informação que está na base da geração dos mapas cognitivos de referência espacial no hipocampo, e que o regime condução da informação entre o hipocampo e as estruturas préfrontais está perturbado durante os processos mnemónicos associados à integração e consolidação da memória espacial.

REFERÊNCIAS BIBLIOGRÁFICAS

Adhikari A, Topiwala MA, Gordon JA (2010) Synchronized activity between the ventral hippocampus and the medial prefrontal cortex during anxiety. Neuron 65:257-269.

Ainge JA, van der Meer MA, Langston RF, Wood ER (2007) Exploring the role of context-dependent hippocampal activity in spatial alternation behavior. Hippocampus 17:988-1002.

Alkire MT, Hudetz AG, Tononi G (2008) Consciousness and anesthesia. Science 322:876-880.

Alkire MT, McReynolds JR, Hahn EL, Trivedi AN (2007) Thalamic microinjection of nicotine reverses sevoflurane-induced loss of righting reflex in the rat. Anesthesiology 107:264-272.

Andersen ML, Tufik S (2000) Altered sleep and behavioral patterns of arthritic rats. Sleep Res Online 3:161-167.

Andersen ML, Tufik S (2003) Sleep patterns over 21-day period in rats with chronic constriction of sciatic nerve. Brain Research 984:84-92.

Apkarian AV, Hashmi JA, Baliki MN (2011) Pain and the brain: specificity and plasticity of the brain in clinical chronic pain. Pain 152:S49-64.

Apkarian AV, Sosa Y, Sonty S, Levy RM, Harden RN, Parrish TB, Gitelman DR (2004a) Chronic back pain is associated with decreased prefrontal and thalamic gray matter density. J Neurosci 24:10410-10415.

Apkarian AV, Sosa Y, Krauss BR, Thomas PS, Fredrickson BE, Levy RE, Harden RN, Chialvo DR (2004b) Chronic pain patients are impaired on an emotional decision-making task. Pain 108:129-136.

Awh E, Vogel E, Oh S (2006) Interactions between attention and working memory. Neuroscience 139.

Baliki MN, Geha PY, Apkarian AV, Chialvo DR (2008) Beyond feeling: chronic pain hurts the brain, disrupting the default-mode network dynamics. J Neurosci 28:1398-1403.

Barnes CA, Suster MS, Shen JM, McNaughton BL (1997) Multistability of cognitive maps in the hippocampus of old rats. Nature 388:272-275.

Boyette-Davis JA, Thompson CD, Fuchs PN (2008) Alterations in attentional mechanisms in response to acute inflammatory pain and morphine administration. Neuroscience 151:558-563.

Buhle J, Wager TD (2010) Performance-dependent inhibition of pain by an executive working memory task. Pain 149:19-26.

Carli G, Montesano A, Rapezzi S, Paluffi G (1987) Differential-Effects of Persistent Nociceptive Stimulation on Sleep Stages. Behav Brain Res 26:89-98.

Castro-Alamancos M (2004) Dynamics of sensory thalamocortical synaptic networks during information processing states. Prog Neurobiology 74:213-247.

Cauda F, Sacco K, Duca S, Cocito D, D'Agata F, Geminiani GC, Canavero S (2009) Altered resting state in diabetic neuropathic pain. PLoSONE 4:e4542.

Chai SC, Kung JC, Shyu BC (2010) Roles of the anterior cingulate cortex and medial thalamus in short-term and long-term aversive information processing. Mol Pain 6:42.

Choi DS, Choi DY, Whittington RA, Nedeljković SS (2007) Sudden amnesia resulting in pain relief: the relationship between memory and pain. Pain 132:206-210.

Colgin LL, Moser EI, Moser MB (2008) Understanding memory through hippocampal remapping. Trends Neurosci 31:469-477.

Contreras D, Destexhe A, Sejnowski TJ, Steriade M (1996) Control of spatiotemporal coherence of a thalamic oscillation by corticothalamic feedback. Science 274:771-774.

Conway AR, Kane MJ, Engle RW (2003) Working memory capacity and its relation to general intelligence. Trends Cogn Sci 7:547-552.

DeCoteau WE, Thorn C, Gibson DJ, Courtemanche R, Mitra P, Kubota Y, Graybiel AM (2007) Learning-related coordination of striatal and hippocampal theta rhythms during acquisition of a procedural maze task. Proc Natl Acad Sci U S A 104(13):5644-5649.

Detsch O, Kochs E, Siemers M, Bromm B, Vahle-Hinz C (2002) Increased responsiveness of cortical neurons in contrast to thalamic neurons during isoflurane-induced EEG bursts in rats. Neurosci Lett 317:9-12.

Dick B, Eccleston C, Crombez G (2002) Attentional functioning in fibromyalgia, rheumatoid arthritis, and musculoskeletal pain patients. Arthritis Rheum 47:639-644.

Dick BD, Rashiq S (2007) Disruption of attention and working memory traces in individuals with chronic pain. AnesthAnalg 104:1223-1229.

Eichenbaum H, Dudchenko P, Wood E, Shapiro M, Tanila H (1999) The hippocampus, memory, and place cells: Is it spatial memory or a memory space? Neuron 23:209-226.

Garcia-Larrea L, Maarrawi J, Peyron R, Costes N, Mertens P, Magnin M, Laurent B (2006) On the relation between sensory deafferentation, pain and thalamic activity in Wallenberg's syndrome: a PET-scan study before and after motor cortex stimulation. Eur J Pain 10:677-688.

Hentschke H, Schwarz C, Antkowiak B (2005) Neocortex is the major target of sedative concentrations of volatile anaesthetics: strong depression of firing rates and increase of GABAA receptor-mediated inhibition. Eur J Neurosci 21:93-102.

Huang J, Chang J, Woodward D, Baccalá L, Han J, Wang J, Luo F (2006) Dynamic neuronal responses in cortical and thalamic areas during different phases of formalin test in rats. Exp Neurol 200:124-134.

Hyman JM, Zilli EA, Paley AM, Hasselmo ME (2005) Medial prefrontal cortex cells show dynamic modulation with the hippocampal theta rhythm dependent on behavior. Hippocampus 15:739-749.

Iadarola MJ, Max MB, Berman KF, Byas-Smith MG, Coghill RC, Gracely RH, Bennett GJ (1995) Unilateral decrease in thalamic activity observed with positron emission tomography in patients with chronic neuropathic pain. Pain 63:55-64.

Isseroff A, Rosvold HE, Galkin TW, Goldman-Rakic PS (1982) Spatial memory impairments following damage to the mediodorsal nucleus of the thalamus in rhesus monkeys. Brain Res 232:97-113.

Jones E (2001) The thalamic matrix and thalamocortical synchrony. Trends Neurosci 24:595-601.

Jones MW, Wilson MA (2005) Phase precession of medial prefrontal cortical activity relative to the hippocampal theta rhythm. Hippocampus 15:867-873.

Karbowski K (1994) [The heyday of neurology in the 19th century]. Schweiz Rundsch Med Prax 83:457.

Keay KA, Monassi CR, Levison DB, Bandler R (2004) Peripheral nerve injury evokes disabilities and sensory dysfunction in a subpopulation of rats: a closer model to human chronic neuropathic pain? Neurosci Lett 361:188-191.

Kentros C, Hargreaves E, Hawkins RD, Kandel ER, Shapiro M, Muller RV (1998) Abolition of long-term stability of new hippocampal place cell maps by NMDA receptor blockade. Science 280:2121-2126.

Kim J, Lee H, Welday A, Song E, Cho J, Sharp P, Jung M, Blair H (2007) Stress-induced alterations in hippocampal plasticity, place cells, and spatial memory. Proc Natl Acad Sci U S A 104:18297-18302.

Klingberg T (2010) Training and plasticity of working memory. Trends Cogn Sci 14:317-324.

Kobayashi T, Nishijo H, Fukuda M, Bures J, Ono T (1997) Task-dependent representations in rat hippocampal place neurons. J Neurophysiol 78:597-613.

Kontinen VK, Ahnaou A, Drinkenburg WH, Meert TF (2003) Sleep and EEG patterns in the chronic constriction injury model of neuropathic pain. Physiol Behav 78:241-246.

Korotkova T, Fuchs EC, Ponomarenko A, von Engelhardt J, Monyer H (2010) NMDA receptor ablation on parvalbumin-positive interneurons impairs hippocampal synchrony, spatial representations, and working memory. Neuron 68:557-569.

LaBuda CJ, Fuchs PN (2000) A behavioral test paradigm to measure the aversive quality of inflammatory and neuropathic pain in rats. ExpNeurol 163:490-494.

Landis CA, Levine JD, Robinson CR (1989) Decreased Slow-Wave and Paradoxical Sleep in A Rat Chronic Pain Model. Sleep 12:167-177.

Legatt AD, Arezzo J, Vaughan HG (1980) Averaged multiple unit activity as an estimate of phasic changes in local neuronal activity: effects of volume-conducted potentials. J Neurosci Methods 2:203-217.

Leite-Almeida H, Almeida-Torres L, Mesquita AR, Pertovaara A, Sousa N, Cerqueira JJ, Almeida A (2009) The impact of age on emotional and cognitive behaviours triggered by experimental neuropathy in rats. Pain 144:57-65.

Leutgeb S, Letugeb JK, Barnes CA, Moser EI, McNaughton BL, Moser MB (2005) Independent codes for spatial and episodic memory in hippocampal neuronal ensembles. Science 309:619-623.

Llinás R, Ribary U, Contreras D, Pedroarena C (1998) The neuronal basis for consciousness. Philos Trans R Soc Lond B Biol Sci 353:1841-1849.

Llinás R, Ribary U, Jeanmonod D, Kronberg E, Mitra P (1999) Thalamocortical dysrhythmia: A neurological and neuropsychiatric syndrome characterized by magnetoencephalography. Proc Natl Acad Sci U S A 96:15222-15227.

Llinás R, Urbano FJ, Leznik E, Ramírez RR, van Marle HJ (2005) Rhythmic and dysrhythmic thalamocortical dynamics: GABA systems and the edge effect. Trends Neurosci 28:325-333.
Lopes da Silva F (1991) Neural mechanisms underlying brain waves: from neural membranes to networks. Electroencephalogr Clin Neurophysiol 79:81-93.
Lumer E, Edelman G, Tononi G (1997) Neural dynamics in a model of the thalamocortical system. II. The role of neural synchrony tested through perturbations of spike timing. Cereb Cortex 7:228-236.
Markowitsch HJ (1982) Retention performance of a learned delayed-alternation task after chemical lesions of the cats mediodorsal nucleus. Behav Brain Res 4:263-277.
McNab F, Klingberg T (2008) Prefrontal cortex and basal ganglia control access to working memory. Nat Neurosci 11:103-107.
McNab F, Varrone A, Farde L, Jucaite A, Bystritsky P, Forssberg H, Klingberg T (2009) Changes in cortical dopamine D1 receptor binding associated with cognitive training. Science 323:800-802.
Mehta MR, Barnes CA, McNaughton BL (1997) Experience-dependent, asymmetric expansion of hippocampal place fields. Proc Natl Acad Sci U S A 94:8918-8921.
Mehta MR, Quirk MC, Wilson MA (2000) Experience-dependent asymmetric shape of hippocampal receptive fields. Neuron 25:707-715.
Millecamps M, Etienne M, Jourdan D, Eschalier A, Ardid D (2004) Decrease in non-selective, non-sustained attention induced by a chronic visceral inflammatory state as a new pain evaluation in rats. Pain 109:214-224.
Mitchell AS, Dalrymple-Alford JC (2005) Dissociable memory effects after medial thalamus lesions in the rat. Eur J Neurosci 22:973-985.
Monassi CR, Bandler R, Keay KA (2003) A subpopulation of rats show social and sleep-waking changes typical of chronic neuropathic pain following peripheral nerve injury. Eur J Neurosci 17:1907-1920.
Moriarty O, McGuire BE, Finn DP (2011) The effect of pain on cognitive function: A review of clinical and preclinical research. Prog Neurobiol.
Munoz M, Esteve R (2005) Reports of memory functioning by patients with chronic pain. Clin J Pain 21:287-291.
Olton DS, Isaacson RL (1967) Effects of lateral and dorsomedial thalamic lesions on retention of active avoidance tasks. J Comp Physiol Psychol 64:256-261.
Pais-Vieira M, Lima D, Galhardo V (2009) Sustained attention deficits in rats with chronic inflammatory pain. Neurosci Lett 463:98-102.
Park DC, Glass JM, Minear M, Crofford LJ (2001) Cognitive function in fibromyalgia patients. Arthritis Rheum 44:2125-2133.
Rainer G, Miller EK (2000) Effects of visual experience on the representation of objects in the prefrontal cortex. Neuron 27:179-189.
Rauschecker JP (1997) Mechanisms of compensatory plasticity in the cerebral cortex. Brain Plasticity 73:137-146.
Ray N, Jenkinson N, Kringelbach M, Hansen P, Pereira E, Brittain J, Holland P, Holliday I, Owen S, Stein J, Aziz T (2009) Abnormal thalamocortical dynamics may be altered by deep brain stimulation: using magnetoencephalography to study phantom limb pain. J Clin Neurosci 16:32-36.
Renaudineau S, Poucet B, Laroche S, Davis S, Save E (2009) Impaired long-term stability of CA1 place cell representation in mice lacking the transcription factor zif268/egr1. Proc Natl Acad Sci U S A 106:11771-11775.
Ribary U (2005) Dynamics of thalamo-cortical network oscillations and human perception. Prog Brain Res 150:127-142.
Sava S, Markus EJ (2008) Activation of the medial septum reverses age-related hippocampal encoding deficits: a place field analysis. J Neurosci 28:1841-1853.
Schmidt-Wilcke T, Wood P, Lürding R (2010) Cognitive impairment in patients suffering from fibromyalgia. An underestimated problem. Schmerz 24:46-53.
Schneider G, Kochs EF (2007) The search for structures and mechanisms controlling anesthesia-induced unconsciousness. Anesthesiology 107:195-198.
Seminowicz DA, Davis KD (2007) Interactions of pain intensity and cognitive load: the brain stays on task. Cerebral Cortex 17:1412-1422.
Shen J, Barnes CA, McNaughton BL, Skaggs WE, Weaver KL (1997) The effect of aging on experience-dependent plasticity of hippocampal place cells. J Neurosci 17:6769-6782.

Siapas AG, Lubenov EV, Wilson MA (2005) Prefrontal phase locking to hippocampal theta oscillations. Neuron 46:141-151.
Sikes RW, Vogt BA (1992) Nociceptive neurons in area 24 of rabbit cingulate cortex. J Neurophysiol 68:1720-1732.
Sirota A, Montgomery S, Fujisawa S, Isomura Y, Zugaro M, Buzsáki G (2008) Entrainment of neocortical neurons and gamma oscillations by the hippocampal theta rhythm. Neuron 60:683-697.
Skaggs WE, McNaughton BL, Gothard KM, Markus EJ (1993) An Information-theoretic approach to deciphering the hippocampal code. In: Advances in neural information processing (Hanson SJ, Cowan JD, Giles CL, eds), pp 1030-1037. San Mateo: Morgan Kaufmann.
Sleigh JW, Steyn-Ross DA, Steyn-Ross ML, Williams ML, Smith P (2001) Comparison of changes in electroencephalographic measures during induction of general anaesthesia: influence of the gamma frequency band and electromyogram signal. Br J Anaesth 86:50-58.
Smith DM, Freeman JH, Nicholson D, Gabriel M (2002) Limbic thalamic lesions, appetitively motivated discrimination learning, and training-induced neuronal activity in rabbits. J Neurosci 22:8212-8221.
Söderqvist S, Bergman Nutley S, Peyrard-Janvid M, Matsson H, Humphreys K, Kere J, Klingberg T (2011) Dopamine, working memory, and training induced plasticity: Implications for developmental research. Dev Psychol.
Sorensen L, Siddall P, Trenell M, Yue D (2008) Differences in metabolites in pain-processing brain regions in patients with diabetes and painful neuropathy. Diabetes Care 31:980-981.
Suga N, Zhang YF, Yan J (1997) Sharpening of frequency tuning by inhibition in the thalamic auditory nucleus of the mustached bat. J Neurophysiol 77:2098-2114.
Suga N, Gao EQ, Zhang YF, Ma XF, Olsen JF (2000) The corticofugal system for hearing: Recent progress. Proc Natl Acad Sci U S A 97:11807-11814.
Todd JJ, Marois R (2004) Capacity limit of visual short-term memory in human posterior parietal cortex. Nature 428:751-754.
Tononi G (2004) An information integration theory of consciousness. BMC Neurosci 5:42.
Tropp J, Figueiredo CM, Markus EJ (2005) Stability of hippocampal place cell activity across the rat estrous cycle. Hippocampus 15:154-165.
Tu Y, Yu T, Fu XY, Xie P, Lu S, Huang XQ, Gong QY (2011) Altered thalamocortical functional connectivity by propofol anesthesia in rats. Pharmacology 88:322-326.
Velly LJ, Rey MF, Bruder NJ, Gouvitsos FA, Witjas T, Regis JM, Peragut JC, Gouin FM (2007) Differential dynamic of action on cortical and subcortical structures of anesthetic agents during induction of anesthesia. Anesthesiology 107:202-212.
Vertes RP (2006) Interactions among the medial prefrontal cortex, hippocampus and midline thalamus in emotional and cognitive processing in the rat. Neuroscience 142:1-20.
Walton K, Dubois M, Llinás R (2010) Abnormal thalamocortical activity in patients with Complex Regional Pain Syndrome (CRPS) Type I. Pain 150:41-51.
Wang J, Chang J, Woodward D, Baccalá L, Han J, Luo F (2007) Corticofugal influences on thalamic neurons during nociceptive transmission in awake rats. Synapse 61:335-342.
Yang JW, Shih HC, Shyu BC (2006) Intracortical circuits in rat anterior cingulate cortex are activated by nociceptive inputs mediated by medial thalamus. J Neurophysiol 96:3409-3422.
Zhou J, Liu X, Song W, Yang Y, Zhao Z, Ling F, Hudetz AG, Li SJ (2011) Specific and nonspecific thalamocortical functional connectivity in normal and vegetative states. Conscious Cogn 20:257-268.

RESUMO E CONCLUSÕES IV

RESUMO E CONCLUSÕES

A experiência dolorosa constitui um fenómeno sensorial com características únicas que a colocam num especial patamar de interacção neurobiológica entre os processos sensoriais e os processos cognitivos. A perturbação da actividade oscilatória do circuito tálamo-cortical surge associada a alterações, não só ao nível do processamento da informação sensorial e memória de experiências sensoriais passadas, mas também ao nível dos processos de atenção e consciência. Os resultados da presente dissertação demonstraram que após o estabelecimento de uma condição de dor neuropática, a dinâmica funcional do eixo tálamo-cortical está alterada. Os animais com neuropatia exibiram um aumento do nível de sincronismo entre o tálamo lateral e o córtex somatosensitivo, sugerindo que o regime de processamento e coordenação da informação no circuito é efectuado de forma mais precisa. Adicionalmente, foi também observada uma redução significativa da quantidade de informação partilhada entre ambas as regiões, embora esta redução seja mais expressiva na projecção descendente do circuito, sugerindo que a actividade global do tálamo tem um menor peso sobre a actividade cortical. Por outro lado, estes dados reforçam também a ideia de que a projecção descendente cortico-talâmica possa estar a exercer um efeito inibitório sobre o tálamo, o que explica em parte essa redução do fluxo de informação no circuito. Esta hipótese é também reforçada por estudos clínicos que indicam que em pacientes com dor crónica existe uma hipoactividade talâmica e uma perturbação da conectividade nativa das redes corticais e subcorticais.

A perda de consciência induzida por anestésicos ocorre pela perturbação da comunicação entre os diversos circuitos do cérebro, através de uma redução gradual da sua capacidade de integração de informação. O circuito tálamo-cortical tem vindo a ser apontado como um candidato para o suporte instrumental dos mecanismos da consciência. Os nossos dados provaram que as populações de neurónios deste circuito permanecem estruturalmente funcionais durante a perda de consciência induzida pelo anestésico volátil isoflurano. Ambas as regiões exibiram um elevado nível de coerência no seu regime de actividade durante o estado estacionário da anestesia e também durante a exposição a concentrações mais elevadas do anestésico. É importante referir

que este padrão é mantido mesmo na presença das flutuações da potência do sinal em frequência que decorrem da concentração do anestésico. Por outro lado, essa actividade apresentou um elevado grau de correlação em função da concentração do anestésico na aplicação de índices clássicos de monitorização da profundidade da anestesia, apresentando-se como uma alternativa promissora em relação a outros índices comerciais baseados na actividade de EEG. Estes resultados suportam a ideia da existência de um diálogo cortico-talâmico contínuo mesmo durante a anestesia, e que a perda de consciência não passa necessariamente pela inactivação dos neurónios deste circuito.

A disfunção cognitiva dos doentes de dor crónica é simultaneamente uma questão crucial e paradoxal uma vez que é absolutamente desconhecida a etiologia deste problema e não se compreende de que forma um síndrome doloroso pode levar a perturbações nos circuitos neuronais de memória e aprendizagem. No presente trabalho de dissertação, procedeu-se à caracterização dos mecanismos de plasticidade no processamento da informação nociceptiva durante a competição com funções associativas e cognitivas. Esta análise foi efectuada em dois níveis do circuito fronto-hipocampal. Primeiro, na integração e processamento da informação associada à geração dos mapas espaciais pelos neurónios piramidais da região CA1 dorsal do hipocampo. Em segundo, ao nível do circuito fronto-hipocampal durante a codificação e retenção da memória de referência espacial, aspecto crucial para a performance de tarefas cognitivas. Os nossos dados demonstraram existir uma instabilidade nas propriedades de codificação espacial dos neurónios piramidais da região CA1 dorsal do hipocampo durante a instalação de uma condição de dor neuropática. Essa instabilidade é traduzida por uma redução do índice de especificidade espacial, indicando que esses neurónios providenciam menos informação acerca da localização do animal após a lesão periférica do nervo. Foram também observadas perturbações na codificação dos mapas espaciais, nomeadamente no número de campos codificados por neurónio, dimensão e coerência de disparo interna.

Os dados demonstraram ainda que o nível de performance associado à memória espacial de trabalho está afectado após a instalação da condição de dor neuropática, e que essas alterações então correlacionadas com perturbações na actividade dos

circuitos entre o córtex pré-frontal e o hipocampo. Em termos da estrutura temporal da actividade dos neurónios do circuito fronto-hipocampal, ambas as populações de neurónios aumentaram a sua precisão de disparo em relação ao ritmo “theta” do hipocampo. Os dados demonstram ainda uma redução significativa da quantidade de informação que é partilhada pelo circuito, a qual ocorre em bandas de frequência diferentes dependendo da resposta correcta ou incorrecta do animal na selecção do percurso a efectuar para localizar a recompensa. Essa redução da conectividade também foi observada nas interacções entre o córtex pré-frontal medial e o tálamo mediodorsal (embora de forma mais evidente no sentido do tálamo mediodorsal para o córtex pré-frontal medial e numa gama mais ampla de frequências de oscilação).

Em conclusão, os dados reunidos na dissertação detalham o papel das oscilações tálamo-corticais no processamento da informação sensorial e como o equilíbrio nessas oscilações é afectado durante a integração da informação nociceptiva e durante os processos de redução da consciência. Os resultados obtidos mostram ainda que condições de dor prolongada afectam a estabilidade da codificação da informação que está na base da geração dos mapas cognitivos de referência espacial no hipocampo, e que o regime de distribuição da informação entre o hipocampo e as estruturas pré-frontais está perturbado durante os processos mnemónicos associados à integração e consolidação da memória espacial.

ABSTRACT AND CONCLUSIONS V

SUMMARY AND CONCLUSIONS

The experience of pain is a sensory phenomenon with unique features, such as the dynamic interaction between sensory and cognitive neurobiological processes. The impairment of the thalamocortical circuit oscillatory activity is associated with changes not only in the processing of sensory information and memory of past sensory experiences, but also in the attention and awareness processes. The results presented in this dissertation demonstrate that the functional activity of the thalamocortical axis is changed after the establishment of a neuropathic pain condition. The animals with neuropathy exhibited an increased level of synchronism between the lateral thalamus and somatosensory cortex, suggesting that the processing and coordination of the information in the circuit is carried out more accurately. In addition, we observed a significant reduction in the amount of information shared by both regions; this decrease is more significant across the downward circuit projection, suggesting that the cortical activity has a larger burden over the thalamic activity. Moreover, these data also reinforce the idea that the corticothalamic descending projection may be carrying out an inhibitory effect on the thalamus, which partly explains the reduction in the flow of information of the circuit. This hypothesis is also supported by clinical studies of chronic pain patients that indicate the presence of a thalamic hypoactivity and a disturbance of the native connectivity of cortical and subcortical networks.

The loss of consciousness induced by anesthesia occurs by the disruption of the communication between several brain circuits, leading to a gradual reduction of its ability to integrate information. The thalamocortical circuit has been identified as a candidate for the instrumental support of the consciousness mechanisms. Our data shows that the neuronal populations of this circuit remain functional during the loss of consciousness induced by the volatile isoflurane anesthetic. Both regions exhibit a high level of consistency in their activity during the anesthesia steady-state, as well as during the exposure to high concentrations of anesthetic. It should be noted that this pattern is maintained even in the presence of fluctuations in the signal power that result from the anesthetic concentration. Furthermore – using conventional monitoring indexes of the depth of anesthesia that are a promising alternative to commercial indexes based in EEG

activity – the corticothalamic signals presented a high degree of correlation degree with depth pf anesthesia. These results support the idea that the corticothalamic dialogue is maintained during anesthesia, and that the loss of consciousness does not necessarily cause an inactivation of the neurons in this circuit.

The cognitive dysfunction of patients with chronic pain is simultaneously critical and paradoxical since the etiology of this problem is absolutely unknown, and it is not understood how a painful syndrome can lead to disturbances in the neuronal circuits of memory and learning. In this dissertation, we have proceeded to characterize the mechanisms of plasticity associated spatial working memory processing in animal models of pain. This analysis has been performed on two levels of the fronto-hippocampal circuit. First, in the integration and processing of information associated with the generation of spatial maps by CA1 pyramidal neurons of the dorsal hippocampus. Second, in the encoding and retention of spatial reference memory in the fronto-hippocampal circuit, crucial for the performance of cognitive tasks. Our data showed an instability in the spatial coding properties of the CA1 pyramidal neurons of the dorsal hippocampus during the installation of a neuropathic pain condition. This instability is translated into a reduction of the spatial specificity, indicating that these neurons provide less information about the animal location in the environment after the peripheral nerve injury. We also observed disruptions in the encoding of spatial maps, including the number of fields coded by neuron, the size of each field, and the internal field firing coherence.

Our data also showed that the performance level associated to spatial working memory is affected by the onset of a neuropathic pain condition, and that these changes are correlated with an impairment in the circuit activity between the prefrontal cortex and the hippocampus. The temporal structure of the activity of neurons in this circuit is modified after pain, with both populations increasing their firing accuracy in respect to hippocampal theta oscillations. The data also demonstrates a significant reduction in the amount of information that is shared by the circuit, which occurs in different frequency bands depending on the correct or incorrect path selected by the animal in order to locate the reward. This reduction was also observed in the connectivity between the medial prefrontal cortex and the mediodorsal thalamus (albeit more evident in the

direction from the thalamus to the cortex and in a wider range of oscillation frequencies).

In conclusion, the data gathered in this dissertation details the role of the corticalthalamic oscillations in the processing of sensory information, and how the balance of these oscillations is affected during the integration of nociceptive information and loss of consciousness. These results also show that prolonged pain conditions affect the ability to encode information that underlies the generation of spatial maps in the hippocampus, and that the distribution of information between the hippocampus and prefrontal structures is disturbed during the mnemonic processes associated with the integration and consolidation of the spatial reference memory.